UNIVERSIDADE FEDERAL DA BAHIA
FACULDADE DE MEDICINA
FUNDAÇÃO OSWALDO CRUZ
INSTITUTO GONÇALO MONIZ

UFBA **FIOCRUZ**

Curso de Pós-Graduação em Patologia

TESE DE DOUTORADO

PAPEL DA GALECTINA-3 NA PATOGÊNESE E NO TRATAMENTO DA MIOCARDIOPATIA CHAGÁSICA CRÔNICA

BRUNO SOLANO DE FREITAS SOUZA

Salvador - Bahia
2016

UNIVERSIDADE FEDERAL DA BAHIA
FACULDADE DE MEDICINA
FUNDAÇÃO OSWALDO CRUZ
INSTITUTO GONÇALO MONIZ

Curso de Pós-Graduação em Patologia

PAPEL DA GALECTINA-3 NA PATOGÊNESE E NO TRATAMENTO DA MIOCARDIOPATIA CHAGÁSICA CRÔNICA

BRUNO SOLANO DE FREITAS SOUZA

Orientadora: Dra. Milena Botelho Pereira Soares

Tese apresentada ao Curso de Pós-Graduação em Patologia Humana para a obtenção do grau de Doutor.

Salvador – Bahia
2016

Ficha Catalográfica elaborada pela Biblioteca do
Centro de Pesquisas Gonçalo Moniz / FIOCRUZ - Salvador - Bahia.

Souza, Bruno Solano de Freitas
S726p Papel da galectina-3 na patogênese e no tratamento da miocardiopatia chagásica crônica / Bruno Solano de Freitas Souza. - 2016.
110 f. : il. ; 30 cm.

Orientador: Dra. Milena Botelho Pereira Soares, Laboratório de Engenharia Tecidual e Imunofarmacologia.
Tese (Doutorado em Patologia) – Universidade Federal da Bahia. Fundação Oswaldo Cruz, Instituto Gonçalo Moniz, 2016.

1. Doença de Chagas. 2. *Trypanosoma cruzi.* 3. Galectina-3. 4. Cardiopatia. 5. Fibrose. 6. Miocardite. 7. Células-tronco mesenquimais. I. Título.

CDU 616.937

"PAPEL DA GALECTINA-3 NA PATOGÊNESE E NO TRATAMENTO DA MIOCARDIOPATIA CHAGÁSICA CRÔNICA"

BRUNO SOLANO DE FREITAS SOUZA

FOLHA DE APROVAÇÃO

Salvador, 24 de outubro de 2016

COMISSÃO EXAMINADORA

Dr. Antônio Carlos Campos de Carvalho
Professor Titular
UFRJ

Dra. Patrícia Sampaio Tavares Veras
Pesquisadora Titular
IGM/ Fiocruz

Dra. Clarissa Araujo Gurgel Rocha
Pesquisadora
IGM/Fiocruz

Dr. Fábio Rocha Formiga
Pesquisador
IGM/Fiocruz

Dra. Milena Botelho Pereira Soares
Pesquisadora
IGM/Fiocruz

SOUZA, Bruno Solano de Freitas. Papel da galectina-3 na patogênese e no tratamento da miocardiopatia chagásica crônica. 119 f. il. Tese (Doutorado em Patologia) – Universidade Federal da Bahia. Fundação Oswaldo Cruz, Instituto Gonçalo Moniz, Salvador, 2016.

RESUMO

INTRODUÇÃO: A doença de Chagas é uma relevante causa de insuficiência cardíaca na América Latina, onde cerca de 30% dos indivíduos infectados por *Trypanosoma cruzi* desenvolvem a cardiopatia chagásica crônica (CCC). Fatores relacionados à interação parasito-hospedeiro, resposta imune, reparo e regeneração tecidual participam da fisiopatologia da doença. A identificação de novos alvos terapêuticos depende de um melhor entendimento destes processos. Anteriormente, demonstramos que a galectina-3 (Gal-3), uma lectina com capacidade de ligação a β-galactosídeos, é superexpressa no tecido cardíaco em um modelo experimental de CCC. **OBJETIVOS**: O objetivo deste estudo foi investigar o papel exercido pela Gal-3 na patogênese da CCC e seu potencial uso como alvo terapêutico. **MATERIAIS E MÉTODOS**: A expressão de Gal-3 foi avaliada no coração de camundongos C57Bl/6 infectados com *T. cruzi* e amostras de indivíduos com CCC. Realizou-se bloqueio da expressão de Gal-3 com RNAi em fibroblastos de camundongos, seguido de avaliações de proliferação, apoptose e síntese de matriz. Camundongos infectados foram submetidos ao tratamento com inibidor farmacológico de Gal-3 e acompanhados quanto à função cardíca, análises morfológicas e de expressão gênica por PCR. Os efeitos do bloqueio da Gal-3 com RNAi em células-tronco MSC foi realizado *in vitro* através de imunofenotipagem, potencial de diferenciação celular, proliferação, avaliações de migração celular e ensaios de imunomodulação. MSC com *knockdown* de Gal-3 e controles foram transplantadas a camundongos cronicamente infectados com *T. cruzi* e os efeitos da terapia foram avaliados através de morfometria e análises de expressão gênica no coração. **RESULTADOS**: A cinética de expressão de Gal-3 durante a infecção por *T. cruzi* em camundongos se correlacionou com a cinética de infiltrado de células inflamatórias no coração. Observamos presença de células Gal-3^{+} no infiltrado inflamatório em secções de corações de pacientes com CCC. Detectamos expressão aumentada de Gal-3 em macrófagos, linfócitos T, fibroblastos, fibrócitos e células-tronco mesenquimais (MSC). O *knockdown* da Gal-3 em fibroblastos cardíacos reduziu a proliferação celular, sobrevivência e a síntese de colágeno. O bloqueio farmacológico de Gal-3 em camundongos na fase crônica da infecção por *T. cruzi* reduziu a fibrose e a migração de células inflamatórias para o coração, além de modular a expressão de mediadores inflamatórios e quimiocinas no coração, tais como IFNγ e TNFα. O *knockdown* de Gal-3 em MSC não alterou a expressão de marcadores de superfície característicos de células MSC, nem a sua capacidade de diferenciação. No entanto, as MSC *knockdown* para Gal-3 apresentam redução na taxa de proliferação e migração celular *in vitro* e *in vivo*. Quando transplantadas em camundongos cronicamente infectados por *T. cruzi*, as MSC controle promoveram a modulação de inflamação e fibrose cardíaca, enquanto que estas ações foram perdidas nas MSC com *knockdown* de Gal-3. **CONCLUSÕES**: Os nossos resultados demonstram que, no contexto da CCC, a Gal-3 participa do processo de migração de células recrutadas para o tecido cardíaco e contribui para o processo de fibrogênese, sendo, portanto, um alvo terapêutico potencial. Além disso, demonstram que a Gal-3 é um importante mediador de ações imunomodulatórias desempenhadas pelas MSC *in vitro* e no modelo de CCC.

Palavras-Chave: Doença de Chagas; *Trypanosoma cruzi*; Galectina-3; Cardiopatia; Fibrose; Miocardite; Células-Tronco Mesenquimais

SOUZA, Bruno Solano de Freitas. Role of galectin-3 in the pathogenesis and treatment of chronic Chagas disease cardiomyopathy. 119 f. il. Tese (Doutorado em Patologia) – Universidade Federal da Bahia. Fundação Oswaldo Cruz, Instituto Gonçalo Moniz, Salvador, 2016.

ABSTRACT

INTRODUCTION: Chagas disease is a relevant cause of heart failure in Latin America, where about 30% of individuals infected with *Trypanosoma cruzi* develop chronic Chagas' disease cardiomyopathy (CCC). Several factors related to host-parasite interactions, immune response, tissue repair and regeneration participate in the pathophysiology of the disease. The identification of novel therapeutic targets relies on a better understanding of these processes. Previously, we have demonstrated that the galectin-3 (Gal-3) - a β-galactoside binding lectin - is overexpressed in the cardiac tissue in an experimental model of CCC. **AIM**: The aim of this study was to investigate the role of Gal-3 in the pathogenesis of CCC and its potential use as a therapeutic target. **MATERIALS AND METHODS**: The expression of Gal-3 was assessed in the hearts of *T. cruzi* infected C57BL/6 mice and in samples of human subjects with CCC. Gal-3 knockdown was performed in fibroblast followed by proliferation, apoptosis and collagen synthesis. Infected mice were subjected to treatment with a pharmacological inhibitor of Gal-3, followed by cardiac function, morphological and gene expression analyses. Gal-3 knockdown in mesenchymal stem cells (MSC) was performed *in vitro*, followed by immunophenotyping, trilineage differentiation assay, proliferation, cell migration and immunomodulation assays. Gal-3 knockdown and control MSC were transplanted to mice chronically infected with T. cruzi and the therapy effects were evaluated by morphometry and analysis of gene expression in the heart. **RESULTS:** Gal-3 expression kinetics during *T. cruzi* infection in mice correlated with the kinetics of infiltration of inflammatory cells into the heart. Gal-3^+ cells were found in the inflammatory infiltrates in heart sections obtained from patients with CCC. Analysis of chagasic hearts of mice by flow cytometry and confocal microscopy demonstrated the high expression of Gal-3 in macrophages, T lymphocytes, fibroblasts, fibrocytes, and mesenchymal stromal cells (MSC). We perfomed *in vitro* studies to block Gal-3 gene expression in cardiac fibroblasts using RNA interference, and showed that Gal-3 inhibition affects cell proliferation, survival and collagen synthesis. Pharmacological blockade of Gal-3 reduced fibrosis, migration of inflammatory cells into the heart, and modulated the gene expression of inflammatory mediators and chemokines in the heart, such as TNF-α and IFN-γ. Next, we investigated the role of Gal-3 expression in MSC. Blockade of Gal-3 gene expression in bone marrow-derived MSC did not alter the expression of characteristic surface markers of MSC or their differentiation capacity. However, MSC knockdown for Gal-3 show a reduction in the rate of cell proliferation and migration *in vitro* and *in vivo*. When transplanted into mice chronically infected with *T. cruzi*, control MSC promoted modulation of inflammation and cardiac fibrosis, while these actions were lost in the MSC with Gal-3 knockdown. **CONCLUSION:** Our results demonstrate that, in the context of CCC, Gal-3 participates in the cell migration to the cardiac tissue and contributes to the fibrogenesis process and is therefore a potential therapeutic target. Furthermore, they show that the Gal-3 is an important mediator of the immunomodulatory actions performed by the MSC *in vitro* and in CCC model.

Keywords: Chagas disease; *Trypanosoma cruzi*; Galectin-3; Heart Disease; Fibrosis; Myocarditis; Mesenchymal Stem Cells

LISTA DE FIGURAS

LISTA DE TABELAS

LISTA DE ABREVIATURAS

AKT	Proteína quinase B
BCL-2	Linfoma de células B 2
BNP	Peptídeo natriurético cerebral
CCC	Cardiopatia chagásica crônica
CXCR4	Receptor de quimiciona C-X-C tipo 4
DAMP	Padrões moleculares associados ao dano
DNA	Ácido desoxirribonucleico
ECA	Enzima conversora da angiotensina
ELISA	do inglês *Enzyme Linked ImmunonoSorbent Assay*
GAL-3	Galectina-3
G-CSF	Fator de crescimento de colônia de granulócitos
HGF	Fator de crescimento de hepatócitos
ICC	Insuficiência cardíaca congestiva
IDO	Indoleamina 2,3 dioxigenase
IFN-γ	Interferon gama
IGF-1	Fator de crescimento semelhante à insulina 1
IgG	Imunoglobulina G
IL-13	Interleucina 13
IL-2	Interleucina 2
IL-4	Interleucina 4
IL-5	Interleucina 5
IL-6	Interleucina 6
IL-10	Interleucina 10
IL-1β	Interleucina 1β
iNOS	Oxido nítrico sintetase induzível
I.P.	Intraperitoneal
LAMC1	Subunidade gama 1 da laminina
LAMP1	Proteína 1 associada à membrana de lisossomos
LAMP2	Proteína 2 associada à membrana de lisossomos
LGALS3	Lectina, ligante de galactosídeo, solúvel 3
LPS	Lipopolissacarídeo

M1	Macrófago tipo 1 ou classicamente ativado
M2	Macrófago tipo 1 ou alternativamente ativado
MDSC	Células supressoras derivadas de linhagem mielóide
MEC	Matriz extracelular
mRNA	RNA mensageiro
MSC	Células-tronco mesenquimais
NAPDH	Fosfato de dinucleótido de nicotinamida adenosina
NT-proBNP	Peptídeo natriurético tipo pro-B N-terminal
NYHA	*New York Heart Association*
PCR	Reação em cadeia da polimerase
PBS	Tampão fosfato-salino
PGE2	Prostaglandina E2
RNA	Ácido ribonucleico
RNAi	RNA de interferência
shRNA	Do inglês *short hairpin RNA*
Smad3	Membro 3 da família SMAD
T-bet	Fator de transcrição t-box
TCR	Receptor de células T
TGF-β	Fator de crescimento de transformação β
Th1	Linfócito T auxiliar tipo 1
Th2	Linfócito T auxiliar tipo 2
Th17	Linfócito T auxiliar tipo 17
THBS1	Trombospondina 1
TNF-α	Fator de necrose tumoral α
Treg	Linfócito T regulatório
SDF-1	Fator derivado de estroma 1
SNP	Polimorfismo de nucleotídeo único
α-SMA	Actina α de músculo liso

SUMÁRIO

1 INTRODUÇÃO

1.1 DOENÇA DE CHAGAS: ASPECTOS GERAIS

Descrita no início do século XX por Carlos Chagas, a doença de Chagas, causada pela infecção por *Trypanosoma cruzi,* é uma doença parasitária de grande prevalência em países latino-americanos. Nestes países, a cardiopatia chagásica crônica (CCC) é uma causa importante de morbimortalidade (NUNES *et al.*, 2013). Atualmente, estima-se que entre seis e sete milhões de pessoas estejam infectadas, principalmente na América Latina. Recentemente, casos da doença também vêm sendo reportados em países desenvolvidos, como Estados Unidos, Canadá e países da Europa, denotando um fenômeno de globalização da doença de Chagas nos últimos anos, em decorrência dos fluxos migratórios (ANDRADE *et al.*, 2014).

O *T. cruzi* é um protozoário flagelado pertencente à ordem kinetoplastida. Este protozoário é vetorialmente transmitido por insetos hematófagos de gêneros que incluem *Rhodnius, Panstrongylus e Triatoma,* pertencentes à família *Reduviidae*, *popularmente* conhecidos no Brasil como barbeiros. Formas infectantes do *T. cruzi* são encontradas nas fezes destes insetos, que podem então ser inoculadas nas feridas provenientes da picada do inseto após o repasto sanguíneo. O *T. cruz*i possui uma passagem obrigatória por hospedeiros mamíferos como parte do seu ciclo evolutivo (Figura 1). Assim, na natureza, o *T. cruzi* infecta diversas espécies de mamíferos que funcionam como reservatórios do parasito, além da infecção em seres humanos (DEVERA *et al.*, 2003).

O parasito possui três formas no seu ciclo evolutivo: epimastigota (forma de vida extracelular presente no intestino dos insetos vetores), tripomastigota (forma flagelada infectante para células de mamíferos) e amastigota (forma de vida intracelular, com capacidade de proliferação dentro da célula de mamífero (DE SOUZA *et al.*, 2002). Historicamente, a maioria das transmissões do *T. cruzi* para seres humanos tem sido causada por via vetorial, porém esta via de transmissão tem sido reduzida significativamente nos países endêmicos, em decorrência do combate ao vetor. A transmissão por via transfusional também ocorreu amplamente no passado, antes de ser praticamente eliminada através da inclusão da triagem sorológica para infecção por *T. cruzi* nos bancos de sangue. Outra via de transmissão ocasional é através do transplante de órgãos sólidos a partir de doadores com infecção crônica, em países onde não é realizada a triagem sorológica. A transmissão congênita permanece ocorrendo sem nenhuma medida de combate, a não ser pela própria redução da incidência da doença. Por fim,

a transmissão por via oral é considerada hoje a mais frequente no Brasil, devido a surtos de fase aguda da doença de Chagas ocorridos nos últimos anos no país, causados pela ingestão de alimentos contaminados (VALENTE *et al*, 2009; PINTO *et al*, 2008; SOUZA-LIMA *et al*, 2013).

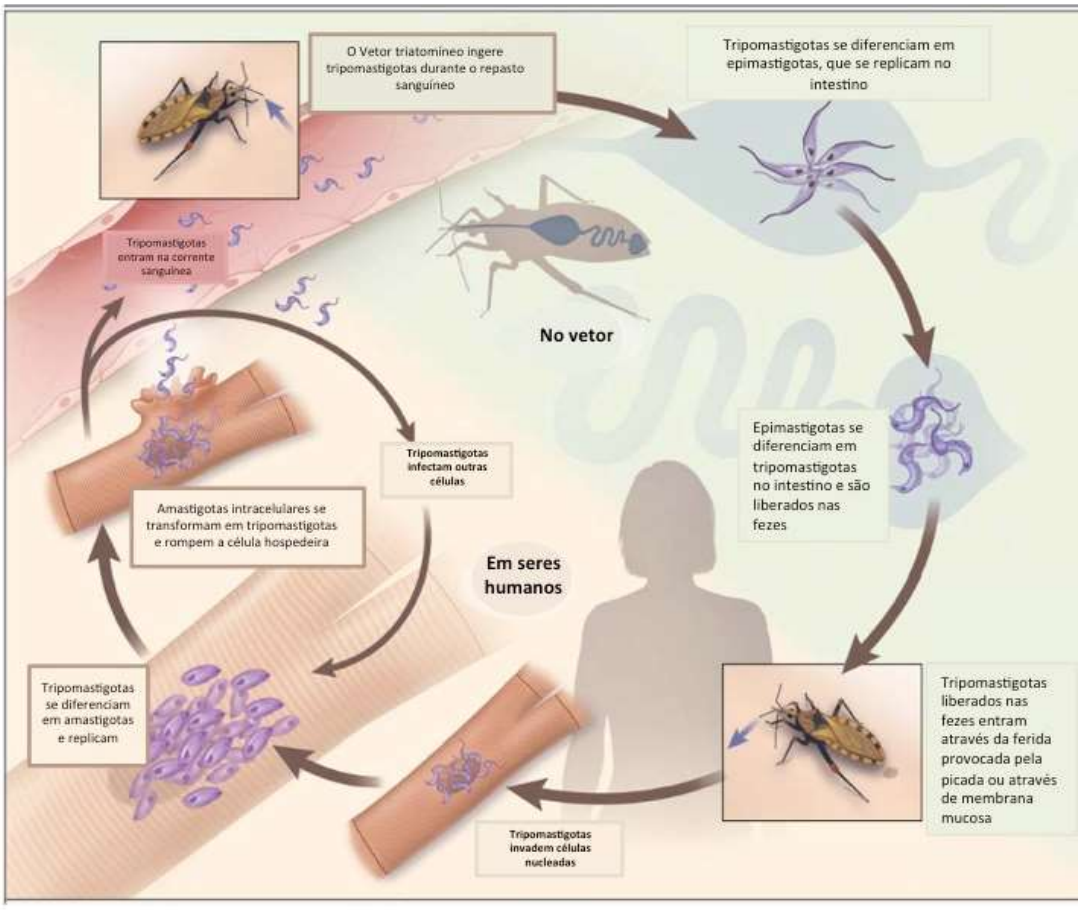

Figura 1. Ciclo de vida do *T. cruzi*. O ciclo de vida é iniciado quando o vetor triatomíneo ingere tripomastigotas circulantes durante o repasto sanguíneo em mamíferos hospedeiros. As formas tripomastigotas se transformam em epimastigotas, formas replicativas presentes no intestino do vetor. As formas epimastigotas se diferenciam em tripomastigotas metacíclicos infectantes, que são excretados com as fezes do vetor durante o repasto sanguíneo. Os tripomastigotas metacíclicos entram através da ferida provocada pela picada ou através de membrana mucosa e invadem células nucleadas. No citoplasma, os tripomastigotas se diferenciam na forma amastigota, que se replica, posteriormente se transformando em tripomastigotas, que rompem a membrana da célula, sendo liberados na circulação. Os parasitas circulantes podem então invadir novas células ou infectar vetores. Adaptado de BERN *et al*, 2015.

Após a entrada do *T. cruzi* no organismo podem ser encontrados sinais clínicos associados à porta de entrada do parasito no organismo, como o clássico sinal de Romaña. A fase aguda da doença é iniciada após um período de incubação que varia de uma a duas semanas,

e pode durar até três meses. Nessa fase, as formas tripomastigotas podem ser visualizadas no sangue periférico, enquanto que os indivíduos infectados se apresentam geralmente oligossintomáticos, com uma doença febril com sinais e sintomas inespecíficos, ou mesmo assintomáticos. A mortalidade nesta fase é baixa e resulta frequentemente de miocardite ou pericardite (TANOWITZ *et al*, 1992). A maioria dos pacientes sobrevive à fase aguda, uma vez que uma resposta imune adaptativa capaz de controlar a infecção é estabelecida, porém sem erradicar completamente o parasito, mantendo uma relação de equilíbrio dinâmico parasito-hospedeiro (BERN, 2015).

A fase crônica da infecção se inicia assintomática, o que caracteriza a forma indeterminada, que se estende por toda a vida em aproximadamente 70% dos casos. Não existe um marcador capaz de prever a progressão da doença ou manutenção da forma indeterminada. No entanto, de 10 a 30 anos após a infecção com *T. cruzi*, 20-30% dos pacientes irão apresentar a grave forma cardíaca da doença, que pode se caracterizar por distúrbios do ritmo e de condução – forma arrítmica – ou por dilatação das câmaras cardíacas, levando à insuficiência cardíaca – forma dilatada. Arritmias graves e morte súbita são as maiores causas de mortalidade nestes casos. Cerca de 10% dos pacientes cronicamente infectados pelo *T. cruzi* apresentam a forma digestiva, caracterizada por megaesôfago e/ou megacólon, enquanto que uma minoria dos pacientes pode apresentar uma combinação das formas cardíaca e digestiva (BERN, 2015).

Apesar da ausência de parasitemia na fase crônica, há persistência do parasito no organismo, o que fica evidenciado pela ocorrência de reagudização da doença em indivíduos imunosuprimidos (ZHANG & TARLETON, 1999; BELLOTTI *et al*, 1996). Esta reativação é caracterizada pelo aumento da multiplicação dos parasitos, com parasitemia detectável e sintomas típicos da fase aguda (PEREZ *et al*, 2015).

A confirmação da infecção através do diagnóstico laboratorial pode ser realizada pela pesquisa do parasito por microscopia em amostras de sangue na fase aguda, enquanto que, na fase crônica, ensaios sorológicos por ELISA, hemaglutinação indireta ou imunofluorescência indireta podem ser utilizados para detectar a presença de IgG específica para antígeno do *T. cruzi* (BERN, 2015).

Em relação às opções terapêuticas, o nifurtimox e o benzonidazol são as únicas drogas com comprovada eficácia para o tratamento da infecção por *T. cruzi.* O benzonidazol é um derivado nitroimidazólico considerado como droga de primeira linha para o tratamento etiológico, uma vez que apresenta maiores evidências de eficácia, e comparativamente menores efeitos colaterais (BERN *et al*, 2007). No entanto, trata-se de uma droga que possui diversos efeitos colaterais, que incluem reações dermatológicas, febre, linfadenopatia e neuropatia

periférica dose-dependente. O nifurtimox é uma alternativa para pacientes que não toleram benzonidazol. Trata-se de uma droga que atua contribuindo para a formação de radicais livres, afetando a sobrevivência do *T. cruzi*. Anorexia, perda de peso, náuseas e vômitos podem ocorrer em até 70% dos pacientes, enquanto que outros eventos adversos associados à neurotoxicidade, incluindo parestesias, polineuropatia e neurite periférica são complicações graves, embora de rara ocorrência (JACKSON *et al*, 2010).

Em pacientes na fase aguda da doença de Chagas, tanto o benzonidazol quanto o nifurtimox podem ser utilizados e são eficazes na redução de sintomas, parasitemia e levam à cura em aproximadamente 80 a 90% dos casos (BERN, 2015). Estudos em pacientes pediátricos indicaram cura sorológica em 60% dos casos crônicos tratados com benzonidazol, de 3 a 4 anos após o início do tratamento (DE ANDRADE *et al*, 1996). Mais recentemente, o estudo BENEFIT foi realizado com desenho de ensaio clínico multicêntrico duplo-cego randomizado e controlado por placebo, com o objetivo de avaliar a eficácia do tratamento com benzonidazol em pacientes com miocardiopatia chagásica crônica leve a moderada. Nestes indivíduos, foi observada uma negativação da PCR para *T. cruzi* em aproximadamente 66% dos casos tratados versus 33% no grupo controle. No entanto, não houve melhora do quadro clínico cardiológico dentro de um período de 5 anos de seguimento (MORILLO *et al*, 2015*)*. Diante destes dados, recomenda-se que os pacientes com miocardiopatia chagásica crônica recebam o tratamento padrão para insuficiência cardíaca de qualquer etiologia, com drogas com alvo em controle sintomático, aumento de sobrevida e prevenção de remodelamento, como os diuréticos, inotrópicos, inibidores da ECA, bloqueadores do receptor de angiotensina, dentre outros (ANDRADE *et al*, 2011; YANCY *et al*, 2016). A única opção para pacientes com miocardiopatia chagásica crônica em estágio final é o transplante cardíaco, que se trata de um procedimento de alto custo e complexidade, complicado pelas consequências da imunossupressão envolvendo reagudização da doença de Chagas, além da indisponibilidade de órgãos e baixa difusão de centros capacitados no Brasil, especialmente nas regiões norte e nordeste (Ministério da Saúde, 2015).

Tendo em vista a limitação de opções terapêuticas e ausência de indicação para o tratamento etiológico em pacientes com miocardiopatia chagásica crônica estabelecida, mais estudos são necessários para a melhor compreensão fisiopatológica, identificação de novos alvos moleculares, descoberta de drogas e desenvolvimento de terapias que possam ser eficazes para o tratamento desses pacientes. Tendo por base a importância dos mecanismos de lesão imunomediada no cenário da doença de Chagas, nosso grupo de pesquisas tem se dedicado a buscar alternativas terapêuticas para a miocardiopatia chagásica crônica, enfocando a

modulação de inflamação e fibrose no coração, utilizando drogas, fatores de crescimento e células-tronco.

1.2 IMUNOPATOLOGIA DA MIOCARDIOPATIA CHAGÁSICA CRÔNICA

A resposta imune é crucial para o controle do parasito, mas também possui um papel central na patogênese da doença (HIGUCHI *et al*, 1987). Logo após a infecção pelo *T. cruzi*, ocorre a ativação da reposta imune inata via receptores *Toll-like* (TLR), que reconhecem padrões moleculares associados a patógenos (PAMP), incluindo DNA e moléculas glicosiladas (BAFICA *et al*, 2006). Deste modo, os macrófagos e as células dendríticas são ativados, levando à secreção de um conjunto de moléculas pró-inflamatórias, incluindo citocinas como TNF-α, quimiocinas e produção de espécies reativas de oxigênio, que contribuem para o ataque ao parasita (PENAS *et al*, 2015). Ocorre, então, uma ativação de células T, com produção de IFN-γ, caracterizando células Th1, que atuam no controle do parasitismo (SAMUDIO *et al*, 1998; ABEL *et al*, 2001).

Na fase crônica, observa-se a persistência de níveis elevados de citocinas com padrão Th1, como IFN-γ e TNF-α. Observa-se, ainda, o aumento da expressão de T-bet, um fator de transcrição presente em linfócitos Th1, no miocárdio de indivíduos com miocardiopatia (NOGUEIRA *et al*, 2014). Comparando indivíduos com sorologia positiva para doença de Chagas que desenvolveram miocardiopatia com aqueles que se apresentam na forma indeterminada, observou-se um aumento de linfócitos T CD4 e CD8 produtores de IFN-γ no sangue periférico, além de redução na população de células T reguladoras (ABEL *et al*, 2001). Estes dados indicam a persistência de uma resposta Th1 exacerbada em indivíduos com miocardiopatia chagásica.

Os achados de citocinas Th1 aumentadas na periferia refletem um processo fisiopatológico que afeta enormemente o coração, onde ocorre dano persistente aos cardiomiócitos, que morrem por necrose em decorrência de diversos mecanismos. A destruição tecidual que ocorre no coração na doença de Chagas é devida a danos imuno-mediados envolvendo tanto a resposta imune direcionada ao *T. cruzi* quanto a auto-antígenos cardíacos (SOARES *et al*, 2001; GIRONÈS & FRESNO, 2003). Diversos mecanismos foram apontados para explicar este acometimento cardíaco observados em indivíduos afetados pela doença de Chagas. Uma das hipóteses sugere que o dano aos cardiomiócitos observado na fase crônica seja decorrente da persistência do parasito no tecido cardíaco. Este achado explicaria o dano aos cardiomiócitos tanto pela lise celular mediada pelo parasito, tanto pelo dano colateral

provocado pela resposta imune direcionada ao *T. cruzi*. Esta hipótese tem suporte pela detecção de DNA ou antígeno de parasitos em algumas lesões inflamatórias no coração, apesar de não serem detectados parasitos intactos no coração durante a fase crônica da doença.

Além da hipótese da persistência do parasito, outros mecanismos têm sido apontados como participantes da patogênese da miocardiopatia chagásica crônica. Diversos estudos independentes reportaram o comprometimento da inervação cardíaca, com perda de neurônios principalmente parassimpáticos (KÖBERLE, 1968). Estas alterações precedem a disfunção ventricular (RIBEIRO *et al*, 2001). O envolvimento da microvasculatura, levando à isquemia e inflamação, também foi previamente descrito (ROSSI, 1990). Por fim, a hipótese da auto-imunidade sugere que o dano provocado pelo parasito levaria à quebra de tolerância a antígenos próprios, possivelmente através de um processo de mimetismo molecular entre antígenos do parasito e do hospedeiro (BONNEY & ENGMAN, 2015; KAPLAN *et al*, 1997; MOTRÁN *et al*, 2000; TARLETON, *et al*, 1997; HYLAND *et al*, 2007). Estas hipóteses não são mutuamente excludentes já que, por exemplo, a persistência do parasito no tecido cardíaco também é importante para o recrutamento de células autoreativas (SOARES *et al*, 2001).

Apesar dos processos que levam ao desenvolvimento da forma cardíaca não estarem completamente esclarecidos, vários estudos sugerem o envolvimento da ativação de linfócitos Th1, que produzem altos níveis de IFN-γ, em um processo de reatividade que se assemelha a uma reação de hipersensibilidade tardia (SOARES *et al*, 2001; GOMES *et al*, 2003). Uma associação entre a progressão para forma cardíaca grave e alta produção de IFN-γ por células T do sangue periférico foi observada em pacientes com doença de Chagas (GOMES *et al*, 2003). O infiltrado inflamatório presente nos corações de camundongos com CCC é composto principalmente por células mononucleares, muitas vezes encontradas na proximidade de fibras cardíacas (ROSENBAUM, 1964). Os macrófagos são uma das principais populações celulares encontradas no sítio inflamatório cardíaco, e são altamente ativados pelo IFN-γ e TNF-α (REIFENBERG *et al*, 2007). Consistentemente, estudos prévios demonstraram que a produção das citocinas IFN-γ e TNF-α está aumentada no coração de camundongos cronicamente infectados por *T. cruzi* em relação aos controles não infectados. Além disso, a expressão de vários genes relacionados à resposta inflamatória e a estas duas citocinas está aumentada nos corações de camundongos infectados (SOARES *et al*, 2010). Esta perda de miócitos leva a uma resposta hipertrófica compensatória no miocárdio, além da infiltração de células inflamatórias com predomínio mononuclear no tecido cardíaco. Através de análises histológicas observa-se uma miocardite difusa com focos de infiltrados inflamatórios associados à miocitólise e também uma fibrose intensa, que estão presentes mesmo sem que parasitos sejam visualizados.

Nestes infiltrados inflamatórios, predominam linfócitos T e macrófagos, mas eosinófilos, neutrófilos e mastócitos também se fazem presentes (REIS *et al*, 1993). Como consequência ao dano aos cardiomiócitos, a fibrose no miocárdio se desenvolve ao longo da infecção, causando, juntamente com o processo de remodelamento, o desenvolvimento de arritmias, distúrbios de condução e insuficiência cardíaca.

Nos últimos anos, estudos de biologia de sistemas têm contribuído para a identificação de vias de sinalização envolvidas na patogênese da doença. Análises de transcriptoma realizadas comparando amostras de tecidos cardíacos obtidos de indivíduos com miocardiopatia chagásica, miocardiopatia dilatada idiopática e corações saudáveis demonstraram ativação de genes relacionados à resposta imune induzidos por IFN-γ, que incluem o peptídeo natriurético atrial, de modo significativamente maior no grupo chagásico. Estes estudos têm revelado os efeitos que mediadores inflamatórios exercem sobre o miocárdio, contribuindo para a disfunção cardíaca através de diferentes mecanismos, que incluem a apoptose de cardiomiócitos (TOSTES *et al*, 2005).

Estudos de expressão gênica global desenvolvidos anteriormente pelo nosso grupo demonstraram, ainda, o aumento da expressão de galectina-3 e sindecan-4, moléculas que estão intimamente associados à resposta inflamatória e que exercem importante papel sobre o processo de fibrogênese e remodelamento cardíaco (SOARES *et al*, 2010).

1.3 REMODELAMENTO CARDÍACO

Entende-se por remodelamento cardíaco o processo de modificação de tamanho, massa, geometria e função do coração, em resposta a uma lesão aguda ou sobrecarga crônica. Este processo decorre de uma série de fatores genéticos, moleculares, neuro-humorais e celulares (COHN *et al*, 2000). Após uma lesão ou sobrecarga, o mecanismo fisiopatológico de Frank-Starling é desencadeado de modo compensatório. No entanto, a persistência da dilatação levará a danos ao miocárdio e insuficiência cardíaca (HOLUBARSCH *et al*, 1996). O remodelamento é o processo que leva à insuficiência cardíaca, sendo que pacientes com maior remodelamento apresentam piora da função cardíaca, resultando em aumento de morbidade e mortalidade (JOHNSON, 2014).

Tendo em vista que o processo de remodelamento cardíaco está diretamente associado à progressão da insuficiência cardíaca e aumentada morbimortalidade, o tratamento da insuficiência cardíaca, segundo as diretrizes de 2016 da *American Heart Association*, visa não apenas à melhora dos sintomas, mas também à redução da progressão do remodelamento.

Drogas que possuem comprovada eficácia no retardo do processo de remodelamento incluem os inibidores da ECA, bloqueadores do receptor da angiotensina e β-bloqueadores, por suas efeitos neuro-humorais (COHN *et al*, 2000).

O processo de remodelamento cardíaco é dependente de alterações estruturais em cardiomiócitos associadas a um processo de reparo tecidual com fibrogênese, decorrente de interações entre diferentes tipos celulares (HULSMANS *et al*, 2016; ZHANG *et al*, 2012). Destacam-se aqui como principais células envolvidas no processo de remodelamento cardíaco: cardiomiócitos, fibroblastos e macrófagos.

Os cardiomiócitos estão diretamente relacionados ao processo de remodelamento. Danos agudos ou sobrecargas crônicas ao coração resultam na redução do número de miócitos. Os miócitos remanescentes passam por um processo adaptativo, tornando-se alongados ou hipertrofiados, como parte de mecanismo compensatório, de modo a manter a função sistólica (DISTEFANO *et al*, 2012).

Os fibroblastos cardíacos são células de origem mesenquimal que residem no interstício cardíaco, compondo um dos tipos celulares mais abundantes no coração de mamíferos (CAMELLITI *et al*, 2005). Há evidências de que os fibroblastos cardíacos derivam, durante a embriogênese, de células provenientes do epicárdio, que passam por um processo de transição epitélio-mesenquimal (LIE-VENEMA *et al*, 2007). Estas células participam ativamente da homeostase da matriz extracelular. Outra fonte de fibroblastos no coração é o endotélio valvar, que passa por um processo de transição endotélio-mesenquimal, dando origem aos fibroblastos valvulares, que contribuem durante o desenvolvimento para a formação da estrutura fibrosa que circunda os vasos (DE LANGE *et al*, 2004).

Quando ocorre uma lesão no miocárdio, por conta da limitada capacidade de regeneração do coração, é disparada uma resposta de reparo tecidual, com ativação de fibroblastos. Os fibroblastos cardíacos residentes proliferam no sítio da lesão e se tornam o tipo celular que mais contribui para o processo de fibrogênese no coração. Estas células proliferam e, eventualmente, tornam-se miofibroblastos, apresentando aparato contrátil e capacidade de síntese de componentes da matriz extracelular aumentada, apresentando positividade para o antígeno α-SMA (PETROV *et al*, 2002). Pericitos e células perivasculares também podem contribuir no processo de fibrogênese, em diferentes tecidos (HUMPHREYS *et al*, 2010). Por fim, em situações de resposta à lesão no miocárdio com formação de cicatriz fibrosa, há um papel significativo de células derivadas da medula óssea, que foram denominadas fibrócitos (KRENNING *et al*, 2010). Estas células expressam marcadores de superfície característicos de células derivadas da medula óssea, como CD45, e marcadores de fibroblastos, tal como a

vimentina (ABE *et al*, 2001). Há indícios de que os fibrócitos derivados da medula óssea desempenham um papel importante no processo de reparo tecidual no coração, tendo sido considerados como fonte de 60% da população de fibroblastos e miofibroblastos em um modelo experimental de miocardite autoimune (KANIA *et al*, 2009).

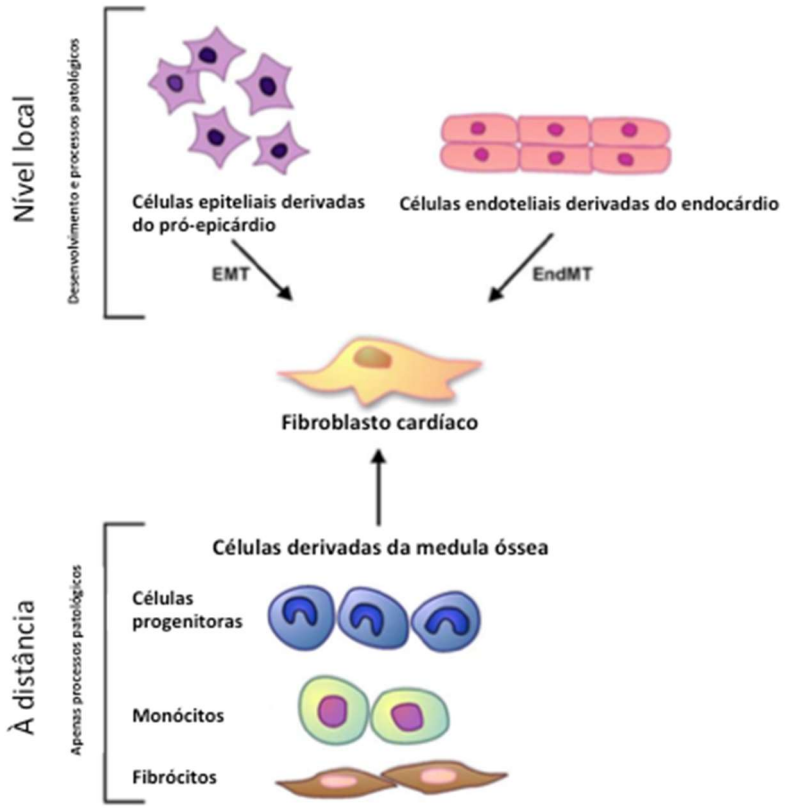

Figura 2. Origem dos fibroblastos cardíacos durante o desenvolvimento e em doenças. Durante o desenvolvimento, células derivadas do epicárdio sofrem transição epitélio-mesenquimal (EMT), enquanto que células endoteliais do endocárdio podem sofrer transição endotélio-mesenquimal (EndMT), transformando-se em fibroblastos cardíacos. Após uma lesão miocárdica, células derivadas da medula óssea (monócitos, células progenitoras e fibrócitos) podem ser recrutadas para o local da lesão, transformando-se em fibroblastos cardíacos. Além deste processo, também pode ocorrer EMT e EndMT em processos patológicos. Adaptado de FAN *et al*, 2012.

Outro tipo celular que desempenha um papel significativo no processo de remodelamento cardíaco é o macrófago. Após uma lesão no miocárdio, há a ativação de macrófagos do tipo M1, pró-inflamatórios, seguida de uma ativação M2, de ações anti-inflamatórias e pró-reparo tecidual. Os macrófagos atuam na resolução de uma lesão tecidual através de diferentes mecanismos: (I) remoção de debris por fagocitose; (II) promoção de angiogênese através da secreção de fatores parácrinos que atuam células endoteliais; (III) indução de fibrose, através da secreção de moléculas que estimulam a proliferação de

fibroblastos e síntese de matriz extracelular, como galectina-3, IGF-1 e TGF-β (FUJIU *et al*, 2014). Além destas ações sobre o processo de reparo, que faz parte do remodelamento cardíaco, há ainda outras consequências da ativação de macrófagos diretamente sobre o músculo cardíaco. É bastante conhecido, por exemplo, que o TNF-α, secretado no coração por macrófagos pró-inflamatórios, afeta a contratilidade dos cardiomiócitos, contribuindo para a disfunção cardíaca em cenários de doença (FELDMAN *et al*, 2000).

O envolvimento dos macrófagos cardíacos é bem descrito na resposta ao infarto agudo do miocárdio. Neste cenário, observa-se a necrose de áreas extensas do miocárdio e liberação de conteúdo intracelular, muitos atuando como DAMPs (do inglês *damage associated molecular patterns*) ou padrões moleculares associados ao dano. Os DAMPs se ligam a receptores de células da resposta imune inata, incluindo os TLR. Ocorre o recrutamento de neutrófilos dentro de 24 horas, fagocitando debris teciduais. Monócitos são recrutados por quimiocinas, tal como a MCP-1, e se diferenciam em macrófagos. Nos primeiros 5 dias ocorre o predomínio de macrófagos M1, caracterizados por suas ações fibrolíticas, fagocíticas e inflamatórias, liberando citocinas como TNF-α, IL-6, IL-1β, quimiocinas e espécies reativas de oxigênio. Em seguida, a partir do 7º dia pós-infarto, inicia-se a fase de resolução, com ativação predominante de macrófagos M2, com ações anti-inflamatórias, angiogênicas e fibrogênicas (NAHRENDORF *et al*, 2007).

No cenário da miocardiopatia chagásica, apesar de não ser tão bem descrito como no infarto agudo do miocárdio, é observada uma ativação de macrófagos M1, que se relaciona diretamente ao combate ao parasito, com persistente dano imuno-mediado aos miócitos, embora também se observe a ativação M2, que contribui para o processo de fibrose (PENAS *et al*, 2015).

1.4 GALECTINA-3

A galectina-3 (Gal-3) é uma lectina com capacidade de ligação a β-galactosídeos, também conhecida como Mac-2. Trata-se de uma proteína de 26-kDa codificada por um único gene, LGALS3, localizado no cromossomo 14, locus q21–q22 (RAIMOND *et al*, 1997). Esta molécula é capaz de atuar tanto no ambiente intracelular quanto no ambiente extracelular, afetando diferentes processos, que incluem adesão celular, vias de sinalização, proliferação, diferenciação e apoptose (KRZEŚLAK *et al*, 2004). As ações desempenhadas por Gal-3 na adesão celular decorrem da sua capacidade de oligomerização, conectando moléculas da

superfície celular com a matriz extracelular. A laminina é um dos componentes da matriz que se liga a Gal-3 com maior afinidade (MASSA *et al*, 1993).

As ações exercidas pela Gal-3 são pleiotrópicas, variando com o tipo celular e com a localização da molécula, isto é, no compartimento extracelular ou intracelular (KRZEŚLAK *et al*, 2004). Dentro da célula, a Gal-3 é encontrada no citoplasma, mas também pode sofrer translocação para o núcleo, onde está envolvida na regulação da expressão gênica e *splicing* alternativo (LIN *et al*, 2002). Foi previamente descrito que a Gal-3 se liga e interage com outras proteínas no ambiente intracelular, incluindo Bcl-2 (YANG *et al*, 1996), Gemin4 (PARK *et al*, 2001) e β-catenina (SHIMURA *et al*, 2004). A Gal-3 apresenta semelhanças em sua sequência com o domínio ativo da molécula anti-apoptótica Bcl-2 (YANG *et al, 1996)*, o que explica suas ações promotoras de sobrevivência celular. Por outro lado, a sua associação intracelular com a Gemin4, um componente do *spliceossomo*, justifica o papel desempenhado na regulação de *splicing* alternativo. Por fim, sua ação sobre a proliferação celular pode ser explicada pela interação com a β-catenina.

O papel da Gal-3 na modulação de respostas imunes é bem descrito na literatura. A Gal-3 exerce diversas funções sobre o sistema imune, agindo diretamente em diferentes tipos celulares (Tabela I). Ela é expressa por linfócitos T ativados (JOO *et al*, 2001) e está envolvida em diferentes processos nestas células (Figura 3). Estas ações variam de acordo com a localização (intracelular vs. extracelular), gerando alguns efeitos comuns, como, por exemplo, a inibição da sinalização do TCR (DEMETRIOU *et al*, 2001), e alguns efeitos antagônicos, como, por exemplo, a indução apoptose no meio extracelular versus efeito anti-apoptótico no meio intracelular (Figura 3). Alguns efeitos estão exclusivamente associados com a presença da Gal-3 no meio intracelular, como é o caso do crescimento celular, enquanto outros são exclusivamente desencadeados pela Gal-3 em meio extracelular, como ativação e migração celular (HSU *et al,* 2009).

A Gal-3 também é altamente expressa em populações de monócitos e macrófagos (LIU *et al*, 1995). Tem sido demonstrado que macrófagos classicamente ativados, também conhecidos como macrófagos pró-inflamatórios ou M1, são a maior fonte da Gal-3 em sua forma secretada para o meio extracelular. Por outro lado, a Gal-3 também está presente em macrófagos alternativamente ativados, também conhecidos como anti-inflamatórios ou M2 (NOVAK *et al*, 2012). Além das ações em macrófagos anti-inflamatórios, Gal-3 atua em outras populações de células com conhecida ação regulatória sobre o sistema imune, como é o caso das células-tronco mesenquimais, onde parece contribuir para ações imunomoduladoras (LIU *et al*, 2013; SIOUD *et al*, 2011).

Tabela I. Funções de galectina-3 em células imunes.

Tipo celular	Ações	Referências
Neutrófilos	↑ Atividade de NADPH-oxidase ↑ Produção de ânion superóxido ↑ Adesão à laminina ↑ Extravasamento ↑ Atividade fagocítica ↑ Expressão de CD66	FEUK-LAGERSTEDT *et al*, 1999 KUWABARA *et al*, 1996 SATO *et al*, 2002 FERNÁNDEZ *et al*, 2005
Monócitos / macrófagos	↑ Produção de ânion superóxido ↑ Produção de IL-1 induzida por LPS ↑ Quimiotaxia ↑ Fagocitose ↓ Apoptose	LIU *et al,* 1995 SANO *et al*, 2000 SANO *et al,* 2003
Linfócitos T	↑ Produção de IL-2 ↑ Apoptose (extracelular) ↑ Proliferação ↑ Interação entre linfócitos T naïve e células dendríticas ↓ Apoptose (intracelular) ↓ Sinalização do TCR	SWARTE *et al*, 1998 HSU *et al,* 2009 DEMETRIOU *et al*, 2001
Linfócitos B	↓ Diferenciação em plasmócitos ↓Apoptose	ACOSTA-RODRIGUEZ *et al*, 2004
Eosinófilos	↓ Produção de IL-5	CORTEGANO *et al*, 1998
Mastócitos	↑ Liberação de mediadores	FRIGERI *et al*, 1993

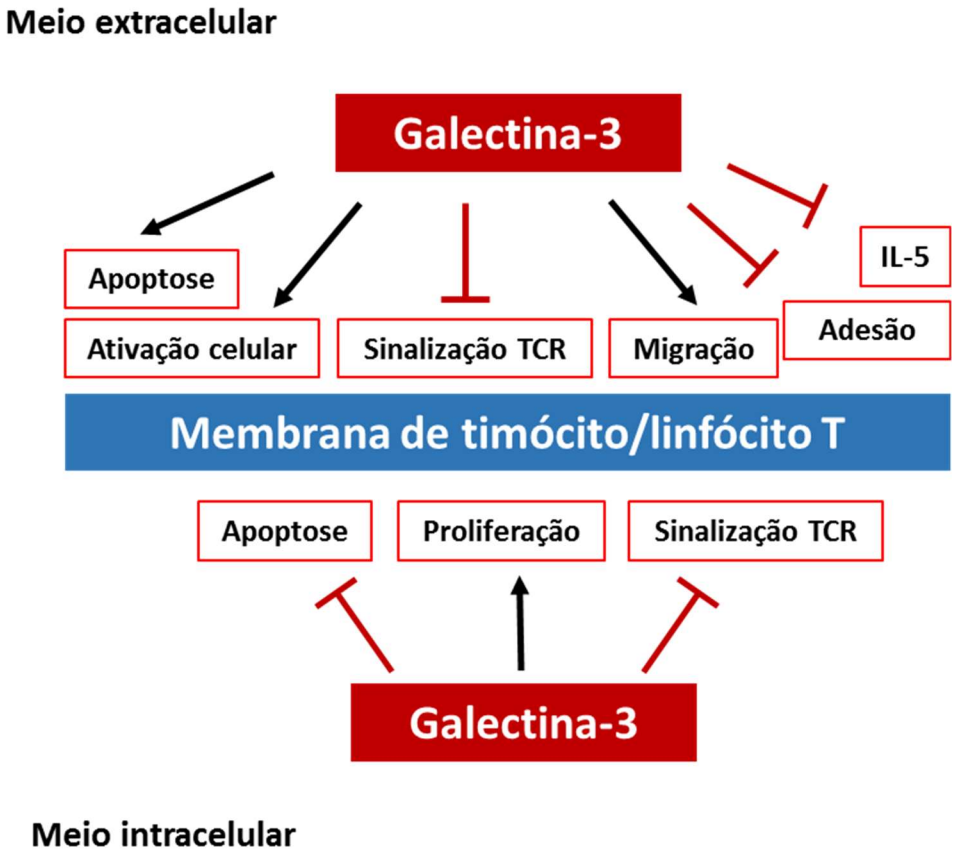

Figura 3. Funções desempenhadas pela Gal-3 em linfócitos T, de acordo com a localização. Funções extracelulares: galectina-3 induz apoptose em linfócitos T, ativação celular e inibição de sinalização do TCR. Promove, ainda, a migração e interfere na adesão de timócitos, e suprime a produção de IL-5. Funções intracelulares: galectina-3 inibe a apoptose, promove o crescimento celular e inibe a sinalização via TCR. Adaptado de HSU *et al*, 2009.

Além disso, foi demonstrado que a Gal-3 é expressa por fibroblastos e está envolvida no processo de fibrogênese. Isto tem sido extensamente descrito em experimentos utilizando camundongos *knockout* para Gal-3, que demonstram a redução na fibrogênese. Em células endoteliais, a presença de Gal-3 estimula a proliferação e angiogênese (WAN *et al*, 2011). O papel proeminente da Gal-3 no estímulo à fibrogênese foi demonstrado em diferentes órgãos, incluindo o coração, fígado, pulmão e rins (MACKINNON *et al*, 2012; HENDERSON *et al*, 2006; KOLATSI-JOANNOU *et al*, 2011).

Diante do exposto, fica claro o envolvimento de Gal-3 em processos de inflamação e reparo tecidual. Após uma lesão tecidual, ocorre a ativação de macrófagos e diferenciação M1. Estes macrófagos então secretam Gal-3, que irá agir em outras células, no compartimento extracelular, levando à ativação e proliferação de células T, ativação de neutrófilos, levando à

"explosão oxidativa", além de mediar interações célula-célula e célula-matriz. Por outro lado, a Gal-3 intracelular terá um papel importante em ações anti-inflamatórias mediadas por macrófagos M2, exercendo também um papel crucial no reparo tecidual, seja estimulando a neovascularização pela sua ação em células progenitoras endoteliais ou formação de cicatriz pelas suas ações em fibroblastos.

1.4.1 A Gal-3 e insuficiência cardíaca

A insuficiência cardíaca é uma síndrome complexa, que envolve numerosos mecanismos fisiopatológicos. O envolvimento da Gal-3 na patogênese da insuficiência cardíaca de diferentes etiologias vem sendo demonstrado nos últimos anos, através de estudos experimentais e clínicos.

Apesar de ser reconhecido o papel da interação entre macrófagos e células secretoras de matriz, como miofibroblastos, em situações de inflamação crônica, os mecanismos moleculares envolvidos ainda são pouco claros. Do ponto de vista experimental, os dados indicam que a Gal-3 possui um papel importante ao estabelecer uma ligação entre ativação de macrófagos e o subsequente estímulo à fibrogênese. A Gal-3 é secretada por macrófagos ativados, para o meio extracelular, ativando outras células como, por exemplo, fibroblastos, estimulando a síntese de matriz extracelular.

A secreção de Gal-3 parece promover aumento da sinalização da via do TGF-β/Smad3, o que resulta no aumento de expressão de α-SMA e colágeno (MACKINNON *et al*, 2011). No entanto, também já foram descritos mecanismos de ativação celular e estímulo à fibrogênese, mediados por Gal-3, que ocorrem independentemente da via do TGF-β (HENDERSON, *et al*, 2006).

Em modelo experimental de insuficiência cardíaca em ratos, a Gal-3 foi encontrada altamente expressa e secretada por macrófagos, associando-se à proliferação de fibroblastos e deposição de colágeno. A infusão de Gal-3 diretamente no saco pericárdico em camundongos causou a infiltração de macrófagos e aumento da fibrose miocárdica, hipertrofia cardíaca, aumento de expressão de TGF-β e disfunção cardíaca (SHARMA *et al*, 2004)

A expressão de Gal-3 é detectada principalmente em macrófagos ativados no miocárdio, e o tratamento de ratos com Gal-3 recombinante induziu a proliferação de fibroblastos cardíacos, a produção de colágeno e a disfunção do ventrículo esquerdo (SHARMA *et al*, 2004). Além disso, a Gal-3 é conhecida por desempenhar um papel importante na resposta inflamatória, incluindo a supressão de apoptose das células T, sendo a sua expressão induzida

pelo IFNγ em macrófagos encontrados no infiltrado inflamatório no coração (REIFENBERG *et al*, 2007). O bloqueio genético e farmacológico de Gal-3 se associou à reduzida deposição de fibrose e disfunção cardíaca em modelo animal de insuficiência cardíaca hipertensiva (YU *et al*, 2013).

Em decorrência dos resultados obtidos em estudos experimentais, a Gal-3 vem sendo estudada através de estudos clínicos. Os níveis de Gal-3 estão aumentados em pacientes com descompensação aguda da ICC, e por isso esta molécula tem sido recentemente apontada como um biomarcador de ICC em pacientes (LOK *et al*, 2010). Através de um estudo de corte transversal, foi inicialmente demonstrado que níveis séricos de Gal-3 acima da mediana (15,3 ng/mL) estavam presentes em indivíduos de idade mais avançada, apresentando insuficiência cardíaca mais grave, segundo a classificação NYHA, além de maiores níveis de creatinina, NT-proBNP e outros marcadores de reconhecida relevância clínica (UELAND *et al*, 2011). O aumento de níveis séricos de Gal-3 também foi observado em pacientes com insuficiência cardíaca com fração de ejeção preservada, correlacionando-se com a gravidade da doença (POLAT *et al*, 2016). Curiosamente, a Gal-3 perde o valor prognóstico e preditor de mortalidade por ICC em indivíduos afro-descendentes (MCEVOY *et al*, 2016).

Um estudo de coorte envolvendo indivíduos que deram entrada no setor de emergência devido à descompensação por ICC foi realizado, visando avaliar se a mensuração dos níveis séricos de Gal-3 poderia colaborar com a estratificação de risco, quando associada ao BNP. Foi observado que indivíduos com Gal-3 apresentavam pior quadro de insuficiência renal, mas não foi observada associação prognóstica (FERMANN *et al*, 2012). Em outro estudo, aproximadamente 600 indivíduos que se apresentaram ao serviço de emergência com descompensação de ICC foram avaliados, demonstrando que a combinação de NTproBNP e Gal-3 era capaz de identificar aqueles que apresentavam maior risco de morte em 30 dias. Em relação ao risco de morte em 60 dias, o nível aumentado de Gal-3 se apresentou como um fator de risco independente (VAN KIMMENADE *et al*, 2006). Além disso, diversos outros estudos demonstraram que níveis de Gal-3 superiores a 17,8 ng/mL se associam a maior risco de re-hospitalização em 30 dias (PEACOCK, 2014).

Tendo por base o achado de que Gal-3 se associa com fibrose miocárdica, hipotetizou-se que esta poderia estar elevada precedendo a sintomatologia clínica de ICC. Realizou-se, então, a mensuração dos níveis séricos de Gal-3 em 3353 participantes da coorte Framingham. Níveis aumentados de Gal-3 se associaram a uma maior incidência de insuficiência cardíaca na comunidade (HO *et al*, 2012). Resultados semelhantes foram observados no estudo de coorte FINRISK, envolvendo 8444 pacientes (JAGODZINSKI *et al*, 2015).

Mais recentemente, realizou-se um estudo envolvendo duas coortes indepententes, em pacientes com ICC de etiologia hipertensiva. Trinta e nove pacientes foram submetidos à biópsia endomiocárdica, durante procedimento de cateterismo cardíaco e as amostras foram avaliadas do ponto de vista histológico e molecular. Observou-se o aumento da expressão de Gal-3 no miocárdio, nos níveis do mRNA e da proteína. Além disso, os níveis de Gal-3 no miocárdio se correlacionaram linearmente com os níveis plasmáticos de Gal-3. No entanto, não se observou associação entre os níveis de Gal-3 no plasma ou miocárdio, com marcadores de fibrose miocárdica, nestes pacientes com ICC de etiologia hipertensiva (LÓPEZ *et al*, 2015). Apesar de ter sido estabelecida uma associação entre Gal-3 e disfunção ventricular em modelos animais, não foi possível se estabelecer uma associação clara entre os níveis circulantes de Gal-3 e a gravidade do remodelamento cardíaco ou da ICC (ABOUEZZEDDINE *et al*, 2015). Conjuntamente, no entanto, os estudos concordam, que os níveis circulantes de Gal-3 estão aumentados em pacientes com ICC e que este achado se correlaciona com um pior prognóstico em termos de mortalidade e reinternação.

1.4.2 A Gal-3 na doença de Chagas

O interesse pelo estudo da Gal-3 na doença de Chagas inicialmente ocorreu devido a lacunas no conhecimento da própria biologia do *T. cruzi*. Tendo em vista que o *T. cruzi* precisa circular pela matriz extracelular antes mesmo que possa penetrar na célula hospedeira, estudos foram realizados de modo a entender melhor como ocorre a interação entre o parasito e moléculas presentes no meio extracelular. Devido ao seu papel em processos de adesão celular e interação com diversas moléculas da matriz extracelular, a Gal-3 era uma candidata importante no processo de migração do *T. cruzi*. Foi demonstrado que a Gal-3 auxilia a ligação de mucina do *T. cruzi* com laminina (MOODY *et al*, 2000). Posteriormente, foi demonstrado que Gal-3, expressa por células musculares lisas, auxilia a entrada do *T. cruzi* na célula, processo que era aumentado após adição de Gal-3 exógena e bloqueado quando era realizado *knockdown* de Gal-3 (KLESHCHENKO *et al*, 2004). Através de análises de transcriptoma, observou-se que o *T. cruzi* altera a expressão de componentes da matriz extracelular, favorecendo a migração e entrada na célula do hospedeiro. Dentre os genes aumentados pela infecção por *T. cruzi*, está o LGALS3 (gene que codifica Gal-3), além de THBS1, LAMC1 e fibronectina (CARDENAS *et al*, 2010). A Gal-3 é também um importante componente de fagossomos e interage com duas proteínas de endossomo tardio e lisossomos: LAMP1 e

LAMP2. Foi demonstrado que a Gal-3 é recrutada pelo *T. cruzi* e participa do processo de escape do vacúolo parasitóforo em macrófagos (REIGNAULT *et al*, 2014).

A infecção por *T. cruzi* também leva ao aumento da expressão de Gal-3 em células B. Nessas células, o aumento de Gal-3 observado após a infecção por *T. cruzi* interfere nas ações de IL-4, inibindo a diferenciação em plasmócitos e produção de imunoglobulinas (ACOSTA-RODRÍGUEZ *et al*, 2004). Após a infecção por *T cruzi*, observou-se também o aumento de expressão de Gal-3 no timo, que se associou a depleção de timócitos em decorrência de morte celular e migração prematura (SILVA-MONTEIRO *et al*, 2007).

Através de análise por microarranjo de DNA, observamos que o gene LGALS3, que codifica a Gal-3, está superexpresso nos corações de camundongos cronicamente infectados por *T. cruzi* (SOARES *et al*, 2011). Esta expressão foi modulada pela terapia com células mononucleares de medula óssea. Utilizando análise por imunofluorescência, demonstramos que Gal-3 é expressa principalmente por células do infiltrado inflamatório no coração de camundongos infectados. A diminuição da expressão de Gal-3 foi também observada após o tratamento com fator de crescimento de colônia de granulócitos (G-CSF) (MIRANDOLA *et al*, 2011, VASCONCELOS *et al*, 2013).

Estes dados levaram o nosso grupo a realizar estudos com o objetivo de avaliar o potencial de Gal-3 como biomarcador na CCC. Foram avaliadas as frequências de polimorfismos no gene LGALS3 em uma amostra de indivíduos com CCC, comparando forma arrítmica e dilatada e buscando uma associação com diferentes variáveis, como percentual de fibrose miocárdica mensurada pela ressonância magnética. Não se observou associação estatística entre nenhum dos SNP avaliados com a gravidade do acometimento cardíaco (CRUZ *et al*, 2015; Anexo IV). Os níveis plasmáticos de Gal-3 também foram avaliados na mesma amostra de pacientes, em um estudo de corte transversal, sendo que também não houve associação com a gravidade da doença (NOYA-RABELO *et al*, no prelo). Houve, no entanto, uma correlação entre os níveis de BNP e a gravidade da doença. Apesar das limitações de um estudo de corte transversal e que, portanto, de não terem sido avaliados desfechos clínicos como mortalidade e número de internações, com foco na determinação de prognóstico, estes dados refutam o valor de Gal-3 como biomarcador na CCC.

No entanto, outros dois trabalhos trouxeram dados que sugerem um papel da Gal-3 na patogênese da miocardiopatia chagásica. Foi demonstrado que a infecção experimental por *T. cruzi* eleva a expressão gênica de colágeno tipo I (Col I), α-SMA, Gal-3, IFN-γ e IL-13 e que, em áreas de fibrose e inflamação no miocárdio, se observa a presença de células com expressão de Col I, Gal-3 e α-SMA (FERRER *et al*, 2014). Mais recentemente, foi demonstrado que

camundongos *knockout* para Gal-3 infectados por *T. cruzi* apresentam níveis de parasitemia elevados e bloqueio na expressão de citocinas e, subsequentemente, infiltrados de células inflamatórias e fibrose reduzidos no coração (PINEDA *et al*, 2015).

1.5 DESENVOLVIMENTO DE TERAPIAS PARA MIOCARDIOPATIA CHAGÁSICA

Tendo em vista que a miocardiopatia chagásica crônica é a maior causa de mortalidade nos indivíduos infectados por *T. cruzi*, novas abordagens são necessárias para desenvolver tratamentos para indivíduos com a forma cardíaca da doença de Chagas. Atenuar ou reverter a miocardiopatia chagásica envolve o desenvolvimento de terapias que atuem sobre a resposta inflamatória sem comprometer a imunidade anti-*T. cruzi*, atenuar fibrose e melhorar a função miocárdica.

1.5.1 Terapias celulares na doença de Chagas

Desde a descoberta do potencial terapêutico das células-tronco, vários estudos pré-clínicos e clínicos foram desenvolvidos visando à recuperação da função de órgãos e tecidos lesados, incluindo o coração.

Nosso grupo de pesquisas foi pioneiro no estudo de terapias celulares para doença de Chagas, tanto no modelo animal (SOARES *et al*, 2004) quanto em estudos clínicos (VILAS-BOAS *et al*, 2006; RIBEIRO-DOS-SANTOS *et al*, 2012). Esses trabalhos iniciais demonstraram que as células mononucleares da medula óssea causaram redução de inflamação e fibrose no coração dos animais na fase crônica da infecção. Posteriormente, observamos que a administração dessas células reduz significativamente as alterações de expressão gênica no coração dos animais crônicos, sobretudo de genes relacionados à inflamação e fibrose (SOARES *et al*, 2011). No entanto, apesar de os estudos iniciais sugerirem efeitos benéficos da terapia em pacientes (VILAS-BOAS *et al*, 2006) o estudo clínico de fase III não demonstrou melhora superior à de pacientes do grupo placebo (RIBEIRO-DOS-SANTOS *et al*, 2012). Desse modo, iniciamos estudos utilizando outros tipos de células-tronco no modelo experimental. Um dos tipos de células-tronco que vem sendo mais investigado em estudos pré-clínicos e clínicos são as células-tronco mesenquimais, descritas a seguir.

1.5.2 Células-tronco mesenquimais

As células-tronco mesenquimais (MSC) são células multipotentes, com potencial para diferenciação em células de origem mesodérmica, como condrócitos, osteócitos e adipócitos (DOMINICI *et al*, 2006). Estas células podem ser obtidas do indivíduo adulto a partir de diferentes órgãos e tecidos, dos quais a medula óssea e o tecido adiposo tem sido os mais amplamente utilizados, devido à facilidade de acesso. As MSC são morfologicamente semelhantes a fibroblastos e possuem elevada capacidade de adesão à superfície plástica (FRIEDENSTEIN *et al*, 1970). Deste modo, as MSC são obtidas a partir da coleta de uma amostra heterogênea de células e purificadas pela sua aderência e pelas condições de cultivo celular.

A caracterização das MSC é realizada através de imunofenotipagem e ensaios funcionais, notadamente a demonstração do potencial para diferenciação condrogênica, osteogênica e adipogênica. A imunofenotipagem é realizada de modo a determinar quantitativamente a frequência de expressão de marcadores característicos de MSC, que devem ser encontrados em níveis elevados, além de negatividade ou baixa frequência de expressão de marcadores de células de origem hematopoiética, que são contaminantes frequentes nestas culturas (DOMINICI *et al*, 2006).

A potencial utilização de MSC para tratar doenças inflamatórias e auto-imunes decorre de sua capacidade de imunomodulação. Dentre as ações imunmodulatórias mais amplamente descritas para MSC na literatura, destacam-se: a supressão da ativação de linfócitos T e B e redução da diferenciação em plasmócitos; inibição da maturação, ativação e apresentação de antígenos em células dendríticas; inibição da ativação de células NK; estímulo à diferenciação em Treg (GAO *et al*, 2016). Estas ações são decorrentes da secreção de fatores parácrinos e de contato celular, por MSC em microambientes inflamatórios, ricos em IFN-γ. Os fatores parácrinos secretados por MSC incluem: TGF-β, PGE2, HGF, IDO (para células humanas), iNOS (para células de camundongo) e IL-10. Alguns trabalhos reportaram o envolvimento de galectinas, incluindo Gal-3, como parte dos fatores associados à imunomodulação mediada por MSC (SIOUD *et al*, 2011; SIOUD *et al*, 2010). Apesar do efeito imunomodulador das MSC ter sido claramente demonstrado, cada vez mais é reconhecido o papel do microambiente na regulação deste potencial. Recentemente, foram descritos dois fenótipos distintos de MSC: MSC1, com ações pró-inflamatórias e MSC2, com ações anti-inflamatórias (WATERMAN *et al*, 2010). Por se tratar de um conceito relativamente recente, os mecanismos e fatores que induzem as MSC a atuarem como imunomoduladoras ou pró-inflamatórias ainda não são totalmente conhecidos.

Nosso grupo realizou estudos envolvendo transplante de células-tronco mesenquimais obtidas do tecido adiposo e do coração, em camundongos cronicamente infectados por *T. cruzi*. Em ambos os casos foi observada a modulação da resposta imune no coração (LAROCCA *et al*, 2013; SILVA *et al*, 2014, Anexo II).

2 JUSTIFICATIVA E HIPÓTESE

A necessidade de desenvolver terapias mais eficazes para indivíduos com CCC depende de um melhor entendimento fisiopatológico dos determinantes da doença, bem como da identificação de novos alvos terapêuticos. Os dados disponíveis na literatura sugerem o envolvimento de Gal-3 na fisiopatologia de doenças que apresentam um componente inflamatório significativo, bem como no processo de remodelamento cardíaco. Tendo em vista que danos imunomediados ao miocárdio e a fibrose cardíaca fazem parte da fisiopatologia da doença de Chagas, a Gal-3 pode representar um novo alvo para o tratamento para a doença, demonstrando a necessidade de investigações mais aprofundadas sobre as ações dessa molécula no contexto da infecção por *T. cruzi*.

Atualmente, há crescente interesse no uso clínico de MSC com finalidades terapêuticas em diferentes doenças, incluindo doenças cardíacas, como a CCC. Levando-se em consideração que a Gal-3 é expressa por MSC e superexpressa no coração após a infecção por *T. cruzi*, faz-se necessário um melhor entendimento sobre o papel desta molécula na biologia das MSC e no contexto da CCC.

Uma vez que a Gal-3 possui diversas funções no organismo e participa da interação parasito-hospedeiro e de processos envolvidos na invasão pelo *T. cruzi* durante a fase aguda da infecção por *T. cruzi*, a avaliação de Gal-3 como alvo terapêutico na CCC deve ser realizada experimentalmente na fase crônica já estabelecida da doença, de modo a não interferir no modelo de CCC. Experimentalmente, isto pode ser realizado através de algumas ferramentas, dentre elas o bloqueio farmacológico, através da administração de moléculas capazes de se ligar à Gal-3 e inibir a sua ação, como é o caso da N-acetil-D-lactosamina, além da utilização da tecnologia de RNAi. O presente estudo visou avaliar o papel da Gal-3 na fisiopatologia da cardiopatia chagásica crônica, através de estudos experimentais *in vitro* e *in vivo*, utilizando esta e outras ferramentas, assim como explorar o potencial papel dessa molécula no tratamento da doença de Chagas e nas propriedades imunomodulatórias das MSC no modelo de CCC.

A hipótese deste trabalho é de que a infecção por *T. cruzi* induz o aumento da expressão de Gal-3 em células envolvidas na resposta imune, no processo de reparo e regeneração tecidual, contribuindo para a inflamação e fibrose no coração.

3 OBJETIVOS

3.1 GERAL:

Investigar o papel da Gal-3 na patogênese e como alvo terapêutico na cardiopatia chagásica crônica

3.2 ESPECÍFICOS:

- Determinar a cinética de expressão de Gal-3 nos corações de camundongos infectados com *T. cruzi*, correlacionando-a com a inflamação e fibrose cardíaca;
- Quantificar a expressão de Gal-3, ao longo da infecção experimental, em células presentes no tecido cardíaco;
- Avaliar a presença e localização de Gal-3 em amostras de corações de pacientes com insuficiência cardíaca de etiologia chagásica;
- Investigar os efeitos da inibição da expressão gênica da Gal-3 em fibroblastos cardíacos de camundongos;
- Investigar as repercussões do bloqueio farmacológico da Gal-3 sobre a função cardíaca, intensidade de miocardite e fibrose, além da expressão gênica diferencial no coração, em modelo experimental de CCC em camundongos;
- Avaliar o efeito do bloqueio da expressão da Gal-3 sobre as propriedades das MSC in vitro;
- Investigar as consequências da inibição da expressão gênica da Gal-3 em MSC in vitro e in vivo, no modelo de CCC em camundongos.

4 RESULTADOS

CAPÍTULO I

Neste capítulo, a associação entre Gal-3, miocardite e fibrose no contexto da CCC foi investigada através de estudos *in vitro*, *in vivo* no modelo de infecção por *T. cruzi* em camundongos e avaliação histológica de amostras de corações humanos obtidas de indivíduos com CCC avançada submetidos a transplante cardíaco.

Artigo submetido à revista *American Journal of Pathology*, sob o código de identificação AJP16-0219.

Association of increased cardiac expression of galectin-3, myocarditis and fibrosis in chronic Chagas disease cardiomyopathy

Bruno Solano de Freitas Souza[*,†], Daniela Nascimento Silva[†], Rejane Hughes Carvalho[†], Gabriela Louise de Almeida Sampaio[†], Bruno Diaz Paredes[†], Luciana Aragão França[†], Carine Machado Azevedo[*,†], Juliana Fraga Vasconcelos[*,†], Cassio Santana Meira[*,†], Paulo Chenaud Neto[†], Simone Garcia Macambira[*,†,‡], Kátia Nunes da Silva[†], Fabio Tavora[§], João David de Souza Neto[§], Ricardo Ribeiro dos Santos[†], and Milena Botelho Pereira Soares[*,†,]

Association of increased cardiac expression of galectin-3, myocarditis and fibrosis in chronic Chagas disease cardiomyopathy

Bruno Solano de Freitas Souza[*,†], Daniela Nascimento Silva[†], Rejane Hughes Carvalho[†], Gabriela Louise de Almeida Sampaio[†], Bruno Diaz Paredes[†], Luciana Aragão França[†], Carine Machado Azevedo[*,†], Juliana Fraga Vasconcelos[*,†], Cassio Santana Meira[*,†], Paulo Chenaud Neto[†], Simone Garcia Macambira[*,†,‡], Kátia Nunes da Silva[†], Fabio Tavora[§], João David de Souza Neto[§], Ricardo Ribeiro dos Santos[†], and Milena Botelho Pereira Soares[*,†,]

[*]Gonçalo Moniz Research Center, FIOCRUZ, Salvador, Bahia, Brazil;
[†]Center for Biotechnology and Cell Therapy, São Rafael Hospital, Salvador, Bahia, Brazil;
[‡]Federal University of Bahia, Salvador, Bahia, Brazil (S.G.M.);
[§]Messejana Hospital, Fortaleza, Ceará, Brazil (F.T., J.D.S.L.).

Number of text pages: 26; number of tables: 01; number of figures: 08.

Short running head: **Role of galectin-3 in Chagas disease**

Sources of funding

This study was supported by funds from National Council for Scientific and Technological Development (CNPq) and Bahia Research Foundation (FAPESB)

Corresponding author: Milena B. P. Soares, Centro de Pesquisas Gonçalo Moniz, Fundação Oswaldo Cruz, Rua Waldemar Falcão, 121, Candeal, Salvador, Bahia, Brazil. CEP: 40296-710. Phone: (55) (71) 3176-2260; Fax: (55) (71) 3176-2272

E-mail address: milena@bahia.fiocruz.br

Abstract

Chronic Chagas disease cardiomyopathy, caused by *Trypanosoma cruzi* infection, is a major cause of heart failure in Latin America. Galectin-3 has been linked to cardiac remodeling and poor prognosis in heart failure of different etiologies. Here we investigated the involvement of galectin-3 in the disease pathogenesis and its role as a target for disease intervention. Galectin-3 expression in mouse hearts was evaluated during *T. cruzi* infection by confocal microscopy and flow cytometry analysis, showing a high expression in macrophages, T cells and fibroblasts. *In vitro* studies using a galectin-3 knockdown with shRNA in cardiac fibroblasts demonstrated that galectin-3 regulates cell survival, proliferation and type I collagen synthesis. *In vivo* blockade of galectin-3 with N-acetyl-D-lactosamine in *T. cruzi*-infected mice led to a remarkable reduction of cardiac fibrosis and migration of inflammatory cells to the heart. Moreover, a modulation in the expression of pro-inflammatory genes in the heart was observed. Finally, histological analysis in human heart samples obtained from subjects with Chagas disease that underwent heart transplantation showed the expression of Gal-3 in areas of inflammation, similar to the pattern observed in the mouse model. Our results demonstrate that galectin-3 plays an important role in the pathogenesis of experimental chronic Chagas disease, favoring inflammation and fibrogenesis. Moreover, the finding of galectin-3 expression in human hearts reinforces this protein as a novel target for drug and therapy development for Chagas cardiomyopathy.

Keywords: galectin-3; Chagas' disease cardiomyopathy; *Trypanosoma cruzi;* fibrosis; myocarditis

Introduction

Chronic Chagas disease cardiomyopathy (CCC), caused by *Trypanosoma cruzi* infection, is an important cause of morbidity and mortality in endemic countries. It is estimated that approximately 7 million people are infected worldwide, with high prevalence in Latin America and growing incidence in developed countries due to globalization.[1,2] It is estimated that the cardiac form of the disease occurs in approximately 20-30% of infected subjects.[2] Antiparasitic drugs are effective during acute infection, but fail to improve established CCC.[3,4] Besides standard heart failure treatment, patients with advanced CCC rely on heart transplantation, which is limited by organ availability and complications relative to parasite reactivation after immunosuppression.[5]

During CCC, cardiomyocytes are lost as a result of damage caused by immune responses directed to the parasites that persist in the heart, as well as to autoreactive cells directed to heart antigens.[6,7] Although the mechanisms of pathogenesis are not completely understood, several studies indicate the involvement of Th1 lymphocytes associated with high production of interferon-γ (IFN-γ), resembling a delayed hypersensitivity reaction.[6] An association between progression to severe chronic forms and a high production of IFN-γ was observed in patients with Chagas disease.[8] Macrophages, a major cell population found in the inflammatory sites, can be activated by IFN-γ and TNF-α, two inflammatory cytokines overexpressed in the hearts of mice chronically infected with *T. cruzi*. Furthermore, several genes related to the inflammatory response are upregulated in the heart tissue during the chronic phase of *T. cruzi* infection.[9]

Previous studies suggested that activated macrophages secrete galectin-3 (Gal-3), a molecule involved in the pathogenesis of cardiac dysfunction.[10] Gal-3 is a soluble beta-galactoside binding lectin involved in a variety of cellular processes, including proliferation, migration and apoptosis.[11] The importance of this protein in the regulation of cardiac fibrosis and remodeling has been highlighted by the demonstration of its contribution to the development and progression of heart failure in different experimental settings.[12-14] Serum Gal-3 concentrations are also increased in patients with acute decompensated heart failure. Based on these findings, the value of Gal-3 as a prognostic biomarker in patients with chronic heart failure has been investigated.[15]

Previously, we performed transcriptomic analysis in the cardiac tissue of mice chronically infected with *T. cruzi*, and found that LGALS3, the gene encoding for Gal-3, is amongst the most overexpressed genes.[16] By immunofluorescence analysis, we showed that Gal-3 is mainly expressed in inflammatory cells in the hearts of *T. cruzi*-infected mice. We

hypothesized that Gal-3 plays a role in the pathogenesis of CCC, contributing to the progression of inflammation and fibrosis. In the present study, we evaluated the expression of Gal-3 during *T. cruzi* infection in mice. Gal-3 expression was also investigated in human heart samples, in order to validate the expression of this protein in the human disease setting. Finally, we conducted *in vitro* and *in vivo* studies involving genetic and pharmacological blockages of Gal-3 in order to investigate its potential role in the pathogenesis of the disease and its usefulness as a target for therapeutic development.

Materials and methods

Animal procedures

Six-to-eight week-old female C57BL/6 mice were used for *T. cruzi* infection and as normal controls. All animals were raised and maintained at the animal facility of the Center for Biotechnology and Cell Therapy, Hospital São Rafael, in rooms with controlled temperature (22 ± 2º C) and humidity (55 ± 10%), and continuous air flow. Animals were housed in a 12 h light/12 h dark cycle (6 am - 6 pm) and provided with rodent diet and water *ad libitum*. Animals were handled according to the NIH guidelines for animal experimentation. All procedures described had prior approval from the local institutional animal ethics committee at Hospital São Rafael (01/13).

Trypanosoma cruzi infection

Trypomastigotes of the myotropic Colombian *T. cruzi* strain were obtained from culture supernatants of infected LLC-MK2 cells, as previously described.[9] Infection of C57BL/6 mice was performed by intraperitoneal injection of 1000 *T. cruzi* trypomastigotes in saline, and was confirmed through evaluation of parasitemia at different time points after infection.

Pharmacological blockade of Gal-3 with N-Lac

C57Bl/6 female mice (n=11) chronically infected with *T. cruzi* (6 m.p.i.) were treated with N-acetyl-D-Lactosamine (N-Lac) (Sigma-Aldrich; 5 mg/kg per day, i.p. injections) 3x a week, for 60 days. Chronically infected mice injected with saline (n=10) and same age naïve mice (n=8) served as controls. Functional analyses were performed, as described bellow. Mice were euthanized, by cervical dislocation under anesthesia with 5% ketamine (Vetanarcol®; Konig) and 2% xylazine (Sedomin®; Konig), the week following the last N-Lac injection. Heart samples were collected for qPCR and histology analysis.

Functional analyses

Electrocardiography was performed using the Bio Amp PowerLab System (PowerLab 2/20; ADInstruments), recording the bipolar lead I. All animals were anesthetized by intraperitoneal injection of xylazine at 10 mg/kg body weight and ketamine at 100 mg/kg body weight to obtain the records. All data were acquired for computer analysis using Chart 5 for Windows (PowerLab). The ECG analysis included heart rate, PR interval, P wave duration, QT interval, QTc and arrhythmias. The QTc was calculated as the ratio of QT interval by square roots of RR interval.

A motor-driven treadmill chamber for one animal (LE 8700; Panlab) was used to exercise the animals. The speed of the treadmill and the intensity of the shock (mA) were controlled by a potentiometer (LE 8700 treadmill control; Panlab). After an adaptation period in the treadmill chamber, the mice exercised at 5 different velocities (7.2, 14.4, 21.6, 28.8 and 36.0 m/min), with increasing velocity after 5 min of exercise at a given speed. Velocity was increased until the animal could no longer sustain a given speed and remained > 5 s on an electrified stainless-steel grid. Total running distance was recorded.

Morphometric analyses

Two months after the therapy mice were euthanized as mentioned before and hearts were collected and fixed in 10% buffered formalin. Heart sections were analyzed by light microscopy after paraffin embedding, followed by standard hematoxylin and eosin (H&E) staining. Inflammatory cells infiltrating heart tissue were counted using a digital morphometric evaluation system. Images were digitized using the slide scanner Scan Scope (Leica). Morphometric analyses were performed using the software Image Pro Plus v.7.0 (Media Cybernetics). The inflammatory cells were counted in 10 fields (400x magnification) per heart. The percentage of fibrosis was determined using Sirius red-stained heart sections and the Image Pro Plus v.7.0. Two blinded investigators performed the analyses.

Immunofluorescence analyses

Frozen (10 μm) or formalin-fixed paraffin embedded (3 μm) hearts sections were obtained. Paraffin embedded tissues were deparaffinized and submitted to a heat-induced antigen retrieval step by incubation in citrate buffer (pH=6.0). Then, sections were incubated overnight at 4ºC with the following primary antibodies: anti-Gal-3, diluted 1:400 (Santa Cruz Biotechnology) and anti-CD11b, diluted 1:400 (BD Biosciences). Next the sections were

incubated for 1 h with secondary antibodies anti-goat IgG Alexa fluor 488-conjugated and anti-rat IgG Alexa fluor 594-conjugated (1:400, Thermo Scientific). Immunostainings for *in vitro* experiments were performed in cardiac fibroblasts or bone marrow-derived macrophages plated on coverslips. The cells were fixed with paraformaldehyde 4% and incubated with the primary antibodies: goat anti-Gal-3, diluted 1:400 (Santa Cruz Biotechnology) or rabbit anti-collagen type I, diluted 1:50 (Novotec). On the following day, sections were incubated for 1 h with Phalloidin conjugated with Alexa fluor 633 or 488 conjugated, diluted 1:50, mixed with the secondary antibodies anti-goat IgG Alexa fluor 488-conjugated (1:400) or anti-rabbit IgG Alexa fluor 568-conjugated (1:200; all from Thermo Scientific) respectively. Nuclei were stained with 4,6-diamidino-2-phenylindole (VectaShield mounting medium with DAPI H-1200; Vector Laboratories). The presence of fluorescent cells was determined by observation on a FluoView 1000 confocal microscope (Olympus) and A1+ confocal microscope (Nikon). Quantifications of Gal-3^+ cells were performed in 10 random fields captured under 400x magnification, using the Image Pro Plus v.7.0 software (Media Cybernetics).

Flow cytometry analysis

Control and *T. cruzi*-infected mice were euthanized, hearts were collected, perfused with PBS to remove blood cells, and processed by enzymatic digestion using 0.1 % collagenase IV (Sigma) and 10 µg/ml DNAse (Roche), for 40 min, at 37°C. To evaluate the subpopulations of digested cardiac tissue samples, cell suspensions were allowed to pass through a 70 µm cell strainer (BD Biosciences) and counted. Aliquots of 10^6 cells were used for each test tube and 1 µL of Fc blocking reagent (BD Biosciences) was added. The fluorochrome-conjugated antibody panels used for each subpopulation were: a) T lymphocytes - CD45-APC-Cy7, CD3-APC, CD4-PE-Cy5, CD8-PE (BD Biosciences); b) Macrophages - CD45-APC-Cy7, CD11b-APC (eBiociences); c) Fibroblast/Fibrocyte - CD45-APC-Cy7, Vimentin-APC (Cell Signaling). Each antibody was diluted as suggested on the product datasheet. Samples were incubated for 20 minutes at RT in the dark. For intracellular staining of Gal-3, samples were washed once in PBS and CytoFix/CytoPerm kit (BD Biosciences) was used as directed on datasheet protocol. Anti-Gal-3-PE (R&D Systems) antibody was added to Macrophages and Fibroblast/Fibrocyte sample tubes, while non-conjugated anti-Gal-3 (Santa Cruz Biotechnology) was added on T lymphocytes sample tube and its detection was performed by addition of anti-mouse IgG-Alexa Fluor 488 (Thermo Scientific). Each incubation step was performed during 30 minutes at RT in the dark. Samples were washed twice and resuspended in PBS and added with Hoecsht 33258

to exclude cell debris from analysis. Apoptosis was evaluated by Annexin V-PI assay. Cells were harvested from culture flasks by adding TrypLE solution (Thermo Scientific) and incubating for 5 minutes at 37^{o}C. Cell suspensions were collected and washed with PBS by centrifugation at 300 g. After discarding supernatant, pellets were resuspended in Binding buffer (Thermo Scientific) and cells were counted. Apoptosis assays were performed using Annexin-V-APC and PI (BD Biosciences) according to the manufacturer's recomendations. Sample acquisition was performed using a BD LSRFortessa SORP cytometer using BD FacsDiva v.6.2. Ten thousand events were acquired per sample, and the data were analyzed using FlowJo v7.5 (FlowJo Interprise).

Real time reverse transcription polymerase chain reaction (RT-qPCR)

Total RNA was isolated from heart samples with TRIzol reagent (Thermo Scientific) and the concentration was determined by spectrophotometry. High Capacity cDNA Reverse Transcription Kit (Thermo Scientific) was used to synthesize cDNA of 1 μg RNA following manufacturer's recommendations. RT-qPCR assays were performed to detect the expression levels of *Tbet (*Mm_00450960_m1), *GATA3 (*Mm_00484683_m1), TNF (Mm_00443258_m1), IFNg (Mm_00801778_m1), IL10 (Mm_00439616_m1), FOXP3 (Mm_00475162_m1), LGALS3 (Mm_00802901_m1), MMP9 (Mm_00444299_m1). . Other primer sequences used in Real Time PCR analyses: COL1A1: 5'-GTCCCTCGACTCCTACATCTTCTGA-3' and 5'-AAACCCGAGGTATGCTTGATCTGTA'; CCND1: 5' TCCGCAAGCATGCACAGA 3' and 5' GGTGGGTTGGAAATGAACTTCA 3'. The RT-qPCR amplification mixtures contained 20 ηg template cDNA, Taqman Master Mix (10 μL) and probes in a final volume of 20 μL (all from Thermo Scientific). All reactions were run in duplicate on an ABI7500 Sequence Detection System (Thermo Scientific) under standard thermal cycling conditions. The mean Ct (cycle threshold) values from duplicate measurements were used to calculate expression of the target gene, with normalization to an internal control (*GAPDH*) using the 2–DCt formula. Experiments with coefficients of variation greater than 5% were excluded. A non-template control and non-reverse transcription controls were also included.

Design of shRNAs and production of lentiviral vectors

To stably knockdown LGALS3 expression, we designed shRNA against different regions of the LGALS3 coding sequence, and a scramble shRNA as control. Target sequences were designed with the help of the online tool siRNA Wizard v3.1 (Invivogen). All suggested sequences were

blasted against the mouse RNA reference sequence database, and the three with the lowest degree of homology to other sequences were chose: Lgals3_shRNA1 5' - GATTTCAGGAGAGGGAATGAT - 3'; Lgals3_shRNA2 5' - GGTCAACGATGCTCACCTACT - 3'; Lgals3_shRNA3 5' - CATGCTGATCACAATCATGG - 3', and one Lgals3_scrbl_shRNA 5' - AGGTATGAGTCGAGATTGAGA - 3'. Sense and anti-sense single strands, containing the target sequence, a loop sequence (TCAAGAG) and restriction enzyme sites for Mlu at the sense sequence and ClaI at the antisense sequence, were synthesized separately. Annealing of both strands to form double-stranded shRNAs was performed by incubating 2.5 µmol/L of the sense and anti-sense strand of each shRNA in 10 mmol/L Tris-HCl (pH 7.5), 0.1 M NaCl and 1 mM EDTA at 95°C for 5 min and then letting the reaction cool down to room temperature for at least 2 h. The double-stranded shRNAs were then phosphorylated using T4 PNK (New England Biolabs) following manufacturer protocol. The shRNAs were cloned into the pLVTHM lentiviral vector (a gift from Didier Trono, Addgene plasmid # 12247), specifically designed for gene knockdown with shRNAs[17], after the vector was linearized by digestion with MluI and ClaI (New England Biolabs) according to manufacturer instructions. Each of the produced shRNAs constructs were confirmed by sequencing using ABI 3500 platform (Thermo Scientific). For lentiviral vector production, HEK293 FT cells were co-transfected with each of the shRNA constructs, plus psPAX2 (Addgene plasmid # 12260) and pMD2.G (Addgene plasmid # 12247) for production of the lentivirus particles, in a proportion of 3:2:1. Viral supernatants were harvested 48 and 72 h later, pooled, centrifuged to remove cell debris, filtered through 0.45-µm filters (Millipore), and concentrated by ultracentrifugation. Cardiac fibroblasts were transduced with the lentivirus by overnight incubation in medium containing lentiviral particles and polybrene (6 µg/ml). Knockdown efficiency for each shRNA was evaluated by qPCR using TaqMan probes for LGALS3 (mm00802901_m1), GAPDH (mm99999915_g1), ACTB (mm00607939_s1) and HPRT (mm00496968_m1) and TaqMan Universal PCR master mix (Thermo Scientific), according to the manufacturer's instructions. Assay was performed in triplicate, and the empty vector was used as control. Cycle threshold (Ct) for LGALS3 was normalized taking into account the geometric mean of the Ct for GAPDH, ACTB and HPRT (ΔCt). The relative expression was then calculated by the normalized Ct between each LGALS3 shRNA construct and the empty vector (ΔΔCt).

In vitro studies with cardiac fibroblasts and bone marrow-derived macrophages

Cardiac fibroblasts were isolated from hearts of adult C57Bl/6 mice, euthanized as described above. Hearts were minced into pieces of 1 mm and incubated with 0.1% collagenase type A (Sigma-Aldrich) at 37°C for 30 min, under constant stirring. The cell suspension was passed through a 70 μm cell strainer (BD Biosciences), and plastic-adherent cells were selected by 1 h incubation in gelatin-coated flasks (Sigma-Aldrich). Non-adherent cells from supernatant were removed and adherent cells were cultured with DMEM supplemented with 10% FBS and 1% penicillin and streptomycin (all from Thermo Scientific), in a humidified incubator at 37°C with 5% CO_2. Culture medium was changed every 3 days, and cells were trypsinized (Trypsin-EDTA 0.05%; Thermo Scientific) when 80% confluence was reached. Cell cycle studies were performed with CFSE Cell Proliferation Kit (Thermo Scientific), according to the manufacturer's instructions. Proliferation of cardiac fibroblasts was measured by the measurement of ^{3}H-thymidine uptake. Cells were plated in 96-well plates, at a density of 10^4 cells/well, in a final volume of 200 μL, in triplicate, and cultured in the absence or presence of 30 μg/mL rmGal-3 (R&D Systems), with or without 1% modified citrus pectin (MCP; ecoNugenics). After 24 h, plates were pulsed with 1 μCi of methyl-^{3}H thymidine (PerkinElmer) for 18 h, and proliferation was assessed by measurement of ^{3}H-thymidine uptake by using a Chameleon β-plate counter (Hydex). Comparison of proliferation capacity of Gal-3 knockdown and control cell lines was also done by ^{3}H-thymidine incorporation.

To obtain macrophages, bone marrow cells were harvested from femurs of C57BL/6 mice by flushing with cold RPMI medium. Bone marrow cells were induced to differentiate into macrophages by culture in RPMI 1640 supplemented with 10% FBS (Thermo Scientific), 50 units/mL of penicillin, 50 μg/mL of streptomycin, 2.0 g/L of sodium bicarbonate, 25 mM HEPES, 2 mM glutamine and 30% supernatant obtained from X63-GM-CSF[18] cell line culture, at 37 °C and 5% CO_2. Cells were cultured for 7 days, with half medium changes every 3 days. Differentiated macrophages were plated onto 24-well plates and incubated in medium alone or with 1 μg/ml LPS (Sigma-Aldrich) with or without 50 ng/ml IFN-γ (R&D Systems). After 24 h, macrophages were detached using a cell scraper and analyzed for Gal-3 expression by flow cytometry, as described above.

Human samples

The procedures involving human samples received prior approval by the local Ethics committee at Hospital São Rafael (approval number 51025115.3.0000.0048). Samples were obtained at Messejana Hospital in Fortaleza, Ceará, a specialized medical center for heart transplantation in Brazil. Fragments of explanted hearts from three patients with Chagas disease, confirmed by serological assay, were obtained from left ventricle and septum. Samples were included in paraffin and stained with H&E and Sirius Red, or used for immunostaining for detection of Gal-3, as described above.

Lymphoproliferation assay

C57BL/6 splenocyte suspensions were prepared in DMEM medium supplemented with 10 % of FBS and 50 µg/mL of gentamycin. Splenocytes were cultured in 96-well plates at 1 x 10^6 cells/well, in triplicate, and lymphocyte proliferation was stimulated or not with concanavalin A (Con A; 2 µg/mL, Sigma-Aldrich) or Dynabeads® mouse T-activator CD3/CD28 (Gibco, Grand Island, NY) according to the manufacturer's instructions. Cell proliferation was induced in the absence or presence of various concentrations of N-Lac (10, 1 and 0.1 µM). After 48 h of incubation, 1 µCi of ^{3}H- thymidine was added to each well, and the plate was incubated for 18 h. Plates were frozen at -70 ºC and thawed and transferred to UniFilter-96 GF/B PEI coated plates (PerkinElmer, Waltham, MA) with assistance of a cell harvester. After drying, 50 mL of scintillation cocktail was added in each well, sealed and plate read at liquid scintillation microplate counter. Dexamethasone (10 µM) was used as positive control. Three independent experiments were performed.

Inhibition of cell migration assay

C57BL/6 mice, 8-12 week-old, were submitted to euthanasia by cervical dislocation under anesthesia. Spleens were collected, minced, cells were resuspended in PBS and passed through a 70 µm cell strainer. The cells were resuspendend and maintained RPMI 1640 medium (Gibco), without serum, supplemented with 2 mM L-glutamine (Gibco), 0,1% RMPI vitamin solution (Sigma Aldrich), 1 mM sodium pyruvate, 10 mM Hepes, 50 µM 2-mercaptoetanol and penicillin/streptomycin solution (all from Gibco). Splenocytes were incubated for for starvation during 24 h at 37ºC and 5% CO_2, in the presence or absence of 10 µM N-Lac. Migration assay was performed using the QCM Chemotaxis Cell Migration Assay, 24-well 3µm pore

(Millipore), according to the manufacturer's instructions. Briefly, splenocytes were counted and 10^7 cells in 250 μL were placed in the upper chamber, in serum-free medium, in the presence or absence of N-Lac. RPMI medium supplemented with 10% FBS (Gibco) with or without 10 μM N-Lac was placed in the bottom chamber. Cells present in the bottom chamber were counted after overnight incubation.

Statistical analyses

All continuous variables are presented as means ± SEM. Continuous variables were tested for normal distribution using Kolmogorov–Smirnov test. Parametric data were analyzed using unpaired *t* tests, for comparisons between two groups, and 1-way ANOVA, followed by Bonferroni post hoc test for multiple-comparison test, using Prism 6.0 (GraphPad Software). Values of $P < 0.05$ were considered statistically significant.

Results

Gal-3 expression is increased during experimental *T. cruzi* infection

We first analyzed the expression of Gal-3 in mouse heart sections obtained at different time points of infection. *T. cruzi* infection led to the expression of Gal-3^+ cells in the myocardium, as shown by confocal microscopy (Figures 1A-B). Quantification of Gal-3 expression showed a significant increase in all time points analyzed, in comparison with uninfected controls (Fig. 1E). The number of Gal-3^+ cells was higher at the peak of parasitemia (1 m.p.i.), when an intense acute inflammatory response is found in the heart (Figure 1F). The numbers of Gal-3^+ cells during the chronic phase were sustained, while the percentage of fibrosis increased with time (Figure 1G). The population of Gal-3^+ cells in the heart included macrophages (CD11b$^+$ cells; Figure 1C) and cardiac fibroblasts (Figure 1D). To investigate the role of pro-inflammatory signals in the expression of Gal-3 by macrophages, we performed *in vitro* studies to analyze the expression of Gal-3 in activated macrophages. Bone marrow-derived macrophages activated with IFN-γ and TLR4 ligand LPS had an increased expression of Gal-3, as demonstrated by flow cytometry analysis (Figure 1H).

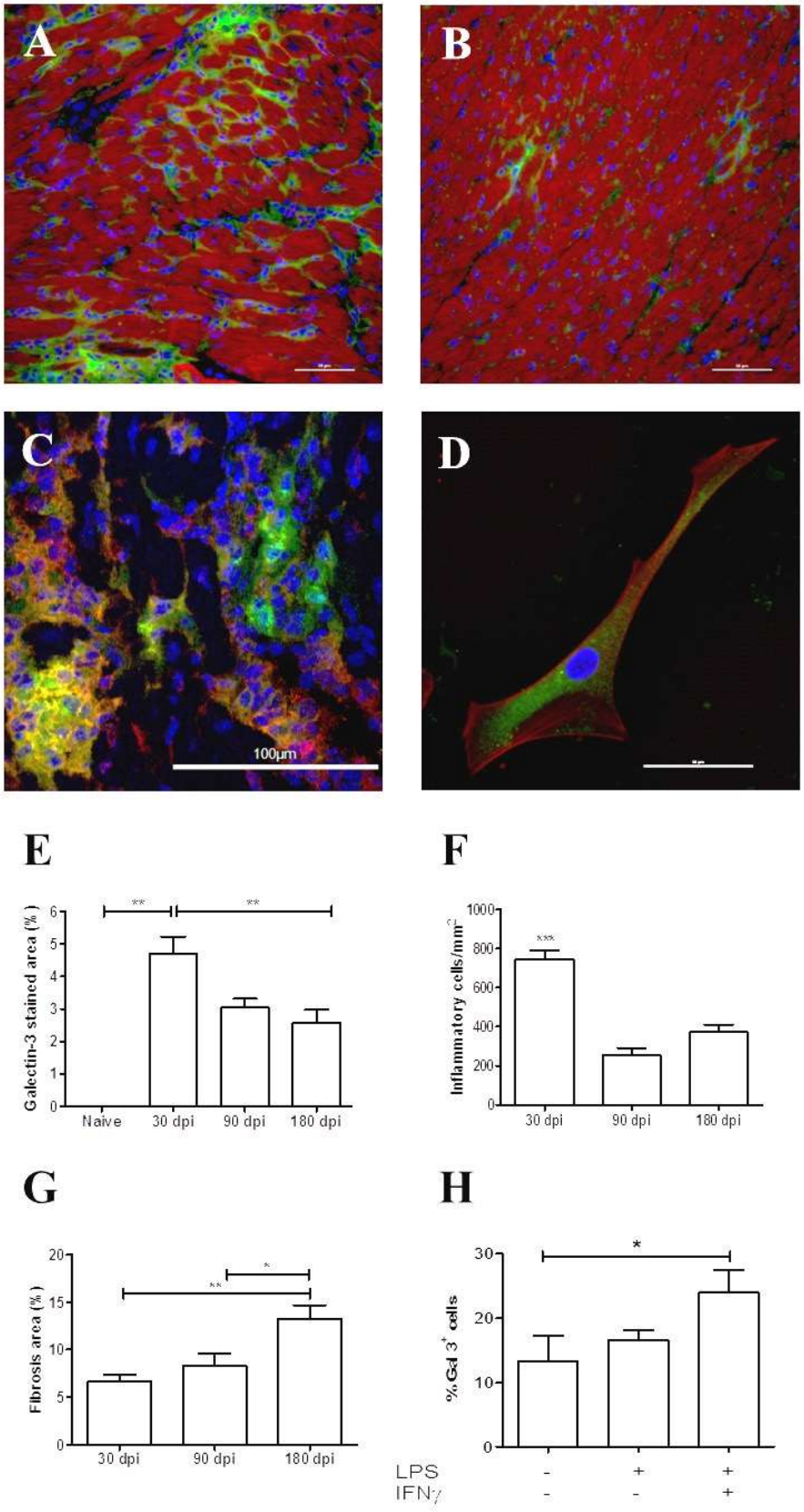

Figure 1. Gal-3 is overexpressed in mouse hearts after *T. cruzi* infection. Confocal microscopy analysis demonstrated the presence of Gal-3^{+} cells (green), mainly in areas of inflammatory infiltrates, at 1 (**A**) and 6 (**B**) months post-infection (m.p.i.). Cardiac muscle was stained for

actin-F (red) and nuclei were stained with DAPI (blue). (**C**) Most cells expressing Gal-3 (green) co-expressed the monocyte/macrophage marker CD11b (red). (**D**) Cardiac fibroblasts isolated by enzymatic digestion of heart tissue also expressed Gal-3 (green). Actin-F is seen in red, and nucleus in blue. (**E**) The cardiac expression of Gal-3 peaked at 1 m.p.i., but remained elevated during the chronic phase of infection, when compared to naïve mice. (**F**) A similar pattern is observed for the number of inflammatory cells infiltrating the heart, while the percentage of fibrosis increased with time (**G**). Bone marrow-derived macrophages stimulated *in vitro* with pro-inflammatory (M1) inductors IFN-γ and LPS increased the expression of Gal-3 (**H**). * $P<0.05$; ** $P<0.01$; *** $P<0.001$.

To better characterize the cell populations expressing Gal-3, we performed flow cytometry analysis of cells isolated from hearts of *T. cruzi*-infected mice (Fig. 2). Both CD4+ and CD8+ T cell had increased Gal-3 expression at 3 and 15 m.p.i when compared to uninfected controls. Additionally, macrophages, characterized as $CD45^{+}/CD11b^{+,}$ composed the cell populations expressing the highest mean fluorescence intensity of Gal-3 (Figure 2). Gal-3 was expressed at low levels in fibroblasts ($vimentin^{+}/CD45^{-}$) in control hearts, and was increased by 52.5% at 3 m.p.i. Interestingly, Gal-3 intensity of expression in fibroblasts at 15 m.p.i. returned to levels similar to those found in controls. However, a major increase in Gal-3 expression was detected in a population of $vimentin^{+}/CD45^{+}$ cells, characterized as bone-marrow derived fibrocytes, at 3 and 15 m.p.i. when compared to controls (Figure 2).

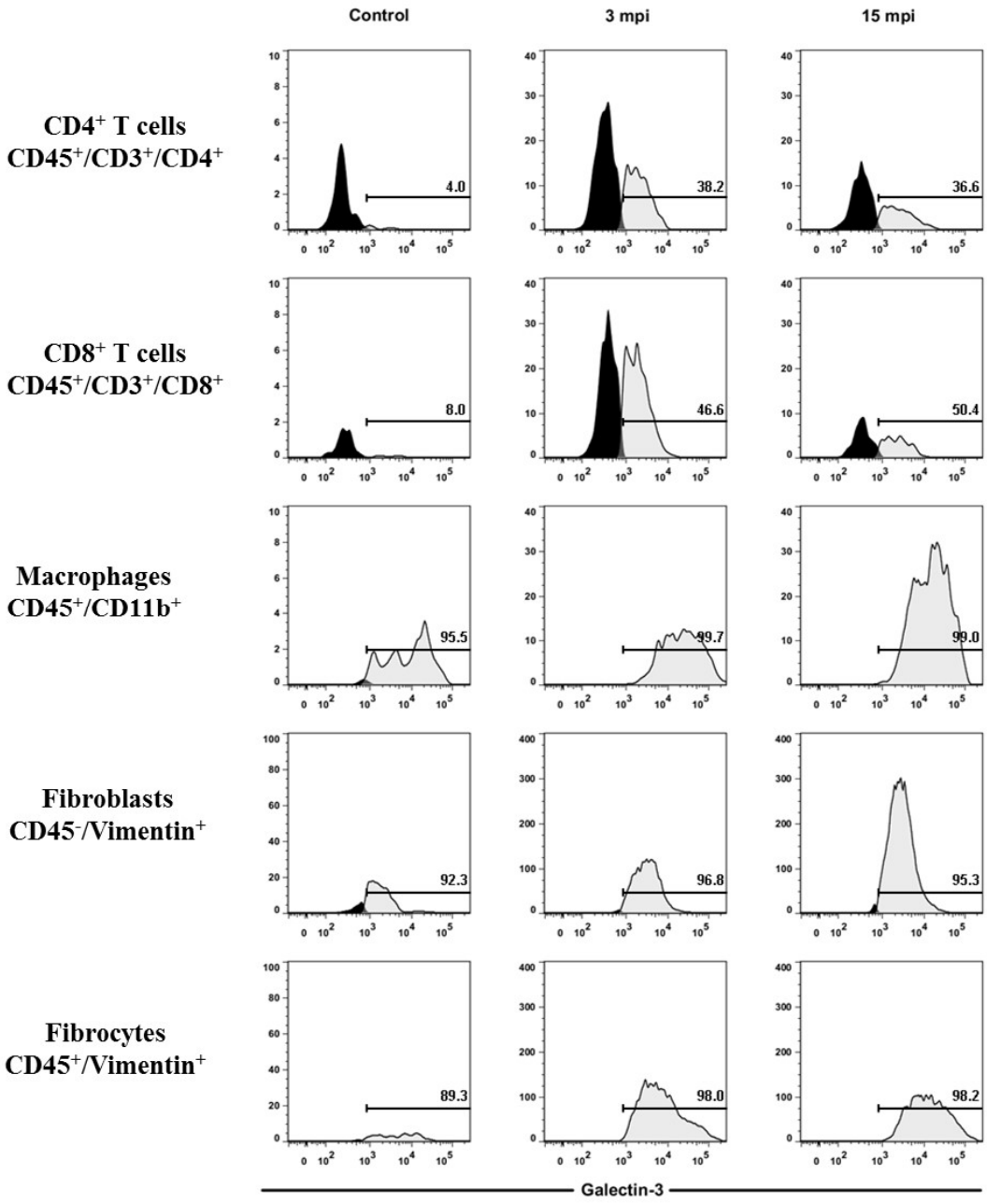

Figure 2. Gal-3 is increased in different cell types involved in inflammation and tissue repair. Histograms showing flow cytometry analysis from digested heart tissue, obtained from naïve and infected mice, at 3 and 15 m.p.i. Gal-3$^+$ T CD4$^+$ and CD8$^+$ lymphocytes expressing Gal-3 are increased in 3 and 15 m.p.i. when compared to naïve controls. The majority of macrophages (CD45$^+$/CD11b$^+$), fibroblasts (CD45$^-$/vimentin$^+$) and bone marrow-derived fibrocytes (CD45$^+$vimentin$^+$) express Gal-3 (>90%) in all groups, but the mean fluorescence intensity is increased with time of infection.

Expression of Gal-3 in the hearts of subjects with CCC

In order to evaluate if the presence of Gal-3^{+} cells in the myocardium of infected mice could be translatable to the human disease, we performed analysis in human heart samples obtained from explants of subjects with chronic Chagas disease cardiomyopathy that underwent heart transplantation. Heart sections were prepared and stained with H&E for histological analysis, demonstrating the presence of foci of myocarditis, with an inflammatory infiltrate composed mainly of mononuclear cells, leading to the destruction of myofibers (Figures 3A and B). Additionally, an extensive area of diffuse fibrotic scar was found in Sirius red stained sections (Figures 3C and D). The expression of Gal-3 in human heart samples was evaluated by analysis using confocal microscopy. We observed the presence of cells, within the inflammatory foci and surrounding the myofibers, expressing variable levels of Gal-3 (Figures 3E and F).

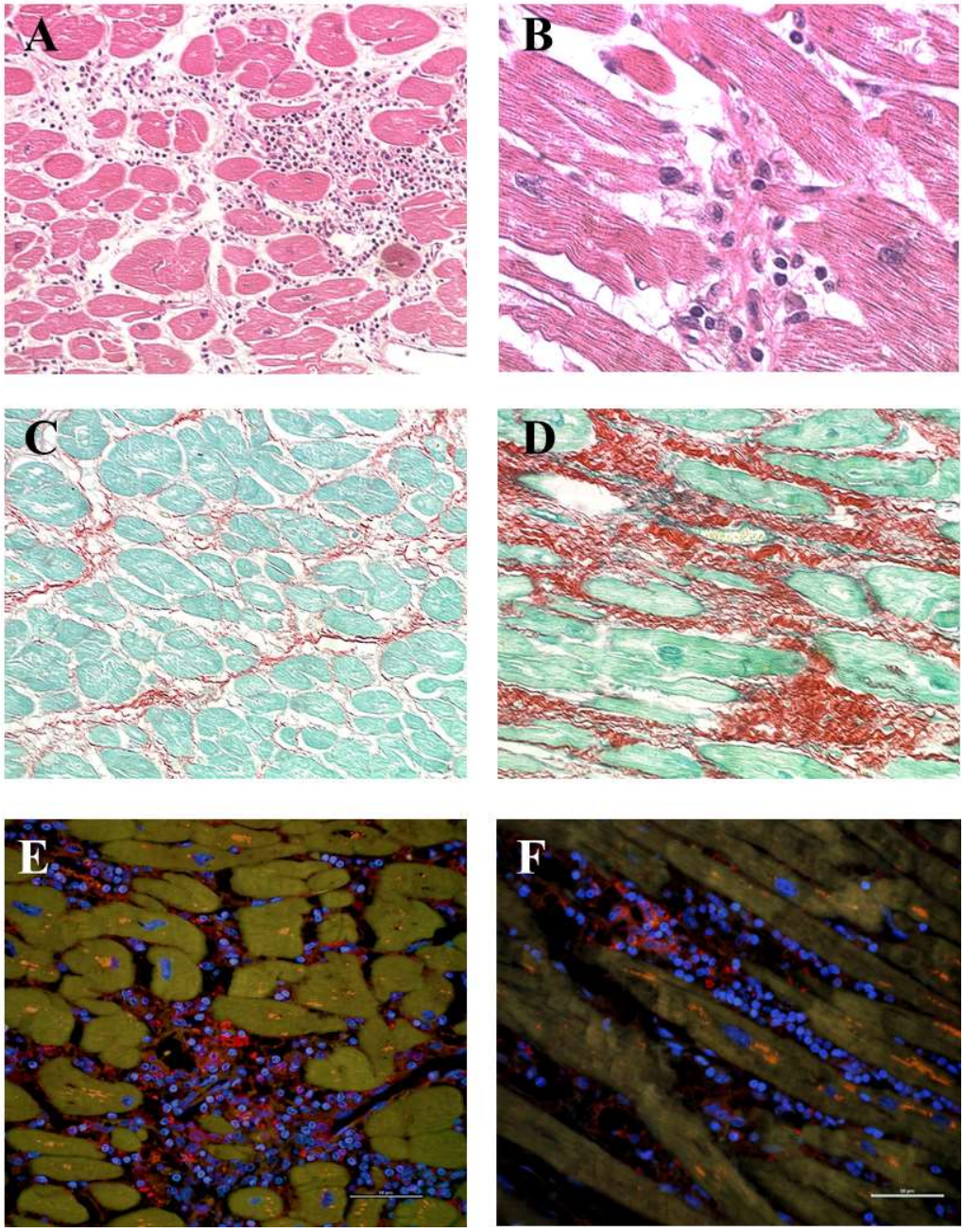

Figure 3. Gal-3 expression in heart samples from subjects with end-stage Chagas cardiomyopathy. Representative images obtained from explanted heart sections of two subjects with end-stage Chagas cardiomyopathy that underwent heart transplantation. Heart sections were stained with H&E, showing inflammatory infiltrates composed of mononuclear cells surrounding myofibers (**A**, 100x magnification); and in areas of myocytolysis (**B**, 400x magnification). Heart sections stained with Sirius red showing areas of mild (**C**) and extensive (**D**) cardiac fibrosis. (**E-F**) Confocal microscopy analysis, showing Gal-3^{+} cells (red) in areas of inflammatory infiltrates. Nuclei are stained with DAPI (blue).

Gal-3 is a major regulator of fibroblast function

Based on the findings of increased Gal-3 expression in fibroblasts during the development of CCC, we performed *in vitro* studies aiming to investigate the role of Gal-3 on different aspects of the biology of these cells. Cardiac fibroblasts isolated from mouse hearts were incubated with mouse recombinant Gal-3 to evaluate their proliferative rate. We found that exogenous recombinant Gal-3, at a micromolar concentration, increased the proliferation of cardiac fibroblasts, whereas addition of modified citrus pectin (MCP), a binding partner of Gal-3, blocked the effect of Gal-3 (Figure 5A).

Considering that this effect was observed at high concentrations of exogenous Gal-3, and given the high expression of intracellular Gal-3 in cardiac fibroblasts in experimental CCC, we sought to evaluate the role of endogenous Gal-3 in cardiac fibroblasts. For this purpose, we generated lentiviral vectors encoding shRNA targeting the LGALS3 gene, together with GFP expression as a reporter gene. Then, cardiac fibroblasts were transduced by lentiviral infection to cause the knockdown of Gal-3. The efficiencies of lentiviral infection and knockdown were confirmed by GFP reporter gene expression and by quantification of Gal-3 gene and protein expressions by qPCR and immunofluorescence analysis, respectively (>90%; Figures 4A-E). Importantly, Gal-3 knockdown in cardiac fibroblasts led to a downregulation of type I collagen expression (Figure 4F-H).

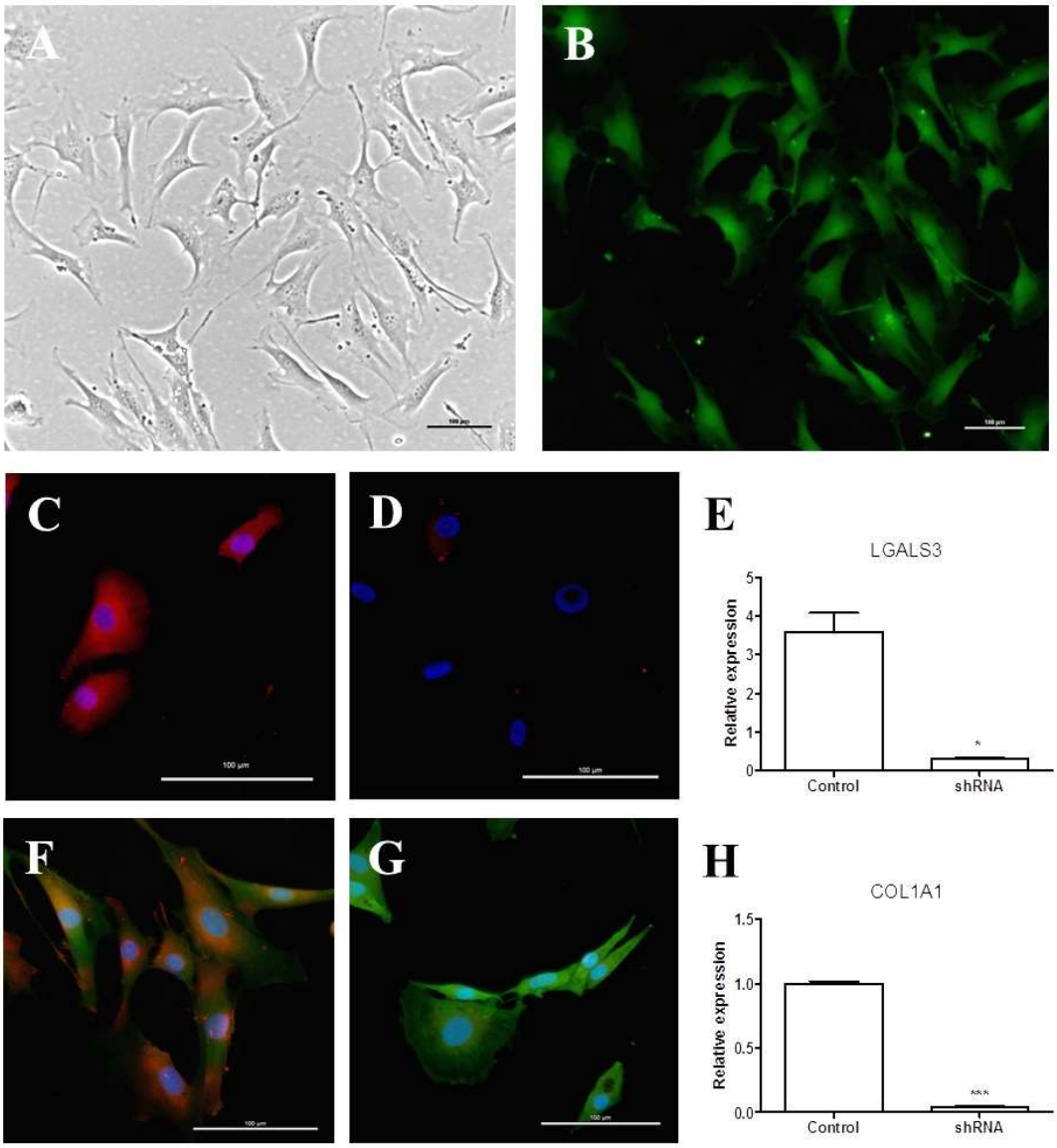

Figure 4. Gal-3 knockdown in cardiac fibroblasts leads to a marked reduction in type I collagen synthesis. (**A**) Cardiac fibroblasts from naïve mice were isolated by enzymatic digestion and expanded *in vitro*. (**B**) The efficiency of lentiviral transduction was evaluated by fluorescence microscopy to detect the expression of GFP, a reporter gene. Immunofluorescence analysis demonstrated that control cardiac fibroblasts expressed Gal-3 (**C**, red), while cells transduced with shRNA vector had a marked reduction of Gal-3 expression (**D**). Nuclei are stained with DAPI (blue). Gal-3 knockdown efficiency was confirmed by qPCR (**E**). Cells transduced with a control vector displayed GFP (green) and type I collagen (red) expression (**F**), while the cells transduced with shRNA vector had a diminished expression of collagen type I (**G**). The expression of type I collagen mRNA was quantified by qPCR, showing a marked reduction in Gal-3 knockdown fibroblasts (**H**). * $P<0.05$; *** $P<0.001$.

Gal-3 knockdown was associated with a marked reduction in the proliferative rate of cardiac fibroblasts (Figure 5B). This finding was accompanied by a reduction of cyclin D1 gene expression (Figure 5C). Flow cytometry analysis showed cell cycle arrest in Gal-3 knockdown when compared to control cells (increased percentage of G0/G1 and decreased S and G2/M phases; Figures 5D-F).

In order to evaluate if knockdown of Gal-3 also affects cell survival, we evaluated the frequency of apoptosis in the culture of cardiac fibroblasts, by Annexin V/PI staining and flow cytometry analysis. A higher percentage of apoptotic cells was detected in cultures of cardiac fibroblasts with Gal-3 knockdown when compared to controls (Figure 5G).

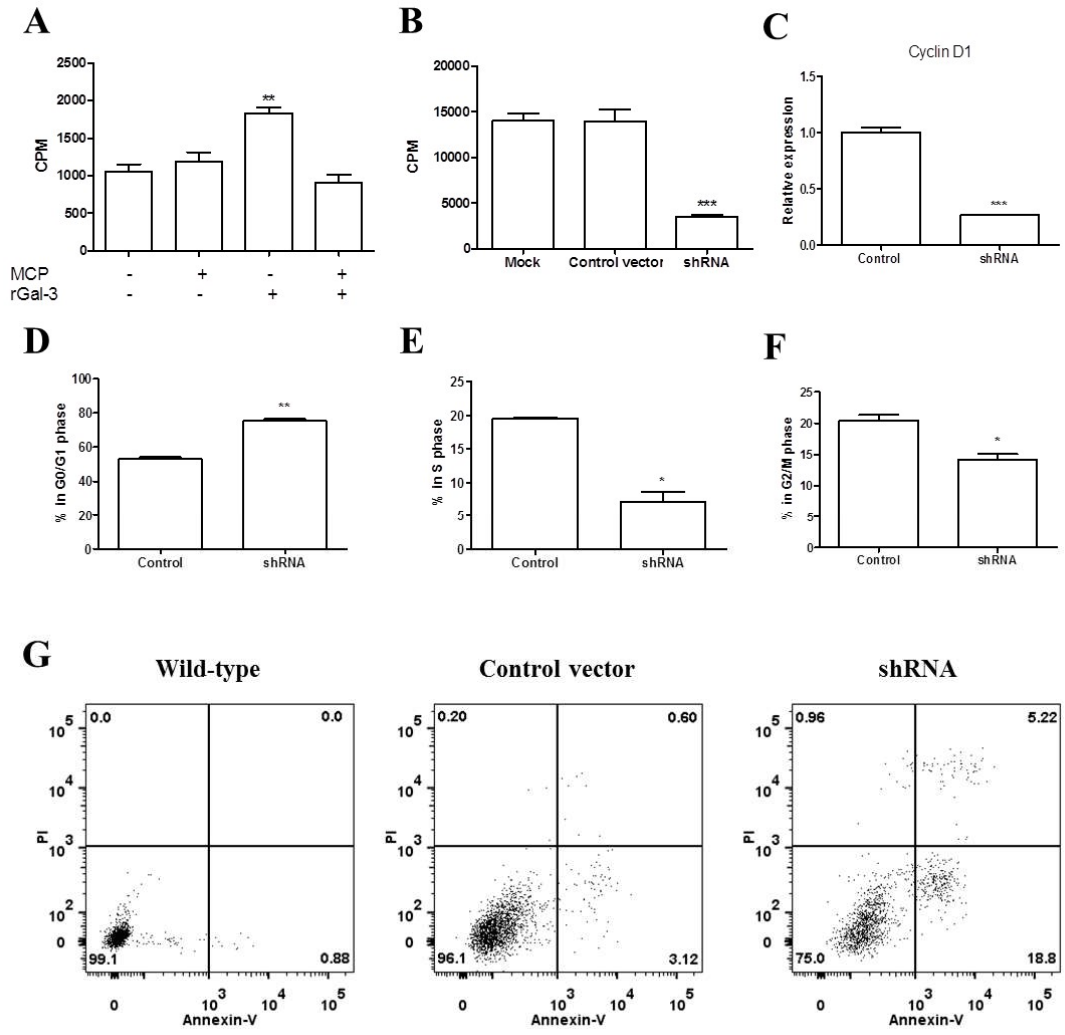

Figure 5. Gal-3 is crucial for cardiac fibroblast proliferation and survival. Recombinant Gal-3 was added to the cardiac fibroblast culture medium and cell proliferation was measured by ^{3}H-thymidine incorporation assay. Extracellular Gal-3 induced cardiac fibroblast proliferation, which was abolished by addition of MCP, a Gal-3 binding partner (**A**). Gal-3 knockdown in

cardiac fibroblasts markedly reduced cell proliferation, as evaluated by ^{3}H-thymidine incorporation assay (**B**). A reduction in gene expression of cyclin D1 was found by qPCR analysis (**C**). Cell cycle analysis was performed by flow cytometry with CFSE assay, demonstrating that Gal-3 knockdown in cardiac fibroblasts is associated with cell cycle arrest in G0/G1 phases (**D**) and reduced number of cells in the S (**E**) and G2/M (**F**) phases. Gal-3 knockdown was associated with increased frequency of apoptosis, as evaluated by Annexin V assay (**G**). * $P<0.05$; ** $P<0.01$; *** $P<0.001$.

Treatment with the Gal-3 blocking agent N-lac reduces inflammation and fibrosis in experimental CCC

To study the role of Gal-3 on the pathogenesis of CCC, we performed a pharmacological blockade of Gal-3 using N-acetyl-D-lactosamine (N-Lac; Figure 6A), during the chronic phase of the infection, when cardiac fibrosis is increased significantly (6 and 8 m.p.i.). We performed functional evaluations (ECG analysis and treadmill test) before treatment (6 m.p.i.) and after the treatment with N-Lac (8 m.p.i.). *T. cruzi* infection caused the development of arrhythmias and cardiac conduction disturbances, such as atrioventricular block, ventricular tachycardia and ventricular bigeminy. Treatment with N-Lac did not alter the frequencies or the severity of arrhythmias when compared to those found in saline-treated controls (Table I). Regarding the exercise capacity, *T cruzi* infected mice had an impaired performance when compared to uninfected controls six months after infection (data not shown). N-Lac treatment did not cause any improvement in exercise capacity, since mice treated with this Gal-3 blocker had similar performance in treadmill test to saline-treated mice and a reduced capacity when compared to uninfected controls (Figure 6B).

Histological analysis demonstrated the presence of inflammatory infiltrate in the hearts of mice infected with *T. cruzi*, mainly composed by mononuclear cells. However, the number of inflammatory cells infiltrating the heart was significantly reduced in N-Lac treated mice, compared to saline treated controls (Figures 6C and D). Additionally, the percentage of heart fibrosis was significantly reduced after N-Lac treatment when compared to saline-treated mice (Figures 6C and E).

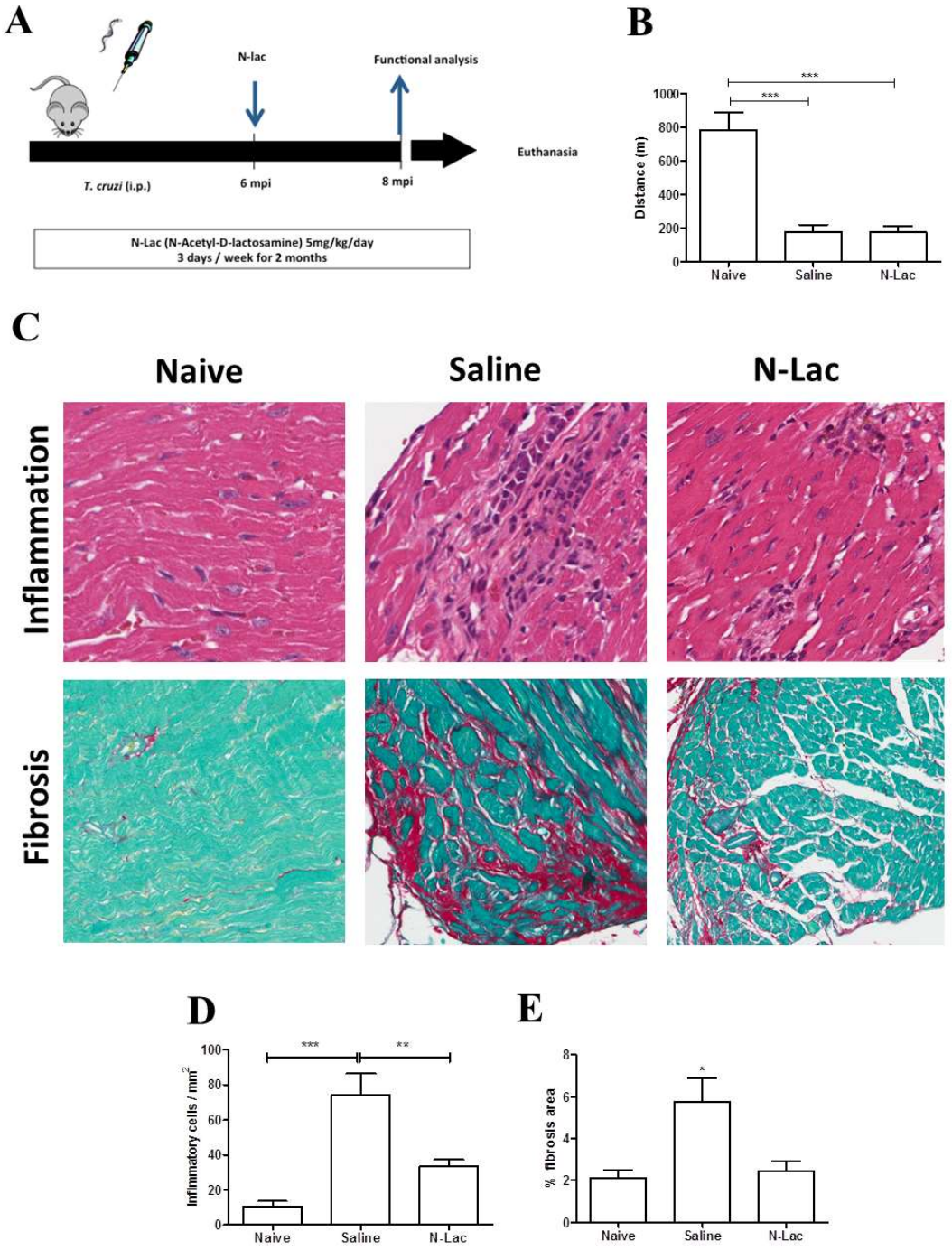

Figure 6. *In vivo* pharmacological blockade of Gal-3 during the chronic phase of experimental *T. cruzi* infection reduces inflammation and fibrosis. (**A**) Experimental design. (**B**) A lack of functional recovery was observed by analysis of performance in treadmill test two months after the beginning of treatment with N-Lac. (**C**) A significant reduction in the intensity of cardiac inflammation and fibrosis is observed in heart sections of mice treated with N-Lac stained with H&E (upper) and Sirius red (bottom). Quantifications of the number of inflammatory cells infiltrating the heart (**D**) and cardiac fibrosis area (**E**), showing histological improvement in N-Lac treated mice. * $P<0.05$; ** $P<0.01$; *** $P<0.001$.

Table 1. ECG analysis in uninfected and *T. cruzi*-infected mice.

ECG findings	Uninfected (n=7)	Pre-treatment (n=19)	Saline (n=9)	N-Lac (n=10)
No alterations	-	1	-	-
Atrial overload	-	1	1	-
IACD*	-	-	2	-
JR†	-	1	1	-
AVB 1st degree‡	-	6	3	2
AVB 3rd degree‡	-	5	2	3
SVT§	-	2	1	-
Ventricular bigeminy	-	-	-	3
Isorhythmic AVD‖	-	2	1	-
AVD‖	-	-	1	-
IVCD#	-	1	1	-

* Intra-atrial conduction delay (IACD); † Junctional rhythm (JR); ‡ Atrioventricular block (AVB); § Supraventricular tachycardia (SVT); ‖ Atrioventricular dissociation (AVD); # Intraventricular conduction delay (IVCD).

In order to investigate whether N-Lac caused modulation of inflammatory mediators, we performed gene expression analysis in the heart tissue (Figure 7). N-Lac-treated mice had reduced levels of the inflammatory cytokines TNF-α and IFN-γ when compared to saline-treated mice. The regulatory cytokine IL-10 was increased in *T. cruzi*-infected mice when compared to uninfected controls, both in saline as well as in N-Lac-treated mice. Moreover, the expression of transcription factors T-bet, GATA-3 and FoxP3, associated with T cell subtypes Th1, Th2 and Treg, respectively, was increased by *T. cruzi* infection and reduced in mice treated with N-Lac. The gene expression of CCL8 (MCP2) and the chemokine receptor CCR5, which are increased by *T. cruzi* infection, was also reduced after N-Lac treatment. Importantly, treatment with N-Lac reduced the gene expression of Gal-3 in the hearts of *T. cruzi*-infected mice (Figure 7).

To better investigate the mechanisms by which N-Lac caused reduction of inflammation, we performed lymphoproliferation and migration assays. Mouse splenocytes were stimulated in vitro with concanavalin A or anti-CD3/CD28. Addition of N-Lac at the highest concentration tested (10 μM) caused a small reduction of lymphoproliferation stimulated by both polyclonal activators (Figures 8 A and B). In contrast, the positive control dexamethasone inhibited the proliferation induced by both stimuli. Lastly, we tested the effects of N-Lac in cell migration. Addition of N-Lac significantly inhibited leukocyte migration in a transwell system (Figures 8C and D).

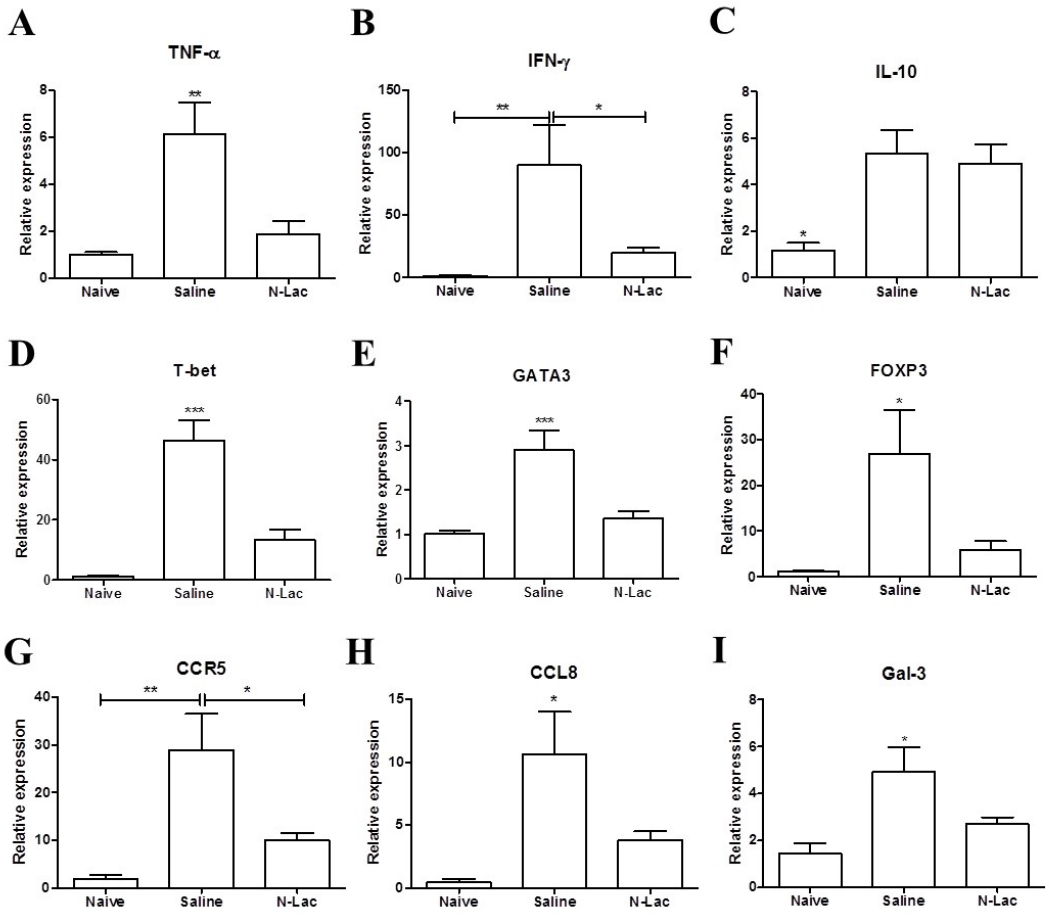

Figure 7. Modulation of gene expression in chagasic heart after N-Lac treatment. RTqPCR analysis of gene expression in the heart tissue demonstrated that N-Lac treatment was associated with a reduction of inflammatory cytokines TNF-α (**A**) and IFN-γ (**B**), and did not alter the expression of IL-10 (**C**), when compared to saline treated mice. T lymphocyte subtype-specific transcription factors associated with Th1 - T-bet (**D**), Th2 – GATA-3 (**E**), and Treg – FOXP3 (**F**) were reduced in N-Lac treated mice. Genes associated with leukocyte migration and chemotaxis CCR5 (**G**), CCL8 (**H**), and Gal-3 (I) were also reduced after N-Lac treatment. * $P<0.05$; ** $P<0.01$; *** $P<0.001$.

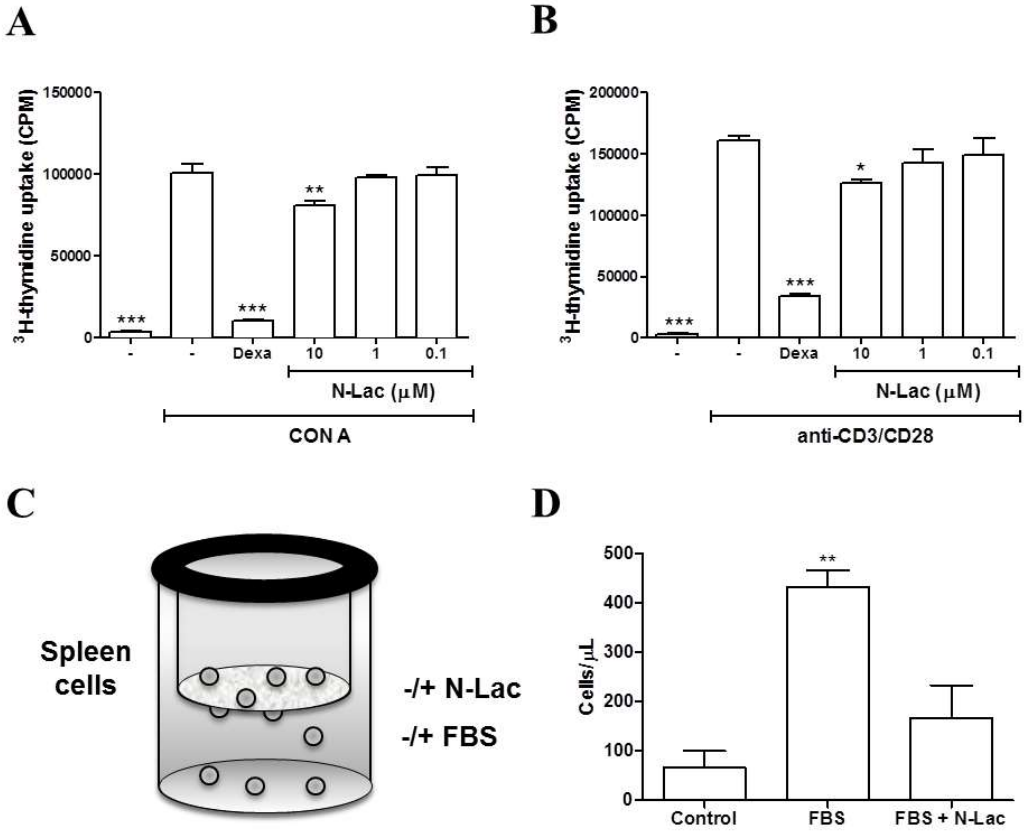

Figure 8. Effects of N-Lac on splenocyte proliferation and migration *in vitro*. Mouse splenocytes obtained from naïve C57Bl/6 mice were stimulated with concanavalin A (Con A) or anti-CD3/CD28 (**A** and **B**, respectively) in the absence or presence of N-Lac or dexamethasone (Dexa; 10 μM). Lymphoproliferation was assessed by ^{3}H-thymidine uptake. (**C** and **D**) Mouse splenocytes were submitted to starvation and placed in the upper compartment of a transwell system in the presence or absence of N-Lac (10 μM). Medium with or without fetal bovine serum (FBS) was placed in the lower chamber as chemoattractant (C). Cell concentration in the lower chamber after overnight incubation (D). Values represent the means±SEM. * P<0.05; *** P<0.01; ***P<0.001 compared to the other groups.

Discussion

Gal-3 is a multifunctional lectin that can be found in various cells and tissues, being detected in the nucleus, cytoplasm, as well as in the extracellular compartment.[11] Notably, Gal-3 may have different, concordant or opposite actions depending on the cell type and whether it is present in the extracellular or intracellular compartments.[11] Previous studies from our group and others have shown a correlation between inflammation and fibrosis in the heart and Gal-3

expression. In the present study, we demonstrated the production of Gal-3 in different cell populations and its role in the promotion of heart inflammation and fibrosis in *T. cruzi*-infected mice. This was achieved by (i) immunostaining in Chronic Chagas disease human and mouse heart samples showing the presence of Gal-3^{+} cells, including macrophages, T cells, fibroblasts and fibrocytes; (ii) blockage of Gal-3 expression in cardiac fibroblasts, showing its role on proliferation and collagen production; and (iii) pharmacological blockage in vivo in the experimental model, showing significant reduction of inflammation, fibrosis and production of key inflammatory mediators in the heart.

Previous studies have highlighted a role for Gal-3 in the cardiac remodeling process in different experimental settings, including experimental models of hypertrophic cardiomyopathy and myocardial infarction.[12-14] These reports have focused on Gal-3 effects in cardiac fibroblasts, contributing for cell survival, proliferation and extracellular matrix synthesis. In CCC, however, a massive infiltration of immune cells is observed in the heart, which leads to persistent immune-mediated myocyte damage, ultimately triggering a progressive fibrogenic response.[6-9]

In the present study we demonstrated the dynamic expression of Gal-3 in different periods during *T. cruzi* experimental infection and correlated with the findings of human heart analysis, in sections obtained from hearts of subjects with end-stage heart failure due to CCC. Gal-3 expression was observed in a similar pattern in human and mouse heart samples, mainly in areas of inflammatory infiltrates. Gal-3 has been previously described in immune cells and to participate in different aspects of innate and adaptive immune responses.[19-24] In the experimental model, we showed expression of Gal-3 in macrophages and T cells, two main cell types present in the inflammatory foci in Chagas disease hearts. Moreover, we demonstrated that inflammatory stimuli increase the expression of Gal-3 in macrophages *in vitro*. Since IFN-γ and TNF-α are produced in hearts of mice with CCC, their action may account for the increased expression in macrophages present in the hearts of infected mice. The described roles for Gal-3 in T cell biology include the promotion of cell survival, proliferation, TCR signaling and migration.[25] In our study we observed reduction of cell migration, but not of lymphocyte proliferation, by the Gal-3 inhibitor N-Lac, indicating that the reduction of inflammation in the hearts of infected mice after N-Lac treatment is mainly due to reduction of cell migration.

In our study we found that *T cruzi* infection also increased the expression of Gal-3 in cardiac fibroblasts and, even more intensely, in a population of bone marrow-derived fibrocytes. Although cardiac fibroblasts have been classically described as the most important cell type involved in cardiac fibrosis, different studies show that bone marrow-derived

fibrocytes play relevant roles in fibrogenesis and remodeling.[26-28] Our data provided from *in vitro* assays in cardiac fibroblasts demonstrated the role of exogenous and endogenous Gal-3 in cell survival, proliferation, and type I collagen synthesis, which is in accordance with the literature.[12-14] Gal-3 has been previously shown to enhance cyclin D1 promoter activity,[29] a fact that correlates with the cell cycle arrest and decreased expression of cyclin D1 gene in Gal-3 knockdown fibroblasts found in our study.

We have previously shown that LGALS3 gene expression is upregulated in the hearts of mice during chronic *T. cruzi* infection.[9,16]. The correlation between intensity of myocarditis and presence of collagen type I, Gal-3 and α-SMA-positive cells was also seen in a mouse model of *T. cruzi* infection.[30] Gal-3 was implicated in the process of *T. cruzi* invasion.[31] Altogether, these data suggest that Gal-3 is involved in different aspects of the pathogenesis of CCC, from *T. cruzi* infection to immune response, inflammation and tissue repair. Interestingly, a reduction of Gal-3 expression in the heart was observed accompanying decreased fibrosis and myocarditis after G-CSF treatment or cell therapy in chronically infected mice.[16,32]

In the present study, we showed that the Gal-3 pharmacological blockage with N-Lac dramatically modulated the immune response in the hearts of CCC mice, reducing migration of immune cells to the myocardium, decreasing the expression of inflammatory Th1 cytokines and markers of Th2 and Treg lymphocyte subtypes, until the level of naïve control mice. Notably, the anti-inflammatory cytokine IL-10 was increased when compared to naïve mice. This finding, together with the observed reduced levels of IFN-γ and TNF-α gene expression, demonstrates a potent anti-inflammatory effect of N-Lac. Moreover, N-Lac treatment was associated with a significant reduction of myocardial fibrosis, which is in accordance with a previous report in a different experimental model.[14] Despite the reduction of inflammation and fibrosis, our results did not correlate with any improvement in functional parameters after N-Lac treatment. This finding does not exclude the possibility of long-term beneficial effects of Gal-3 blockage, nor that N-Lac treatment, at an earlier stage of the infection, may prevent the deterioration of cardiac function.

In conclusion, we demonstrated that Gal-3 plays an important role in the pathogenesis of experimental chronic Chagas disease, acting in different cell compartments and promoting cardiac inflammation and fibrosis. The finding of Gal-3 expression in human heart samples, in a similar pattern as observed in the mouse model, reinforces its potential as a novel target for drug and therapy development for CCC.

Acknowledgements

We acknowledge the help of Ms. Pamela Daltro for technical assistance in the cardiac functional analysis.

Disclosures section: None.

References

1. Andrade DV, Gollob KJ, Dutra WO: Acute chagas disease: New global challenges for an old neglected disease. PLoS Negl Trop Dis 2014, 8:e3010.
2. WHO. Chagas disease in Latin America: an epidemiological update based on 2010 estimates. Wkly Epidemiol Rec 2015, 90:33-44.
3. Bern C, Montgomery SP, Herwaldt BL, Rassi A Jr, Marin-Neto JA, Dantas RO, Maguire JH, Acquatella H, Morillo C, Kirchhoff LV, Gilman RH, Reyes PA, Salvatella R, Moore AC: Evaluation and treatment of Chagas disease in the United States: a systematic review. JAMA 2007, 298:2171-2181.
4. Morillo CA, Marin-Neto JA, Avezum A, BENEFIT Investigators: Randomized Trial of Benznidazole for Chronic Chagas' Cardiomyopathy. N Engl J Med 2015, 373:1295-1306.
5. Burgos JM, Diez M, Vigliano C, Bisio M, Risso M, Duffy T, Cura C, Brusses B, Favaloro L, Leguizamon MS, Lucero RH, Laguens R, Levin MJ, Favaloro R, Schijman AG: Molecular identification of Trypanosoma cruzi discrete typing units in end-stage chronic Chagas heart disease and reactivation after heart transplantation. Clin Infect Dis 2010, 51:485-495.
6. Soares MB, Pontes-De-Carvalho L, Ribeiro-Dos-Santos R: The pathogenesis of Chagas' disease: when autoimmune and parasite-specific immune responses meet. An Acad Bras Cienc 2001, 73:547-559.
7. Bonney KM, Engman DM: Autoimmune pathogenesis of Chagas heart disease: looking back, looking ahead. Am J Pathol 2015, 185:1537-1547.
8. Gomes JA, Bahia-Oliveira LM, Rocha MO, Martins-Filho OA, Gazzinelli G, Correa-Oliveira R: Evidence that development of severe cardiomyopathy in human Chagas' disease is due to a Th1-specific immune response. Infect Immun 2003, 71:1185-1193.
9. Soares MB, de Lima RS, Rocha LL, Vasconcelos JF, Rogatto SR, dos Santos RR, Iacobas S, Goldenberg RC, Iacobas DA, Tanowitz HB, de Carvalho AC, Spray DC:

Gene expression changes associated with myocarditis and fibrosis in hearts of mice with chronic chagasic cardiomyopathy. J Infect Dis 2010, 202:416-426.

10. Boer RA, Voors AA, van Veldhuisen DJ: Galectin-3: a novel mediator of heart failure development and progression. Eur J Heart Fail 2009, 11:811–817.
11. Krześlak A, Lipińska A: Galectin-3 as a multifunctional protein. Cell Mol Biol Lett 2004, 9:305-328.
12. Sharma U, Pokharel S, Pinto YM: Galectin-3 Marks Activated Macrophages in Failure-Prone Hypertrophied Hearts and Contributes to Cardiac Dysfunction. Circulation 2004, 110:3121-3128.
13. González GE, Cassaglia P, Noli Truant S, Fernández MM, Wilensky L, Volberg V, Malchiodi EL, Morales C, Gelpi RJ: Galectin-3 is essential for early wound healing and ventricular remodeling after myocardial infarction in mice. Int J Cardiol 2014, 176:1423-1425.
14. Ruifrok WP, Meissner M, Bos EM, van Goor H, Sanjabi B, van der Harst P, Pitt B, Goldstein IJ, Koerts JA, van Veldhuisen DJ, Bank RA, van Gilst WH, Silljé HH, de Boer RA: Genetic and pharmacological inhibition of galectin-3 prevents cardiac remodeling by interfering with myocardial fibrogenesis. Circ Heart Fail 2013, 6:107-117.
15. Chen A, Hou W, Zhang Y, Chen Y, He B: Prognostic value of serum galectin-3 in patients with heart failure: a meta-analysis. Int J Cardiol 2015, 182:168-170.
16. Soares MBP, Lima RS, Souza BSF, Vasconcelos JF, Rocha LL, dos-Santos RR, Iacobas S, Goldenberg RC, Lisanti MP, Iacobas DA, Tanowitz HB, Spray DC, Campos-de-Carvalho AC: Reversion of gene expression alterations in hearts of mice with chronic chagasic cardiomyopathy after transplantation of bone marrow cells. Cell Cycle 2011, 10:1448–1455.
17. Wiznerowicz, M and Trono, D: Conditional Suppression of Cellular Genes: Lentivirus Vector-Mediated Drug-Inducible RNA Interference. J Virol 2003, 77: 8957–8961.
18. Karasuyama H, F. Melchers: Establishment of mouse cell lines which constitutively secrete large quantities of interleukins 2, 3, 4, or 5 using modified cDNA expression vectors. Eur J Immunol 1988, 18:97-104.
19. Henderson NC, Sethi T: The regulation of inflammation by galectin-3. Immunol Rev 2009, 230:160-171.
20. Hsu DK, Yang RY, Pan Z, Yu L, Salomon DR, Fung-Leung WP, Liu FT: Targeted

disruption of the galectin-3 gene results in attenuated peritoneal inflammatory responses. Am J Pathol 2000, 156:1073-1083.

21. Jeon SB, Yoon HJ, Chang CY, Koh HS, Jeon SH, Park EJ: Galectin-3 exerts cytokine-like regulatory actions through the jak-stat pathway. J Immunol 2010, 185:7037-7046.
22. MacKinnon AC, Farnworth SL, Hodkinson PS, Henderson NC, Atkinson KM, Leffler H, Nilsson UJ, Haslett C, Forbes SJ, Sethi T: Regulation of alternative macrophage activation by galectin-3. J Immunol 2008, 180:2650-2658.
23. Yang RY, Hsu DK, Liu FT: Expression of galectin-3 modulates t-cell growth and apoptosis. Proc Natl Acad Sci U S A 1996, 93:6737-6742.
24. Chen SS, Sun LW, Brickner H, Sun PQ: Downregulating galectin-3 inhibits proinflammatory cytokine production by human monocyte-derived dendritic cells via rna interference. Cell Immunol 2015, 294:44-53.
25. Tribulatti MV, Figini MG, Carabelli J, Cattaneo V, Campetella O: Redundant and antagonistic functions of galectin-1, -3, and -8 in the elicitation of t cell responses. J Immunol 2012, 188:2991-2999.
26. Chu PY, Mariani J, Finch S, McMullen JR, Sadoshima J, Marshall T, Kaye DM: Bone marrow-derived cells contribute to fibrosis in the chronically failing heart. Am J Pathol 2010, 176:1735-1742.
27. van Amerongen MJ, Bou-Gharios G, Popa E, van Ark J, Petersen AH, van Dam GM, van Luyn MJ, Harmsen MC: Bone marrow-derived myofibroblasts contribute functionally to scar formation after myocardial infarction. J Pathol 2008, 214:377-386.
28. Haudek SB, Cheng J, Du J, Wang Y, Hermosillo-Rodriguez J, Trial J, Taffet GE, Entman ML: Monocytic fibroblast precursors mediate fibrosis in angiotensin-II-induced cardiac hypertrophy. J Mol Cell Cardiol 2010, 49:499-507.
29. Lin HM, Pestell RG, Raz A, Kim HR: Galectin-3 enhances cyclin d(1) promoter activity through sp1 and a camp-responsive element in human breast epithelial cells. Oncogene 2002, 21:8001-8010.
30. Ferrer MF, Pascuale CA, Gomez RM, Leguizamón MS: DTU I isolates of Trypanosoma cruzi induce upregulation of galectin-3 in murine myocarditis and fibrosis. Parasitology 2014, 141:849-858.
31. Machado FC, Cruz L, da Silva AA, Cruz MC, Mortara RA, Roque-Barreira MC, da Silva CV: Recruitment of galectin-3 during cell invasion and intracellular

trafficking of *Trypanosoma cruzi* extracellular amastigotes. Glycobiology 2014, 24:179-184.

32. Vasconcelos JF, Souza BS, Lins TF, Garcia LM, Kaneto CM, Sampaio GP, de Alcântara AC, Meira CS, Macambira SG, Ribeiro-dos-Santos R, Soares MB: Administration of granulocyte colony-stimulating factor induces immunomodulation, recruitment of T regulatory cells, reduction of myocarditis and decrease of parasite load in a mouse model of chronic Chagas disease cardiomyopathy. FASEB J 2013, 27(12):4691-4702.

CAPÍTULO II

Neste capítulo é descrito o estudo no qual comparamos as propriedades das células-tronco mesenquimais *knockdown* para Gal-3 e seus controles *in vitro*, além de uma avaliação dos efeitos imunomoduladores dessas células no modelo experimental de miocardiopatia chagásica em camundongos.

Artigo em preparação.

Galectin-3 knockdown impairs the ability of mesenchymal stem cells to promote immunomodulation and decrease cardiac inflammation in a mouse model of Chagas' disease cardiomyopathy

Bruno Solano de Freitas Souza[*,†], Kátia Nunes da Silva[†], Daniela Nascimento Silva[†], Bruno Diaz Paredes[†], Carine Machado Azevedo[*,†], Juliana Fraga Vasconcelos[*,†], Ricardo Ribeiro dos Santos[†], and Milena Botelho Pereira Soares[*,†,]

Galectin-3 knockdown impairs migration and immunomodulatory actions of mesenchymal stromal cells in a mouse model of Chagas disease cardiomyopathy

Bruno Solano de Freitas Souza[*,†], Kátia Nunes da Silva[†], Daniela Nascimento Silva[†], Bruno Diaz Paredes[†], Carine Machado Azevedo[*,†], Vinícius Pinto Costa Rocha*, Carolina Kymie Nonaka[*,†], Gisele Batista Carvalho[†], Juliana Fraga Vasconcelos[*,†], Ricardo Ribeiro dos Santos[†], and Milena Botelho Pereira Soares[*,†,]

[*]Gonçalo Moniz Institute, FIOCRUZ, Salvador, Bahia, Brazil;

[†]Center for Biotechnology and Cell Therapy, São Rafael Hospital, Salvador, Bahia, Brazil;

Corresponding author: Milena B. P. Soares, Centro de Pesquisas Gonçalo Moniz, Fundação Oswaldo Cruz, Rua Waldemar Falcão, 121, Candeal, Salvador, Bahia, Brazil. CEP: 40296-710. Phone: (55) (71) 3176-2260; Fax: (55) (71) 3176-2272

E-mail address: milena@bahia.fiocruz.br

Abstract

Therapies based on transplantation of mesenchymal stromal cells (MSC) are currently under pre-clinical and clinical investigation and hold promise for the management of several inflammatory disorders. In Chagas disease cardiomyopathy (CCC), caused by chronic infection with *Trypanosoma cruzi*, the exacerbated immune response plays a critical pathophysiological role. Previous studies have shown the ability of MSC to decrease myocarditis and fibrosis in the experimental model of *T. cruzi* infection. However, the mechanisms involved in the modulatory action of MSC in CCC still need to be investigated. Galectin-3 (Gal-3), a beta-galactoside-binding lectin with several actions on immune responses and repair process, has been suggested as a regulator of immunosuppression induced by MSC. Here we investigated the role of Gal-3 on the immunomodulatory potential of MSC, through *in vitro* and *in vivo* studies. We found that Gal-3 knockdown in MSC did not affect the immunophenotype or the ability to undergo osteogenic, chondrogenic and adipogenic differentiations. However, Gal-3 knockdown MSC lost the ability to suppress T cell proliferation in vitro in a co-culture lymphocyte proliferation assay. Additionally, Gal-3 knockdown MSC showed decreased migration and displacement by *in vitro* wound healing and cell tracking assays, respectively. Additionally, when injected intraperitoneally, Gal-3 knockdown MSC were significantly less detected in the spleens, when compared to control MSC, demonstrating an impaired migration *in vivo*. Transplantation of control MSC into mice with CCC caused a suppression of cardiac inflammation, as shown by gene expression analysis of PTPRC and inflammatory cytokines such as TNFα, IL-1β, IL-6, while increasing the cardiac expression of anti-inflammatory cytokine IL-10. In contrast, Gal-3 knockdown MSC were unable to suppress the immune response, and even increased IFN-γ, as well as TGFβ and Gal-3 production in the heart. Similarly, while control MSC decreased cardiac collagen type I gene expression, transplantation of Gal-3 knockdown MSC lead to increased cardiac fibrosis and collagen type I gene expression. These findings demonstrate that Gal-3 expression regulates the ability of MSC to migrate and to promote immunomodulation in CCC.

Keywords: Mesenchymal stromal cells; Chagas disease cardiomyopathy; Galectin-3

Introduction

Mesenchymal stromal cells (MSC) are multipotent stem cells with the ability to differentiate into mesoderm-derived cell lineages, such as chondrocytes, osteocytes and adipocytes (DOMINICI *et al.*, 2006). Described by Friedenstein and colleagues (1970), MSC are plastic-adherent, morphologically similar to fibroblasts and can be characterized by the expression of specific surface markers and demonstration of tri-lineage differentiation potential. MSC can be easily obtained from different organs and tissues of adult individuals, being presently among the most studied cell types for cellular therapies (DOMINICI *et al.*, 2006).

The potential use of MSC to treat inflammatory and autoimmune disorders relies on several described immunomodulatory actions, including inhibition of the activation of T and B lymphocytes, NK cells, dendritic cells and stimulation of regulatory T cell differentiation (GAO *et al.*, 2016). The anti-inflammatory actions of MSC are well studied and found to be mediated by IL-10, TGF-β, PGE2, HGF and IDO (for human cells) or iNOS (for mouse cells). Galectin-3 (Gal-3) has also been pointed as a mediator of immunodulatory actions of human MSC (SIOUD *et al.*, 2011; SIOUD *et al.*, 2010).

Galectins are a group of galactoside-binding lectins that regulate various biological processes. Gal-3 is present in the extracellular and intracellular compartments, being involved in cell adhesion, migration, apoptosis, inflammation and tissue repair (KRZEŚLAK & LIPIŃSKA, 2004). Expression of Gal-3 in fibroblasts is associated with proliferation and synthesis of extracellular matrix components, contributing to scar formation (MACKINNON *et al.*, 2012; HENDERSON *et al.*, 2006; KOLATSI-JOANNOU *et al.*, 2011). In endothelial precursor cells, Gal-3 promotes proliferation and angiogenesis (WAN *et al.*, 2011). While the role of Gal-3 in immune cells has been extensively studied, the actions affected by Gal-3 expression in MSC are not well established. Being highly expressed in inflammatory and fibrogenic microenvironments in tissues, such as the heart, liver, kidney and joints, Gal-3 is likely to affect MSC biology and response, naturally or in a cell therapy scenario.

Cell therapy has been investigated as a potential alternative treatment for Chagas disease cardiomyopathy, a relevant cause of chronic heart failure in Latin America which results from *Trypanosoma cruzi* infection (NUNES *et al.*, 2013; SOARES *et al.*, 2011). An exacerbated immune response directed against the parasite and to host antigens plays a central role in the pathogenesis of CCC, leading to progressive cardiomyocyte loss, fibrosis, arrhythmia and loss of ventricular function (SOARES *et al.*, 2001). Previously, we have demonstrated that transplantation of MSC into mice chronically infected with *T. cruzi* caused reduction of

myocarditis and modulation of fibrosis (LAROCCA *et al.*, 2013; SILVA *et al.*, 2014). Additionally, we have shown that Gal-3 expression is increased in the hearts of chronic chagasic mice (SOARES *et al.*, 2011). *T. cruzi* infection induces increased Gal-3 expression in different cell types, which favors parasite adhesion, migration, invasion, and reduces anti-parasitic immune responses (MOODY *et al.*, 2000; KLESHCHENKO *et al.*, 2004; REIGNAULT *et al.*, 2014; ACOSTA-RODRÍGUEZ *et al.*, 2004; SILVA-MONTEIRO *et al.*, 2007). Here we investigated the potential involvement of Gal-3 as a mediator of the immunomodulatory potential of MSC in a mouse model of CCC.

Materials and Methods

Animal procedures

Six-to-eight week-old female C57BL/6 mice were used in this study. All animals were raised and maintained at the animal facility of the Center for Biotechnology and Cell Therapy, Hospital São Rafael, in rooms with controlled temperature (22 ± 2º C) and humidity (55 ± 10%), continuous air flow, with 12 h light/12 h dark cycles (6 am - 6 pm) and provided with rodent diet and water *ad libitum*. Mice were handled according to the NIH guidelines for animal experimentation, and the study received prior approval by the animal ethics committee at Hospital São Rafael.

Isolation and culture of MSC

Bone marrow cells were obtained from the tibiae and femurs by flushing, and cultured in Dulbecco's Modified Eagle's Medium (DMEM; ThermoFisher Scientific, CA, USA), 10% fetal bovine serum (ThermoFisher Scientific) and 1% penicillin/streptomycin (ThermoFisher Scientific) in a humidified incubator at 37° C with 5% atmospheric CO_2. The medium was changed every 2-3 days and, when the culture reached 90% confluency, the cells were passaged with trypsin-EDTA 0,25% solution (ThermoFisher Scientific).

Galectin-3 knockdown

Stable Gal-3 knockdown was achieved by transduction of MSC with a lentiviral vector carrying a shRNA sequence targeting LGALS3 gene or scrambled control (Lgals3_shRNA1 5' - GATTTCAGGAGAGGGAATGAT - 3'; one Lgals3_scrbl_shRNA 5' - AGGTATGAGTCGAGATTGAGA - 3'). Sense and anti-sense single strands, containing the target sequence, a loop sequence (TCAAGAG) and restriction enzyme sites. These sequences

were cloned to pLVTHM (Addgene plasmid #12247) vector under the ClaI and Mlu1 sites. For lentiviral particles production, HEK293FT were co-transfected, with the calcium-phosphate method, in a ratio of 2:1:3, respectively with: psPAX2, a packaging plasmid (Addgene plasmid #12260); pMD2.G, envelope protein expressing plasmid (Addgene plasmid #12259); and the transfer vector containing either the shRNA sequence targeting LGALS3 or scrambled non-targeting sequence. The culture supernatants containing viral particles were collected 48 and 72 h after transfection, concentrated by ultracentrifugation and stored at -80ºC. The transduction of MSC was performed by incubating the cells overnight with the concentrated lentiviral vectors in the presence of 6 μg/ml polybrene. Culture medium was replaced and the cells were cultured for additional 48 h, being assessed for GFP reporter gene expression by using an inverted fluorescence microscope (Eclipse Ti-E; Nikon, Tokyo, Japan). The cells were expanded and knockdown efficiency for each shRNA was evaluated by confocal microscopy and qPCR analyses, as described below.

Flow cytometry analysis

For immunophenotyping, MSC lines were passaged, centrifuged and the pellet was resuspended in PBS. A total of $5x10^5$ cells was used for labeling with the following antibodies in the concentration 1/50: Sca1PE-Cy7 (BD Biosciences, San Jose, CA, USA), CD45-PerCP (eBioscience, San Diego, CA, USA), CD44-PE (BD Bioscience), CD29-PE (eBioscience) and CD11b-APC (eBioscience). After the incubation period, cells were washed two times with PBS, and the data acquisition and analysis were performed in LRSFortessa flow cytometer (BD Biosciences). At least 10,000 events were acquired and analyzed.

Trilineage differentiation assay

Adipogenic, osteogenic and chondrogenic differentiation were performed using commercially available kits, following the manufacturer's instructions (all kits from ThermoFisher Scientific). For adipogenic differentiation, cells were cultured in 24-well plates in adipogenic induction medium - StemPro Adipogenesis Differentiation Kit. Lipid inclusions were detected on differentiation day 14, by fixation in 4% paraformaldehyde and staining with Oil red solution. For osteogenic differentiation, the cells were cultured in a specific osteogenic differentiation medium, StemPro Osteogenesis Differentiation Kit. Half the differentiation medium was changed every two days. Calcium-rich matrix deposition was observed by staining with Alizarin red 2%. For chondrogenic differentiation, cells were cultured for 21 days in chondrogenic differentiation medium, StemPro Chondrogenesis Differentiation Kit.

Proteoglycan synthesis was evaluated after staining with Alcian Blue solution. The images were captured with an inverted microscope (Eclipse Ti, Nikon, Tokyo, Japan).

Endothelial cell differentiation

Differentiation of MSC to endothelial cells was performed by incubating the cells with EGM-2 medium (Lonza, Basel, Switzerland), as previously described (SILVA *et al.*, 2014). Endothelial tube formation assay was performed to observe capillary-like 3-D structures by plating the differentiated cells on Matrigel (Corning, Corning, NY, USA). The images were captured with an inverted microscope (Eclipse Ti, Nikon, Tokyo, Japan).

Proliferation assays

To evaluate the immunomodulatory potential of MSC, an *in vitro* lymphocyte proliferation inhibition assay based on their co-culture with activated splenocytes was performed, as previously described (SILVA *et al.*, 2014). Briefly, splenocytes were isolated from C57BL/6 mice, cultured in 96-well plates, in RPMI supplemented with 10% FBS (All from ThermoFisher Scientific). Lymphocyte proliferation was induced by concanavalin A (Con A; 5 µg/mL, Sigma-Aldrich). Splenocytes were cultured in the absence or presence of irradiated (3000 rads) MSC cell lines, at different ratios (MSC:splenocytes 1:1, 1:10, 1:100, 1:1000, 1:10000). After 48 h of incubation, plates were pulsed with 1 µCi of methyl-^{3}H-thymidine (PerkinElmer, Amersham, Little Chalfont, England) for 18 h. Cell proliferation was assessed by measurement of ^{3}H-thymidine uptake using a β-plate counter (Hydex). The percent inhibition of lymphoproliferation was determined in relation to controls stimulated by Con A in absence of MSC.

For comparative evaluation of the proliferation rate among different MSC lines, the cells were plated in 96-well plates, at a density of 10^4 cells/well, in a final volume of 200 µL, in triplicate, and cultured in DMEM supplemented with 10% FBS. After 24 h, plates were pulsed with 1 µCi of methyl-^{3}H thymidine (PerkinElmer) for 18 h, and proliferation was assessed by measurement of ^{3}H-thymidine uptake by using a Chameleon β-plate counter.

Cell migration analyses

MSC were plated in wells of a 24-well plate, at a cell density of $5x10^4$ cells/cm^2. Live cell imaging was performed using the Operetta High Content Imaging System (Perkin Elmer, Waltham, MA, USA) under controlled temperature (37 °C) and atmospheric CO_2 (5%). Digital

phase contrast images were acquired at 10X magnification (10X high NA objective) using Operetta's automatic digital phase contrast algorithm. Image acquisition interval was set to 10 min during 16 h. Images were segmented using the Find Cells building block of the Harmony 3.5.2 software (Perkin Elmer), which provides a dedicated algorithm for segmenting digital phase contrast images. The segmented cells were subjected to cell tracking using the Track Objects building block. Properties that describe cell migration per time point were calculated, such as displacement. For *in vitro* wound healing assay, MSC were cultured in a 6 well-plate until a monolayer was formed. A pipette tip was used to make a scratch along the well, and the area was photographed after 3 days.

T. cruzi infection and cell transplantation

Trypomastigotes of the myotropic Colombian *T. cruzi* strain were obtained from culture supernatants of infected LLC-MK2 cells, as previously described (SOARES *et al.*, 2010). Then, C57BL/6 mice were infected by intraperitoneal injection with 1000 *T. cruzi* trypomastigotes in PBS. Infection was confirmed by following parasitemia at different time points after infection. Six months after infection, mice were randomly assigned into three groups; control MSC, Gal-3 knockdown MSC or saline. Mice received one weekly injection of saline or 10^6 MSC in a 100 µl by intraperitoneal route, during five weeks. Mice were euthanized by cervical dislocation under anesthesia with ketamine (100 mg/kg) and xylazine (10 mg/kg), on the 7th week after the beginning of the treatment, for analysis.

Real time reverse transcription polymerase chain reaction (RT-qPCR)

Dissociated cells, heart and spleen samples were subjected to total RNA extraction using TRIzol reagent (Thermo Scientific). The RNA concentration was determined by spectrophotometry. Next, cDNA was synthetized, starting with 1 µg RNA using High Capacity cDNA Reverse Transcription Kit (Thermo Scientific), following manufacturer's instructions. RT-qPCR assays were performed to detect the expression levels of *Tbet (*Mm_00450960_m1), TNFα (Mm_00443258_m1), IFNγ (Mm_00801778_m1), IL10 (Mm_00439616_m1), LGALS3 (Mm_00802901_m1), COL1A1 (Mm_0801666_g1), IL-1β (Mm_0043228_m1), IL-6 (Mm_00446190_m1), PTPCR (Mm_01293577_m1), and TGF-β (Mm_00441724_m1). The RT-qPCR amplification mixtures contained 20 ηg template cDNA, Taqman Master Mix (10 µL) and probes in a final volume of 20 µL (all from Thermo Scientific). The reactions were run in duplicate on an ABI7500 Sequence Detection System (Thermo Scientific) under standard thermal cycling conditions. The mean Ct (cycle threshold) values from duplicate measurements

were used to calculate expression of the target gene, with normalization to an internal control - *GAPDH (*mm99999915_g1), using the 2–DCt formula. Experiments with coefficients of variation greater than 5% were excluded. A non-template control and non-reverse transcription controls were also included.

Histology and morphometric analyses

Hearts were collected and fixed in 10% buffered formalin. Heart sections were analyzed by light microscopy after paraffin embedding, followed by standard hematoxylin and eosin (H&E), or Sirius red staining. Sirius red stained sections were entirely digitalized using a confocal microscope A1+ (Nikon). The percentage of fibrosis was determined by analysis of whole sections stained with Sirius red-stained heart sections and semi-automatic morphometric quantification using Image Pro Plus v.7.0. Two blinded investigators performed the analyses. For determining the relative fibrosis area, the result of the collagen stained area was subtracted from the mean value obtained in the naïve control group.

Immunofluorescence analysis

Immunostainings for detection of Gal-3 expression were performed in MSC plated on coverslips. The cells were fixed with paraformaldehyde 4% and incubated overnight at 4ºC with the primary antibody goat anti-Gal-3, diluted 1:400 (Santa Cruz Biotechnology). On the following day, sections were incubated for 1 h with Phalloidin conjugated with Alexa fluor 488 (1:200; ThermoFisher Scientific) mixed with the secondary antibody anti-goat IgG Alexa fluor 568 (1:1000; ThermoFisher Scientific) respectively. Nuclei were stained with 4,6-diamidino-2-phenylindole (VectaShield mounting medium with DAPI H-1200; Vector Laboratories). The presence of fluorescent cells was determined by observation using an A1+ confocal microscope (Nikon).

Statistical analyses

Continuous variables are presented as means ± SEM. Parametric data were analyzed using Student's unpaired *t* test, for comparisons between two groups, and 1-way ANOVA, followed by Bonferroni post hoc test for multiple-comparison test, using Prism 6.0 (GraphPad Software). Values of $P < 0.05$ were considered statistically significant.

Results

Bone marrow-derived MSC lines were generated, by transduction with lentiviral vectors containing the shRNA sequence targeting Gal-3 gene, a non-targeting scrambled sequence of an empty vector encoding only GFP. The MSC lines were assessed for Gal-3 expression, in order to confirm the knockdown efficiency by confocal microscopy and qPCR (Figures 1A-C). Gal-3 was expressed on the cytoplasm and inside the nuclei of wild type (Figure 1A) and control vector-transduced MSC lines. Cells transduced with the vector containing the shRNA sequence for Gal-3 knockdown showed a marked reduction of Gal-3 expression (Figure 1B). This finding was confirmed quantitatively at the mRNA level by RT-qPCR analysis (Figure 1C).

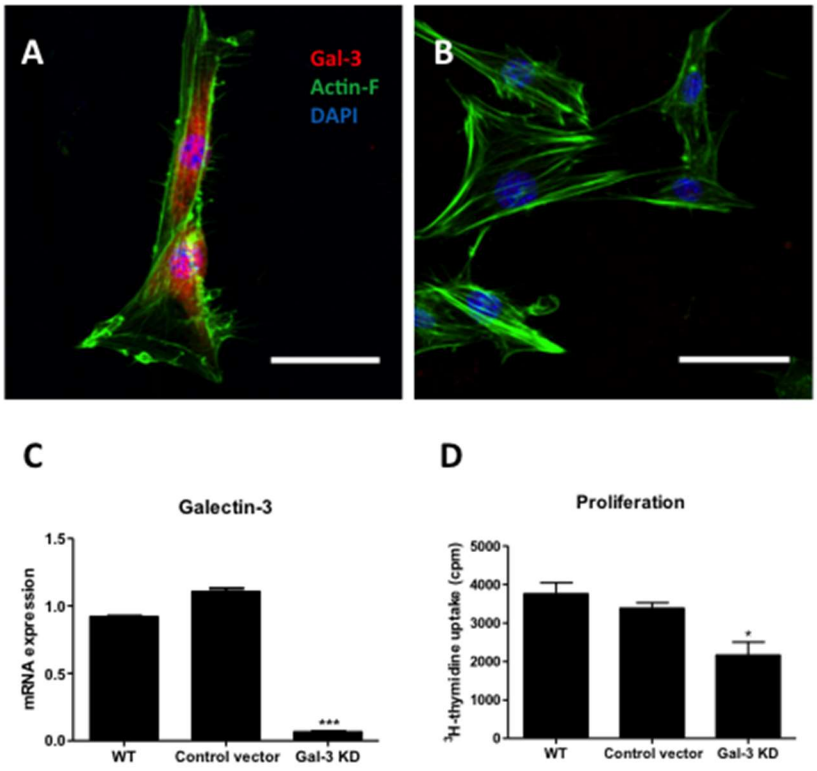

Figure 1. Evaluation of Gal-3 knockdown efficiency. Confocal microscopy images showing Gal-3 expression (red) in wild type (A) and Gal-3 knockdown MSC (B). Scale bars = 20 μm. (C) Gene expression analysis of LGALS3 gene expression by qRT-PCR. (D) Proliferation rate in different MSC lines, evaluated by ^{3}H-thymidine incorporation assay. WT = Wild type MSC; Control vector = MSC transduced with a non-targeting shRNA vector; Gal-3 KD = Gal-3 knockdown. *P<0.05; ***P<0.001.

After confirming the knockdown efficiency, the cell lines were characterized in order to ensure the maintenance of the phenotype and biological properties that define MSC.

Immunophenotyping by flow cytometry showed a similar pattern of expression of surface markers by the different cell lines, with a positive staining for the MSC markers CD44, CD29 and Sca-1, and low frequency of cells expressing hematopoietic lineage markers CD45 and CD11b. Thus, Gal-3 knockdown did not alter the expression of the surface markers analyzed (Table I). Next, we assessed the multipotential by a trilineage differentiation assay *in vitro*. Upon induction by specific culture media, Gal-3 knockdown and control MSC lines were able to efficiently undergo osteogenic, chondrogenic and adipogenic differentiation (Figure 2A). Additionally, knockdown of Gal-3 in MSC did not interfere with their ability to form capilary-like structures when cultured in endothelium-inducer medium (Figure 2B).

Table I – Immunophenotype of MSC lines

MSC line	Cell surface markers (%)				
	CD44$^+$	**CD29$^+$**	**Sca-1$^+$**	**CD45$^+$**	**CD11b$^+$**
WT	**92.4**	**99.7**	**93.5**	**0.3**	**2.8**
Control vector	**99.1**	**98.9**	**97.8**	**0.7**	**2.5**
Gal-3 KD	**93.7**	**97.9**	**97.1**	**0.3**	**0.6**

WT = wild type MSC; Control vector = MSC transduced with a non-targeting shRNA vector; Gal-3 KD = Gal-3 knockdown.

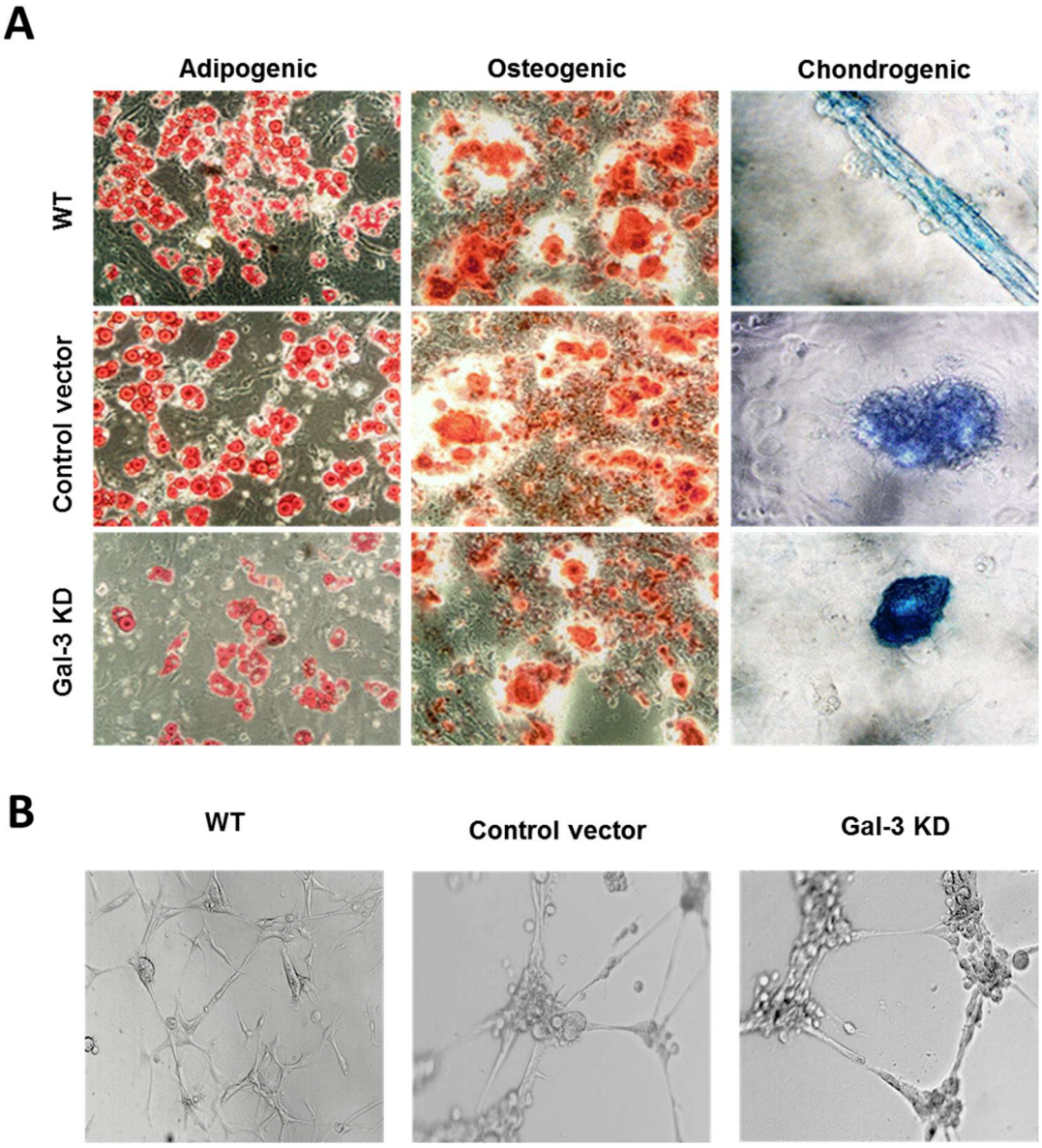

Figure 2. Differentiation potential of MSC is not affected by Gal-3 knockdown. (A) Trilineage differentiation assay was performed to generate adipocytes, visualized by Oil red staining, osteocytes, visualized by Alizarin red staining, and chondrocytes, visualized by Alcian blue staining, respectively. (B) Angiogenic ability demonstrated by endothelial tube formation assay on Matrigel. WT = Wild type MSC; Control vector = MSC transduced with a non-targeting shRNA vector; Gal-3 KD = Gal-3 knockdown. Magnification = 200x.

To evaluate the immunomodulatory potential of MSC lines, we performed an *in vitro* co-culture assay with activated lymphocytes. Wild-type and vector control MSC were able to

block concanavalin A-induced lymphocyte proliferation when co-cultured in different ratios (Figures 3A and B). Gal-3 knockdown MSC, however, did not inhibit lymphocyte proliferation even at a 1:1 ratio (Figure 3C).

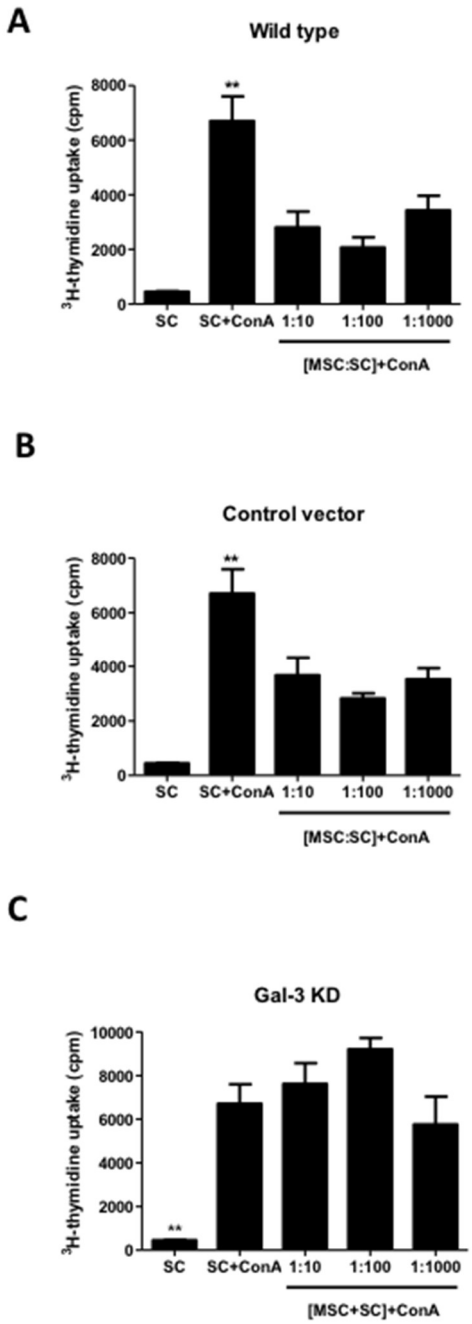

Figure 3. Immumodulatory effects of MSC on lymphocyte proliferation induced by mitogen *in vitro*. Mouse splenocytes were activated with Con-A and co-cultured with different amounts of the MSC lines: (A) wild type; (B) transduced with a non-targeting shRNA vector; or (C) Gal-3 knockdown. Lymphocyte proliferation was measured by by ^{3}H-thymidine

incorporation assay. SC = splenocytes; ConA = concanavalin A; MSC = mesenchymal stromal cells. *P<0.05; **P<0.01.

Galectin 3 is known to affect cell-extracellular matrix protein binding and cell migration processes (POLLI *et al.*, 2013; GAO *et al.*, 2014). To investigate whether Gal-3 knockdown interferes with migration of MSC, we assessed the *in vitro* migratory ability of Gal-3 knockdown MSC and control cell lines *in vitro*. Gal-3 knockdown caused a decreased migration *in vitro* in a wound healing assay when compared to control MSC (Figures 4A-C). Additionally, by using displacement cell tracking by time lapse image analysis, we found that Gal-3 knockdown caused a reduction in the mobility of MSC when compared to controls (Figures 4D-F).

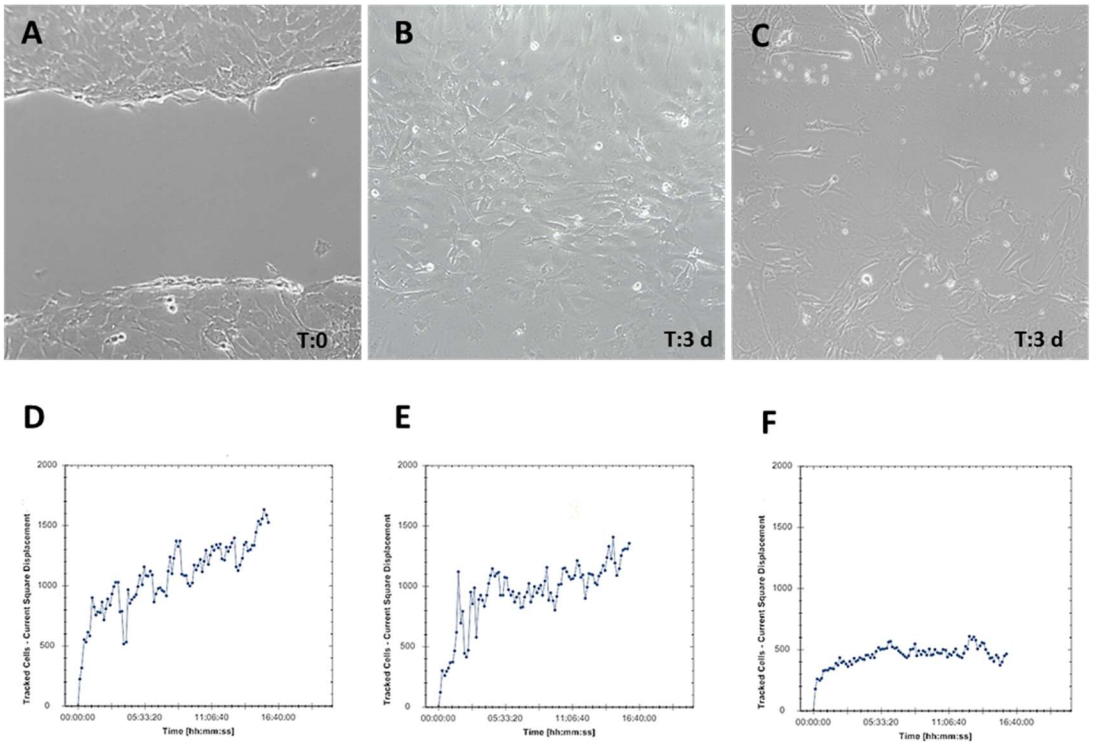

Figure 4. Gal-3 knockdown MSC exhibit defective migration and displacement *in vitro*. Migration was evaluated by the wound healing assay. Phase contrast representative images showing scratch area at day 0 (A), and at day 3 for wild-type MSC (B) and Gal-3 knockdown MSC (C). (D-F) Mean square displacements were obtained by individually tracked cells at various time points, from the time of the first position, until the end of the overnight incubation of wild-type MSC (D), MSC transduced with control vector (E) and Gal-3 knockdown MSC (F).

In order to test if Gal-3 knockdown could impair MSC therapeutic actions in an *in vivo* setting, the cells were administered i.p. into mice chronically infected with *T. cruzi*, a model of chronic Chagas disease cardiomyopathy (Figure 5A). First, the ability of MSC to migrate to spleen and heart was evaluated shortly after transplantation, by qPCR analysis of GFP mRNA expression. As shown in figure 6B, the expression of GFP was found in the spleen as early as 30 min after cell transplantation and increased at the 3 h time point. However, significantly lower levels of GFP expression were detected in the spleens of mice transplanted with MSC-RNAi when compared to control MSC, both 30 min and 3 h after the cell administration. Negligible levels of GFP were detected in the hearts at the same time points (Figure 5B).

Next we investigated the long term effects of cell transplantation in *T. cruzi*-infected mice. Groups of mice received weekly i.p. injections of 10^6 MSC – control or Gal-3 knockdown cell line, for five weeks. A vehicle control group was injected with equal volumes of saline solution (Figure 5A). Seven weeks after the beginning of the treatment, mice were euthanized for histological and molecular evaluations.

Histological analysis of heart sections revealed the presence of multifocal inflammatory infiltrates predominantly composed by mononuclear cells in *T. cruzi*-infected mice (Figure 5C-F). We did not detect statistically significant changes in the number of inflammatory cells infiltrating the heart among the groups, as measured by morphometry (Figure 6G). The gene expression levels PTPRC – which encodes for CD45, a pan-leukocyte marker - in heart samples, were decreased in the hearts of mice treated with wild type MSC, but not with Gal-3 knockdown MSC (Figure 5H). Similarly, treatment with wild type MSC, but not with Gal-3 knockdown MSC, reduced the expression of genes in the heart which are associated with inflammation, such as TNF-α, IL-6 and IL-1β (Figure 6). The levels of expression of IFN-γ were not modulated by wild type MSC treatment, however, the expression of the transcription factor T-bet, associated with Th1 responses, was significantly reduced by treatment with wild-type MSC. Interestingly, treatment with Gal-3 knockdown MSC did not reduce T-bet expression, and increased significantly the expression of IFN-γ (Figure 6). The gene expression of the anti-inflammatory cytokine IL-10 was found to be increased in the group treated with wild type MSC, but not with Gal-3 knockdown MSC.

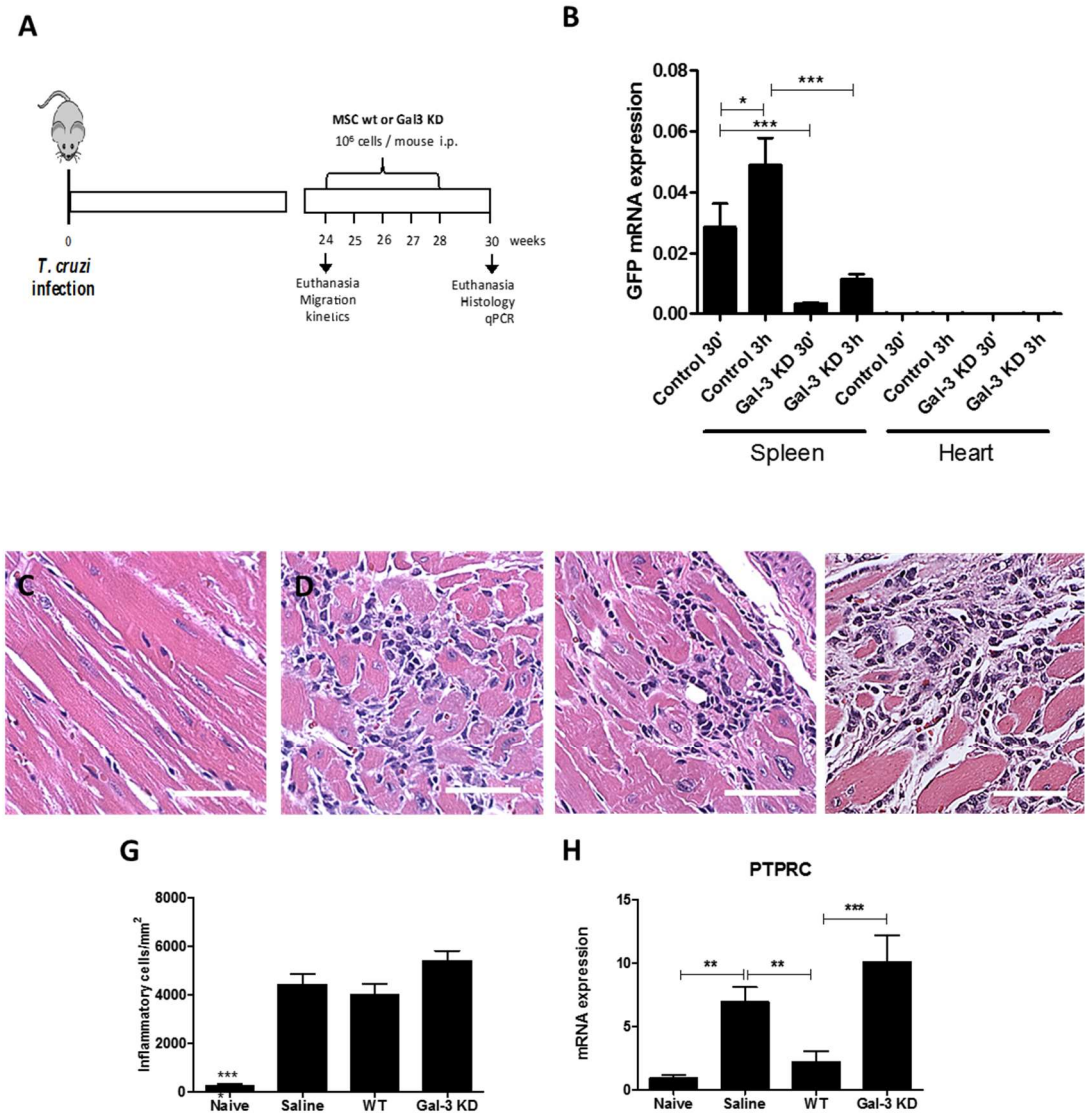

Figure 5. Modulation of inflammation and cell migration by wild type and Gal-3 knockdown MSC in *T. cruzi* infected mice. (A) Study design. (B) Cell migration and homing to spleens and hearts was evaluated by amplification of GFP mRNA by qRT-PCR. (C-F) Representative images of H&E stained heart sections of naïve mice (C), infected and administered with saline (D), wild type MSC (E) or Gal-3 knockdown MSC (F). Quantification of infiltrating inflammatory cells by morphometry (G) and mRNA expression levels of CD45 coding gene (CD45), evaluated qRT-PCR (H). ***P*<0.01; ****P*<0.001.

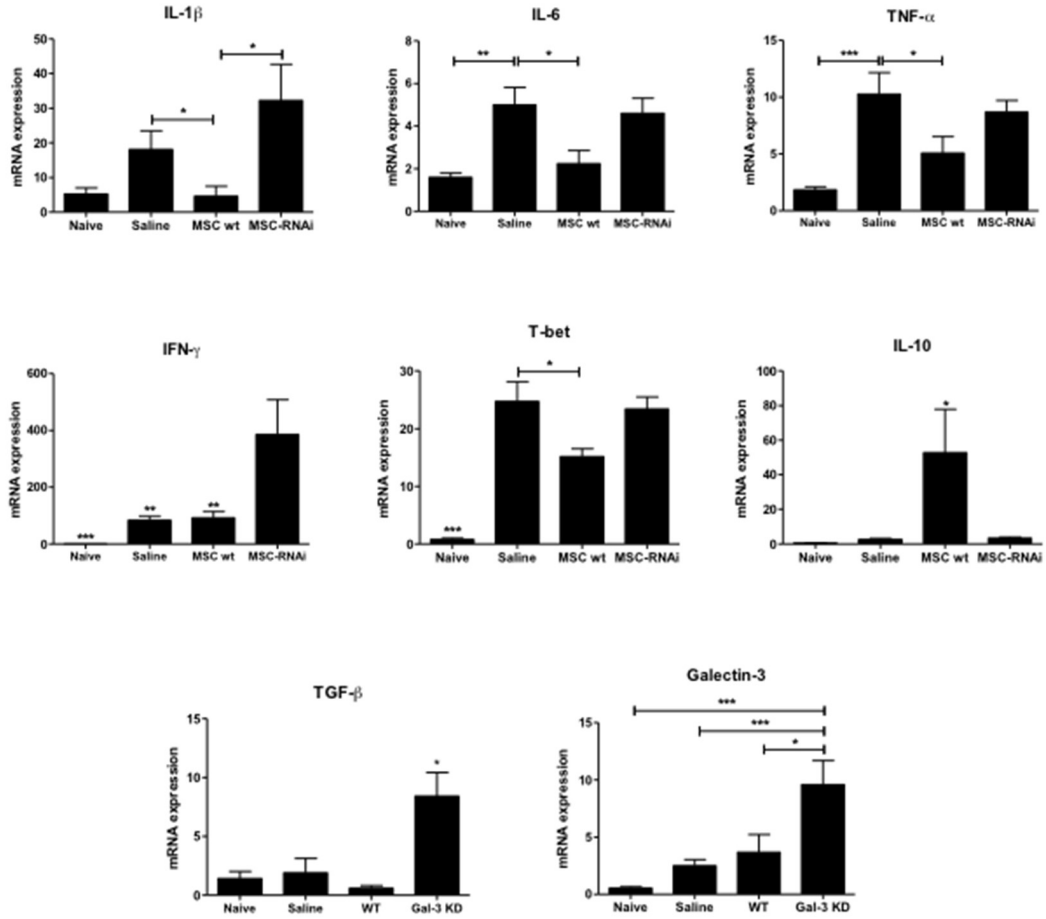

Figure 6. Modulation of gene expression in the hearts of *T. cruzi* infected mice after transplantation of MSC. RTqPCR analysis of gene expression in the heart tissue of the cytokines TNF-α, IL1-β, IL-6, IFN-γ, IL-10 and TGF-β, Th1-associated transcription factor T-bet, and Galectin-3. * $P<0.05$; ** $P<0.01$; *** $P<0.001$.

The analysis of Sirius red-stained heart sections of *T. cruzi*-infected mice showed extensive areas of fibrosis (Figure 7A-C). Wild type MSC reduced the percentage of fibrosis when compared to saline-treated control mice (Figure 8D). In contrast, a significant increase in fibrosis was observed in the group treated with Gal-3 knockdown MSC (Figure 7D). Similarly, collagen type I (COL1A1) gene expression was reduced by wild type MSC, but not by Gal-3 knockdown MSC (Figure 8E). The transcriptional levels of TGF-β, and Gal-3 (LGALS3), two genes associated with the repair process and fibrosis, were also evaluated. Similar expression levels of TGF-β and Gal-3 were found when saline and wild type MSC-treated mice were compared (Figure 7). Transplantation of Gal-3 knockdown MSC, however, significantly increased the expression of Gal-3 and TGFβ in the hearts of *T. cruzi*-infected mice (Figure 6).

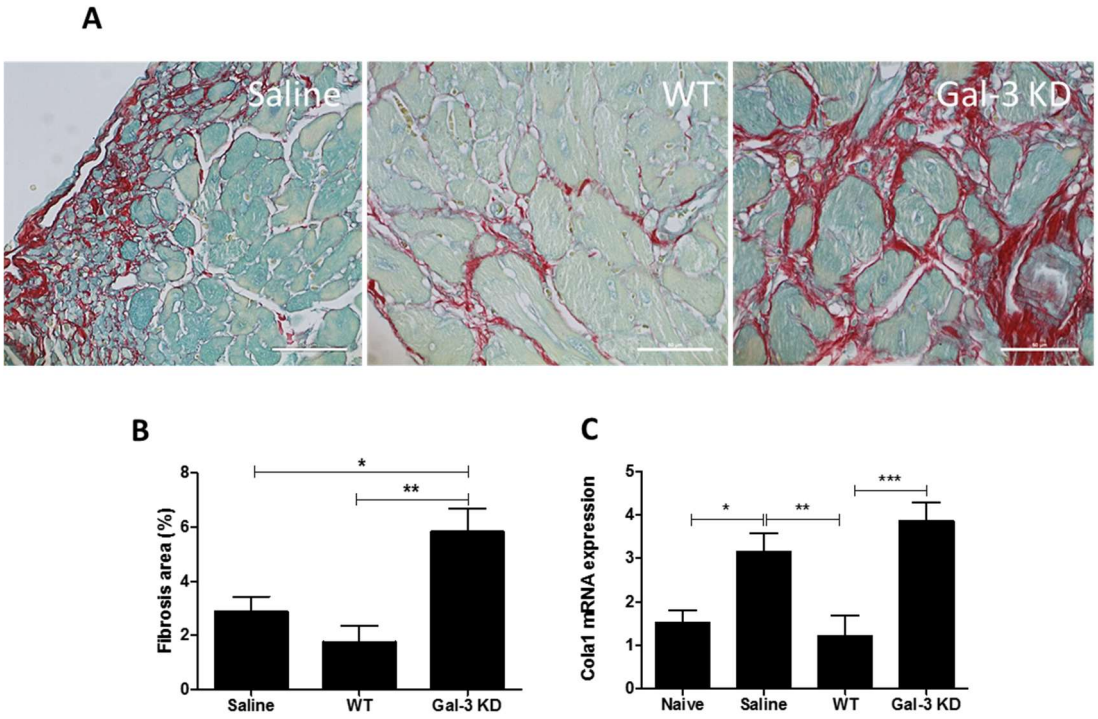

Figure 7. Modulation of collagen synthesis and cardiac fibrosis after administration of MSC. (A) Representative images of Sirius red stained heart sections of *T. cruzi* infected mice administered with saline, wild type MSC (WT) or Gal-3 knockdown MSC (Gal-3 KD). (B) Quantification of the cardiac fibrosis area by morphometry. (C) Type I collagen (Col1a1) gene expression analysis by qRT-PCR in the heart tissue. * $P<0.05$; ** $P<0.01$; *** $P<0.001$.

Discussion

Gal-3 is a multifunctional lectin with diverse, concordant and occasionally opposing actions, when expressed by different cell types and either in extracellular or intracellular compartments (KRZEŚLAK & LIPIŃSKA, 2004). Adhesion, proliferation and migration are processes that are consistently favored by Gal-3 expression in different cell types, and increased Gal-3 expression play a role in migration and invasion by neoplastic cells (FORTUNA-COSTA *et al.*, 2014). In the present study we showed that Gal-3 knockdown in MSC was associated with decreased migration and proliferative capacity. These results are in accordance with a recent study using bone marrow-derived MSC obtained from miniature pigs (GAO *et al.*, 2016).

The process of migration and homing of MSC to areas of inflammation is still poorly understood and may involve different adhesion molecules, chemokines and receptors, such as the CXCR4/SDF-1 axis (LEIBACHER *et al.*, 2016). Gal-3 was recently found to promote

migration of MSC through inhibition of RhoA-GTP activity, enhancement of p-AKT (ser473) expression, and regulation of p-Erk1/2 levels (GAO *et al.*, 2016). Based on these data and in our findings, it is reasonable to suggest that Gal-3 plays a significant role in MSC migration and homing, which could have several implications in a cell transplantation setting. Considering that decreased migration and engraftment can result in decreased therapeutic effects and poor outcomes, evaluation of Gal-3 expression could potentially be applied as a predictive biomarker, as part of the quality control on cell preparations to be therapeutically applied, but this merits further investigation.

In the chronic Chagas disease model, Gal-3 expression by MSC was associated with increased migration from the peritoneal cavity to the spleen. The spleen was also characterized as a reservoir for inflammatory monocytes that emigrate from the subcapsular red pulp and populate inflammatory sites (SWIRSKI et al., 2009). By reaching the spleens, MSC may be able to exert immunomodulatory actions, with systemic repercussions, as observed previously in another experimental model (ACOSTA *et al.*, 2015). Besides regulating lymphocyte populations, MSC also were shown to promote expansion of regulatory populations of monocytes and granulocytes, known as myeloid-derived suppressor cells (MDSC), through HGF secretion (YEN *et al.*, 2013). By migrating to heart tissues of *T. cruzi* mice, MDSC were shown to suppress T lymphocytes present in the infiltrate (CUERVO et al., 2011). Indeed, i.p. transplanted MSC showed negligible migration to the heart, but were still able to promote immunomodulation with detectable effects in the heart disease. In mice transplanted with Gal-3 knockdown MSC, however, in which a reduced cell migration to the spleens was observed, inflammation and fibrosis remained at the level of saline controls or even worsened.

Gal-3 knockdown did not affect the immunophenotype or differentiation potential of MSC, but was associated with an impaired ability to promote immunomodulatory actions, both *in vitro* and *in vivo*. This finding is in accordance with previous publications showing that secretion of Gal-3 by human cord blood or bone marrow derived MSC modulates T cell responses in mixed lymphocyte reaction (SIOUD *et al.*, 2010; SIOUD *et al.*, 2011).

During the chronic phase of Chagas disease cardiomyopathy, different mechanisms are associated with the exacerbated immune response found in the heart, including parasite persistence and autoimmunity (SOARES *et al.*, 2001). The ability of transplanted MSC to decrease cardiac inflammation in experimental CCC in mice was shown before in studies that applied systemic and local delivery routes for cell transplantation (LAROCCA *et al.*, 2013; SILVA *et al.*, 2014; MELLO *et al.*, 2015). Here we demonstrated that transplanted MSC caused downregulation of inflammatory cytokines directly involved in the disease pathogenesis, such

as TNF-α and IFN-γ. (SOARES *et al.*, 2001). Moreover, MSC were able to induce the expression of the anti-inflammatory cytokine IL-10 in the cardiac tissue. The immunomodulatory effects observed in the heart tissue were not associated with a high recruitment and homing of MSC to the cardiac tissue, favoring the hypothesis that these cells exert a systemic modulatory action at lymphoid organs such as the spleen, where we did observe migration of MSC. This is corroborated by our finding that Gal-3 knockdown MSC had a significantly lower migration efficiency to the spleen and exerted a lower immunomodulatory action than wild-type MSC.

Conflicting results in clinical trials aiming immunomodulation by MSC transplantation in different immune-mediated diseases, which were described to be either completely or partially controlled, unaltered, or even worsened in some cases (MA *et al.*, 2014). Current knowledge recognizes that MSC respond to the surrounding microenvironment by polarizing into a pro-inflammatory – MSC1 – phenotype or an anti-inflammatory – MSC2 – phenotype (WATERMAN *et al.*, 2010). Further studies are needed in order to better clarify the mechanisms that guide MSC polarization and interactions with immune cells and to investigate whether Gal-3 plays a role in this process.

In conclusion, our data that reinforces an important role of Gal-3 as a mediator of immunomodulatory actions of MSC *in vitro* and *in vivo* in a chronic inflammatory model of Chagas disease cardiomyopathy, by regulating the ability of MSC to modulate T cell activation, and by promoting cell migration and homing after systemic transplantation.

Acknowledgements

This work was supported by funding from CNPq, FAPESB, and FINEP.

References

Acosta SA, Tajiri N, Hoover J, Kaneko Y, Borlongan CV. Intravenous Bone Marrow Stem Cell Grafts Preferentially Migrate to Spleen and Abrogate Chronic Inflammation in Stroke. Stroke. 2015 Sep;46(9):2616-27.

Acosta-Rodríguez, E. V. *et al*. Galectin-3 mediates IL-4-induced survival and differentiation of B cells: functional cross-talk and implications during *Trypanosoma cruzi* infection. J Immunol, v. 172, n. 1, p. 493-502, Jan 2004.

Cuervo H, Guerrero NA, Carbajosa S, Beschin A, De Baetselier P, Gironès N, Fresno M. Myeloid-derived suppressor cells infiltrate the heart in acute *Trypanosoma cruzi* infection. J Immunol. 2011 Sep 1;187(5):2656-65.

Dominici M, Le Blanc K, Mueller I, Slaper-Cortenbach I, Marini F, Krause D, Deans R, Keating A, Prockop Dj, Horwitz E. Minimal criteria for defining multipotent mesenchymal stromal cells. The International Society for Cellular Therapy position statement. Cytotherapy. 2006;8(4):315-7.

Fortuna-Costa A, Gomes AM, Kozlowski EO, Stelling MP, Pavão MS. Extracellular galectin-3 in tumor progression and metastasis. Front Oncol. 2014 Jun 16;4:138.

Friedenstein AJ, Chailakhjan RK, Lalykina KS. The development of fibroblast colonies in monolayer cultures of guinea-pig bone marrow and spleen cells. Cell Tissue Kinet. 1970 Oct;3(4):393-403.

Gao X, Balan V, Tai G, Raz A. Galectin-3 induces cell migration via a calcium-sensitive MAPK/ERK1/2 pathway. Oncotarget. 2014 Apr 30;5(8):2077-84.

Gao F, Chiu SM, Motan DA, Zhang Z, Chen L, Ji HL, Tse HF, Fu QL, Lian Q. Mesenchymal stem cells and immunomodulation: current status and future prospects. Cell Death Dis. 2016 Jan 21;7:e2062.

Henderson, N. C. *et al*. Galectin-3 regulates myofibroblast activation and hepatic fibrosis. Proc Natl Acad Sci U S A, v. 103, n. 13, p. 5060-5, Mar 2006.

Kleshchenko, Y. Y. *et al*. Human galectin-3 promotes *Trypanosoma cruzi* adhesion to human coronary artery smooth muscle cells. Infect Immun, v. 72, n. 11, p. 6717-21, Nov 2004.

Kolatsi-Joannou, M. *et al*. Modified citrus pectin reduces galectin-3 expression and disease severity in experimental acute kidney injury. PLoS One, v. 6, n. 4, p. e18683, 2011. ISSN 1932-6203.

Krześlak A, Lipińska A. Galectin-3 as a multifunctional protein. Cell Mol Biol Lett 2004, 9:305-328.

Larocca, T. F. *et al*. Transplantation of adipose tissue mesenchymal stem cells in experimental chronic chagasic cardiopathy. Arq Bras Cardiol, v. 100, n. 5, p. 460-8, May 2013.

Leibacher J. & Henschler R. Biodistribution, migration and homing of systemically applied mesenchymal stem/stromal cells. Stem Cell Res Ther. 2016; 7: 7.

Ma S, Xie N, Li W, Yuan B, Shi Y, Wang Y. Immunobiology of mesenchymal stem cells. Cell Death Differ. 2014 Feb;21(2):216-25.

Mackinnon, A. C. *et al*. Regulation of transforming growth factor-β1-driven lung fibrosis by galectin-3. Am J Respir Crit Care Med, v. 185, n. 5, p. 537-46, Mar 2012.

Mello DB, Ramos IP, Mesquita FC, Brasil GV, Rocha NN, Takiya CM, Lima AP, Campos de Carvalho AC, Goldenberg RS, Carvalho AB. Adipose Tissue-Derived Mesenchymal Stromal Cells Protect Mice Infected with *Trypanosoma cruzi* from Cardiac Damage through Modulation of Anti-parasite Immunity. PLoS Negl Trop Dis. 2015 Aug 6;9(8):e0003945.

Moody, T. N.; Ochieng, J.; Villalta, F. Novel mechanism that *Trypanosoma cruzi* uses to adhere to the extracellular matrix mediated by human galectin-3. FEBS Lett, v. 470, n. 3, p. 305-8, Mar 2000.

Nunes, M. C. *et al*. Chagas disease: an overview of clinical and epidemiological aspects. J Am Coll Cardiol, v. 62, n. 9, p. 767-76, Aug 2013.

Polli, C. D., *et al.* Monocyte migration driven by galectin-3 occurs though distinct mechanisms involving selective interactions with the extracellular matrix. ISRN Inflamm. 2013; 2013: 259256.

Reignault, L. C. *et al*. Structures containing galectin-3 are recruited to the parasitophorous vacuole containing *Trypanosoma cruzi* in mouse peritoneal macrophages. Parasitol Res, v. 113, n. 6, p. 2323-33, Jun 2014.

Silva, D. N. *et al.* Intramyocardial transplantation of cardiac mesenchymal stem cells reduces myocarditis in a model of chronic Chagas disease cardiomyopathy. Stem Cell Res Ther, v. 5, n. 4, p. 81, 2014.

Silva-Monteiro, E. *et al*. Altered expression of galectin-3 induces cortical thymocyte depletion and premature exit of immature thymocytes during *Trypanosoma cruzi* infection. Am J Pathol, v. 170, n. 2, p. 546-56, Feb 2007.

Sioud, M. New insights into mesenchymal stromal cell-mediated T-cell suppression through galectins. Scand J Immunol, v 73, n. 2, p. 79-84, Feb 2011. ISSN 1365-3083.

Sioud M, Mobergslien A, Boudabous A, Fløisand Y. Evidence for the involvement of galectin-3 in mesenchymal stem cell suppression of allogeneic T-cell proliferation. Scand J Immunol. 2010 Apr;71(4):267-74.

Soares MB, de Lima RS, Rocha LL, Vasconcelos JF, Rogatto SR, dos Santos RR, Iacobas S, Goldenberg RC, Iacobas DA, Tanowitz HB, de Carvalho AC, Spray DC: Gene expression changes associated with myocarditis and fibrosis in hearts of mice with chronic chagasic cardiomyopathy. J Infect Dis 2010, 202:416-426.

Soares, M. *et al*. Reversion of gene expression alterations in hearts of mice with chronic chagasic cardiomyopathy after transplantation of bone marrow cells. Cell Cycle, v. 10, n. 9, p. 1448-55, May 2011.

Soares, M. B.; Pontes-De-Carvalho, L.; Ribeiro-Dos-Santos, R. The pathogenesis of Chagas' disease: when autoimmune and parasite-specific immune responses meet. An Acad Bras Cienc, v. 73, n. 4, p. 547-59, Dec 2001.

Swirski FK, Nahrendorf M, Etzrodt M, Wildgruber M, Cortez-Retamozo V, Panizzi P, Figueiredo JL, Kohler RH, Chudnovskiy A, Waterman P, Aikawa E, Mempel TR, Libby P, Weissleder R, Pittet MJ. Identification of splenic reservoir monocytes and their deployment to inflammatory sites. Science. 2009 Jul 31;325(5940):612-6.

Waterman, R. S. *et al*. A new mesenchymal stem cell (MSC) paradigm: polarization into a pro-inflammatory MSC1 or an Immunosuppressive MSC2 phenotype. PLoS One, v. 5, n. 4, p. e10088, 2010. ISSN 1932-6203.

Yen BL, Yen ML, Hsu PJ, Liu KJ, Wang CJ, Bai CH, Sytwu HK. Multipotent human mesenchymal stromal cells mediate expansion of myeloid-derived suppressor cells via hepatocyte growth factor/c-met and STAT3. Stem Cell Reports. 2013 Jul 25;1(2):139-51.

5 DISCUSSÃO

Durante as fases aguda e crônica da doença, a Gal-3 atua em uma série de processos envolvidos na relação parasito-hospedeiro, que incluem desde mecanismos de infecção até a regulação da resposta imune, fibrose e remodelamento cardíaco (Tabela I; MACKINNON *et al.*, 2012; HENDERSON *et al.*, 2006; KOLATSI-JOANNOU *et al.*, 2011; SHARMA *et al.*, 2004; MOODY *et al.*, 2000; REIGNAULT *et al.*, 2014). O presente estudo traz uma série de evidências que reforçam o envolvimento da Gal-3 na patogênese da doença de Chagas, reforçando a sua participação em processos, incluindo a migração celular, proliferação de fibroblastos e produção de colágeno, produção de fatores fibrogênicos e de mediadores inflamatórios, dentre outros. Portanto, a Gal-3 tem papel importante tanto na inflamação, que causa a descruição progressiva do miocárdio, quanto na fibrose, que são duas características marcantes na CCC.

Nosso grupo reportou, anteriormente, que a expressão gênica de Gal-3 é significativamente aumentada nos corações de camundongos durante a fase crônica da infecção por *T. cruzi* (SOARES *et al.*, 2010; SOARES *et al.*, 2011). No presente estudo, observamos que a expressão de Gal-3 está aumentada no coração ao longo de toda a infecção por *T. cruzi* em camundongos, em concordância com achados de outros trabalhos (FERRER *et al.*, 2014; PINEDA *et al.*, 2015). A correlação entre a intensidade da miocardite e presença de colágeno tipo I, Gal-3 e células α-SMA^{+} também foi descrita em um modelo de infecção por *T. cruzi* em camundongos (FERRER *et al.*, 2014). A Gal-3 também foi implicada no processo de invasão pelo *T. cruzi* (MACHADO *et al.*, 2014; KLESHCHENKO *et al.*, 2004), e a infecção induziu o aumento de expressão de Gal-3 na célula hospedeira (CARDENAS *et al.*, 2010; ACOSTA-RODRÍGUEZ *et al.,* 2004), indicando a sua participação na relação parasito-hospedeiro.

Uma correlação entre os níveis de inflamação e fibrose no coração e a expressão de Gal-3 foram sugeridos anteriormente, e tratamentos capazes de reduzir a miocardite causaram uma redução concomitante na expressão de Gal-3 no coração (FERRER *et al.,* 2014; VASCONCELOS *et al.,* 2013; SOARES *et al.*, 2011; Anexo III). No presente estudo, demonstramos, através de uma análise cinética, que a expressão de Gal-3 se correlaciona com a intensidade do infiltrado inflamatório no coração, apresentando um pico durante a fase aguda da doença, mantendo, em seguida, níveis persistentemente aumentados durante a fase crônica. Também foi observada expressão de Gal-3 por células do infiltrado inflamatório em corações humanos obtidos de indivíduos com CCC avançada que foram submetidos à transplante cardíaco, reforçando a participação da Gal-3 na patogênese da doença de Chagas.

Em nosso modelo experimental, não observamos uma correlação entre o nível de fibrose e a expressão de Gal-3. Estes dados estão de acordo com os resultados de outros estudos, em que foi demonstrado, através de análises em tecido cardíaco obtido de indivíduos com ICC de diferentes causas, que a expressão cardíaca de Gal-3 não se associa com o conteúdo de fibrose no coração (LOPEZ *et al.*, 2015). Em estudo de corte transversal realizado pelo nosso grupo, os níveis séricos de Gal-3 também não se correlacionaram com o percentual de fibrose cardíaca, mensurado por ressonância magnética, em indivíduos com miocardiopatia chagásica crônica (NOYA-RABELO *et al.*, no prelo; Anexo I). De fato, no modelo experimental utilizado no presente estudo, foi observado que o pico de expressão de Gal-3 precedeu o aumento de tecido fibroso no coração. Estes achados, apesar de afastarem a potencial utilidade de Gal-3 como um biomarcador de fibrose miocárdica estabelecida, não afastam sua utilização como alvo terapêutico, tendo em vista o seu papel em processos relacionados à fibrogênese.

Foi descrito previamente que a Gal-3 é expressa por células do sistema imune e participa de diferentes aspectos das respostas imunes inata e adaptativa (HENDERSON *et al.*, 2009; HSU *et al.*, 2000; JEON *et al.*, 2010; MACKINNON *et al.*, 2008; YANG *et al.*, 1996; CHEN *et al.*, 2015). No presente estudo, foram analisadas diferentes populações celulares que expressam Gal-3, no coração de animais cronicamente infectados por *T. cruzi*. As principais populações celulares encontradas que expressam Gal-3 são macrófagos, linfócitos T, fibroblastos e fibrócitos. A Gal-3 também teve sua expressão aumentada em macrófagos após ativação com estímulos inflamatórios *in vitro*. Estímulos inflamatórios, incluindo elevada expressão de citocinas pró-inflamatórias, como IFN-γ e TNF-α, estão presentes nos corações na fase crônica da infecção por *T. cruzi*, o que justifica níveis de Gal-3 consistentemente aumentados nos macrófagos *in vivo* (SOARES *et al.*, 2001; SHARMA *et al.*, 2004).

Em nosso trabalho, a infecção por *T. cruzi* aumentou a expressão da Gal-3 em fibroblastos cardíacos e, ainda mais intensamente, em uma população de fibrócitos derivadas da medula óssea. Embora fibroblastos cardíacos tenham sido classicamente descritos como o tipo de célula mais importante envolvida na fibrose cardíaca, diferentes estudos mostram que fibrócitos derivadas de medula óssea desempenham papéis importantes na fibrogênese e remodelamento cardíaco (CHU *et al.,* 2010; VAN AMERONGEN *et al.,* 2008; HAUDEK *et al.,* 2010). Observamos que a Gal-3 regula diversos processos celulares em fibroblastos, uma vez que o bloqueio da expressão da Gal-3 nessas células foi associado a uma redução na taxa de proliferação, ao aumento de apoptose e à redução na síntese de colágeno. Estes resultados estão de acordo com dados da literatura (SHARMA *et al.,* 2004; GONZÁLEZ *et al.,* 2014; YU *et al.,* 2013). Uma vez que a adição Gal-3 recombinante ao meio de cultura induziu o aumento

na taxa de proliferação celular apenas em concentrações elevadas, é provável que a Gal-3 intracelular desempenha um papel mais importante na regulação do ciclo celular em fibroblastos do que a extracelular. De fato, foi previamente demonstrado que a Gal-3 intracelular aumenta a atividade do promotor de ciclina D1 (SHIMURA *et al.*, 2004), o que se correlaciona com o resultado deste estudo, que demonstra a redução de proliferação celular associada à diminuição da expressão do gene da ciclina D1 em fibroblastos nos quais foi feito bloqueio da expressão de Gal-3.

Os resultados encontrados são compatíveis com o modelo que liga a expressão aumentada de Gal-3, induzida após uma lesão, por estímulos inflamatórios e pela própria infecção por *T. cruzi*, com o desencadeamento de uma resposta de reparo tecidual, dependente da proliferação, sobrevivência e síntese de matriz por fibroblastos (Figura 4). Consistentemente com o modelo proposto, o bloqueio farmacológico *in vivo*, utilizando o N-Lac, um ligante de Gal-3, causou a redução de fibrose e do número de células inflamatórias infiltrantes no coração de camundongos cronicamente infectados por *T. cruzi*. Além disso, a expressão gênica de diferentes mediadores inflamatórios também foi modulada significativamente nos animais tratados com N-Lac. Foi observada diminuição da expressão de citocinas e marcadores de diferentes subtipos de linfócitos, Th1, Th2 e Treg. É importante ressaltar que os níveis de TNF-α e IFN-γ, duas citocinas pró-inflamatórias com papel na CCC já comprovado (SOARES *et al.*, 2001), estavam reduzidos, enquanto que a citocina anti-inflamatória IL-10 manteve-se aumentada, quando comparada aos níveis de camundongos naive.

A utilização de inibidores farmacológicos, em comparação a modelos genéticos, traz algumas vantagens, como a possibilidade de realizar inferências, quanto do desenvolvimento de drogas. Há, no entanto, algumas desvantagens, como é o caso do nível de seletividade, já que inibidores farmacológicos podem não ser totalmente específicos, atuando, assim, em outros alvos, dificultando a interpretação dos resultados. Este é o caso dos inibidores de galectinas, que são derivados de açucares, já que existe uma alta homologia entre as regiões de ligação a carboidrato entre os membros da familía de galectinas (BLANCHARD *et al.*, 2014). A capacidade e a força da ligação entre a Gal-3 e o N-Lac foi demonstrada previamente (VON MACH *et al.*, 2014). Além disso, outros dois estudos utilizaram N-Lac, em esquema posológico e via semelhantes ao aplicado no presente estudo, com o objetivo de inibir a Gal-3 em modelos experimentais de miocardite viral e miocardiopatia hipertensiva (JAQUENOD DE GIUSTI *et al.*, 2015; YU *et al.*, 2013). Outros inibidores de Gal-3, também derivados de açúcares, que estão sendo estudados e se encontram em fase de desenvolvimento pré-clínico ou clínico,

principalmente visando ao tratamento de câncer ou fibrose, são protegidos por patente e ainda não estão disponíveis comercialmente (BLANCHARD *et al.*, 2014).

Já a utilização de modelo genético, através de camundongos Gal-3 *knockout* constitutivos, pode ser considerada inadequada para investigação de aspectos relacionados à fase crônica da infecção, tendo em vista que a ausência de Gal-3 interfere na própria infecção por *T. cruzi*, comprometendo o modelo experimental. A Gal-3 é uma das moléculas utilizadas pelo *T. cruzi* para adesão, migração, ligação à membrana da célula hospedeira, invasão e evasão do vacúolo parasitóforo (MACHADO *et al.*, 2014; KLESHCHENKO *et al.*, 2004). Deste modo, a utilização camundongos Gal-3 *knockout* poderia levar à redução de inflamação e fibrose cardíaca como resultado de uma menor infectividade do *T. cruzi*. De fato, foi demonstrado que camundongos Gal-3 *knockout* apresentam menor intensidade de fibrose e inflamação no coração após a infecção por *T. cruzi* (PINEDA *et al.*, 2015). Uma possibilidade interessante seria a utilização de camundongos com *knockout* induzível, com os quais seria possível bloquear geneticamente a expressão da Gal-3 apenas na fase crônica da infecção por *T. cruzi*. No entanto, esta linhagem de camundongos ainda não foi desenvolvida até o momento.

Dependendo do tipo celular e da localização, a Gal-3 pode apresentar funções diversas, concordantes e, eventualmente, opostas (KRZEŚLAK *et al.*, 2004). Adesão, proliferação e migração são processos celulares consistentemente favorecidos pela expressão de Gal-3, em diferentes tipos de célula e cenários fisiológicos e patológicos (YANG & LIU, 2003). No presente estudo, observamos que o bloqueio da expressão de Gal-3 se associou à redução da capacidade migratória de leucócitos e de MSC *in vitro* e *in vivo*, no contexto da infecção crônica experimental por *T. cruzi*. A redução do infiltrado de células inflamatórias no coração dos animais infectados foi observada após a inibição farmacológica da Gal-3 com N-Lac. Estes dados sugerem que o aumento da expressão de Gal-3 no coração durante a infecção por *T cruzi* desempenha um papel importante no recrutamento e migração de células para o tecido lesionado.

As funções descritas para a Gal-3 na biologia das células T incluem a promoção da sobrevivência, proliferação e migração celular (TRIBULATTI *et al.*, 2012). Apesar da Gal-3 ter sido previamente associada à modulação da polarização Th1/Th2, os resultados do presente estudo são consistentes com uma redução dos diferentes subtipos de linfócitos no coração, provavelmente resultante de um bloqueio sobre a migração de células para o tecido cardíaco. Através de estudos *in vitro*, observamos a redução da migração, mas não da proliferação de linfócitos, pelo inibidor N-Lac, o que indica que a redução da inflamação nos corações de camundongos infectados e tratados com N-Lac é principalmente devida a uma redução da

migração celular. A Gal-3 estimula a migração de leucócitos através de um processo de haptotaxia, caracterizado como um movimento controlado pelas forças e arranjos de adesão (DANELLA POLLI *et al.*, 2013). A redução na migração leucocitária para o coração dos animais infectados é uma possível explicação para os resultados obtidos, já que os infiltrados de células inflamatórias no coração promovem danos imuno-mediados persistentes, o que desencadeia uma resposta fibrogênica progressiva na CCC (SOARES *et al.*, 2001).

Estudos anteriores revelaram um papel da Gal-3 no processo de remodelamento cardíaco em diferentes configurações experimentais, incluindo modelos experimentais de cardiomiopatia hipertrófica e infarto do miocárdio (SHARMA *et al.*, 2004; GONZÁLEZ *et al.*, 2014; YU *et al.*, 2013). No modelo utilizado no presente estudo não foram observadas alterações morfológicas cardíacas através de análises por ecocardiografia. No entanto, é encontrada uma elevada frequência de arritmias graves, o que torna este modelo experimental mais próximo da forma cardíaca arrítmica do que da forma cardíaca dilatada, não permitindo, assim, a avaliação de um possível papel da Gal-3 no remodelamento cardíaco na CCC.

Apesar dos resultados benéficos observados à nível histológico e das análises de expressão gênica, não foi observada uma melhora nas arritmias já estabelecidas após o bloqueio farmacológico com N-lac. De fato, a fibrose miocárdica contribui, mas não é o único determinante do desenvolvimento de arritmias na CCC. De fato, a ausência de correlação entre níveis de fibrose miocárdica e gravidade de arritmias na doença de Chagas foi demonstrada recentemente em pacientes (GADIOLI *et al.*, 2016). O desenvolvimento de arritmias envolve outros processos, dentre os quais foram apontados como determinantes os níveis de expressão reduzidos de conexina-43 e presença de disautonomia (JUNQUEIRA JR, 2012; DE CARVALHO *et al.*, 1994). No entanto, não pode ser excluída a possibilidade de haver benefícios funcionais após o bloqueio farmacológico de Gal-3 em mais longo prazo ou, ainda, se realizado em uma fase mais precoce da infecção, como forma de prevenção da deterioração da função cardíaca.

Uma possibilidade interessante para correlacionar a redução de inflamação e fibrose a melhoras funcionais cardíacas seria associar o bloqueio de Gal-3 a outras estratégias terapêuticas, utilizando células ou moléculas com efeito trófico que participam naturalmente do reparo e regeneração tecidual na doença de Chagas. Previamente, demonstramos que o coração de animais cronicamente infectados com *T. cruzi* expressa altos níveis de quimiocinas, tais como SDF-1, MCP-1, -2 e -3, recrutando diversos tipos celulares derivados da medula óssea, incluindo as MSC (SOUZA *et al.*, 2014). Estas células derivadas da medula óssea participam do processo de reparo e regeneração tecidual na infecção por *T. cruzi*, conforme demonstrado

através da utilização de camundongos quiméricos transplantados com medula óssea provenientes de camundongos transgênicos para a proteína fluorescente verde (GFP). Estes dados sugerem um papel das MSC endógenas na resposta do hospedeiro à infecção por *T. cruzi*, através de mecanismos imunomodulatórios e de reparo tecidual. Esta afirmação é válida para outras doenças que afetam o músculo cardíaco e esquelético. Em pacientes com miocardite aguda viral, também foi observado o recrutamento de MSC circulantes para o coração (SCHMIDT-LUCKE *et al.*, 2015). Em modelo experimental de distrofia muscular Duchenne, de modo similar, foi demonstrado o recrutamento de MSC circulantes endógenas para colaborar com a regeneração muscular (FUJITA *et al.*, 2015).

Além das evidências de que MSC são naturalmente recrutadas e participam da resposta à infecção por *T. cruzi*, alguns estudos utilizaram terapeuticamente estas células de modo a avaliar que processos seriam regulados pelas MSC transplantadas. A capacidade das MSC transplantadas em diminuir a miocardite em modelo experimental de CCC em camundongos foi demonstrada utilizando as vias de administração sistêmica e local para o transplante das células (LAROCCA *et al.*, 2013; SILVA *et al.*, 2014; MELLO *et al.*, 2015).

O processo de migração e *homing* de MSC para áreas de inflamação não é totalmente elucidado e pode envolver diferentes moléculas de adesão, quimiocinas e receptores, com destaque para o eixo CXCR4/SDF-1 (DONG *et al.*, 2012; LEIBACHER *et al.*, 2016). No presente estudo, foi demonstrado que o bloqueio da expressão de Gal-3 em MSC se associou a uma diminuição da migração e capacidade proliferativa. Estes resultados estão de acordo com um estudo recente usando MSC derivadas da medula óssea obtidas a partir de porcos miniatura (GAO *et al.*, 2016). Este estudo demonstrou que Gal-3 promove a migração de MSC através da inibição da atividade RhoA-GTP, aumentando a expressão de p-AKT (Ser473), e regulando os níveis de p-ERK1/2 (GAO *et al.*, 2014). Com base nestes dados, é razoável afirmar que Gal-3 favorece a migração e *homing* das MSC, o que pode ter diversas implicações no contexto da terapia celular. A diminuição da migração e da enxertia pode resultar em ausência de efeitos terapêuticos ou resultados insatisfatórios. Consequentemente, é possível que o monitoramento da expressão de fatores relevantes para a migração celular, tais como a expressão de Gal-3, em preparações de células a serem aplicadas terapeuticamente, poderá servir de marcador a ser utilizado como parte do controle de qualidade.

As MSC transplantadas na fase crônica da infecção por *T. cruzi* em camundongos migraram da cavidade peritoneal até o baço. Em camundongos transplantados com MSC *knockdown* para Gal-3, no entanto, foi observada uma migração celular significativamente reduzida. Este achado se associou à perda do efeito terapêutico das MSC sobre parâmetros

relacionados à resposta inflamatória e fibrose cardíaca, que se mantiveram inalteradas ou até pioraram. A migração de MSC para o baço foi demonstrada como uma das etapas necessárias para a ocorrência de ações imunomodulatórias que tenham repercussão sistêmica (ACOSTA *et al.*, 2015).

O baço foi previamente caracterizado como um reservatório de monócitos inflamatórios, que migram da polpa vermelha subcapsular, infiltrando áreas de inflamação, como por exemplo o coração após um infarto do miocárdio induzido experimentalmente (SWIRSKI *et al.*, 2009). As MSC, além de regular populações linfocitárias, também promovem a expansão de populações regulatórias de monócitos e granulócitos, conhecidas como células supressoras derivadas da linhagem mielóide (MDSC), através da secreção de HGF (YEN *et al.*, 2013). A migração de MDSC para os corações de camundongos infectados por *T. cruzi* foi associada à supressão de linfócitos T presentes no infiltrado (CUERVO et al., 2011). No presente estudo, as MSC transplantadas por via i.p. apresentaram baixa migração para o coração, mas ainda assim foram capazes de promover a imunomodulação com efeitos detectáveis na doença cardíaca, sugerindo que estas possam de fato ter exercido um efeito em órgãos linfoides secundários, tais como o baço.

O *knockdown* de Gal-3 não afetou o imunofenótipo ou potencial de diferenciação que caracterizam as MSC, mas foi associado a uma diminuição da capacidade de promover ações imunomoduladoras, tanto *in vitro* como *in vivo*, já que as MSC selvagens induziu uma potente regulação negativa na produção de citocinas inflamatórias diretamente envolvidas na patogênese da doença, tais como TNF-α e IFN-γ (SOARES *et al.*, 2001). Esta descoberta está de acordo com publicações anteriores que mostram que a expressão de Gal-3 pelas MSC humanas derivadas de sangue do cordão umbilical ou da medula óssea é responsável pela inibição de células T em reação mista linfocitária (SIOUD *et al*., 2010; SIOUD *et al*, 2011). Portanto, nossos dados reforçam um papel importante da Gal-3 como regulador intracelular da atividade imunomoduladora de MSC.

A capacidade de MSC de responder diferencialmente ao microambiente circudante pode explicar a variação de resultados obtidos em cenários de terapias celulares. Atualmente, a experiência clínica com transplante de MSC visando imunomodulação em diferentes doenças tem gerado resultados conflitantes, com respostas completas, parciais, ausentes, ou até mesmo piorando o quadro clínico em alguns casos (MA *et al.*, 2014). O conhecimento atual reconhece que MSC respondem ao microambiente em torno pela polarização em um fenótipo pró-inflamatório - MSC1 - ou um fenótipo anti-inflamatório - MSC2 (WATERMAN *et al.*, 2010). Mais estudos são necessários para esclarecer os mecanismos que orientam a polarização das

MSC e suas interações com células do sistema imunológico, assim como para investigar se a Gal-3 desempenha algum papel neste processo.

Apesar de ainda serem necessários estudos aprofundados sobre este tópico, é possível encontrar respaldo científico, por analogia com os achados de estudos envolvendo camundongos Gal-3 *knockout* em diferentes modelos experimentais e estudos com células dendríticas Gal-3 *knockout*. Foi demonstrado previamente que a expressão de Gal-3 em células dendríticas colabora para o controle da magnitude da ativação de células T. A interação entre células dendríticas *knockout* para Gal-3 e linfócitos aumenta a proliferação e liberação de citocinas inflamatórias por linfócitos T *in vitro* e *in vivo* (BREUILH *et al.*, 2007). É possível que a estimulação de células T pelas MSC *knockdown* para Gal-3 seja responsável pela maior atividade inflamatória no coração, com maiores danos imunomediados e, consequentemente, maior deposição de fibrose, que foi observada neste modelo. Previamente, foi relatado que camundongos *knockout* para Gal-3 apresentam respostas polarizadas Th1 em modelos experimentais de dermatite atópica e infecções por *Schistosoma mansoni* e *Toxoplasma gondii* (BERNARDES *et al.*, 2006; SAEGUSA *et al.*, 2009; BREUILH *et al.*, 2007). De modo semelhante, as células dendríticas $Gal3^{-/-}$ transferidas a camundongos em modelo de infecção por *Candida albicans* aumentaram significativamente a produção de citocinas Th1 e Th17 (FERMIN LEE *et al.*, 2013). É possível que, de modo similar ao que ocorre com células dendríticas, a Gal-3 regule a expressão de citocinas e outros fatores responsáveis pelas interações entre MSC e células do sistema imune. Novos estudos serão necessários para explorar esta hipótese.

Tendo em vista que o aumento de expressão de Gal-3 é induzido pelo *T. cruzi* após a infecção, é possível também inferir que a Gal-3 auxilia a sobrevivência do parasito, não se restringindo apenas a facilitar processos relacionados à biologia do parasito, como adesão à MEC, deslocamento, entrada na célula hospedeira e evasão do vacúolo parasitóforo (MACHADO *et al.*, 2014; KLESHCHENKO *et al.*, 2004). O aumento de Gal-3 também parece causar a modulação de aspectos da resposta imune, tais como a inibição da diferenciação de plasmócitos e produção de imunoglobulinas (ACOSTA-RODRÍGUEZ *et al.*, 2004), estímulo à liberação de células imaturas do timo e modulação da secreção de citocinas estimuladas por células dendríticas (SILVA-MONTEIRO *et al.*, 2007). Os dados do presente estudo sugerem que a expressão de Gal-3 pelas MSC na infecção por *T. cruzi* também contribui para a modulação de resposta imune, o que beneficia a sobrevivência do parasito, principalmente na fase aguda (Figura 4). No entanto, na fase crônica, a modulação de uma resposta Th1 promovida por MSC pode contribuir para redução de danos imunomediados ao tecido cardíaco (SOARES

et al., 2001). O benefício da modulação de expressão de Gal-3 em MSC para o tratamento da CCC deverá ser explorado em novos estudos visando a uma melhor compreensão dos mecanismos envolvidos na regulação do potencial de imunomodulação de MSC por Gal-3, e incluindo validações em células humanas.

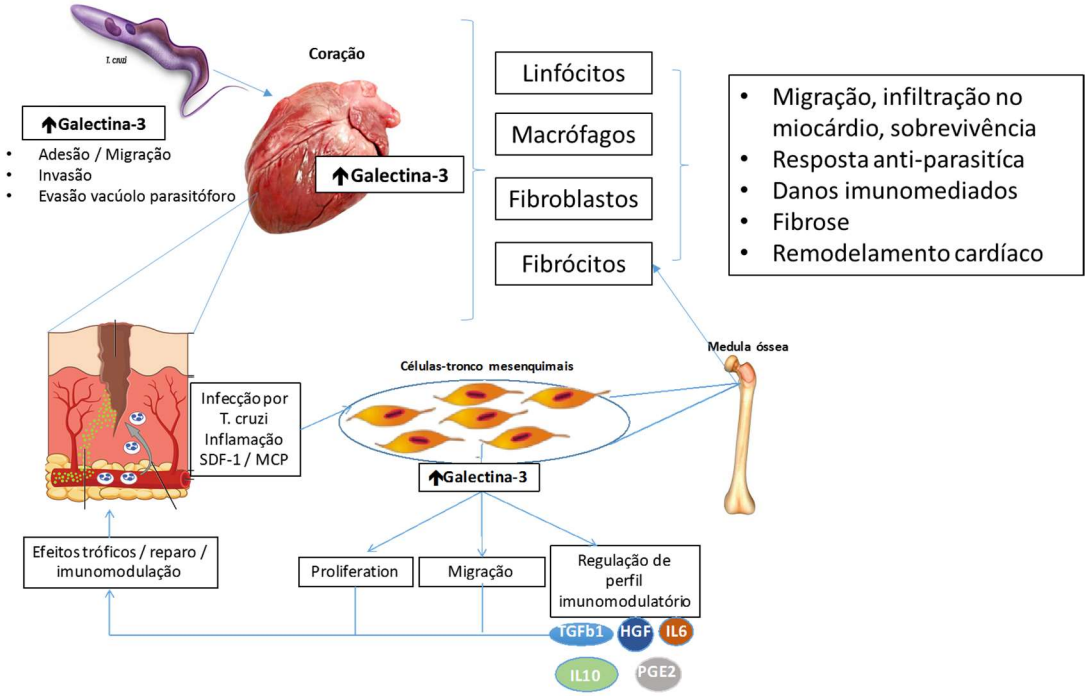

Figura 4: Modelo proposto para participação da Gal-3 na patogênese da doença de Chagas.

6 CONCLUSÃO

O presente estudo demonstra que a Gal-3 desempenha um papel importante na patogênese da doença de Chagas crônica experimental, atuando em diferentes células, contribuindo para o dano imunomediado, uma vez que promove a migração de células inflamatórias para o coração, bem como promovendo fibrose, através de estímulos à proliferação de fibroblastos e síntese de matriz extracelular. A inibição farmacológica de Gal-3 durante a fase crônica da infecção experimental por *T. cruzi* se demonstrou eficaz na redução de inflamação e fibrose cardíaca. Além disso, a expressão de Gal-3 em MSC contribui para que estas células exerçam ações imunomoduladoras no contexto da CCC. Isto é observado pela regulação da capacidade de MSC em modular a ativação de células T e por contribuir para a proliferação e migração celular. O achado de expressão de Gal-3 em amostras de coração humano, com padrão semelhante ao observado no modelo de camundongos, reforça os achados experimentais, sugerindo o envolvimento de Gal-3 na patogênese da doença humana. Deste modo, é possível concluir que a Gal-3 é:

- importante agente promotor de inflamação e fibrose na CCC, atuando em diferentes populações celulares;
- um alvo molecular promissor para o desenvolvimento de novos tratamentos para a CCC visando ao bloqueio da sua ação;
- importante regulador da ação imunomoduladora de MSC in vitro e in vivo.

REFERÊNCIAS

ABE, R. et al. Peripheral blood fibrocytes: differentiation pathway and migration to wound sites. **J. Immunol.,** v. 166, n. 12, p. 755675-62, jun. 2001.

ABEL, L. C. et al. Chronic Chagas' disease cardiomyopathy patients display an increased IFN-gamma response to *Trypanosoma cruzi* infection. **J. Autoimmun.,** v. 17, n. 1, p. 99-107, aug. 2001.

ABOUEZZEDDINE, O. F. et al. Galectin-3 in heart failure with preserved ejection fraction. A RELAX trial substudy (Phosphodiesterase-5 Inhibition to Improve Clinical Status and Exercise Capacity in Diastolic Heart Failure). **JACC Heart Fail.,** v. 3, n. 3, p. 245-252, mar. 2015.

ACOSTA, S. A. et al. Intravenous Bone Marrow Stem Cell Grafts Preferentially Migrate to Spleen and Abrogate Chronic Inflammation in Stroke. **Stroke,** v. 46, n. 9, p. 2616-2267, sep. 2015.

ACOSTA-RODRÍGUEZ, E. V. et al. Galectin-3 mediates IL-4-induced survival and differentiation of B cells: functional cross-talk and implications during *Trypanosoma cruzi* infection. **J. Immunol.,** v. 172, n. 1, p. 493-502, jan. 2004a.

ANDRADE, D. V.; GOLLOB, K. J.; DUTRA, W. O. Acute chagas disease: new global challenges for an old neglected disease. **PLoS Negl. Trop. Dis.,** v. 8, n. 7, p. e3010, 2014.

ANDRADE, J. P. et al. I Latin American Guidelines for the diagnosis and treatment of Chagas' heart disease: executive summary. **Arq. Bras. Cardiol.,** v. 96, n. 6, p. 434-42, jun. 2011.

BAFICA, A. et al. Cutting edge: TLR9 and TLR2 signaling together account for MyD88-dependent control of parasitemia in *Trypanosoma cruzi* infection. **J. Immunol.,** v. 177, n. 6, p. 3515-3519, sep. 2006.

BELLOTTI, G. et al. In vivo detection of *Trypanosoma cruzi* antigens in hearts of patients with chronic Chagas' heart disease. **Am. Heart J.,** v. 131, n. 2, p. 301-307, feb. 1996.

BERN, C. Chagas' Disease. **N. Engl. J. Med.,** v. 373, n. 5, p. 456-466, jul. 2015.

BERN, C. et al. Evaluation and treatment of chagas disease in the United States: a systematic review. **JAMA,** v. 298, n. 18, p. 2171-2181, nov. 2007.

BERNARDES, E. S. et al. *Toxoplasma gondii* infection reveals a novel regulatory role for galectin-3 in the interface of innate and adaptive immunity. **Am. J. Pathol.,** v. 168, n. 6, p. 1910-1920, jun. 2006.

BLANCHARD, H. et al. Galectin-3 inhibitors: a patent review (2008-present). **Expert Opin Ther. Pat.,** v. 24, n. 10, p. 1053-1065, oct. 2014.

BONNEY, K. M.; ENGMAN, D. M. Autoimmune pathogenesis of Chagas heart disease: looking back, looking ahead. **Am. J. Pathol.,** v. 185, n. 6, p. 1537-1547, jun. 2015.

BREUILH, L. et al. Galectin-3 modulates immune and inflammatory responses during helminthic infection: impact of galectin-3 deficiency on the functions of dendritic cells. **Infect. Immun.,** v. 75, n. 11, p. 5148-5157, nov. 2007a.

CAMELLITI, P.; BORG, T. K.; KOHL, P. Structural and functional characterisation of cardiac fibroblasts. **Cardiovasc. Res.,** v. 65, n. 1, p. 40-51, jan. 2005.

CARDENAS, T. C. et al. Regulation of the extracellular matrix interactome by *Trypanosoma cruzi*. **Open Parasitol. J.,** v. 4, p. 72-76, 2010.

CHEN, S. S. et al. Downregulating galectin-3 inhibits proinflammatory cytokine production by human monocyte-derived dendritic cells via RNA interference. **Cell Immunol.,** v. 294, n. 1, p. 44-53, mar. 2015a.

Chagas disease in Latin America: an epidemiological update based on 2010 estimates. **Wkly. Epidemiol. Rec.,** v. 90, n. 6, p. 33-43, feb. 2015.

COHN, J. N.; FERRARI, R.; SHARPE, N. Cardiac remodeling--concepts and clinical implications: a consensus paper from an international forum on cardiac remodeling. Behalf of an International Forum on Cardiac Remodeling. **J. Am. Coll. Cardiol.,** v. 35, n. 3, p. 569-582, mar. 2000.

CORTEGANO, I. et al. Galectin-3 down-regulates IL-5 gene expression on different cell types. **J. Immunol.,** v. 161, n. 1, p. 385-389, jul. 1998.

CRUZ, G. A. S. et al. Assessment of Galectin-3 Polymorphism in Subjects with Chronic Chagas Disease. **Arq. Bras. Cardiol.,** v. 105, n. 5, p. 472-478, nov. 2015.

CUERVO, H. et al. Myeloid-derived suppressor cells infiltrate the heart in acute *Trypanosoma cruzi* infection. **J. Immunol.,** v. 187, n. 5, p. 2656-2665, sep 2011.

DANELLA POLLI, C. et al. Monocyte Migration Driven by Galectin-3 Occurs through Distinct Mechanisms Involving Selective Interactions with the Extracellular Matrix. **ISRN Inflamm.,** v. 2013, p. 259256, 2013.

DE ANDRADE, A. L. et al. Randomised trial of efficacy of benznidazole in treatment of early *Trypanosoma cruzi* infection. **Lancet,** v. 348, n. 9039, p. 1407-1413, nov. 1996

DE CARVALHO, A. C. et al. Conduction defects and arrhythmias in Chagas' disease: possible role of gap junctions and humoral mechanisms. **J. Cardiovasc. Electrophysiol.,** v. 5, n. 8, p. 686-698, aug. 1994.

DE LANGE, F. J. et al. Lineage and morphogenetic analysis of the cardiac valves. **Circ. Res.,** v. 95, n. 6, p. 645-654, sep. 2004.

DE SOUZA, W. Basic cell biology of *Trypanosoma cruzi*. **Curr. Pharm. Des.,** v. 8, n. 4, p. 269-285, 2002.

DEMETRIOU, M. et al. Negative regulation of T-cell activation and autoimmunity by Mgat5 N-glycosylation. **Nature,** v. 409, n. 6821, p. 733-739, feb. 2001.

DEVERA, R.; FERNANDES, O.; COURA, J. R. Should *Trypanosoma cruzi* be called "cruzi" complex? a review of the parasite diversity and the potential of selecting population after in vitro culturing and mice infection. **Mem. Inst. Oswaldo Cruz,** v. 98, n. 1, p. 1-12, jan. 2003. ISSN 0074-0276.

DISTEFANO, G.; SCIACCA, P. Molecular pathogenesis of myocardial remodeling and new potential therapeutic targets in chronic heart failure. **Ital J Pediatr,** v. 38, p. 41, 2012.

DOMINICI, M. et al. Minimal criteria for defining multipotent mesenchymal stromal cells. The International Society for Cellular Therapy position statement. **Cytotherapy,** v. 8, n. 4, p. 315-317, 2006.

DONG, F. et al. Myocardial CXCR4 expression is required for mesenchymal stem cell mediated repair following acute myocardial infarction. **Circulation,** v. 126, n. 3, p. 314-324, jul. 2012.

FAN, D. et al. Cardiac fibroblasts, fibrosis and extracellular matrix remodeling in heart disease. **Fibrog. Tissue Repair,** v. 5, n. 1, p. 15, 2012.

FELDMAN, A. M. et al. The role of tumor necrosis factor in the pathophysiology of heart failure. **J. Am. Coll. Cardiol.,** v. 35, n. 3, p. 537-544, mar. 2000a.

FERMANN, G. J. et al. Galectin 3 complements BNP in risk stratification in acute heart failure. **Biomarkers,** v. 17, n. 8, p. 706-713, dec. 2012.

FERMIN LEE, A. et al. Galectin-3 modulates Th17 responses by regulating dendritic cell cytokines. **Am. J. Pathol.,** v. 183, n. 4, p. 1209-1222, oct. 2013.

FERNÁNDEZ, G. C. et al. Galectin-3 and soluble fibrinogen act in concert to modulate neutrophil activation and survival: involvement of alternative MAPK pathways. **Glycobiology,** v. 15, n. 5, p. 519-527, may. 2005.

FERRER, M. F. et al. DTU I isolates of *Trypanosoma cruzi* induce upregulation of Galectin-3 in murine myocarditis and fibrosis. **Parasitology,** v. 141, n. 6, p. 849-858, may. 2014.

FEUK-LAGERSTEDT, E. et al. Identification of CD66a and CD66b as the major galectin-3 receptor candidates in human neutrophils. **J. Immunol.,** v. 163, n. 10, p. 5592-5598, nov. 1999.

FRIEDENSTEIN, A. J.; CHAILAKHJAN, R. K.; LALYKINA, K. S. The development of fibroblast colonies in monolayer cultures of guinea-pig bone marrow and spleen cells. **Cell Tissue Kinet.,** v. 3, n. 4, p. 393-403, oct. 1970.

FRIGERI, L. G.; ZUBERI, R. I.; LIU, F. T. Epsilon BP, a beta-galactoside-binding animal lectin, recognizes IgE receptor (Fc epsilon RI) and activates mast cells. **Biochemistry,** v. 32, n. 30, p. 7644-7649, aug. 1993.

FUJITA, R. et al. Endogenous mesenchymal stromal cells in bone marrow are required to preserve muscle function in mdx mice. **Stem Cells,** v. 33, n. 3, p. 962-975, mar. 2015.

FUJIU, K.; WANG, J.; NAGAI, R. Cardioprotective function of cardiac macrophages. **Cardiovasc. Res.** v. 102, n. 2, p. 232-239, may. 2014.

GADIOLI, L. P. et al. The severity of ventricular arrhythmia correlates with the extent of myocardial sympathetic denervation, but not with myocardial fibrosis extent in chronic Chagas cardiomyopathy: Chagas disease, denervation and arrhythmia. **J. Nucl. Cardiol.**, jul. 2016.

GAO, F. et al. Mesenchymal stem cells and immunomodulation: current status and future prospects. **Cell Death Dis.,** v. 7, p. e2062, 2016.

GAO, Q. et al. Galectin-3 Enhances Migration of Minature Pig Bone Marrow Mesenchymal Stem Cells Through Inhibition of RhoA-GTP Activity. **Sci. Rep.,** v. 6, p. 26577, 2016.

GAO, X. et al. Galectin-3 induces cell migration via a calcium-sensitive MAPK/ERK1/2 pathway. **Oncotarget,** v. 5, n. 8, p. 2077-2084, apr. 2014.

GIRONÈS, N.; FRESNO, M. Etiology of Chagas disease myocarditis: autoimmunity, parasite persistence, or both? **Trends Parasitol.,** v. 19, n. 1, p. 19-22, jan. 2003.

GOMES, J. A. et al. Evidence that development of severe cardiomyopathy in human Chagas' disease is due to a Th1-specific immune response. **Infect. Immun.,** v. 71, n. 3, p. 1185-1193, mar. 2003.

GONZÁLEZ, G. E. et al. Galectin-3 is essential for early wound healing and ventricular remodeling after myocardial infarction in mice. **Int. J. Cardiol.,** v. 176, n. 3, p. 1423-1425, oct. 2014a.

HAUDEK, S. B. et al. Monocytic fibroblast precursors mediate fibrosis in angiotensin-II-induced cardiac hypertrophy. **J. Mol. Cell. Cardiol.,** v. 49, n. 3, p. 499-507, sep. 2010.

HENDERSON, N. C. et al. Galectin-3 regulates myofibroblast activation and hepatic fibrosis. **Proc. Natl. Acad. Sci. USA,** v. 103, n. 13, p. 5060-5065, mar. 2006.

HIGUCHI, M. L. et al. The role of active myocarditis in the development of heart failure in chronic Chagas' disease: a study based on endomyocardial biopsies. **Clin. Cardiol.,** v. 10, n. 11, p. 665-670, nov. 1987.

HO, J. E. et al. Galectin-3, a marker of cardiac fibrosis, predicts incident heart failure in the community. **J. Am. Coll. Cardiol.,** v. 60, n. 14, p. 1249-1256, oct. 2012

HOLUBARSCH, C. et al. Existence of the Frank-Starling mechanism in the failing human heart. Investigations on the organ, tissue, and sarcomere levels. **Circulation,** v. 94, n. 4, p. 683-689, aug. 1996.

HSU, D. K.; CHEN, H. Y.; LIU, F. T. Galectin-3 regulates T-cell functions. **Immunol. Rev.,** v. 230, n. 1, p. 114-127, jul. 2009.

HULSMANS, M.; SAM, F.; NAHRENDORF, M. Monocyte and macrophage contributions to cardiac remodeling. **J. Mol. Cell. Cardiol.,** v. 93, p. 149-155, apr. 2016.

HUMPHREYS, B. D. et al. Fate tracing reveals the pericyte and not epithelial origin of myofibroblasts in kidney fibrosis. **Am. J. Pathol.,** v. 176, n. 1, p. 85-97, jan. 2010.

HYLAND, K. V. et al. Modulation of autoimmunity by treatment of an infectious disease. **Infect. Immun.,** v. 75, n. 7, p. 3641-3650, jul. 2007.

JACKSON, Y. et al. Tolerance and safety of nifurtimox in patients with chronic chagas disease. **Clin. Infect. Dis.,** v. 51, n. 10, p. e69-75, nov. 2010.

JAGODZINSKI, A. et al. Predictive value of galectin-3 for incident cardiovascular disease and heart failure in the population-based FINRISK 1997 cohort. **Int. J. Cardiol.,** v. 192, p. 33-39, aug. 2015.

JAQUENOD DE GIUSTI, C. et al. Macrophages and galectin 3 play critical roles in CVB3-induced murine acute myocarditis and chronic fibrosis. **J. Mol. Cell. Cardiol.,** v. 85, p. 58-70, aug. 2015.

JEON, S. B. et al. Galectin-3 exerts cytokine-like regulatory actions through the JAK-STAT pathway. **J. Immunol.,** v. 185, n. 11, p. 7037-7046, dec. 2010a.

JOHNSON, F. L. Pathophysiology and etiology of heart failure. **Cardiol. Clin.,** v. 32, n. 1, p. 9-19, feb. 2014.

JOO, H. G. et al. Expression and function of galectin-3, a beta-galactoside-binding protein in activated T lymphocytes. **J. Leukoc. Biol.,** v. 69, n. 4, p. 555-564, apr. 2001.

JUNQUEIRA JR, L. F. Insights into the clinical and functional significance of cardiac autonomic dysfunction in Chagas disease. **Rev. Soc. Bras. Med. Trop.,** v. 45, n. 2, p. 243-252, mar-apr. 2012.

KANIA, G. et al. Heart-infiltrating prominin-1+/CD133+ progenitor cells represent the cellular source of transforming growth factor beta-mediated cardiac fibrosis in experimental autoimmune myocarditis. **Circ. Res.,** v. 105, n. 5, p. 462-470, aug. 2009.

KAPLAN, D. et al. Antibodies to ribosomal P proteins of *Trypanosoma cruzi* in Chagas disease possess functional autoreactivity with heart tissue and differ from anti-P autoantibodies in lupus. **Proc. Natl. Acad. Sci. USA,** v. 94, n. 19, p. 10301-10306, sep. 1997.

KLESHCHENKO, Y. Y. et al. Human galectin-3 promotes *Trypanosoma cruzi* adhesion to human coronary artery smooth muscle cells. **Infect. Immun.,** v. 72, n. 11, p. 6717-6721, nov. 2004.

KOLATSI-JOANNOU, M. et al. Modified citrus pectin reduces galectin-3 expression and disease severity in experimental acute kidney injury. **PLoS One,** v. 6, n. 4, p. e18683, 2011. I

KRENNING, G.; ZEISBERG, E. M.; KALLURI, R. The origin of fibroblasts and mechanism of cardiac fibrosis. **J. Cell Physiol.,** v. 225, n. 3, p. 631-637, nov. 2010.

KRZEŚLAK, A.; LIPIŃSKA, A. Galectin-3 as a multifunctional protein. **Cell. Mol. Biol. Lett.,** v. 9, n. 2, p. 305-328, 2004.

KUWABARA, I.; LIU, F. T. Galectin-3 promotes adhesion of human neutrophils to laminin. **J. Immunol.,** v. 156, n. 10, p. 3939-3944, may. 1996.

KÖBERLE, F. Chagas' disease and Chagas' syndromes: the pathology of American trypanosomiasis. **Adv. Parasitol.,** v. 6, p. 63-116, 1968.

LAROCCA, T. F. et al. Transplantation of adipose tissue mesenchymal stem cells in experimental chronic chagasic cardiopathy. **Arq. Bras. Cardiol.,** v. 100, n. 5, p. 460-468, may. 2013.

LEIBACHER, J.; HENSCHLER, R. Biodistribution, migration and homing of systemically applied mesenchymal stem/stromal cells. **Stem Cell Res. Ther.,** v. 7, p. 7, 2016.

LIE-VENEMA, H. et al. Origin, fate, and function of epicardium-derived cells (EPDCs) in normal and abnormal cardiac development. **Scient. World J.,** v. 7, p. 1777-1798, 2007.

LIN, H. M. et al. Galectin-3 enhances cyclin D(1) promoter activity through SP1 and a cAMP-responsive element in human breast epithelial cells. **Oncogene,** v. 21, n. 52, p. 8001-8010, nov. 2002.

LIU, F. T. et al. Expression and function of galectin-3, a beta-galactoside-binding lectin, in human monocytes and macrophages. **Am. J. Pathol.,** v. 147, n. 4, p. 1016-1028, oct. 1995

LIU, G. Y. et al. Secreted galectin-3 as a possible biomarker for the immunomodulatory potential of human umbilical cord mesenchymal stromal cells. **Cytotherapy,** v. 15, n. 10, p. 1208-1217, oct. 2013.

LOK, D. J. et al. Prognostic value of galectin-3, a novel marker of fibrosis, in patients with chronic heart failure: data from the DEAL-HF study. **Clin Res Cardiol,** v. 99, n. 5, p. 323-328, ,may. 2010.

LÓPEZ, B. et al. Galectin-3 and histological, molecular and biochemical aspects of myocardial fibrosis in heart failure of hypertensive origin. **Eur. J. Heart Fail.,** v. 17, n. 4, p. 385-392, apr. 2015.

MA, S. et al. Immunobiology of mesenchymal stem cells. **Cell Death Differ,** v. 21, n. 2, p. 216-225, feb. 2014a.

MACHADO, F. C. et al. Recruitment of galectin-3 during cell invasion and intracellular trafficking of Trypanosoma cruzi extracellular amastigotes. **Glycobiology,** v. 24, n. 2, p. 179-184, feb. 2014a.

MACKINNON, A. C. et al. Regulation of transforming growth factor-β1-driven lung fibrosis by galectin-3. **Am. J. Respir. Crit. Care Med.,** v. 185, n. 5, p. 537-546, mar. 2012.

MASSA, S. M. et al. L-29, an endogenous lectin, binds to glycoconjugate ligands with positive cooperativity. **Biochemistry,** v. 32, n. 1, p. 260-267, jan. 1993.

MELLO, D. B. et al. Adipose Tissue-Derived Mesenchymal Stromal Cells Protect Mice Infected with Trypanosoma cruzi from Cardiac Damage through Modulation of Anti-parasite Immunity. **PLoS Negl. Trop. Dis.,** v. 9, n. 8, p. e0003945, 2015.

MCEVOY, J. W. et al. Galectin-3 and Risk of Heart Failure and Death in Blacks and Whites. **J. Am. Heart Assoc.,** v. 5, n. 5, 2016.

MIRANDOLA, L. et al. Galectin-3C inhibits tumor growth and increases the anticancer activity of bortezomib in a murine model of human multiple myeloma. **PLoS One,** v. 6, n. 7, p. e21811, 2011.

MOODY, T. N.; OCHIENG, J.; VILLALTA, F. Novel mechanism that *Trypanosoma cruzi* uses to adhere to the extracellular matrix mediated by human galectin-3. **FEBS Lett.,** v. 470, n. 3, p. 305-308, mar. 2000.

MORILLO, C. A. et al. Randomized Trial of Benznidazole for Chronic Chagas' Cardiomyopathy. **N. Engl. J. Med.,** v. 373, n. 14, p. 1295-306, oct. 2015.

MOTRÁN, C. C. et al. Immunization with the C-terminal region of *Trypanosoma cruzi* ribosomal P1 and P2 proteins induces long-term duration cross-reactive antibodies with heart functional and structural alterations in young and aged mice. **Clin. Immunol.,** v. 97, n. 2, p. 89-94, nov. 2000.

NAHRENDORF, M. et al. The healing myocardium sequentially mobilizes two monocyte subsets with divergent and complementary functions. **J. Exp. Med.,** v. 204, n. 12, p. 3037-347, nov. 2007.

NOGUEIRA, L. G. et al. Myocardial gene expression of T-bet, GATA-3, Ror-γt, FoxP3, and hallmark cytokines in chronic Chagas disease cardiomyopathy: an essentially unopposed TH1-type response. **Mediat. Inflamm.,** v. 2014, p. 914326, 2014.

NOVAK, R.; DABELIC, S.; DUMIC, J. Galectin-1 and galectin-3 expression profiles in classically and alternatively activated human macrophages. **Biochim. Biophys. Acta,** v. 1820, n. 9, p. 1383-90, sep. 2012.

NOYA-RABELO, M. M. et al. Evaluation of Galectin-3 as a Novel Biomarker for Chagas Cardiomyopathy. **Cardiology,** v. 136, n. 1, p. 33-39, aug. 2016.

NUNES, M. C. et al. Chagas disease: an overview of clinical and epidemiological aspects. **J Am. Coll. Cardiol.,** v. 62, n. 9, p. 767-776, aug. 2013.

PARK, J. W. et al. Association of galectin-1 and galectin-3 with Gemin4 in complexes containing the SMN protein. **Nucl. Acids Res.,** v. 29, n. 17, p. 3595-3602, sep. 2001.

PEACOCK, W. F. How galectin-3 changes acute heart failure decision making in the emergency department. **Clin. Chem. Lab. Med.,** v. 52, n. 10, p. 1409-1412, oct. 2014.

PENAS, F. et al. Treatment in vitro with PPARα and PPARγ ligands drives M1-to-M2 polarization of macrophages from *T. cruzi*-infected mice. **Biochim. Bioph. Acta,** v. 1852, n. 5, p. 893-904, may. 2015.

PEREZ, C. J.; LYMBERY, A. J.; THOMPSON, R. C. Reactivation of Chagas Disease: Implications for Global Health. **Trends Parasitol.,** v. 31, n. 11, p. 595-603, nov. 2015.

PETROV, V. V.; FAGARD, R. H.; LIJNEN, P. J. Stimulation of collagen production by transforming growth factor-beta1 during differentiation of cardiac fibroblasts to myofibroblasts. **Hypertension,** v. 39, n. 2, p. 258-263, feb. 2002.

PINEDA, M. A. et al. Lack of Galectin-3 Prevents Cardiac Fibrosis and Effective Immune Responses in a Murine Model of *Trypanosoma cruzi* Infection. **J. Infect. Dis.,** v. 212, n. 7, p. 1160-1171, oct. 2015.

PINTO, A. Y. et al. Acute phase of Chagas disease in the Brazilian Amazon region: study of 233 cases from Pará, Amapá and Maranhão observed between 1988 and 2005. **Rev. Soc. Bras. Med. Trop.,** v. 41, n. 6, p. 602-614, 2008 nov-dec. 2008.

POLAT, V. et al. Diagnostic significance of serum galectin-3 levels in heart failure with preserved ejection fraction. **Acta Cardiol.,** v. 71, n. 2, p. 191-197, apr. 2016.

RAIMOND, J. et al. Mapping of the galectin-3 gene (LGALS3) to human chromosome 14 at region 14q21-22. **Mamm. Genome,** v. 8, n. 9, p. 706-707, sep. 1997.

REIFENBERG, K. et al. Interferon-gamma induces chronic active myocarditis and cardiomyopathy in transgenic mice. **Am. J. Pathol.,** v. 171, n. 2, p. 463-72, aug. 2007.

REIGNAULT, L. C. et al. Structures containing galectin-3 are recruited to the parasitophorous vacuole containing *Trypanosoma cruzi* in mouse peritoneal macrophages. **Parasitol. Res.,** v. 113, n. 6, p. 2323-2333, jun. 2014.

REIS, D. D. et al. Characterization of inflammatory infiltrates in chronic chagasic myocardial lesions: presence of tumor necrosis factor-alpha+ cells and dominance of granzyme A+, CD8+ lymphocytes. **Am. J. Trop. Med. Hyg.,** v. 48, n. 5, p. 637-644, may. 1993.

RIBEIRO, A. L. et al. Parasympathetic dysautonomia precedes left ventricular systolic dysfunction in Chagas disease. **Am. Heart J.,** v. 141, n. 2, p. 260-265, feb. 2001.

RIBEIRO DOS SANTOS, R. et al. Cell therapy in Chagas cardiomyopathy (Chagas arm of the multicenter randomized trial of cell therapy in cardiopathies study): a multicenter randomized trial. **Circulation,** v. 125, n. 20, p. 2454-2461, may. 2012.

ROSENBAUM, M. B. CHAGASIC MYOCARDIOPATHY. **Prog Cardiovasc Dis,** v. 7, p. 199-225, nov. 1964.

ROSSI, M. A. Microvascular changes as a cause of chronic cardiomyopathy in Chagas' disease. **Am. Heart J.,** v. 120, n. 1, p. 233-236, jul. 1990.

SAEGUSA, J. et al. Galectin-3 is critical for the development of the allergic inflammatory response in a mouse model of atopic dermatitis. **Am. J. Pathol.,** v. 174, n. 3, p. 922-931, mar. 2009.

SAMUDIO, M. et al. Differential expression of systemic cytokine profiles in Chagas' disease is associated with endemicity of *Trypanosoma cruzi* infections. **Acta Trop.,** v. 69, n. 2, p. 89-97, may. 1998.

SANO, H. et al. Critical role of galectin-3 in phagocytosis by macrophages. **J. Clin. Invest.,** v. 112, n. 3, p. 389-397, aug. 2003.

SANO, H. et al. Human galectin-3 is a novel chemoattractant for monocytes and macrophages. **J. Immunol.,** v. 165, n. 4, p. 2156-2164, aug. 2000.

SATO, S.; HUGHES, R. C. Regulation of secretion and surface expression of Mac-2, a galactoside-binding protein of macrophages. **J. Biol. Chem.,** v. 269, n. 6, p. 4424-4430, feb. 1994.

SCHMIDT-LUCKE, C. et al. Cardiac migration of endogenous mesenchymal stromal cells in patients with inflammatory cardiomyopathy. **Mediat. Inflamm.,** v. 2015, p. 308185, 2015.

SHARMA, U. C. et al. Galectin-3 marks activated macrophages in failure-prone hypertrophied hearts and contributes to cardiac dysfunction. **Circulation,** v. 110, n. 19, p. 3121-3128, nov. 2004.

SHIMURA, T. et al. Galectin-3, a novel binding partner of beta-catenin. **Cancer Res.,** v. 64, n. 18, p. 6363-6367, sep. 2004.

SHIMURA, T. et al. Implication of galectin-3 in Wnt signaling. **Cancer Res.,** v. 65, n. 9, p. 3535-7353, may. 2005.

SILVA, D. N. et al. Intramyocardial transplantation of cardiac mesenchymal stem cells reduces myocarditis in a model of chronic Chagas disease cardiomyopathy. **Stem Cell Res. Ther.,** v. 5, n. 4, p. 81, 2014.

SILVA-MONTEIRO, E. et al. Altered expression of galectin-3 induces cortical thymocyte depletion and premature exit of immature thymocytes during *Trypanosoma cruzi* infection. **Am. J. Pathol.,** v. 170, n. 2, p. 546-556, feb. 2007.

SIOUD, M. et al. Evidence for the involvement of galectin-3 in mesenchymal stem cell suppression of allogeneic T-cell proliferation. **Scand. J. Immunol.,** v. 71, n. 4, p. 267-274, apr. 2010.

SIOUD, M. New insights into mesenchymal stromal cell-mediated T-cell suppression through galectins. **Scand. J. Immunol.,** v 73, n. 2, p. 79-84, feb. 2011.

SOARES, M. et al. Gene expression changes associated with myocarditis and fibrosis in hearts of mice with chronic chagasic cardiomyopathy. **J. Infect. Dis.,** v. 202, n. 3, p. 416-426, aug. 2010.

SOARES, M. et al. Reversion of gene expression alterations in hearts of mice with chronic chagasic cardiomyopathy after transplantation of bone marrow cells. **Cell Cycle,** v. 10, n. 9, p. 1448-1455, may. 2011.

SOARES, M. B.; PONTES-DE-CARVALHO, L.; RIBEIRO-DOS-SANTOS, R. The pathogenesis of Chagas' disease: when autoimmune and parasite-specific immune responses meet. **An. Acad. Bras. Cienc.,** v. 73, n. 4, p. 547-559, dec. 2001.

SOUZA, B. S. et al. Bone marrow cells migrate to the heart and skeletal muscle and participate in tissue repair after Trypanosoma cruzi infection in mice. **Int. J. Exp. Pathol.,** v. 95, n. 5, p. 321-329, oct. 2014.

SOUZA-LIMA, R. E. C. et al. Outbreak of acute Chagas disease associated with oral transmission in the Rio Negro region, Brazilian Amazon. **Rev. Soc. Bras. Med. Trop.,** v. 46, n. 4, p. 510-514, jul-aug 2013a.

SWARTE, V. V. et al. Lymphocyte triggering via L-selectin leads to enhanced galectin-3-mediated binding to dendritic cells. **Eur. J. Immunol.,** v. 28, n. 9, p. 2864-2871, sep. 1998.

SWIRSKI, F. K. et al. Identification of splenic reservoir monocytes and their deployment to inflammatory sites. **Science,** v. 325, n. 5940, p. 612-616, jul. 2009.

TANOWITZ, H. B. et al. Chagas' disease. **Clin. Microbiol. Rev.,** v. 5, n. 4, p. 400-419, oct. 1992.

TARLETON, R. L.; ZHANG, L.; DOWNS, M. O. "Autoimmune rejection" of neonatal heart transplants in experimental Chagas disease is a parasite-specific response to infected host tissue. **Proc. Natl. Acad. Sci. USA,** v. 94, n. 8, p. 3932-3937, apr. 1997.

TOSTES, S. et al. Myocardiocyte apoptosis in heart failure in chronic Chagas' disease. **Int. J. Cardiol.,** v. 99, n. 2, p. 233-237, mar. 2005.

TRIBULATTI, M. V. et al. Redundant and antagonistic functions of galectin-1, -3, and -8 in the elicitation of T cell responses. **J. Immunol.,** v. 188, n. 7, p. 2991-2999, apr. 2012a.

UELAND, T. et al. Galectin-3 in heart failure: high levels are associated with all-cause mortality. **Int. J. Cardiol.,** v. 150, n. 3, p. 361-364, aug. 2011.

VALENTE, S. A. et al. Analysis of an acute Chagas disease outbreak in the Brazilian Amazon: human cases, triatomines, reservoir mammals and parasites. **Trans. R. Soc. Trop. Med. Hyg.,** v. 103, n. 3, p. 291-297, mar. 2009.

VAN AMERONGEN, M. J. et al. Bone marrow-derived myofibroblasts contribute functionally to scar formation after myocardial infarction. **J. Pathol.,** v. 214, n. 3, p. 377-386, feb. 2008.

VAN KIMMENADE, R. R. et al. Utility of amino-terminal pro-brain natriuretic peptide, galectin-3, and apelin for the evaluation of patients with acute heart failure. **J. Am. Coll. Cardiol.,** v. 48, n. 6, p. 1217-1224, sep. 2006.

VASCONCELOS, J. F. et al. Administration of granulocyte colony-stimulating factor induces immunomodulation, recruitment of T regulatory cells, reduction of myocarditis and decrease of parasite load in a mouse model of chronic Chagas disease cardiomyopathy. **FASEB J.,** v. 27, n. 12, p. 4691-4702, dec. 2013.

VILAS-BOAS, F. et al. Early results of bone marrow cell transplantation to the myocardium of patients with heart failure due to Chagas disease. **Arq. Bras. Cardiol.,** v. 87, n. 2, p. 159-166, aug. 2006.

VON MACH, T. et al. Ligand binding and complex formation of galectin-3 is modulated by pH variations. **Biochem. J.,** v. 457, n. 1, p. 107-115, jan. 2014.

WAN, S. Y.; ZHANG, T. F.; DING, Y. Galectin-3 enhances proliferation and angiogenesis of endothelial cells differentiated from bone marrow mesenchymal stem cells. **Transplant. Proc.,** v. 43, n. 10, p. 3933-3938, dec. 2011.

WATERMAN, R. S. et al. A new mesenchymal stem cell (MSC) paradigm: polarization into a pro-inflammatory MSC1 or an Immunosuppressive MSC2 phenotype. **PLoS One,** v. 5, n. 4, p. e10088, 2010.

YANCY, C. W. et al. 2016 ACC/AHA/HFSA Focused Update on New Pharmacological Therapy for Heart Failure: An Update of the 2013 ACCF/AHA Guideline for the Management of Heart Failure: A Report of the American College of Cardiology/American Heart Association Task Force on Clinical Practice Guidelines and the Heart Failure Society of America. **Circulation**, may. 2016.

YANG, R. Y.; HSU, D. K.; LIU, F. T. Expression of galectin-3 modulates T-cell growth and apoptosis. **Proc. Natl. Acad. Sci. USA,** v. 93, n. 13, p. 6737-6742, jun. 1996

YANG, R. Y.; LIU, F. T. Galectins in cell growth and apoptosis. **Cell Mol. Life Sci.,** v. 60, n. 2, p. 267-276, feb. 2003.

YEN, B. L. et al. Multipotent human mesenchymal stromal cells mediate expansion of myeloid-derived suppressor cells via hepatocyte growth factor/c-met and STAT3. **Stem Cell Rep.,** v. 1, n. 2, p. 139-151, 2013.

YU, L. et al. Genetic and pharmacological inhibition of galectin-3 prevents cardiac remodeling by interfering with myocardial fibrogenesis. **Circ. Heart Fail.,** v. 6, n. 1, p. 107-117, jan. 2013.

ZHANG, L.; TARLETON, R. L. Parasite persistence correlates with disease severity and localization in chronic Chagas' disease. **J. Infect. Dis.,** v. 180, n. 2, p. 480-486, aug. 1999.

ZHANG, P.; SU, J.; MENDE, U. Cross talk between cardiac myocytes and fibroblasts: from multiscale investigative approaches to mechanisms and functional consequences. **Am J Physiol. Heart Circ. Physiol.,** v. 303, n. 12, p. H1385-96, dec. 2012.

ANEXOS

ANEXO I

Original Research

CARDIOLOGY

Cardiology 2017;136:33–39
DOI: 10.1159/000447529

Received: February 26, 2016
Accepted after revision: June 30, 2016
Published online: August 23, 2016

Evaluation of Galectin-3 as a Novel Biomarker for Chagas Cardiomyopathy

Márcia Maria Noya-Rabelo[a, b] Ticiana Ferreira Larocca[a, c, d]
Carolina Thé Macêdo[a, c, d] Jorge Andion Torreão[a, b]
Bruno Solano de Freitas Souza[c, d] Juliana Fraga Vasconcelos[c, d]
Luciana Estrella Souza[e] Agnaluce Moreira Silva[e] Ricardo Ribeiro dos Santos[d]
Luís Claudio Lemos Correia[a, b] Milena Botelho Pereira Soares[c, d]

[a]Department of Cardiology, Hospital São Rafael, [b]Escola Bahiana de Medicina e Saúde Pública, [c]Gonçalo Moniz Research Center, CPqGM-Fiocruz/BA, [d]Center for Biotechnology and Cell Therapy, and [e]Clinical Diagnostics Laboratory, Hospital São Rafael, Salvador, Brazil

Key Words
Chagas disease · Biomarkers · Galectin-3

Abstract
Objectives: Chagas cardiomyopathy has worse long-term outcomes than other cardiomyopathies. A biomarker strategy to refer subjects for noninvasive cardiac imaging may help in the early identification of cardiac damage in subjects with Chagas disease. Galectin-3 (Gal-3) is a mediator of cardiac fibrosis shown to be upregulated in animal models of decompensated heart failure. Here we assessed the correlation of Gal-3 with myocardial fibrosis in patients with Chagas disease. ***Methods:*** This study comprised 61 subjects with Chagas disease. All subjects underwent clinical assessments, Doppler echocardiography and magnetic resonance imaging. Plasmatic Gal-3 was determined by ELISA. ***Results:*** Delayed enhancement (DE) was identified in 37 of 61 subjects (64%). The total amount of myocardial fibrosis was 9.4% [interquartile interval (IQI): 2.4–18.4]. No differences were observed in Gal-3 concentration according to the presence or absence of myocardial fibrosis, with a median Gal-3 concentration of 11.7 ng/ml (IQI: 9.4–15) in subjects with DE versus 12.9 ng/ml (IQI: 9.2–14) in subjects without DE (p = 0.18). No correlation was found between myocardial fibrosis and Gal-3 concentration (r = 0.098; p = 0.47). ***Conclusions:*** There is no correlation between the degree of myocardial fibrosis and the concentration of Gal-3 in subjects with Chagas disease.

Introduction

The main symptomatic form of Chagas disease is a cardiomyopathy characterized by heart failure, ventricular arrhythmias, heart blocks, thromboembolic events and sudden death [1]. Previous studies demonstrated that subjects with Chagas disease cardiomyopathy have worse long-term outcomes than subjects with cardiomyopathy due to other etiologies [2]. The worst prognosis has been

The authors take responsibility for all aspects of the reliability and freedom from bias of the data presented and their discussed interpretation.

KARGER

E-Mail karger@karger.com
www.karger.com/crd

Márcia Maria Noya-Rabelo
Av. São Rafael, 2152
São Marcos
Salvador, BA 41253-190 (Brazil)
E-Mail marcianoya@gmail.com

attributed to the continuous myocardial damage due to parasite persistence and immune-mediated mechanisms, leading to interstitial fibrosis throughout the myocardium [3]. Cost-effective strategies to identify subgroups of subjects with progressive fibrosis before the occurrence of extensive remodeling are of great interest.

There is a need to find new biomarkers that may reflect the pathophysiological mechanisms of myocardial fibrosis, in order to support the risk stratification, especially regarding subjects with Chagas disease, thus allowing the application of potentially invasive and expensive therapies to those who are most likely to benefit. To date there are no biomarkers accurate enough to predict myocardial fibrosis for detecting early cardiac involvement.

Galectin-3 (Gal-3) is a beta-galactoside-binding lectin shown to be, in experimental studies, a mediator of cardiac fibrosis [4, 5] and upregulated in animal models of decompensated heart failure, as reviewed by de Boer et al. [6]. We previously demonstrated that Gal-3 is upregulated in the hearts of mice chronically infected with *Trypanosoma cruzi* [7]. Gal-3 may promote fibrosis through the activation of fibroblasts and macrophages, which is a hallmark of cardiac remodeling processes [8]. Current data suggest that Gal-3 secreted by activated macrophages acts on fibroblasts, establishing a link between inflammation and fibrosis [9]. In addition to the involvement in heart diseases, Gal-3 may be involved in other disease settings, such as cancer, liver disease, renal disease and various rheumatologic conditions [10–13]. Moreover, circulating Gal-3 has been found to be elevated in different human diseases associated with fibrosis [14–16]. A pathophysiological role for Gal-3 in heart failure was suggested by previous studies showing that Gal-3 infusion into murine pericardium induced adverse cardiac remodeling whereas coinfusion with a Gal-3 inhibitor counteracted these effects [4, 5].

Here we sought to examine the clinical correlation of plasma Gal-3 with myocardial fibrosis, in subjects with different forms of Chagas disease, using cardiac magnetic resonance imaging (MRI) as the gold standard method to estimate the percentage of myocardium affected by fibrosis.

Methods

Study Population

Subjects with Chagas disease were prospectively recruited between January 2012 and December 2013 in the Chagas disease outpatient clinic at Hospital São Rafael, a tertiary referral center located in Salvador, Bahia, Brazil.

Inclusion criteria were an age of 18–70 years and a diagnosis of Chagas disease confirmed by 2 positive serologic tests for antibodies against *T. cruzi* (indirect hemagglutination and indirect immunofluorescence). Exclusion criteria were: the acute form of Chagas disease, previous myocardial infarction or known coronary atherosclerotic disease (or >2 risk factors for it), primary valve disease, end-stage renal disease on dialysis, active hepatitis or cirrhosis, hematologic, neoplastic or bone diseases and contraindication to MRI.

We classified enrolled patients into 3 groups based on distinct stages of Chagas disease, according to the current Brazilian Chagas disease consensus [1], distributed as follows: (1) a group with the indeterminate form of the disease, comprising 17 asymptomatic subjects without signs of cardiac involvement characterized by normal electrocardiogram, chest X-ray and echocardiography, (2) a group with the cardiac form without ventricular dysfunction, comprising 16 consecutive subjects with known heart involvement defined as abnormal electrocardiogram (typically, right bundle-branch block with left anterior hemiblock) and without left ventricular dysfunction and (3) a group with the cardiac form with ventricular dysfunction, comprising 28 subjects with low left-ventricular ejection fraction, 16 of whom were in New York Heart Association (NYHA) class III/IV.

At the time of enrolment, all subjects underwent clinical assessments consisting of structured medical questionnaires, 12-lead electrocardiography, chest radiography, 24-hour ambulatory electrographic monitoring, exercise testing, conventional Doppler echocardiography and cardiovascular MRI.

The study complied with the Declaration of Helsinki, was approved by the Ethics Committee of the Hospital São Rafael and is registered in ClinicalTrials.gov under the identifier NCT01842854. All subjects signed a written informed consent before their inclusion in the study.

Magnetic Resonance Imaging

Cardiovascular MRI was performed using a Sigma HDx 1.5-T system (General Electric, Fairfield, Conn., USA). For assessment of the LV function, electrocardiography-gated, breath-hold, long-axis, short-axis and 4-chamber views were acquired at the same location in different sequences. Acquisition parameters used for the dynamic sequence included a repetition time (RT) of 3.5 ms, an echo time (ET) of 1.5 ms, a flip angle of 60°, a receiver bandwidth of 125 kHz, a 35 × 35 cm field of view (FOV), a matrix of 256 × 148, a temporal resolution (TR) of 35 ms and a slice thickness of 8.0 mm without gap.

Delayed enhancement (DE) images were acquired every heartbeat, 10–20 min after the administration of a gadolinium-based contrast (0.1 mmol/kg) using an RT of 7.1 ms, an ET of 3.1 ms, a flip angle of 20°, a first cardiac phase, 16/32 views per segment, a matrix size of 256 × 192, a slice thickness of 8.0 mm, a gap between slices of 2 mm, a 32 × 38 cm FOV, an inversion time of 150–300 ms, a receiver bandwidth of 31.25 kHz and 2 excitations. The myocardial DE technique was used to investigate myocardial fibrosis, which was estimated by a quantitative visual method.

Gal-3 and NT-ProBNP

Gal-3 and NT-proBNP concentrations were determined in EDTA plasma samples with the VIDAS® automated enzyme-linked fluorescent assay (BioMérieux, Marcy-l'Étoile, France). The assay principle combines a one-step immunoassay sandwich

Table 1. Subjects' clinical and demographic characteristics

Variable	All subjects (n = 61)	Indeterminate form (n = 17)	Cardiac form without ventricular dysfunction (n = 16)	Cardiac form with ventricular dysfunction (n = 28)
Demographic characteristics				
Age, years	58±8	59±11	59±9	58±7
Female gender	36 (59)	12 (70)	12 (75)	12 (43)
Lived before in house of mud	50 (82)	15 (88)	15 (94)	20 (71)
Chagas-positive parents	39 (64)	11 (65)	14 (88)	14 (50)
Digestive form	4 (6.6)	0	2 (12)	2 (7)
Body mass index	25±4	26±4	27±4	26±3
Coexisting conditions				
Hypertension	44 (72)	14 (82)	12 (75)	18 (64)
Diabetes	9 (15)	4 (23)	0	5 (18)
Syncope	6 (7)	1 (6)	1 (6)	2 (7)
Current smoking	16 (26)	3 (18)	3 (18)	10 (36)
Congestive heart failure NYHA III/IV	16 (26)	0	0	16 (57)*
Laboratory characteristics				
Creatinine, mg/dl	0.88 (0.7–0.99)	0.84 (0.7–0.98)	0.78 (0.6–0.91)	0.94 (0.7–1.0)
Sodium, mmol/dl	140±3	138±2	139±2	139±2
Hemoglobin, g/dl	13.9±0.9	14.2±1.3	13.4±0.7	14.2±1.0
Total cholesterol, mg/dl	193±38	202±40	194±42	200±45
hsCRP, mg/dl	1.15 (0.63–4.02)	1.71 (0.35–6.54)	1.24 (0.51–4.74)	1.09 (0.73–3.62)
NT-proBNP, pg/ml	686 (66–816)	60.5 (34–108)	96.0 (73–181)	839.5** (189–2,271)
Troponin I, ng/ml	0.684 (0.012–0.04)	0.012 (0.012–0.012)	0.012 (0.012–0.028)	0.038 (0.019–0.06)
LVEF, %	54±15	64±3	64±4	43±10**
METS	9±2.5	12±3	9±2	8±2

Data are expressed as mean ± SD or n (%) for discrete variables and median (IQI) for continuous nonnormal variables. LVEF = LV ejection fraction; METS = metabolic equivalent of task; hsCRP = high-sensitivy C-reactive protein. * $p < 0.001$, Fisher's exact test. ** $p < 0.001$, Kruskal-Wallis test, one-way ANOVA.

method with a final fluorescent detection (ELFA). The samples were transferred into the wells containing anti-Gal-3 or anti-NT-proBNP antibodies conjugated with alkaline phosphatase. The intensity of the fluorescence is proportional to the concentration of antigens present in the sample. The measurement range was 3.3–100 ng/l for Gal-3 and 20–25.000 pg/ml for NT-proBNP.

Sample Size Calculation

Gal-3 concentration in patients with heart failure is described as 18.6 ± 7.8 ng/ml [17]. The sample size was calculated for the comparison of the Gal-3 concentration between 2 groups of subjects defined by the presence of myocardial fibrosis assessed by MRI. Considering that subjects with myocardial fibrosis have values close to those described in heart failure patients (18.6 ± 7.8 ng/ml), we determined that the enrolment of 64 participants would provide a power of 80% to reject the null hypothesis if subjects without myocardial fibrosis had Gal-3 values 30% lower than subjects with myocardial fibrosis, with the same standard deviation of 7.8 ng/ml for both groups, at a two-sided alpha level of 0.05.

Statistical Analysis

Categorical variables are presented as numbers and percentages and continuous variables are presented as means (SD) or median (interquartile interval, IQI). The significance of baseline differences was determined by the χ^2 test, the Fisher exact test or the unpaired t test, as appropriate. Comparisons of continuous variables among groups were performed with an analysis of variance (ANOVA) test or the Kruskal-Wallis test, depending on normality assessed by the Shapiro-Wilk test. Correlation between continuous variables was evaluated by the Pearson or Spearman coefficient, depending on normality.

Analyses were performed using SPSS v20.0 (IBM), and a two-sided p value <0.05 was considered to indicate statistical significance.

Results

Baseline Characteristics

We evaluated 61 subjects with Chagas disease, distributed as follow: 17 in group 1 (subjects with no evidence of cardiac involvement or heart failure), 16 in group 2 (cardiac form without ventricular dysfunction or symptoms) and 28 in group 3 (cardiac form with ventricular

Table 2. Myocardial fibrosis on cardiac MRI

	All subjects (n = 61)	Indeterminate form (n = 17)	Cardiac form without ventricular dysfunction (n = 16)	Cardiac form with ventricular dysfunction (n = 28)	p value
DE, n (%)	35 (57)	6 (35)	7 (44)	22 (79)	0.001*
Myocardial fibrotic area, % of LV mass (IQI)	9.4 (2.4–18.4)	4.1 (2.1–10.7)	2.3 (1.0–5.0)	15.2 (7.8–25)	0.004**

* Fisher's exact test. ** Kruskal-Wallis, one-way ANOVA.

Table 3. Myocardial fibrosis and subjects' clinical characteristics

	With fibrosis	Without fibrosis	p value
Age, years	57±9.2	58±7.6	0.53
Female gender	16 (43)	18 (86)	0.002*
Forms of the disease			
Indeterminate	7 (19)	10 (48)	<0.001*
Cardiac without LV dysfunction	7 (19)	9 (43)	
Cardiac with LV dysfunction	23 (62)	2 (9.5)	
Gal-3, ng/ml	11.8 (9.1–12.6)	13.7 (9.2–14.2)	0.67
NT-proBNP, pg/ml	211 (96–1087)	68 (34–346)	0.01
Troponin I, ng/ml	0.032 (0.012–0.048)	0.012 (0.012–0.013)	0.002**
hsCRP, mg/dl	1.1 (0.63–4.0)	1.1 (0.26–46.8)	0.38

Data are expressed as mean ± SD or n (%) for discrete variables and median (IQI) for continuous nonnormal variables. hsCRP = High sensitivity C-reactive protein. * Fisher's exact test. ** Mann-Whitney U test.

dysfunction, with or without symptoms). Mean age was 58 ± 8.5 years and 59% of the participants were women. The majority of subjects (73.8%) were in NYHA functional class I or II and 4 (6.6%) had concomitant gastrointestinal involvement. The prevalence of hypertension, diabetes, hypercholesterolemia and current smoking was similar across the 3 groups. As expected, higher NT-proBNP values and a lower ejection fraction were observed in group 3 ($p < 0.001$). Ventricular tachycardia was detected in 20 (33%) subjects on 24-hour Holter monitoring (none from group 1, 5 from group 2 and 15 from group 3; $p = 0.001$). Clinical and demographic characteristics of the subjects are described in table 1.

Myocardial Fibrosis

DE was identified in 37 of 61 subjects (64%). The total amount of myocardial fibrosis was 9.4% (IQI: 2.4–18.4) with a progressive increase across the different forms of the disease. Myocardial fibrosis was detected in 6 of 17 subjects in the indeterminate form (median 4.1%, IQI: 2.1–10.7), 7 of 16 in the cardiac form without ventricular dysfunction (median 2.3%, IQI: 1.0–5.0) and 22 of 28 subjects in the cardiac form with ventricular dysfunction (median 15.2%, IQI: 7.8–25.0, $p = 0.001$). DE was detected more frequently in the inferolateral and apical segments of the left ventricle. Moreover, subjects with DE showed a lower ejection fraction (68 ± 13 vs. 48 ± 18%; $p < 0.001$), higher NT-proBNP values [197 pg/ml (IQI: 91–2,682) vs. 73 pg/ml (IQI: 34–190); $p = 0.01$; tables 2, 3] and ventricular tachycardia detected on Holter monitoring (43 vs. 15%; $p = 0.03$).

Assessment of Gal-3

The median concentration of Gal-3 in the study sample was 12.1 ng/ml (IQI: 9.4–14.4). No differences were observed in Gal-3 concentration according to the presence or absence of myocardial fibrosis, with a median Gal-3 concentration of 11.7 ng/ml (IQI: 9.4–15) in subjects with DE versus 12.9 ng/m (IQI: 9.2–14) in subjects without DE ($p = 0.67$; fig. 1). No correlation was found between myocardial fibrosis and Gal-3 concentration ($r = 0.098$; $p = 0.47$; fig. 2).

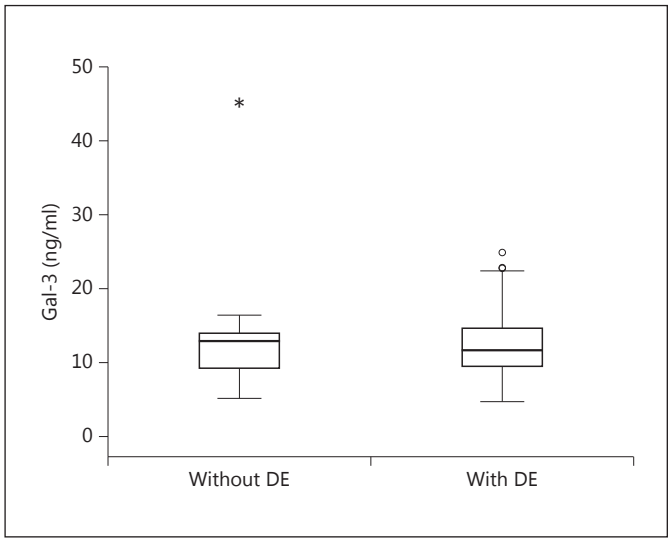

Fig. 1. Plasmatic concentration of Gal-3 assessed by ELISA in subjects with and without DE detected by MRI (Mann-Whitney U test, p = 0.67).

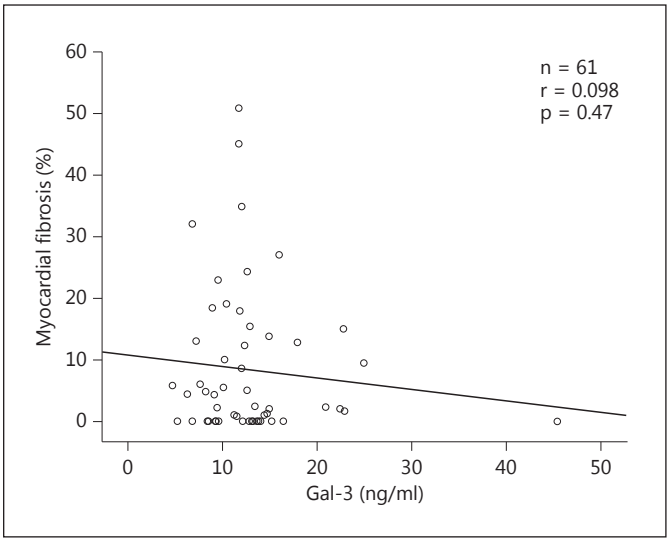

Fig. 2. Correlation between plasmatic concentration of Gal-3 and percentage of myocardial fibrosis assessed by cardiovascular MRI (Spearman's correlation, r = 0.098, p = 0.47).

Higher values of Gal-3 were found in women compared to men, with median Gal-3 concentrations of 13.4 ng/ml (IQI: 10.3–15.1) and 10.4 ng/ml (IQI: 8.9–10.1, p = 0.03), respectively. However, no differences were identified in subjects with a lower ejection fraction (p = 0.45), higher NT-proBNP values (p = 0.26), greater age (p = 0.15), higher troponin (p = 0.26) and high-sensitivity C-reactive protein values (p = 0.86). Additionally, we did not identify differences in Gal-3 concentration comparing groups of patients with different forms of Chagas disease, with a median concentration of 12.1 ng/ml (IQI: 8.8–18.3) in group 1, 12.1 ng/ml (IQI: 10.1–13.9) in group 2 and 12.0 ng/ml (IQI: 11.0–14.8) in group 3 (p = 0.90; fig. 3).

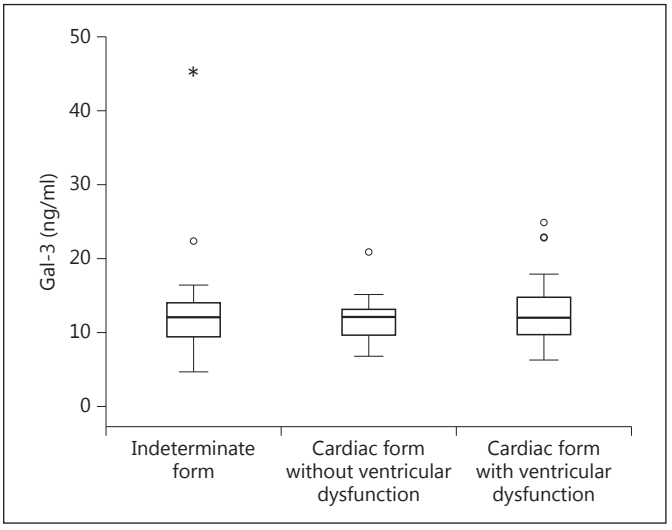

Fig. 3. Plasmatic concentration of Gal-3 assessed by ELISA in subjects with different forms of Chagas disease (Kruskal-Wallis, one-way ANOVA, p = 0.90).

Discussion

A useful biomarker must have a diagnostic or prognostic value or aid therapeutic guidance. Gal-3 has been shown to mediate fibrosis in several disease settings, including cardiac diseases. In animal models, Gal-3 mediates ventricular remodeling, and the administration of Gal-3 leads to a phenotype of progressive fibrosis and LV systolic dysfunction [4]. These observations have led to an increasing interest in Gal-3 as a potential heart failure biomarker that could reflect ongoing ventricular remodeling and progressive fibrosis.

This study provides the first evaluation of the Gal-3 role as a biomarker in a population with Chagas disease. Despite the experimental data on mice indicating a correlation between Gal-3 expression and the progression of Chagas disease [7, 18], our analysis in the clinical setting showed no direct relationship between the amount of myocardial fibrosis and the plasmatic concentration of

Gal-3. In contrast, Lepojärvi et al. [19] demonstrated a positive correlation between myocardial fibrosis and the serum concentration of Gal-3, although their data were obtained from a different population which included subjects with coronary artery disease and preserved LV function. Likewise, in patients with nonischemic dilated cardiomyopathy, Gal-3 is able to predict myocardial fibrosis as DE on cardiovascular MRI [20].

Although the median percentage of fibrosis varied across the different clinical forms of Chagas disease, the median concentration of Gal-3 was nearly identical in all 3 groups. Subjects with the cardiac form and ventricular dysfunction had a higher percentage of myocardial fibrosis than subjects without cardiac involvement, but the concentration of Gal-3 was not significantly different. Nonetheless, our data regarding the higher concentration of Gal-3 in females are in agreement with previously published data. Ho et al. [21] also demonstrated that Gal-3 concentration was significantly higher in women (median: 14.3 ng/ml) compared with men (median: 13.1 ng/ml, $p < 0.05$). Likewise, Daniels et al. [22] found that the concentration of Gal-3 was higher in women [15.3 (12.1–19.8) vs. 13.7 (10.7–17.4) ng/ml, $p < 0.0001$].

The role of circulating Gal-3 as a biomarker in heart failure of different etiologies has been supported by studies that showed that an elevated Gal-3 concentration, after adjusting for other variables, is associated with poorer outcomes in subjects with heart failure [23, 24]. However, these studies have limitations regarding their sample size or the number and type of variables included in their models for multivariate analysis. In contrast, the findings of Felker et al. [25], who included a larger cohort, showed that, after adjusting for more clinical variables (including NT-proBNP), Gal-3 was no longer able to significantly predict outcome in subjects with heart failure. Moreover, Srivatsan et al. [26], in a recent systematic review, found Gal-3 to be ineffective in the prediction of mortality when variables such as estimated glomerular filtration rate, LV ejection fraction and NT-proBNP were considered in the analysis.

There are several limitations to this study that may affect the interpretation of its results. First, it was conducted at a single tertiary and academic hospital, with a small sample size. However, there are also advantages to a single-center location, including the possibility of following all subjects closely for the duration of the study and gathering considerably detailed information on each study participant. The second limitation is that we measured Gal-3 at a single time point, which could not supply information about its importance over time. Lastly, the circulating concentration of Gal-3 may not accurately reflect the expression in the heart tissue.

Conclusion

That there is a lack of correlation between the degree of myocardial fibrosis and the plasma concentration of Gal-3, therefore refuting the hypothesis of a predictive role of this molecule as a biomarker for myocardial fibrosis in subjects with Chagas disease.

Acknowledgements

The authors wish to acknowledge BioMérieux for supplying VIDAS kits for the NT-proBNP and Gal-3 assessments. This work was financially supported by FAPESB.

Conflict of Interest

There were no conflicts of interest.

References

1 Andrade J, Marin-Neto J, Paola A, Vilas-Boas F, Oliveira G, Bacal F, et al; Sociedade Brasileira de Cardiologia: I. Latin American guidelines for the diagnosis and treatment of Chagas cardiomyopathy (in Portuguese). Arq Bras Cardiol 2011;97:1–48.

2 Barbosa AP, Cardinalli Neto A, Otaviano AP, Rocha BF, Bestetti RB: Comparison of outcome between Chagas cardiomyopathy and idiopathic dilated cardiomyopathy. Arq Bras Cardiol 2011;97:517–525.

3 Rassi A Jr, Rassi A, Marin-Neto JA: Chagas heart disease: pathophysiologic mechanisms, prognostic factors and risk stratification. Mem Inst Oswaldo Cruz 2009;104(suppl 1):152–158.

4 Sharma UC, Pokharel S, van Brakel TJ, van Berlo JH, Cleutjens JP, Schroen B, André S, Crijns HJ, Gabius HJ, Maessen J, Pinto YM: Galectin-3 marks activated macrophages in failure-prone hypertrophied hearts and contributes to cardiac dysfunction. Circulation 2004;110:3121–3128.

5 Liu YH, D'Ambrosio M, Liao TD, Peng H, Rhaleb NE, Sharma U, André S, Gabius HJ, Carretero OA: N-Acetyl-seryl-aspartyl-lysyl-proline prevents cardiac remodeling and dysfunction induced by galectin-3, a mammalian adhesion/growth-regulatory lectin. Am J Physiol Heart Circ Physiol 2009;296:H404–H412.

6 de Boer RA, Yu L, van Veldhuisen DJ: Galectin-3 in cardiac remodeling and heart failure. Curr Heart Fail Rep 2010;7:1–8.

7 Soares MB, Lima RS, Souza BS, Vasconcelos JF, Rocha LL, Dos Santos RR, Iacobas S, Goldenberg RC, Lisanti MP, Iacobas DA, et al: Reversion of gene expression alterations in hearts of mice with chronic chagasic cardiomyopathy after transplantation of bone marrow cells. Cell Cycle 2011;10:1448–1455.
8 Sutton MG, Sharpe N: Left ventricular remodeling after myocardial infarction: pathophysiology and therapy. Circulation 2000; 101:2981–2988.
9 Henderson NC, Mackinnon AC, Farnworth SL, Kipari T, Haslett C, Iredale JP, Liu FT, Hughes J, Sethi T: Galectin-3 expression and secretion links macrophages to the promotion of renal fibrosis. Am J Pathol 2008;172: 288–298.
10 Funasaka T, Raz A, Nangia-Makker P: Galectin-3 in angiogenesis and metastasis. Glycobiology 2014;24:886–891.
11 de Oliveira SA, de Freitas Souza BS, Sá Barreto EP, Kaneto CM, Neto HA, Azevedo CM, Guimarães ET, de Freitas LA, Ribeiro-Dos-Santos R, Soares MB: Reduction of galectin-3 expression and liver fibrosis after cell therapy in a mouse model of cirrhosis. Cytotherapy 2012;14:339–349.
12 Kolatsi-Joannou M, Price KL, Winyard PJ, Long DA: Modified citrus pectin reduces galectin-3 expression and disease severity in experimental acute kidney injury. PLoS One 2011;6:e18683.
13 de Oliveira FL, Gatto M, Bassi N, Luisetto R, Ghirardello A, Punzi L, Doria A: Galectin-3 in autoimmunity and autoimmune diseases. Exp Biol Med (Maywood) 2015;240:1019–1028.
14 de Boer RA, Voors AA, Muntendam P, van Gilst WH, van Veldhuisen DJ: Galectin-3: a novel mediator of heart failure development and progression. Eur J Heart Fail 2009;11: 811–817.
15 Nishi Y, Sano H, Kawashima T, Okada T, Kuroda T, Kikkawa K, Kawashima S, Tanabe M, Goto T, Matsuzawa Y, et al: Role of galectin-3 in human pulmonary fibrosis. Allergol Int 2007;56:57–65.
16 Taniguchi T, Asano Y, Akamata K, Noda S, Masui Y, Yamada D, Takahashi T, Ichimura Y, Toyama T, Tamaki Z, et al: Serum levels of galectin-3: possible association with fibrosis, aberrant angiogenesis, and immune activation in patients with systemic sclerosis. J Rheumatol 2012;39:539–544.
17 Lok DJ, Van Der Meer P, de la Porte PW, Lipsic E, Van Wijngaarden J, Hillege HL, van Veldhuisen DJ: Prognostic value of galectin-3, a novel marker of fibrosis, in patients with chronic heart failure: data from the DEAL-HF study. Clin Res Cardiol 2010;99: 323–328.
18 Pineda MA, Cuervo H, Fresno M, Soto M, Bonay P: Lack of galectin-3 prevents cardiac fibrosis and effective immune responses in a murine model of *Trypanosoma cruzi* infection. J Infect Dis 2015;212:1160–1171.
19 Lepojärvi ES, Piira OP, Pääkkö E, Lammentausta E, Risteli J, Miettinen JA, Perkiömäki JS, Huikuri HV, Junttila MJ: Serum PINP, PIIINP, galectin-3, and ST2 as surrogates of myocardial fibrosis and echocardiographic left ventricular diastolic filling properties. Front Physiol 2015;6:200.
20 Vergaro G, Del Franco A, Giannoni A, Prontera C, Ripoli A, Barison A, Masci PG, Aquaro GD, Cohen Solal A, Padeletti L, et al: Galectin-3 and myocardial fibrosis in nonischemic dilated cardiomyopathy. Int J Cardiol 2015;184:96–100.
21 Ho JE, Liu C, Lyass A, Courchesne P, Pencina MJ, Vasan RS, Larson MG, Levy D: Galectin-3, a marker of cardiac fibrosis, predicts incident heart failure in the community. J Am Coll Cardiol 2012;60:1249–1256.
22 Daniels LB, Clopton P, Laughlin GA, Maisel AS, Barrett-Connor E: Galectin-3 is independently associated with cardiovascular mortality in community-dwelling older adults without known cardiovascular disease: the Rancho Bernardo Study. Am Heart J 2014;167: 674–682.e671.
23 Shah RV, Chen-Tournoux AA, Picard MH, van Kimmenade RR, Januzzi JL: Galectin-3, cardiac structure and function, and long-term mortality in patients with acutely decompensated heart failure. Eur J Heart Fail 2010;12: 826–832.
24 Toprak G, Yüksel H, Demirpençe Ö, Islamoglu Y, Evliyaoglu O, Mete N: Fibrosis in heart failure subtypes. Eur Rev Med Pharmacol Sci 2013;17:2302–2309.
25 Felker GM, Fiuzat M, Shaw LK, Clare R, Whellan DJ, Bettari L, Shirolkar SC, Donahue M, Kitzman DW, Zannad F, et al: Galectin-3 in ambulatory patients with heart failure: results from the HF-ACTION study. Circ Heart Fail 2012;5:72–78.
26 Srivatsan V, George M, Shanmugam E: Utility of galectin-3 as a prognostic biomarker in heart failure: where do we stand? Eur J Prev Cardiol 2015;22:1096–1110.

ANEXO II

stem cell research&therapy

RESEARCH Open Access

Intramyocardial transplantation of cardiac mesenchymal stem cells reduces myocarditis in a model of chronic Chagas disease cardiomyopathy

Daniela Nascimento Silva[1,2], Bruno Solano de Freitas Souza[1,2], Carine Machado Azevedo[1,2], Juliana Fraga Vasconcelos[1,2], Rejane Hughes Carvalho[1], Milena Botelho Pereira Soares[1,2*] and Ricardo Ribeiro dos Santos[1]

Abstract

Introduction: New therapeutic options are necessary for patients with chronic Chagas disease, a leading cause of heart failure in Latin American countries. Stem cell therapy focused on improving cardiac function is a promising approach for treating heart disease. Here, we evaluated the therapeutic effects of cardiac mesenchymal stem cells (CMSCs) in a mouse model of chronic Chagas disease.

Methods: CMSCs were isolated from green fluorescent protein (GFP) transgenic C57BL/6 mouse hearts and tested for adipogenic, osteogenic, chondrogenic, endothelial, and cardiogenic differentiation potentials evaluated by histochemical and immunofluorescence techniques. A lymphoproliferation assay was performed to evaluate the immunomodulatory activity of CMSCs. To investigate the therapeutic potential of CMSCs, C57BL/6 mice chronically infected with *Trypanosoma cruzi* were treated with 10^6 CMSCs or saline (control) by echocardiography-guided injection into the left ventricle wall. All animals were submitted to cardiac histopathological and immunofluorescence analysis in heart sections from chagasic mice. Analysis by quantitative real-time reverse transcription polymerase chain reaction (qRT-PCR) was performed in the heart to evaluate the expression of cytokines involved in the inflammatory response.

Results: CMSCs demonstrated adipogenic, osteogenic, and chondrogenic differentiation potentials. Moreover, these cells expressed endothelial cell and cardiomyocyte features upon defined stimulation culture conditions and displayed immunosuppressive activity *in vitro*. After intramyocardial injection, GFP^+ CMSCs were observed in heart sections of chagasic mice one week later; however, no observed GFP^+ cells co-expressed troponin T or connexin-43. Histopathological analysis revealed that CMSC-treated mice had a significantly decreased number of inflammatory cells, but no reduction in fibrotic area, two months after treatment. Analysis by qRT-PCR demonstrated that cell therapy significantly decreased tumor necrosis factor-alpha expression and increased transforming growth factor-beta in heart samples.

Conclusions: We conclude that the CMSCs exert a protective effect in chronic chagasic cardiomyopathy primarily through immunomodulation.

* Correspondence: milena@bahia.fiocruz.br
[1]Centro de Biotecnologia e Terapia Celular, Hospital São Rafael, Av. São Rafael, 2152. São Marcos 41253-190, Salvador, BA, Brazil
[2]Laboratório de Engenharia Tecidual e Imunofarmacologia, Centro de Pesquisas Gonçalo Moniz, Fundação Oswaldo Cruz, Avenida Waldemar Falcão, 121, Candeal, Salvador 40296-710, BA, Brazil

Introduction

Heart disease remains a major cause of worldwide morbidity and mortality. Despite advances in clinical and surgical care of cardiac patients, current therapies are able to treat symptoms, delay clinical deterioration, and increase survival but are not effective in repair induction in a diseased heart. This is the case of chronic cardiac Chagas disease, which is caused by the protozoan parasite *Trypanosoma cruzi* and remains a leading cause of heart failure in Latin America [1]. Therefore, a major effort is under way to develop therapies aiming at regenerating the myocardium or to stimulate endogenous repair programs.

Different cell types, such as bone marrow cells, mesenchymal stem cells (MSCs) from adipose tissue, and skeletal myoblasts, have been tested in basic and applied clinical studies [1-4]. Bone marrow cells have demonstrated limited efficacy in many clinical trials, and this has raised the question of its usefulness as well as increased the investigation of other stem cell sources that may be potentially more effective in heart disease treatment. Moreover, different cell types are likely to have therapeutic potential in various disease settings, depending on the particular cardio-pathogenic mechanisms involved.

Adult cardiac stem cell populations have previously been observed in both murine and human hearts, including tissue-specific MSCs [5-14]. Owing to their multipotentiality and direct action via secretion of a repertoire of molecules that stimulate tissue regeneration and immunomodulation, MSCs have been used in different clinical trials and experimental models that reproduce tissue damage in order to verify their therapeutic potential [15-19].

In this study, we isolated a population of stem cells from the heart tissue that displays cell phenotype and immunosuppressive and differentiation potentials characteristic of MSCs. The therapeutic potential of these cells was evaluated in an experimental model of chronic Chagas disease cardiomyopathy.

Materials and methods

Animals

Male C57BL/6-Tg(CAG-EGFP)1Osb/J (The Jackson Laboratory, Bar Harbor, ME, USA) mice (4 to 8 weeks old) were used to obtain cardiac mesenchymal stem cells (CMSCs). Wild-type female C57BL/6 (4 weeks old) were used for *T. cruzi* infection and as non-infected controls. Animals were maintained in the animal facility of the Center for Biotechnology and Cell Therapy, Hospital São Rafael (Salvador, Bahia, Brazil), with access to food and water *ad libitum*. This study was approved by the local ethics committee for animal use at the Hospital São Rafael (CEUA-HSR).

Isolation and culture of stem cells

Green fluorescent protein (GFP) transgenic mice were deeply anesthetized by using an inhaled isoflurane anesthetic circuit 2% (Abbott, Abbott Park, IL, USA) for 10 minutes and euthanized by cervical dislocation. The hearts were then removed to isolate CMSCs. Cardiac fragments (approximately 1 mm) were dissected and incubated with 0.1% collagenase type A (Sigma-Aldrich, St. Louis, MO, USA) at 37°C for 30 minutes under constant stirring. After chemical and mechanical dissociation, fragments were cultured in Dulbecco's modified Eagle's medium (DMEM) (Gibco, Grand Island, NY, USA) supplemented with 10% fetal bovine serum (FBS) (Gibco) and 1% Pen Strep (Gibco) as explants in sixwell plates and incubated at 37°C with 5% CO_2. Culture medium was changed every 3 days, and on day 8, upon reaching 90% confluence, the explants were removed from the wells and adherent cells were trypsinized (Trypsin-EDTA 0.05%; Gibco) and transferred to tissue culture flasks containing medium supplemented with 10% FBS and 1% Pen Strep. The CMSC culture was maintained in a humidified incubator at 37°C with 5% CO_2 for *in vitro* and *in vivo* studies.

Phenotypic characterization by flow cytometry

CMSCs at passage 8 were trypsinized and resuspended in 0.9% saline. The cells (5×10^5) were incubated for 5 minutes with CD16/CD32 (BD Biosciences, San Diego, CA, USA) with further incubation at 4°C for 30 minutes with the following antibodies (diluted at 1:100): Sca1-PE-Cy5.5 (Caltag Medsystems, Buckingham, UK); CD90.2-APC, CD117-PE, CD45-APC, CD34-Alexa Fluor 647, and CD44-PE (BD Biosciences); and CD29-APC and CD105-PE (BioLegend, San Diego, CA, USA). Isotype-identical antibodies were used as controls. After incubation and two phosphate-buffered saline (PBS) washes, the data were acquired and analyzed on an LSRFortessa flow cytometer (BD Biosciences). At least 50,000 events were collected and analyzed.

Adipogenic, osteogenic, and chondrogenic differentiation

For adipogenic differentiation, cells were cultured in 24-well plates with 13-mm coverslips in complete medium (10^4 cells per well). After reaching 50% to 60% confluence, the medium was removed and replaced with an adipogenic induction medium by using a StemPro Adipogenesis Differentiation Kit (Gibco). To observe the fatty vacuoles after 14 days in culture, the adipocyte differentiated cells and their controls were fixed in 4% paraformaldehyde and stained with Oil red solution. The images were captured by an AX70 microscope (Olympus, Tokyo, Japan) and ImagePro Plus 7.0 software (Media Cybernetics, San Diego, CA, USA). For osteogenic differentiation, the cells were cultured in a specific osteogenic differentiation medium by using a StemPro Osteogenesis Differentiation Kit (Gibco). Half of the differentiation medium was changed every two days. Calcium-rich matrix deposition was observed by staining with Alizarin red 2%. For chondrogenic differentiation, cells were cultured for 21 days in standard

chondrogenic differentiation medium by using a StemPro Chondrogenesis Differentiation Kit (Gibco). Proteoglycan synthesis evaluation was performed in preparations stained with Alcian blue solution.

Cardiomyogenic differentiation

CMSCs were cultured in DMEM and 10% FBS in 24-well plates with 13-mm coverslips with complete medium. After reaching 60% confluence, cells were incubated with 10 μM 5-azacytidine (Sigma-Aldrich). A control group was maintained in complete medium. After 24 hours of incubation, medium was replaced and cells were cultured in complete DMEM for an additional 4 weeks, when the expression of molecular cardiac markers was evaluated by immunofluorescence analysis. Cells were fixed with 4% paraformaldehyde for 30 minutes, washed twice with PBS for 3 minutes, and blocked with 5% bovine serum albumin in PBS for 30 minutes. The following primary antibodies were then applied and incubated at 4°C for 24 hours: anti-GATA-4 and anti-connexin 43 (1:200) (Santa Cruz Biotechnology, Inc., Santa Cruz, CA, USA). Images of differentiated cells and their controls were acquired by confocal microscopy (Olympus) and ImagePro Plus 7.0 software (Media Cybernetics).

Endothelial cell differentiation

CMSCs were used for the endothelial cell induction protocol. Cells were seeded at a density of 3,000 cells per cm^2 on 24-well plates in EGM-2 culture medium with supplements (Lonza, Walkersville, MD, USA) and cultured for 10 days. The expression of CD31, an endothelial cell marker, was then evaluated by immunofluorescence (BD Biosciences). On the following day, sections were incubated with Alexa fluor 594-conjugated anti-goat IgG (Molecular Probes, Carlsbad, CA, USA). To induce the formation of capillary-like structures, 24-well plates were covered with 250 μL of Matrigel (BD Biosciences) diluted 1:1 in EGM-2. CMSCs were seeded at a density of 30,000 cells per cm^2 and cultured for 24 hours. The formation of capillary-like structures was observed over time by using an inverted microscope (Olympus). Additionally, the percentage of CD31 cells before and after EGM-2 induction was evaluated by flow cytometry with APC-conjugated anti-CD31 (BD Biosciences) diluted 1:50 and by analysis with the LSRFortessa flow cytometer.

Lymphoproliferation assay

C57BL/6 spleen cell suspensions were prepared in RPMI medium (Invitrogen, Gibco-BRL, Gaithersburg, MD, USA) supplemented with 10% fetal bovine serum (Invitrogen, Gibco-BRL), 2 mM of L-glutamine, 0.1% RPMI 1640 vitamins solution (Sigma-Aldrich), 1 mM of sodium pyruvate, 10 mM of Hepes, 50 μM of 2-mercaptoethanol, and 50 μg/mL of gentamycin (Sigma-Aldrich). Splenocytes were cultured in 96-well plates at 4×10^5 cells per well, in a final volume of 200 μL, in triplicate, in the presence of 5 μg/mL concanavalin A (Con A) only or in the presence of CMSCs pre-treated with 25 μg/mL mitomycin C, at different ratios (CMSC/splenocyte ratio of 1:1, 1:10, or 1:100). After 48 hours, plates were pulsed with 1 μCi of methyl-3 H thymidine (PerkinElmer, Amersham, Little Chalfont, UK) for 18 hours, and proliferation was assessed by measurement of 3 H-thymidine uptake by using a β-plate counter. The percentage inhibition of spleen cell proliferation was determined in relation to controls stimulated by Con A in the absence of CMSCs.

Trypanosoma cruzi infection and cell therapy

Infection of C57BL/6 mice was performed by intraperitoneal injection of 100 trypomastigotes of the myotropic Colombian *T. cruzi* strain [20]. Groups of 10 chronic chagasic mice (6 months post-infection) were treated by intramyocardial injection with 10^6 GFP^+ CMSCs prepared in 50 μL of sterile 0.9% saline solution and injected into the lateral wall of the left ventricle by using an ultrafine needle (12.7 × 0.33 mm 29 G; BD Biosciences) guided by an echocardiography probe RMV 707B, 30 MHz (Vevo 707; VisualSonics, Toronto, ON, Canada). All animals were anesthetized by using an inhaled isoflurane anesthetic circuit 2% (Abbott) for 10 minutes before and after the intramyocardial injection. Control chagasic mice received the same volume of saline solution (n = 10). One mouse from the cell therapy group died during the intramyocardial injection. Therefore, the cell therapy group was composed of nine mice for the following analysis.

Cell visualization by *in vivo* imaging system

Transplanted CMSCs were visualized by the *in vivo* imaging system (IVIS) Kodak Image Station 4000MM PRO equipped with a charge-coupled device camera (Eastman Kodak Company's Health Group, now known as Carestream Health, Toronto, ON, Canada). For fluorescence imaging, the machine was configured for 550 nm excitation, 600 nm emission, 3 minutes of exposure, 262 binning, and fstop 2.5. The acquired images were analyzed with Carestream MI Application 5.0.2.30 software (Carestream Health). Whole body images were acquired from the ventral surface of the mice. Images were acquired immediately after intramyocardial transplantation, accompanied by an additional follow-up analysis 1 week later, in infected mice (6 months post-infection).

Morphometric analysis

Heart sections were analyzed by light microscopy, and images were digitized by using a color digital video camera (CoolSnap, Montreal, QC, Canada) adapted to a BX41 microscope (Olympus). Morphometric analyses

were performed 2 months after treatment by using software Image Pro Plus version 7.0 (Media Cybernetics). The number of inflammatory cells was determined by counting 10 fields (400×) per heart in hematoxylin-and-eosin-stained sections, and the percentage of fibrosis was determined in Masson's trichrome-stained heart sections (200×) as previously described [3]. All of the analyses were blinded.

Real-time reverse transcription polymerase chain reaction

Total RNA was isolated from heart samples with TRIzol reagent (Invitrogen, Molecular Probes, Eugene, OR, USA), and concentration was determined by photometric measurement. A High Capacity cDNA Reverse Transcription Kit (Applied Biosystems, Foster City, CA, USA) was used to synthesize cDNA from 1 μg of RNA in accordance with the recommendations of the manufacturer. Quantitative real-time reverse transcription polymerase chain reaction (qRT-PCR) assays were performed to detect the expression levels of tumor necrosis factor-alpha (TNF-α) (Mm 00443258 m1), interferon-gamma (IFN-γ) (Mm008017 78m1), interleukin-6 (IL-6) (Mm00446190m1), cyclooxigenase 2 (COX-2) (Mm01307329m1), transforming growth factor-beta (TGF-β) (Mm00441724m1), and IL-10 (Mm00 439616m1). The qRT-PCR amplification mixtures contained template cDNA, TaqMan Master Mix, and probes (all from Applied Biosystems). All reactions were run in triplicate on an ABI7500 Sequence Detection System (Applied Biosystems) under standard thermal cycling conditions. Non-template control (NTC) and non-reverse transcription controls (No-RT) were included.

Confocal immunofluorescence analyses in heart sections of chagasic mice

The hearts obtained from chagasic mice were cryopreserved in Tissue-Tek (Sakura, Alphen aan den Rijn, The Netherlands), and 10-μm sections were obtained in Leica CM 1850 UV cryostat (Leica Microsystems, Wetzlar, Germany). To evaluate the presence of GFP^+ cells in the heart, sections were incubated overnight with the following primary antibodies: anti-connexin 43 and troponin T (Santa Cruz Biotechnology, Inc.). On the following day, sections were incubated with Alexa fluor 594-conjugated anti-goat IgG or Alexa fluor 488-conjugated anti-rabbit IgG (Molecular Probes, Carlsbad, CA, USA). Nuclei were stained with 4,6-diamidino-2-phenylindole (DAPI) by using VectaShield Hard Set mounting medium with DAPI H-1500 (Vector Laboratories, Burlingame, CA, USA). Sections were then analyzed by using a FluoView 1000 confocal microscope (Olympus).

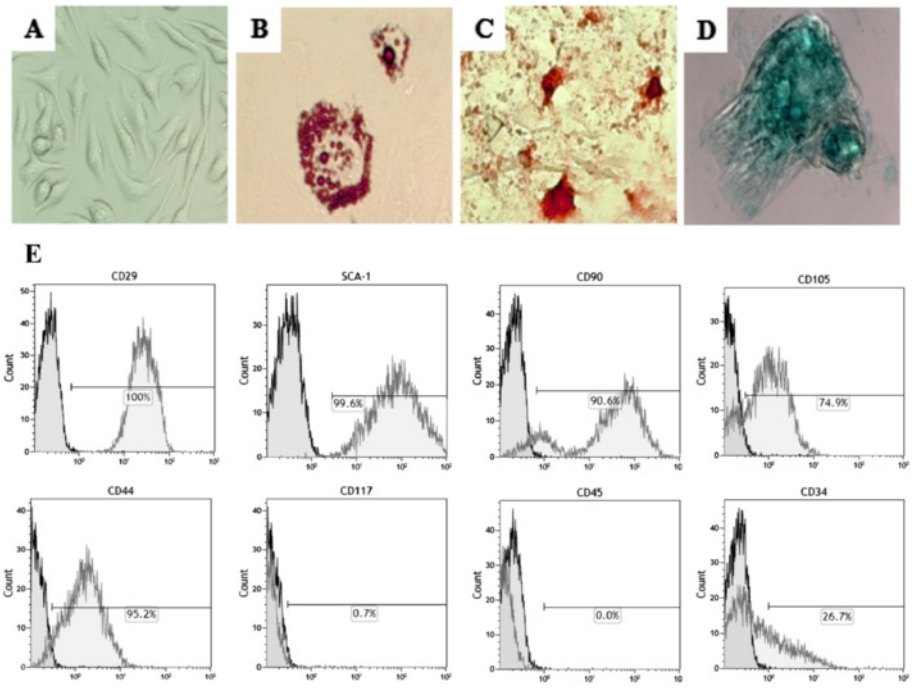

Figure 1 Morphologic and multipotential characterization of cardiac mesenchymal stem cells (CMSCs). (A) Phase contrast microscopy of CMSCs shows a fibroblast-like morphology in culture. **(B-D)** CMSCs were submitted to differentiation protocols into mesenchymal lineages. Cell differentiation was confirmed by positive staining with Oil red for adipocytes **(B)**, Alizarin red for osteocytes **(C)**, and Alcian blue for chondrocytes **(D)**. Magnification: 20×. **(E)** Flow cytometry analysis of CMSCs shows the percentages of CD29, CD90, CD45, Sca-1, CD44, CD105, CD117, and CD34 at passage 8.

Statistical analyses

All continuous variables are presented as mean ± standard error. Lymphoproliferation assay, morphometry, and qRT-PCR were analyzed by using one-way analysis of variance followed by Tukey's multiple-comparison test with Prism 3.0 (GraphPad Software, San Diego, CA, USA). All differences were considered significant at *P* values of less than 0.05.

Results

Morphological and phenotypical characteristics of cardiac mesenchymal stem cells

Stem cells isolated from GFP transgenic mouse hearts had fibroblast-like morphologic characteristics of MSCs (Figure 1A). CMSCs were analyzed by flow cytometry to evaluate the expression of cell surface markers used to

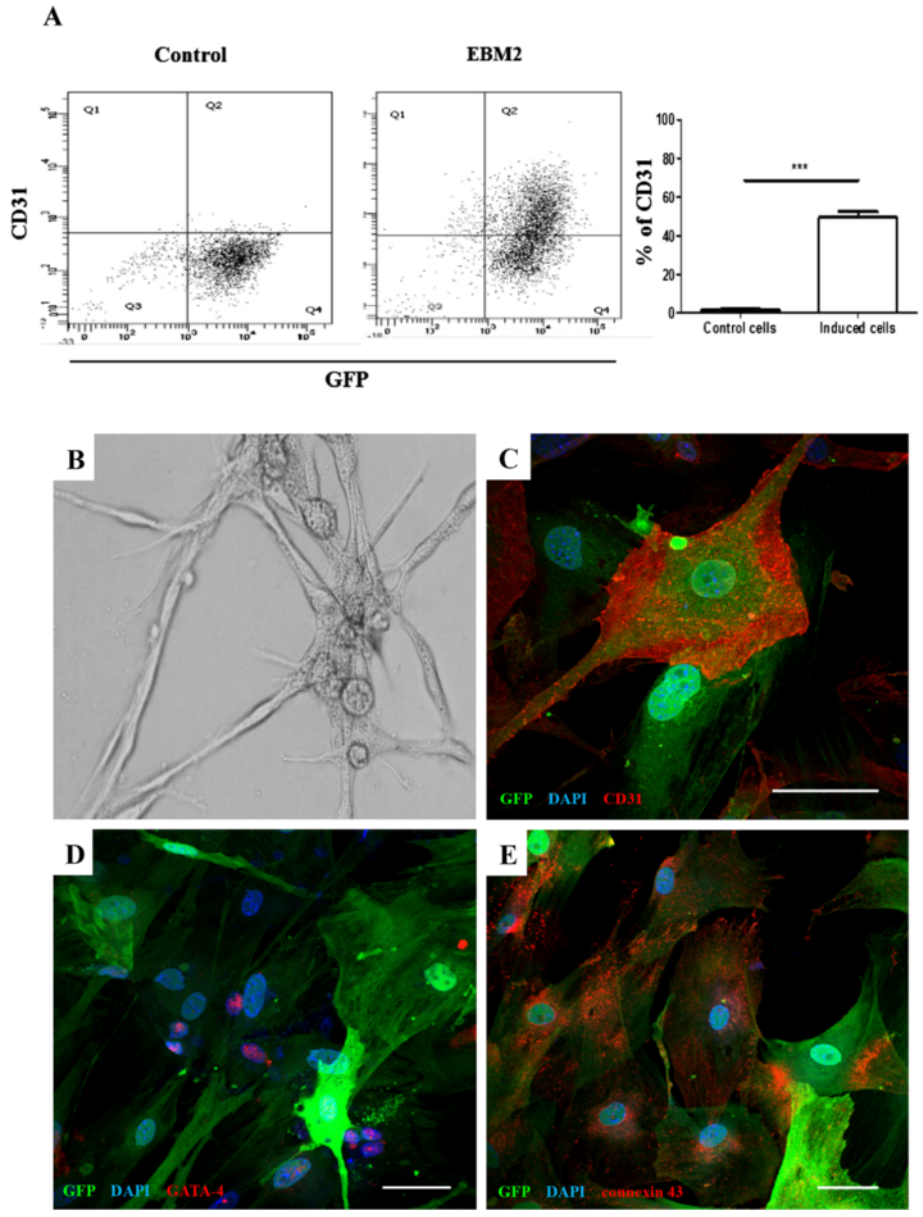

Figure 2 Immunofluorescence, flow cytometry, and capillary-like tube formation analyses of cardiac mesenchymal stem cells (CMSCs) induced for cardiac and endothelial cell differentiation. (A) Flow cytometry analysis of CD31 expression was evaluated in cells cultured or not with EGM-2 medium. An increase in the percentage of CD31 expression was observed in EGM-2 cell cultures. **(B)** Tubular-like structures of induced CMSCs were evaluated following culture on Matrigel for 24 hours induced by EGM-2 medium (magnification: 20×). **(C)** Confocal microscopy analysis of CMSCs after 10 days of endothelial induction by EGM-2 medium reveals positive staining for CD31 (red) in green fluorescent protein-positive (GFP^+) CMSCs (green). **(D, E)** Four weeks after 5′ azacitidine induction, GFP^+ CMSCs (green) began to express the cardiac transcription factor GATA-4 (red) **(D)** and the gap junction protein connexin 43 (red) **(E)**. Sections were co-stained with 4,6-diamidino-2-phenylindole (DAPI) (blue) for nuclei visualization. Bars represent 30 μm in **(B)** and 50 μm in **(D)** and **(E)**. *** $p < 0.001$.

identify different cell populations (Figure 1E). A high percentage of cells expressing GFP was observed in the CMSC population. Additionally, a small percentage of CMSCs showed expression of CD117, whereas the majority of the cells expressed MSC markers (Sca-1, CD44, CD73, and CD90). In contrast, the percentage of cells expressing the hematopoietic cell marker CD45 was low in the passage used (passage 8), whereas the expression of CD34 remained high even at passage 8 (26%).

Adipogenic, osteogenic, and chondrogenic differentiation potential of cardiac mesenchymal stem cells

CMSC cultures lacking differentiation stimuli maintained the undifferentiated state (Figure 1A). Stimulation of CMSCs with adipogenic differentiation medium for 15 days induced the accumulation of intracellular lipid, as shown by Oil red solution staining (Figure 1B). After 14 days of culture in osteogenic differentiation medium, cell clusters from CMSCs underwent osteoblast differentiation, as revealed by staining with Alizarin red 2%, showing the presence of calcium deposits in the cultures (Figure 1C). Twenty-one days after culture of CMSCs in chondrogenic differentiation medium, we observed the initial formation of cell clusters stained with Alcian blue, confirming the production of proteoglycans and chondrogenic differentiation (Figure 1D).

Endothelial cell and cardiomyogenic differentiation of cardiac mesenchymal stem cells

We analyzed whether CMSCs cultured in EGM-2 developed an endothelial cell-like phenotype. Flow cytometry analysis showed an increase in the expression of CD31, an endothelial marker, after induction (Figure 2A). This was confirmed by confocal microscopy analysis (Figure 2C). CMSCs cultured for 10 days in EGM-2 were reseeded on Matrigel for another 24 hours. After this period, we observed the presence of capillary-like tube formation on Matrigel, confirming the endothelial cell differentiation potential (Figure 2B).

CMSCs were cultured for 24 hours in the presence of the cardiomyogenic-inducing agent 5′ azacytidine. We did not observe any spontaneous beating of CMSCs stimulated or not with 5′ azacytidine. After 2 weeks of culture in the presence of 5′ azacytidine, we observed the expression of two cardiomyocyte differentiation markers, Gata-4 (Figure 2D) and connexin-43 (Figure 2E), by confocal microscopy analysis. However, we did not find an increase in troponin T gene expression by qRT-PCR analysis during the 3 weeks of induction with 5′ azacytidine (data not shown).

Immunomodulatory potential of cardiac mesenchymal stem cells *in vitro*

To analyze the immunomodulatory potential of CMSCs, we performed a lymphoproliferation assay by using splenocytes

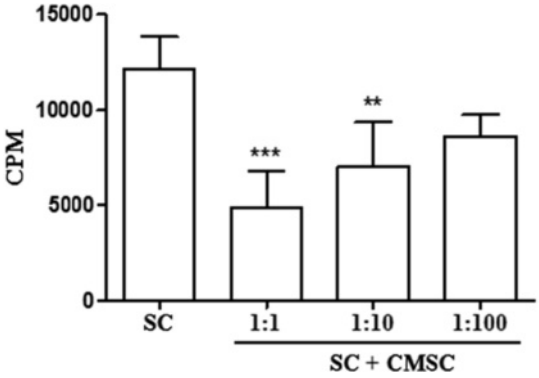

Figure 3 Concentration-dependent inhibitory effect of cardiac mesenchymal stem cells (CMSCs) on concanavalin A-stimulated splenocytes. Mouse splenocytes (SCs) were incubated for 2 days with concanavalin A in the presence of different numbers of mitomycin-treated CMSCs (CMSC/SC ratios of 1:1, 1:10, and 1:100). Spleen cell proliferation was assessed on day 3 by pulsing with ^{3}H-thymidine for 18 hours. Values represent the mean ± standard error of the mean from four independent experiments performed in triplicate. CPM = counts per minute. ** $p < 0.01$, *** $p < 0.001$.

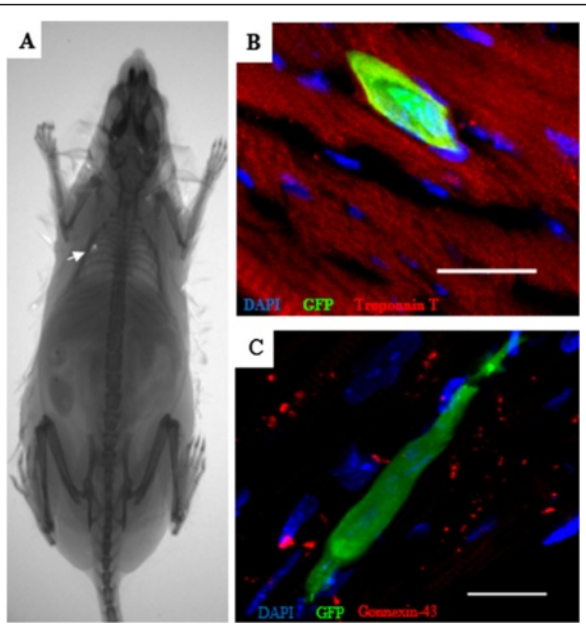

Figure 4 Engraftment and survival of green fluorescent protein-positive (GFP^{+}) cardiac mesenchymal stem cells (CMSCs) immediately and 1 week after cell transplantation in chagasic mice. (A) The tracking of GFP^{+} CMSCs in chagasic mice was performed immediately in cell transplantation by using an *in vivo* image system. Arrow indicates a GFP^{+} fluorescent dot in the heart of a chagasic mouse after intramyocardial injection in the left ventricle wall. **(B, C)** Heart sections of CMSC-treated mice 1 week after intramyocardial injection show the engraftment and survival of GFP^{+} cells (green) in chagasic heart by confocal microscopy analysis. GFP^{+} cells in the tissue did not co-express the cardiomyocyte markers (red) troponin T **(B)** or connexin 43 **(C)**. Sections were co-stained with 4,6-diamidino-2-phenylindole (DAPI) (blue) for nuclei visualization. Bars represent 20 μm.

stimulated with the mitogen Con A in the presence or absence of CMSCs. As shown in Figure 3, the addition of CMSCs to the cultures of activated splenocytes caused a concentration-dependent inhibition of proliferation, demonstrating its immunosuppressive potential *in vitro*.

Presence of green fluorescent protein-positive cardiac mesenchymal stem cells in the heart and expression of cardiac markers after intramyocardial injection in chronic chagasic mice

Transplanted GFP$^+$ CMSCs were observed after intramyocardial injection guided by echocardiography. A fluorescent dot was visualized in the heart immediately after injection by using an *in vivo* imaging system in three of the nine analyzed mice, but no signal was detected in control mice (Figure 4A). One week after intramyocardial injection, *in vivo* imaging analysis was repeated and no signal was detected. However, GFP$^+$ cells could be observed, 1 week after injections, in heart sections of CMSC-transplanted chagasic mice. However, none of the GFP$^+$ cells observed co-expressed the cardiomyocyte proteins troponin T (Figure 4B) or connexin-43 (Figure 4C).

Intramyocardial injection of cardiac mesenchymal stem cells modulates inflammation in chronic chagasic mice

Heart fibrosis and inflammation, typical features of chronic chagasic cardiomyopathy, were observed in *T. cruzi*-infected mice. Morphometric analysis demonstrated a significant reduction in the number of inflammatory cells, but not in the fibrotic area, 2 months after CMSC intramyocardial injection, when compared with saline-treated controls (Figure 5).

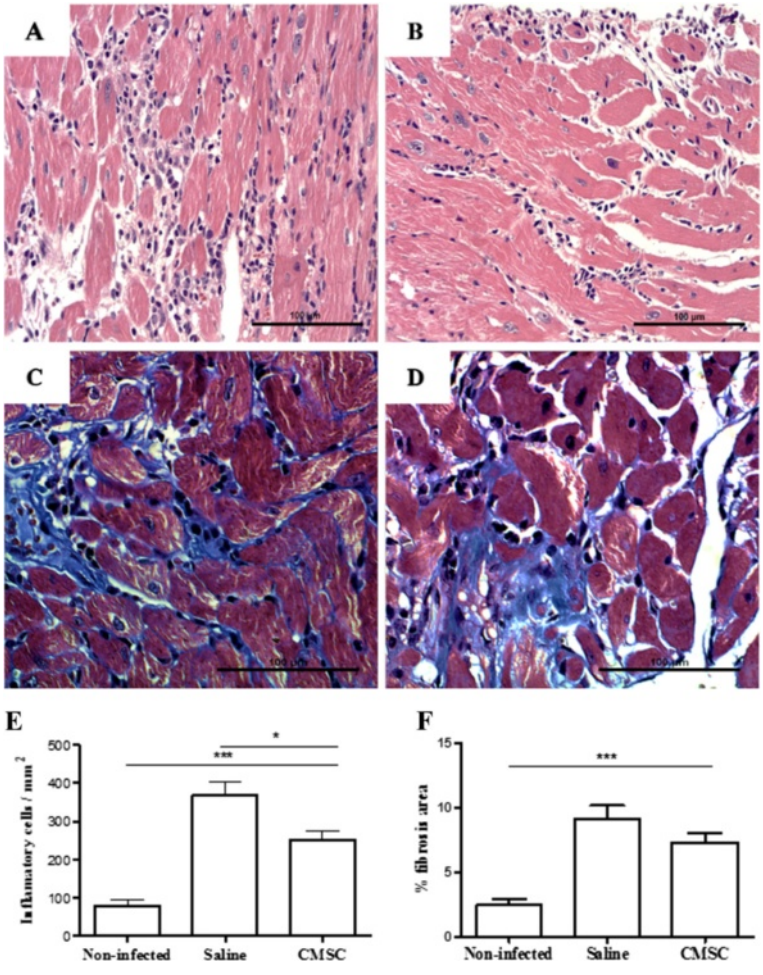

Figure 5 Morphometric analysis of heart sections from uninfected and chagasic mice treated with cardiac mesenchymal stem cells (CMSCs) or saline. Representative images of sections of hearts from mice euthanized 2 months after cell therapy with CMSCs and untreated controls are shown: heart sections of animals untreated **(A)** and treated **(B)** stained with hematoxylin and eosin (H&E) and heart sections stained with Masson's trichrome obtained from untreated **(C)** and treated **(D)** mice. **(E)** Number of inflammatory cells per mm^2 measured in sections stained with H&E. **(F)** Percentage of fibrosis quantified in sections stained with Masson's trichrome. Results are expressed as mean ± standard error of the mean of 5 to 10 animals per group. *P <0.05. *** p < 0.001.

Additionally, gene expression of pro-inflammatory and anti-inflammatory factors was evaluated in heart samples. Treatment with CMSCs produced a statistically significant reduction in the expression of TNF-α, but TGF-β gene expression was increased after CMSC transplantation (Figure 6B and C). No significant differences were observed in IL-6, COX-2, IFN-γ, and IL-10 gene expression between CMSC- and saline-treated groups (Figure 6A, D, E, and F).

Discussion

Owing particularly to recent data suggesting their increased cardiomyogenic potential, heart-derived stem cells have been considered a promising source for use in cell therapy for cardiac diseases [14]. Additionally, MSCs have been isolated from the heart [7,14] by using previously protocols for cardiac fibroblast isolation [21].

In the present study, we isolated stem cells from the mouse heart and showed their mesenchymal features. The analysis of CMSC surface markers showed a pattern similar to that of MSCs obtained from different sources [22]. A small percentage of CMSCs presented CD117 (c-kit) expression. The low expression frequency of CD117 on cultured MSCs obtained from different organs has been previously described [23,24]. Similar characteristics have been described for fibroblasts obtained from different

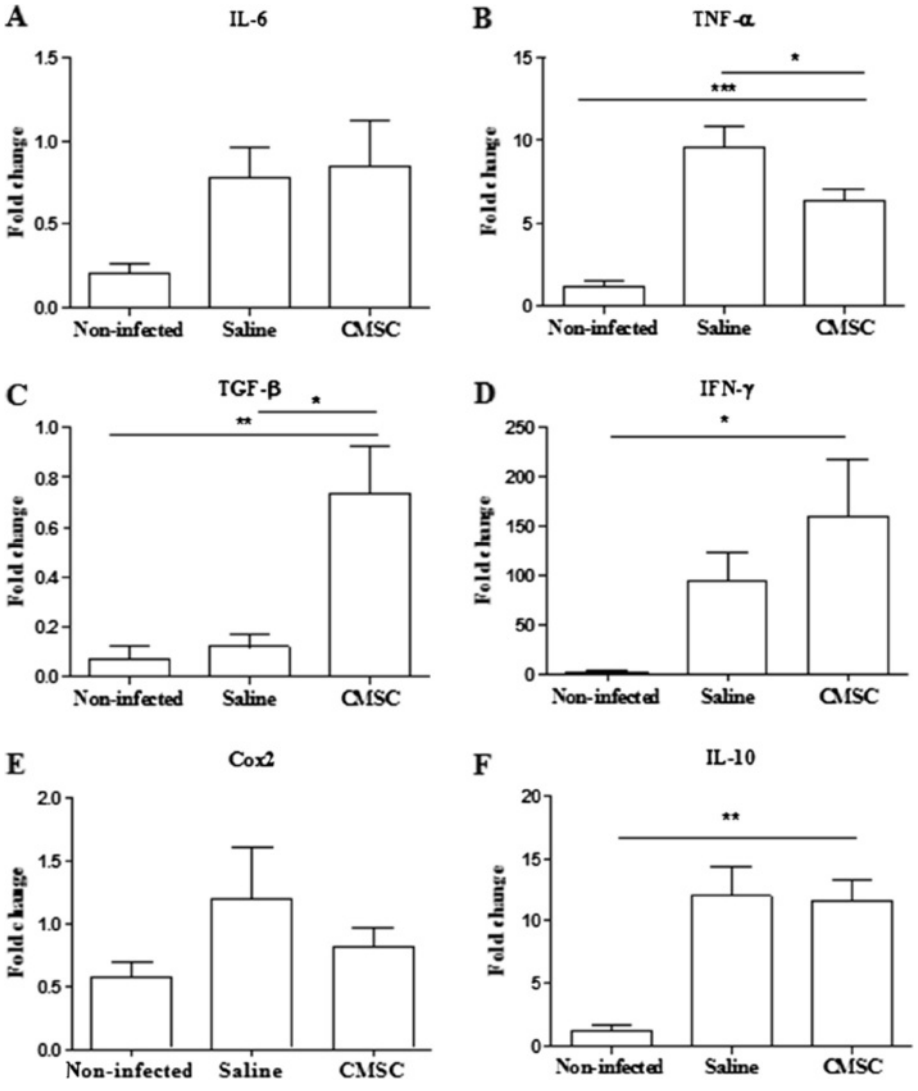

Figure 6 Gene expression of inflammatory mediators in the heart. Heart samples of uninfected or chagasic mice treated with saline or cardiac mesenchymal stem cells (CMSCs) were removed 2 months after therapy and analyzed by quantitative real-time reverse transcription polymerase chain reaction for the expression of interleukin-6 (IL-6) **(A)**, tumor necrosis factor-alpha (TNF-α) **(B)** (*P <0.05 versus saline and ***P <0.001 versus non-infected), transforming growth factor-beta (TGF-β) **(C)** (*P <0.05 versus saline and **P <0.01 versus non-infected), interferon-gamma (IFN-γ) **(D)** (*P <0.05 versus saline), cyclooxigenase 2 (COX-2) **(E)**, and IL-10 **(F)** (**P <0.01 versus non-infected).

sources, and therefore unequivocal distinction between these two cell populations cannot be made [25].

CMSCs obtained in our study met additional criteria to be defined as MSCs, including differentiation potential into adipocytes, osteocytes, chondrocytes, and endothelial cells. These differentiation potentials are also observed in MSCs obtained from other sources, such as the bone marrow [22,26], and have been observed in additional CMSC studies [14]. However, when stimulated after previously described cardiomyogenic protocols, CMSCs expressed cardiac-lineage specifiers, such as GATA-4, and connexin 43, but failed to differentiate completely into beating cardiomyocytes *in vitro*. Moreover, after intramyocardial transplantation, we did not observe *in vivo* differentiation into cardiomyocytes at the evaluated time points. These findings are in contrast to previous reports describing the generation of differentiated cardiomyocytes *in vitro* by other populations of cardiac stem cells [14,27]. However, the efficiency of differentiation of MSCs into cardiomyocytes *in vitro* described previously is very low and has been constantly questioned [26,27]. Thus, the protocol of induction by using 5′ azacitidine has limitations in the induction of cardiomyogenic differentiation, which was confirmed in the present study.

Interestingly, we demonstrated for the first time that CMSCs have significant immunomodulatory potential both *in vitro* and *in vivo*. When co-cultured in the presence of splenocytes activated by Con A, CMSCs inhibited the lymphoproliferation in a concentration-dependent manner. Although this effect was not reported for cardiac-derived stem cells before, MSCs obtained from other sources, such as the bone marrow, have been well characterized regarding their immunomodulatory properties [28,29].

Furthermore, we demonstrated a reduction in the number inflammatory cells in the hearts of chronic chagasic mice after intramyocardial administration of CMSCs. Experimental infection with the myotropic Colombian strain of *T. cruzi* caused an intense inflammation composed mainly of mononuclear cells (macrophages and $CD4^+$ and $CD8^+$ T cells), which is one of the hallmarks of chronic chagasic cardiomyopathy [4]. Inflammatory cell modulation was accompanied by a reduction of TNF-α gene expression, but TGF-β, an anti-inflammatory cytokine, was upregulated. Previous studies have shown similar results with the use of MSCs obtained from adipose tissue and from bone marrow mononuclear cells [3,30].

Treatment with CMSCs, however, did not reduce the percentage of fibrosis. This may be explained by the fact that CMSCs contribute to scar formation by the abundant secretion of collagen type I deposited in the infarct area, as described by Carlson and colleagues [7] (2011). Moreover, in the present study, it is not possible to determine whether the beneficial effects exerted by CMSCs could be translated into improved heart function, since this experimental model is not associated with impaired heart function at the time points analyzed (unpublished data).

Conclusions

CMSCs demonstrated an immunomodulatory potential in a Chagas disease model but did not reduce fibrosis or contribute to cardiomyocyte formation. These results suggest that MSCs may be beneficial in the context of Chagas disease cardiomyopathy. We speculate that, in combination with other cell types or factors, MSCs may participate in tissue regeneration.

Abbreviations

CMSC: cardiac mesenchymal stem cell; Con A: concanavalin A; COX-2: cyclooxigenase 2; DAPI: 4,6-diamidino-2-phenylindole; DMEM: Dulbecco's modified Eagle's medium; FBS: fetal bovine serum; GFP: green fluorescent protein; IFN-γ: interferon gamma; IL: interleukin; MSC: mesenchymal stem cell; PBS: phosphate-buffered saline; qRT-PCR: quantitative real-time reverse transcription polymerase chain reaction; TGF-β: transforming growth factor-beta; TNF-α: tumor necrosis factors-alpha.

Competing interests

The authors declare that they have no competing interests.

Authors' contributions

DNS contributed to conception and design, critical revision, data collection and analysis, and manuscript writing. BFS contributed to data collection and analysis, critical revision, and manuscript writing. CMA, JFV, and RHC contributed to data collection and analysis. MBPS and RRS contributed to conception and design and to critical revision. All authors read and approved the final manuscript.

Acknowledgments

This work was supported by CNPq, FAPESB, FINEP, and FIOCRUZ. The authors thank Luiz Fernando Quintanilha for technical assistance in flow cytometry analysis.

Received: 8 January 2014 Accepted: 20 June 2014
Published: 1 July 2014

References

1. Ribeiro Dos Santos R, Rassi S, Feitosa G, Grecco OT, Rassi A Jr, da Cunha AB, de Carvalho VB, Guarita-Souza LC, de Oliveira W Jr, Tura BR, Soares MB, de Carvalho AC C, Chagas Arm of the MiHeart Study Investigators: **Cell therapy in Chagas cardiomyopathy (Chagas arm of the multicenter randomized trial of cell therapy in cardiopathies study): a multicenter randomized trial.** *Circulation* 2012, **125:**2454–2461.
2. Guarita-Souza LC, Carvalho KA, Woitowicz V, Rebelatto C, Senegaglia A, Hansen P, Miyague N, Francisco JC, Olandoski M, Faria-Neto JR, Brofman P: **Simultaneous autologous transplantation of cocultured mesenchymal stem cells and skeletal myoblasts improves ventricular function in a murine model of Chagas disease.** *Circulation* 2006, **114:**I120–I124.
3. Larocca TF, Souza BS, Silva CA, Kaneto CM, Alcantara AC, Azevedo CM, Castro MF, Macambira SG, Soares MB, Ribeiro-dos-Santos R: **Transplantation of adipose tissue mesenchymal stem cells in experimental chronic chagasic cardiopathy.** *Arq Bras Cardiol* 2013, **100:**460–468.
4. Soares MB, Pontes-De-Carvalho L, Ribeiro-Dos-Santos R: **The pathogenesis of Chagas' disease: when autoimmune and parasite-specific immune responses meet.** *An Acad Bras Cienc* 2001, **73:**547–559.
5. Heng BC, Haider H, Sim EK, Cao T, Ng SC: **Strategies for directing the differentiation of stem cells into the cardiomyogenic lineage in vitro.** *Cardiovasc Res* 2004, **62:**34–42.
6. Barile L, Messina E, Giacomello A, Marban E: **Endogenous cardiac stem cells.** *Prog Cardiovasc Dis* 2007, **50:**31–48.
7. Carlson S, Trial J, Soeller C, Entman ML: **Cardiac mesenchymal stem cells contribute to scar formation after myocardial infarction.** *Cardiovasc Res* 2011, **91:**99–107.

8. Dawn B, Stein AB, Urbanek K, Rota M, Whang B, Rastaldo R, Torella D, Tang XL, Rezazadeh A, Kajstura J, Leri A, Hunt G, Varma J, Prabhu SD, Anversa P, Bolli R: **Cardiac stem cells delivered intravascularly traverse the vessel barrier, regenerate infarcted myocardium, and improve cardiac function.** *Proc Natl Acad Sci U S A* 2005, **102:**3766–3771.
9. Martin CM, Meeson AP, Robertson SM, Hawke TJ, Richardson JA, Bates S, Goetsch SC, Gallardo TD, Garry DJ: **Persistent expression of the ATP-binding cassette transporter, Abcg2, identifies cardiac SP cells in the developing and adult heart.** *Dev Biol* 2004, **265:**262–275.
10. Matsuura K, Nagai T, Nishigaki N, Oyama T, Nishi J, Wada H, Sano M, Toko H, Akazawa H, Sato T, Nakaya H, Kasanuki H, Komuro I: **Adult cardiac Sca-1-positive cells differentiate into beating cardiomyocytes.** *J Biol Chem* 2004, **279:**11384–11391.
11. Messina E, De Angelis L, Frati G, Morrone S, Chimenti S, Fiordaliso F, Salio M, Battaglia M, Latronico MV, Coletta M, Vivarelli E, Frati L, Cossu G, Giacomello A: **Isolation and expansion of adult cardiac stem cells from human and murine heart.** *Circ Res* 2004, **95:**911–921.
12. Oh H, Bradfute SB, Gallardo TD, Nakamura T, Gaussin V, Mishina Y, Pocius J, Michael LH, Behringer RR, Garry DJ, Entman ML, Schneider MD: **Cardiac progenitor cells from adult myocardium: homing, differentiation, and fusion after infarction.** *Proc Natl Acad Sci U S A* 2003, **100:**12313–12318.
13. Steele A, Jones OY, Gok F, Marikar Y, Steele P, Chamizo W, Scott M, Boucek RJ Jr: **Stem-like cells traffic from heart ex vivo, expand in vitro, and can be transplanted in vivo.** *J Heart Lung Transplant* 2005, **24:**1930–1939.
14. Gambini E, Pompilio G, Biondi A, Alamanni F, Capogrossi MC, Agrifoglio M, Pesce M: **C-kit + cardiac progenitors exhibit mesenchymal markers and preferential cardiovascular commitment.** *Cardiovasc Res* 2011, **89:**362–373.
15. Boyle AJ, Schulman SP, Hare JM, Oettgen P: **Is stem cell therapy ready for patients? Stem Cell Therapy for Cardiac Repair. Ready for the Next Step.** *Circulation* 2006, **114:**339–352.
16. Choi YH, Kurtz A, Stamm C: **Mesenchymal stem cells for cardiac cell therapy.** *Hum Gene Ther* 2011, **22:**3–17.
17. Hackett TL, Knight DA, Sin DD: **Potential role of stem cells in management of COPD.** *Int J Chron Obstruct Pulmon Dis* 2010, **5:**81–88.
18. Salem HK, Thiemermann C: **Mesenchymal stromal cells: current understanding and clinical status.** *Stem Cells* 2010, **28:**585–596.
19. Uccelli A, Pistoia V, Moretta L: **Mesenchymal stem cells: a new strategy for immunosuppression?** *Trends Immunol* 2007, **28:**219–226.
20. Federici EE, Abelmann WH, Neva FA: **Chronic and Progressive Myocarditis and Myositis in C3h Mice Infected with Trypanosoma Cruzi.** *Am J Trop Med Hyg* 1964, **13:**272–280.
21. Ieda M, Fu JD, Delgado-Olguin P, Vedantham V, Hayashi Y, Bruneau BG, Srivastava D: **Direct reprogramming of fibroblasts into functional cardiomyocytes by defined factors.** *Cell* 2010, **142:**375–386.
22. da Silva ML, Chagastelles PC, Nardi NB: **Mesenchymal stem cells reside in virtually all post-natal organs and tissues.** *J Cell Sci* 2006, **119:**2204–2213.
23. Hong SH, Gang EJ, Jeong JA, Ahn C, Hwang SH, Yang IH, Park HK, Han H, Kim H: **In vitro differentiation of human umbilical cord blood-derived mesenchymal stem cells into hepatocyte-like cells.** *Biochem Biophys Res Commun* 2005, **330:**1153–1161.
24. Shin JW, Lee DW, Kim MJ, Song KS, Kim HS, Kim HO: **Isolation of endothelial progenitor cells from cord blood and induction of differentiation by ex vivo expansion.** *Yonsei Med J* 2005, **46:**260–267.
25. Haniffa MA, Collin MP, Buckley CD, Dazzi F: **Mesenchymal stem cells: the fibroblasts' new clothes?** *Haematologica* 2009, **94:**258–263.
26. Zhen-Zhou C, Xiao-Dan J, Gui-Tao L, Jiang-Hua S, Ling-Hui L, Mou-Xuan D, Ru-Xiang X: **Functional and ultrastructural analysis of endothelial-like cells derived from bone marrow stromal cells.** *Cytotherapy* 2008, **10:**611–624.
27. Beltrami AP, Barlucchi L, Torella D, Baker M, Limana F, Chimenti S, Kasahara H, Rota M, Musso E, Urbanek K, Leri A, Kajstura J, Nadal-Ginard B, Anversa P: **Adult cardiac stem cells are multipotent and support myocardial regeneration.** *Cell* 2003, **114:**763–776.
28. Le Blanc K, Tammik C, Rosendahl K, Zetterberg E, Ringden O: **HLA expression and immunologic properties of differentiated and undifferentiated mesenchymal stem cells.** *Exp Hematol* 2003, **31:**890–896.
29. Liu H, Lu K, MacAry PA, Wong KL, Heng A, Cao T, Kemeny DM: **Soluble molecules are key in maintaining the immunomodulatory activity of murine mesenchymal stromal cells.** *J Cell Sci* 2012, **125:**200–208.
30. Soares MB, Lima RS, Rocha LL, Takyia CM, Pontes-de-Carvalho L, de Carvalho AC, Ribeiro-dos-Santos R: **Transplanted bone marrow cells repair heart tissue and reduce myocarditis in chronic chagasic mice.** *Am J Pathol* 2004, **164:**441–447.

doi:10.1186/scrt470
Cite this article as: Silva *et al.*: Intramyocardial transplantation of cardiac mesenchymal stem cells reduces myocarditis in a model of chronic Chagas disease cardiomyopathy. *Stem Cell Research & Therapy* 2014 **5**:81.

ANEXO III

The FASEB Journal article fj.13-229351. Published online August 20, 2013.

Administration of granulocyte colony-stimulating factor induces immunomodulation, recruitment of T regulatory cells, reduction of myocarditis and decrease of parasite load in a mouse model of chronic Chagas disease cardiomyopathy

Juliana F. Vasconcelos,*,† Bruno S. F. Souza,*,† Thayse F. S. Lins,* Letícia M. S. Garcia,† Carla M. Kaneto,†,‡ Geraldo P. Sampaio,† Adriano C. de Alcântara,† Cássio S. Meira,* Simone G. Macambira,*,†,§ Ricardo Ribeiro-dos-Santos,† and Milena B. P. Soares*,†,1

*Centro de Pesquisas Gonçalo Moniz, Fundação Oswaldo Cruz, Salvador, Bahia, Brazil; †Centro de Biotecnologia e Terapia Celular, Hospital São Rafael, Salvador, Bahia, Brazil; ‡Universidade Estadual de Santa Cruz, Ilhéus, Bahia, Brazil; and §Universidade Federal da Bahia, Salvador, Bahia, Brazil

ABSTRACT **Chagas disease, caused by *Trypanosoma cruzi* infection, is a leading cause of heart failure in Latin American countries. In a previous study, we showed beneficial effects of granulocyte colony-stimulating factor (G-CSF) administration in the heart function of mice with chronic *T. cruzi* infection. Presently, we investigated the mechanisms by which this cytokine exerts its beneficial effects. Mice chronically infected with *T. cruzi* were treated with human recombinant G-CSF (3 courses of 200 μg/kg/d for 5 d). Inflammation and fibrosis were reduced in the hearts of G-CSF-treated mice, compared with the hearts of vehicle-treated mice, which correlated with decreased syndecan-4, intercellular adhesion molecule-1, and galectin-3 expressions. Marked reductions in interferon-γ and tumor necrosis factor-α and increased interleukin-10 and transforming growth factor-β were found after G-CSF administration. Because the therapy did not induce a Th1 to Th2 immune response deviation, we investigated the role of regulatory T (T_{reg}) cells. A significant increase in $CD3^+Foxp3^+$ cells was observed in the hearts of G-CSF-treated mice. In addition, a reduction of parasitism was observed after G-CSF treatment. Our results indicate a role of T_{reg} cells in the immunosuppression induced by G-CSF treatment and reinforces its potential therapeutic use for patients with Chagas disease.—Vasconcelos, J. F., Souza, B. S. F., Lins, T. F. S., Garcia, L. M. S., Kaneto, C. M., Smapaio, G. P., de Alcântara, A. C., Meira, C. S., Macambira, S. G., Ribeiro-dos-Santos, R., Soares, M. B. P. Administration of granulocyte colony-stimulating factor induces immunomodulation, recruitment of T regulatory cells, reduction of myocarditis and decrease of parasite load in a mouse model of chronic Chagas disease cardiomyopathy. *FASEB J.* 27, 000–000 (2013). www.fasebj.org**

Key Words: Trypanosoma cruzi · cytokine therapy · inflammation · fibrosis · Th1 modulation

CHAGAS DISEASE, CAUSED BY infection with *Trypanosoma cruzi*, is considered a neglected tropical disease endemic in Latin American countries that mainly affects the poorest populations (1, 2). Although recent data indicate a reduction in the number of infected people as a result of vector transmission control, it is estimated that 10 million individuals are infected and 25 million are at risk of acquiring the disease (3, 4). About 70% of infected individuals remain asymptomatic, whereas 30% will develop the chronic symptomatic form of Chagas disease. Chronic chagasic cardiomyopathy (CCC), the most common symptomatic form of the disease, is one of the leading causes of heart failure. The only available treatment is heart transplantation, a high-cost procedure, that is limited by organ donation and presents severe complications in patients with

Abbreviations: CCC, chronic chagasic cardiomyopathy; DAPI, 4,6-diamidino-2-phenylindole dihydrochloride; DMEM, Dulbecco's modified Eagle's medium; ELISA, enzyme-linked immunosorbent assay; FBS, fetal bovine serum; Foxp3, forkhead box P3; G-CSF, granulocyte colony-stimulating factor; ICAM-1, intercellular adhesion molecule 1; IL, interleukin; IFN-γ, interferon-γ; RT-qPCR, reverse transcription-quantitative polymerase chain reaction; PBS, phosphate-buffered saline; TGF-β, transforming growth factor-β; TNF-α, tumor necrosis factor-α; T_{reg}, regulatory T

[1] Correspondence: Centro de Pesquisas Gonçalo Moniz, Fundação Oswaldo Cruz, Rua Waldemar Falcão, 121, Candeal, Salvador, Bahia, Brazil 40296-710. E-mail: milena@bahia.fiocruz.br

doi: 10.1096/fj.13-229351

This article includes supplemental data. Please visit *http://www.fasebj.org* to obtain this information.

Chagas disease due to infection reactivation after immunosuppressant administration (5).

Granulocyte colony-stimulating factor (G-CSF) is a pleiotropic cytokine that stimulates the production of neutrophils and releases bone marrow stem cells into the peripheral circulation. It has been in clinical use for nearly 2 decades, mainly as an adjunctive medication to chemotherapy or to mobilize stem cells for bone marrow transplantation (6). In addition to neutrophils and their precursors, monocytes are direct target cells of G-CSF action (7, 8). The administration of G-CSF in models of cardiac ischemic diseases has also shown the potential use of this cytokine in regenerative medicine (9–11).

Evidence is now accumulating that G-CSF also has immunomodulatory effects on adaptive immune responses mediated through several mechanisms, including activation of regulatory T (T_{reg}) cells (12). T_{reg} cells express the regulatory lineage factor forkhead box P3 (Foxp3), comprise 5−10% of peripheral $CD4^+$ T cells, and are known as natural T_{reg} cells (13). $CD4^+$ T cells from G-CSF-mobilized stem cell donors are able to suppress alloproliferative responses of autologous T cells in a cell contact-independent manner, by acquiring a T_{reg}-like cytokine profile (14). G-CSF drives the *in vitro* differentiation of human dendritic cells that express tolerogenic markers involved in T_{reg} cell induction (15).

We have previously demonstrated that administration of G-CSF in mice with chronic heart lesions caused by *T. cruzi* infection improved cardiac structure and function (16). Here we investigate the immunomodulatory effects of G-CSF in a mouse model of chronic Chagas disease, by investigating the modulation of key inflammatory mediators and the participation of T_{reg} cells.

MATERIALS AND METHODS

Animals

Four-week-old male C57BL/6 mice were used for *T. cruzi* infection and as normal controls. All animals were raised and maintained at the Gonçalo Moniz Research Center, Fundação Oswaldo Cruz (FIOCRUZ) in rooms with controlled temperature (22±2°C) and humidity (55±10%) and continuous air flow. Animals were housed in a 12 h-light-dark cycle (6:00 AM−6:00 PM) and provided with rodent diet and water *ad libitum*. Animals were handled according to the U.S. National Institutes of Health guidelines for animal experimentation. All procedures described had prior approval from the local animal ethics committee under number L-002/11 (FIOCRUZ, Bahia, Brazil).

T. cruzi infection and G-CSF administration

Trypomastigotes from the myotropic Colombian *T. cruzi* strain (17) were obtained from culture supernatants of infected LLC-MK2 cells. Infection of C57BL/6 mice was performed by intraperitoneal injection of 100 *T. cruzi* trypomastigotes in saline. Parasitemia of infected mice was evaluated at different time points after infection by counting the number of trypomastigotes in peripheral blood aliquots. Groups of chronic chagasic mice (6 mo after infection) were treated intraperitoneally (200 μg/kg/d) with 3 administered courses of human recombinant G-CSF (Filgrastim; Bio Sidus S.A., Buenos Aires, Argentina) for 5 consecutive d with an interval of 9 d between the courses (**Fig. 1**). Control chagasic mice received saline solution in the same regimen.

Morphometric analyses

Groups of mice were euthanized 2 mo after the therapy under anesthesia [5% ketamine (Vetanarcol; Konig, Santana de Parnaíba, Brazil) and 2% xylazine (Sedomin; Konig)], and hearts were removed and fixed in 10% buffered formalin. Heart sections were analyzed by light microscopy after paraffin embedding, followed by standard hematoxylin and eosin staining. Inflammatory cells infiltrating heart tissue were counted using a digital morphometric evaluation system. Images were digitized using a color digital video camera (CoolSnap, Photometrics, Montreal, QC, Canada) adapted to a BX41 microscope (Olympus, Tokyo, Japan). Morphometric analyses were performed using the software Image-Pro Plus v.7.0 (Media Cybernetics, San Diego, CA, USA). The inflammatory cells were counted in 10 fields (×400 view)/heart. The percentage of fibrosis was determined using Sirius red-stained heart sections and Image-Pro Plus v.7.0 to integrate the areas; 10 fields per animal were captured using ×200 view. All of the analyses were performed in a blinded fashion.

Confocal immunofluorescence analyses

Frozen or formalin-fixed paraffin-embedded hearts were sectioned, and 4-μm-thick sections were used for detection of syndecan-4, intercellular adhesion molecule-1 (ICAM-1), galectin-3, CD3, Foxp3, and interleukin (IL)-10 expression by immunofluorescence. First, paraffin-embedded sections were deparaffinized and submitted to a heat-induced antigen retrieval step by incubation in citrate buffer (pH 6.0). Then,

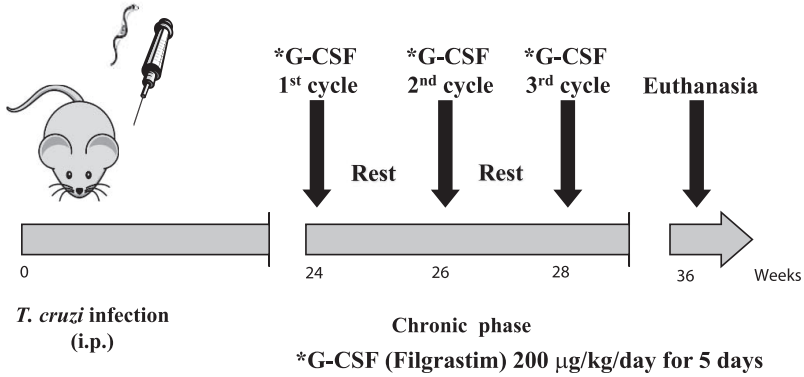

Figure 1. Experimental design. C57BL/6 mice were infected with 100 Colombian strain *T. cruzi* trypomastigotes and treated during the chronic phase of infection with human recombinant G-CSF, as indicated.

sections were incubated overnight with the following primary antibodies: anti-syndecan-4 (1:50; Santa Cruz Biotechnology, Santa Cruz, CA, USA), anti-ICAM-1 (1:50; BD Biosciences, San Jose, CA, USA), anti-CD3 (1:400; BD Biosciences), anti-Foxp3 (1:400; Dako, Glostrup, Denmark), or anti-IL-10 (1:100; BD Biosciences). On the following day, sections were incubated for 1 h with Alexa Fluor 633- or Alexa Fluor 488-conjugated phalloidin (1:200), mixed with one of the following secondary antibodies: Alexa Fluor 594-conjugated anti-goat IgG (1:200) or Alexa Fluor 488-conjugated anti-rabbit IgG (1:200; Molecular Probes, Carlsbad, CA, USA). Nuclei were stained with 4,6-diamidino-2-phenylindole (DAPI; VectaShield Hard Set mounting medium with DAPI H-1500; Vector Laboratories, Burlingame, CA, USA). The presence of fluorescent cells was determined by observation on a FluoView 1000 confocal microscope (Olympus). Quantifications of galectin-3$^+$ cells, syndecan-4$^+$ blood vessels, and ICAM-1$^+$ percentual area were performed in 10 random fields captured under ×400 magnification, using Image-Pro Plus v.7.0.

Real-time reverse transcription-quantitative polymerase chain reaction (RT-qPCR)

Total RNA was isolated from heart samples with TRIzol reagent (Molecular Probes) and concentration was determined by photometric measurement. A High Capacity cDNA Reverse Transcription Kit (Applied Biosystems, Foster City, CA, USA) was used to synthesize cDNA from 1 μg of RNA following the manufacturer's recommendations. RT-qPCR assays were performed to detect the expression levels of *Tbet* (Mm_00450960_m1), *GATA3* (Mm_00484683_m1), and *G-CSF* (Mm 00438334_m1). The RT-qPCR amplification mixtures contained 20 ng of template cDNA, TaqMan Master Mix (10 μl), and probes in a final volume of 20 μl (all from Applied Biosystems). All reactions were run in duplicate on an ABI 7500 sequence detection system (Applied Biosystems) under standard thermal cycling conditions. The mean C_t (cycle threshold) values from duplicate measurements were used to calculate expression of the target gene, with normalization to an internal control (*GAPDH*) using the $2^{-\Delta\Delta Ct}$ formula. Experiments with coefficients of variation $> 5\%$ were excluded. A nontemplate control and nonreverse transcription controls were also included.

Flow cytometry analysis

Quantitative analysis of T_{reg} cells was performed in the bone marrow and spleen of G-CSF- or saline-treated chronic chagasic mice, by flow cytometry. In brief, mice were treated with one course of G-CSF or saline and were euthanized under anesthesia the day after the final dose. Bone marrow cells were obtained from mice femurs. The bone marrow was collected by flushing the bones with Dulbecco's modified Eagle's medium (DMEM), followed by cell purification by centrifugation in Ficoll (Histopaque 1119 and 1077, 1:1; Sigma-Aldrich, St. Louis, MO, USA) gradient at 1000 *g* for 15 min. The spleens were collected, washed in DMEM, and homogenized by pressing through a 40-mm cell strainer. Bone marrow and spleen cells were counted and resuspended in phosphate-buffered saline (PBS) buffer [1% fetal bovine serum (FBS) in PBS]. For flow cytometry, cells were stained with labeled anti-CD4 PE-Cy5.5 and CD25 APC antibodies (BD Biosciences) for 20 min at room temperature. Cells were washed and analyzed using a cell analyzer (LSRFortessa; BD Biosciences) with FACSDiva software (version 6.1.3; BD Biosciences).

Cytokine assessment

Cytokine concentrations were measured in total spleen or heart protein extracts and in sera. Tissue proteins were extracted at 50 mg of tissue/500 ml of PBS to which 0.4 M NaCl, 0.05% Tween 20, and protease inhibitors (0.1 mM phenylmethylsulfonyl fluoride, 0.1 mM benzethonium chloride, 10 mM EDTA, and 20 kIU of aprotinin A/100 ml) were added. The samples were centrifuged for 10 min at 3000 *g*, and the supernatants were immediately used in enzyme-linked immunosorbent assays (ELISAs) or frozen at −70°C for later quantification. Interferon-γ (IFN-γ), tumor necrosis factor-α (TNF-α), transforming growth factor-β (TGF-β), IL-4, IL-6, IL-10, or IL-17 was quantified from individual mice by ELISA using specific antibody kits (R&D Systems, Minneapolis, MN, USA), according to the manufacturer's instructions. In brief, 96-well plates were blocked and incubated at room temperature for 1 h. Samples were added in duplicate and incubated overnight at 4°C. Biotinylated antibodies were added, and plates were incubated for 2 h at room temperature. A 0.5-h incubation with streptavidin-horseradish peroxidase conjugate was followed by detection using 3,3′,5,5′-tetramethylbenzidine peroxidase substrate and reading at 450 nm.

Quantification of parasite load

T. cruzi DNA was quantified in heart samples by qPCR analysis. For DNA extraction, heart fragments were submitted to DNA extraction using the NucleoSpin Tissue Kit (Machenerey-Nagel, Düren, Germany), as recommended by the manufacturer. In brief, 10 mg of each heart sample was submitted to DNA extraction, and the DNA amount and purity (260/280 nm) were analyzed by Nanodrop 2000 spectrophotometry (Thermo Fisher Scientific, Waltham, MA, USA). Kapa Probe Fast Universal 2X qPCR Master Mix was used to perform the qPCR in 20-μl reactions, including ROX low as the passive reference, as recommended by the manufacturer (Kapa Biosystems Inc., Woburn, MA, USA). Primers were designed based on the report by Schijman *et al.* (18), and the amounts used per reaction were 0.4 μM concentrations of both primers (primer 1, 5′-GTTCACACACTGGACACCAA-3′ and primer 2, 5′-TCGAAAACGATCAGCCGAST-3′) and a 0.2 μM concentration of the probe (SatDNA specific probe, 5′-/56-FAM/AATTCCTCC/ZEN/AAGCAGCGGATA/3IABkFQ/-3′), all included in a Mini PrimeTime qPCR assay (Integrated DNA Technologies, Inc., Coralville, IA, USA). Amounts of 1 μl for each point of the standard curve, samples, and controls were applied to different wells of a PCR microplate (Axygen, Union City, CA, USA), film sealed, and submitted to amplification. Cycles were performed in an ABI 7500 system (Applied Biosystems) as follows: first, 3 min at 95°C for *Taq* activation; and second, 45 cycles at 95°C for 10 s followed by 55°C for 30 s. To calculate the number of parasites per milligram of tissue, each plate contained an 8-log standard curve of DNA extracted from trypomastigotes of the Colombian *T. cruzi* strain (ranging from 4.7×10^{-1} to 4.7×10^{6}) in duplicate. Data were analyzed using 7500 software 2.0.1 (Applied Biosystems).

Assessment of trypanocidal activity

T. cruzi epimastigotes (Colombian strain) were maintained at 26°C in liver infusion tryptose medium supplemented with 10% FBS, 1% hemin (Sigma-Aldrich), 1% R9 medium (Sigma-Aldrich), and 50 μg/ml gentamicin. Parasites were counted in a hemocytometer and then dispensed into 96-well plates at a cell density of 5×10^6 cells/ml in the absence or presence of the human recombinant G-CSF at 3, 10, or 30 μg/ml in triplicate. The plate was incubated for 5 d at 26°C, aliquots of

each well were collected, and the number of viable parasites was counted in a Neubauer chamber. Trypomastigote forms of *T. cruzi* were obtained from supernatants of LLC-MK2 cells previously infected and cultured in 96-well plates at a cell density of 2×10^6 cells/ml in RPMI 1640 medium (Sigma-Aldrich) supplemented with 10% FBS and 50 μg/ml gentamicin in the absence or presence of human recombinant G-CSF. After 24 h of incubation, the number of viable parasites, based on parasite motility, was assessed in a Neubauer chamber and compared with that of an untreated parasite culture to calculate the percentage of inhibition. Benznidazole (30 μg/ml) was used as a positive control. For *in vitro* infection, peritoneal macrophages obtained from C57BL/6 mice were seeded at a cell density of 2×10^5 cells/ml in a 24-well plate with rounded coverslips on the bottom in RPMI 1640 medium supplemented with 10% FBS and 50 μg/ml gentamicin and incubated for 24 h. Cells were then infected with trypomastigotes (1:10) for 2 h. Free trypomastigotes were removed by successive washes using saline solution. Cultures were incubated in complete medium alone or with G-CSF (2, 6, or 10 μg/ml) or benznidazole (10 μg/ml) for 6 h. The medium was then replaced by fresh medium, and the plate was incubated for 3 d at 37°C. Cells were fixed in absolute alcohol, and the percentage of infected macrophages and the mean number of amastigotes/100 infected macrophages was determined by manual counting after hematoxylin and eosin staining using an optical microscope (Olympus).

Evaluation of anti-*T. cruzi* antibodies

T. cruzi-specific, total IgG, IgG1, and IgG2 antibodies were detected in the sera of naive or G-CSF- or saline-treated chronic chagasic mice by ELISA. Microtiter plates were coated overnight at 4°C with *T. cruzi* trypomastigote antigen (3 μg/ml) in 50 μl of carbonate-bicarbonate buffer (pH 9.6). The plates were washed 3 times with PBS containing 0.05% Tween 20 and then blocked by incubation at room temperature for 1 h with PBS-5% nonfat milk. After washing, the plates were incubated with 50 μl of a 1:200 (IgG) or 1:100 (IgG1 or IgG2a) dilution of each serum sample at 37°C for 2 h. The plates were washed, and a 1:1000 dilution of goat anti-mouse IgG (Sigma-Aldrich) or rat anti-mouse IgG1 or IgG2a (BD Biosciences) was incubated for 1 h at room temperature. After washing, peroxidase-conjugated anti-mouse polyvalent immunoglobulins (Sigma-Aldrich) diluted 1:1000 were dispensed into each well, and the plate was incubated for 30 min at room temperature followed by detection using 3,3′,5,5′-tetramethylbenzidine peroxidase substrate and read at 450 nm.

Statistical analyses

All continuous variables are presented as means ± SEM. Morphometric and cytokine levels were analyzed using 1-way analysis of variance, followed by a Newman-Keuls multiple comparison test with Prism 3.0 (GraphPad Software, San Diego, CA, USA). All differences were considered significant at values of $P < 0.05$.

RESULTS

Administration of G-CSF reduces inflammation and fibrosis in hearts of chronic chagasic mice

Multifocal inflammation, mainly composed of mononuclear cells, and fibrosis were found in the hearts of *T. cruzi*-infected mice during the chronic phase of the disease (**Fig. 2*A*, *B***). Administration of G-CSF reduced the number of inflammatory cells and the fibrotic area in chronic chagasic hearts (Fig. 2*C*, *D*). Morphometric analysis showed a statistically significant reduction of inflammation and fibrosis after G-CSF treatment, compared with the saline-treated controls (Fig. 2*E*, *F*).

Reduction of syndecan-4, ICAM-1, and galectin-3 expression in the hearts of G-CSF-treated mice

We have previously shown the overexpression of syndecan-4, ICAM-1, and galectin-3 in the hearts of chronic chagasic mice (19). To evaluate the effects of G-CSF on the expression of these inflammation markers, we performed confocal microscopy analysis in heart sections of mice from the 3 different groups. A marked decrease in syndecan-4 production, which is highly expressed in blood vessels of chagasic hearts, was seen after G-CSF treatment (**Fig. 3*A*, *B***). Morphological analyses revealed a statistically significance difference (Fig. 3*C*). Similarly, the expression of ICAM-1, mainly in inflammatory cells and cardiomyocytes in hearts of chronic chagasic mice, was significantly decreased after G-CSF treatment (Fig. 3*D*−*F*). Moreover, the high expression of galectin-3 in inflammatory cells was down-regulated in mouse hearts treated with G-CSF, which correlated to decreased inflammation (Fig. 3*G*−*I*).

Modulation of cytokine production after G-CSF administration

CCC has been associated with increased IFN-γ and TNF-α production in mice and in humans (19, 20). The concentrations of these two proinflammatory cytokines were increased in heart extracts from saline-treated chagasic mice, compared with those in normal mice. The administration of G-CSF promoted a statistically significant reduction in the concentrations of both cytokines (**Fig. 4*A*,*B***). In contrast, a significant increase in TGF-β and IL-10 concentrations was observed in G-CSF-treated chagasic mice hearts compared with that in saline-treated controls (Fig. 4*C*, *D*). No significant differences were measured in IL-17 and IL-4 concentrations (Fig. 4*E*. *F*). Moreover, RT-qPCR analysis showed a significant decrease in *Tbet* gene expression after G-CSF administration (Fig. 4*G*), but no significant alterations in *GATA3* gene expression were observed in the hearts of chronic chagasic mice (Fig. 4*H*).

The systemic effects of G-CSF on cytokine production were also investigated. G-CSF increased IL-10 production in the spleens of chagasic mice compared with that in uninfected and saline-treated mice (**Fig. 5*A***). This effect was also correlated with a reversion in the overexpression of IL-17, TNF-α, and IFN-γ in sera or in the spleens of G-CSF-treated mice (Fig. 5*B*−*E*). In addition, G-CSF administration also induced an increase in *G-CSF* gene expression in the spleens of chagasic mice (Fig. 5*F*).

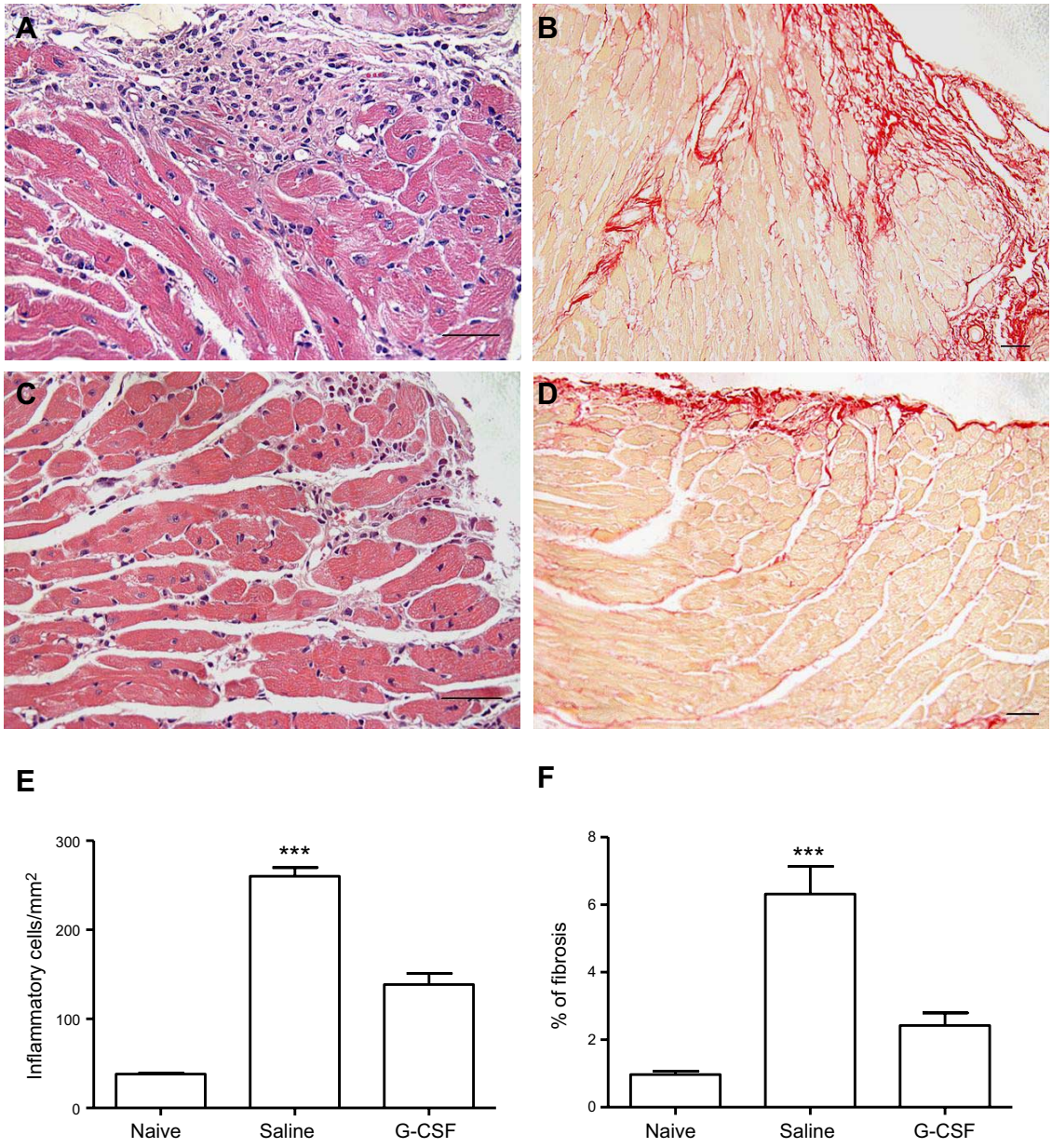

Figure 2. Reduction of inflammation and fibrosis in the hearts of chagasic mice after G-CSF administration. Groups of C57BL/6 mice in the chronic phase of infection (6 mo) were treated with saline (*A*, *B*) or G-CSF (*C*, *D*). *A*, *C*) heart sections stained with hematoxylin and eosin. *B*, *D*) Heart sections stained with Sirius red. *E*) Inflammatory cells were quantified in heart sections of naive mice, saline-treated chagasic mice, or G-CSF-treated chagasic mice and integrated by area. *F*) Fibrotic area is represented by percentage of collagen deposition in heart sections. Bars represent means ± SEM of 9−10 mice/group. ***$P < 0.001$.

G-CSF therapy increases the percentage of T_{reg} cells in the hearts of chagasic mice

Next, we examined whether G-CSF administration altered the number of T_{reg} cells in chagasic mice. G-CSF caused a decrease in the percentage of $CD4^+CD25^+$ cells in the bone marrow of chagasic mice (**Fig. 6*A*−*C***). Foxp3 expression was analyzed in cardiac $CD3^+$ cells by immunofluorescence. A higher percentage of $CD3^+$ $Foxp3^+$ T-cell expression was found in the hearts of G-CSF-treated mice compared with those of saline-treated mice (Fig. 6*D*−*F*). A partial recovery of $CD4^+CD25^+$ cells in the spleens of chagasic mice was observed after G-CSF administration (Fig. 6*G*), and splenic $Foxp3^+$ cells coexpressed IL-10 (Fig. 6*H*).

Effects of G-CSF administration on *T. cruzi* infection

To investigate whether the suppressive response induced by G-CSF treatment affected the immune response against the parasite, we first analyzed parasite-specific antibody levels in the sera of mice from the different experimental groups. Total IgG anti-*T. cruzi* antibody levels were similar between G-CSF and saline-treated chagasic mice (**Fig. 7*A***). A significant increase in IgG1 but not in IgG2 anti-*T. cruzi* antibodies was

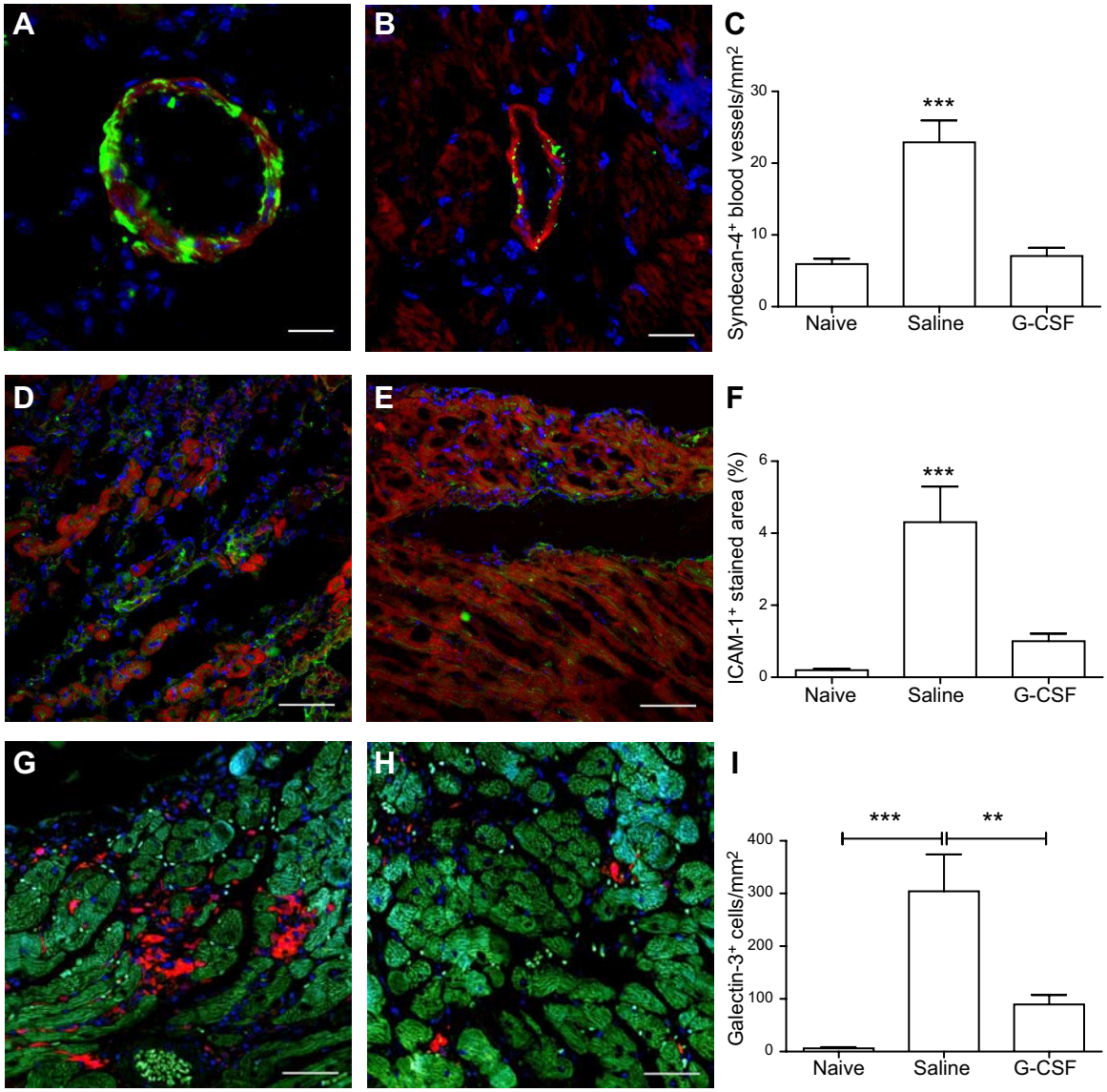

Figure 3. Reduction of syndecan-4, ICAM-1, and galectin-3 in hearts of chronic chagasic mice after G-CSF administration. Heart sections of saline-treated (*A*, *D*, *G*) or G-CSF-treated (*B*, *E*, *H*) mice were stained with anti-syndecan-4 (green; *A*, *B*), anti-ICAM-1 (green; *D*, *E*), or anti-galectin-3 (red; *G*, *H*) antibodies. F-actin stained with phalloidin 633 (red; *A*, *B*, *D*, *E*) or 488 (green; *G*, *H*). All sections were stained with DAPI for nuclear visualization (blue). Scale bars = 50 μm. *C*, *F*, *I*) Morphometric analyses in heart sections of naive mice or chagasic mice treated with saline or G-CSF. Bars represent means ± SEM of 3 animals/group. $^{**}P < 0.01$; $^{***}P < 0.001$.

found in the group treated with G-CSF compared with the saline-treated controls (Fig. 7*B*, *C*).

To evaluate whether G-CSF administration in chronic chagasic mice affected the residual *T. cruzi* infection, we performed RT-qPCR analysis to quantify the parasite load in the hearts of the mice. As shown in Fig. 7*D*, a significant reduction in the parasite load was observed in the hearts of G-CSF-treated mice compared with that in saline-treated controls. To determine whether G-CSF acts directly on the parasite, we analyzed the effects of G-CSF on *T. cruzi* cultures. Addition of G-CSF at various concentrations in axenic cultures of *T. cruzi* epimastigotes had little effect on viability at 30 μg/ml (**Table 1**). In contrast, a concentration-dependent trypanocidal effect was seen in cultures of isolated trypomastigotes (Table 1). In addition, when G-CSF was added to macrophage cultures infected with *T. cruzi*, a concentration-dependent decrease in the percentage of infected cells, as well as in the number of intracellular amastigotes, was observed (Fig. 7*E*, *F*).

DISCUSSION

The hallmark of CCC is the presence of a multifocal inflammatory response mainly composed of lymphocytes and macrophages, which promotes myocytolysis, fibrosis deposition, and myocardial remodeling (21). This is a progressively debilitating condition that occurs during a phase of the disease when parasitism is very scarce. Although the pathogenic mechanisms are still a matter of debate (22), the correlation of disease

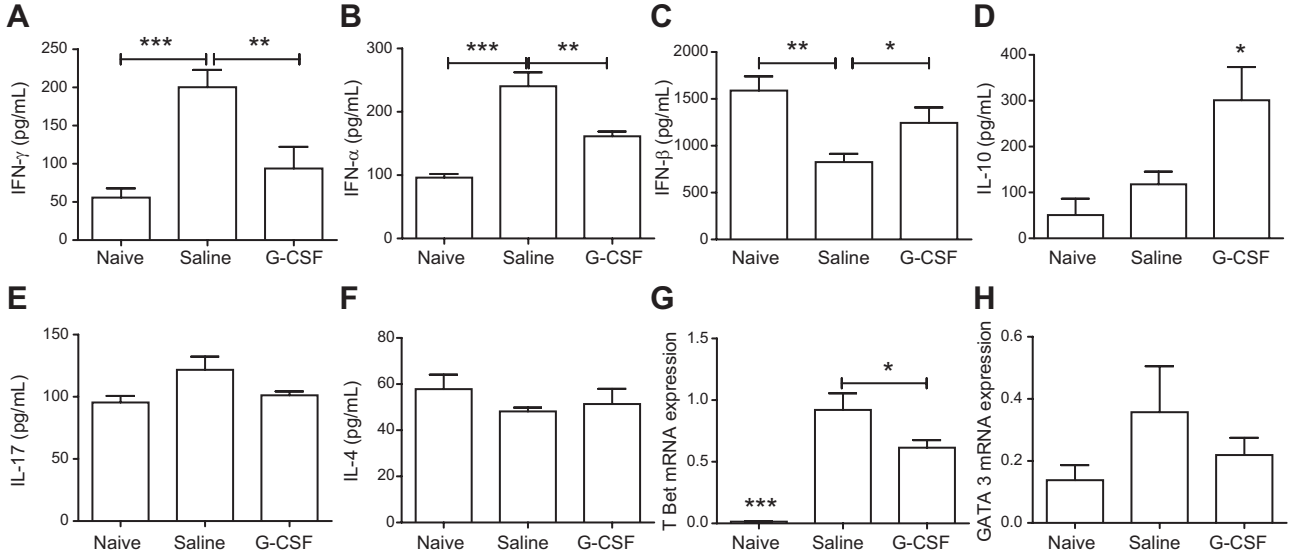

Figure 4. Modulation of cytokine production after G-CSF treatment. Concentrations of IFN-γ (*A*), TNF-α (*B*), TGF-β (*C*), IL-10 (*D*), IL-17 (*E*), and IL-4 (*F*) were determined in heart homogenates from naive (n=3) or chagasic mice treated with saline (n=7) or G-CSF (n=10), by ELISA. Analysis of *Tbet* (*G*) and *GATA3* (*H*) was performed by real-time RT-qPCR using cDNA samples prepared from mRNA extracted from hearts of naive and chronic chagasic mice treated with saline or G-CSF (n=9−10 mice/group). Values represent means ± SEM. *$P < 0.05$; **$P < 0.01$; ***$P < 0.001$.

severity and IFN-γ production has been well demonstrated (23, 24). The fact that the parasite persists in *T. cruzi*-infected individuals renders any immunosuppressive condition a risk for reactivation of parasitemia (25, 26).

In the present study, we have demonstrated that systemic administration of G-CSF, a cytokine widely used in the clinical setting, modulates the inflammatory response, decreasing the production of key inflammatory mediators such as IFN-γ and TNF-α, in the main target organ, the heart. Different cytokine profiles are involved in the control of both the immune response and pathology during *T. cruzi* infection. The control of parasitism during the acute phase of Chagas disease is critically dependent on effective macrophage activation by cytokines, such as IFN-γ and TNF-α, which are

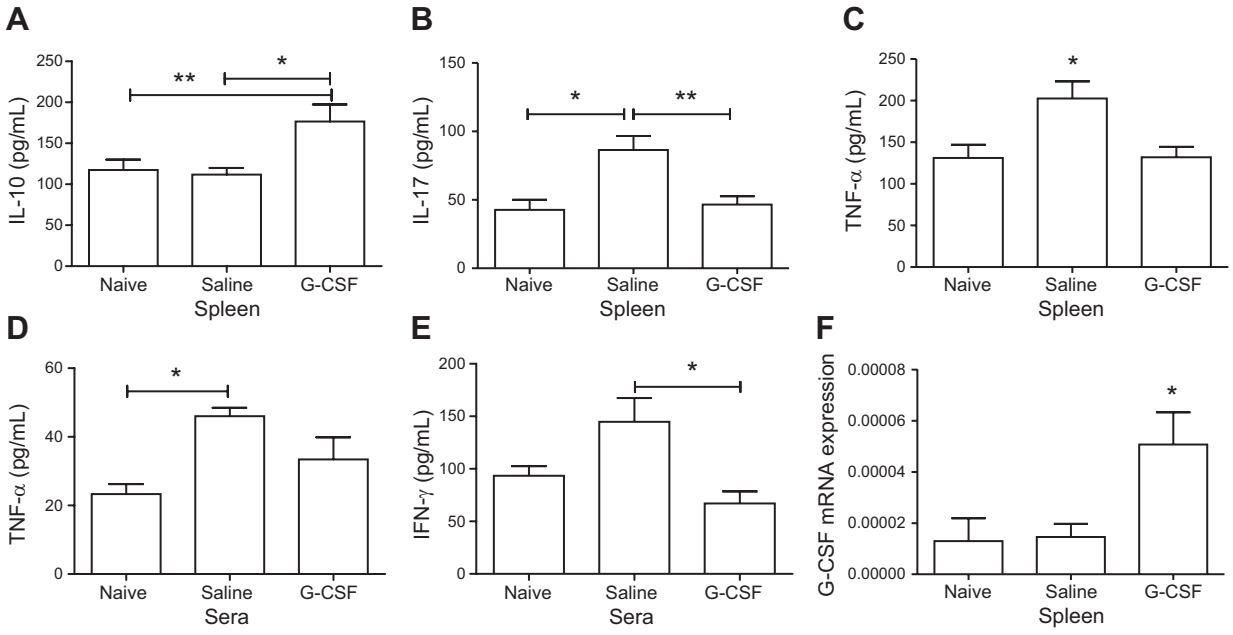

Figure 5. Modulation of systemic cytokine production in chronic chagasic mice treated with G-CSF. *A–E*) Concentrations of IL-10 (*A*), IL-17 (*B*), and TNF-α (*C*) were determined by ELISA in spleen homogenates and TNF-α (*D*) and IFN-γ (*E*) in the sera from naive (n=3) and chagasic mice treated with saline (n=7) or G-CSF (n=10). *F*) G-CSF mRNA expression was determined by real-time RT-qPCR using cDNA samples prepared from mRNA extracted from spleens of naive and chronic chagasic mice treated with saline or G-CSF. Values represent means ± SEM. *$P < 0.05$; **$P < 0.01$.

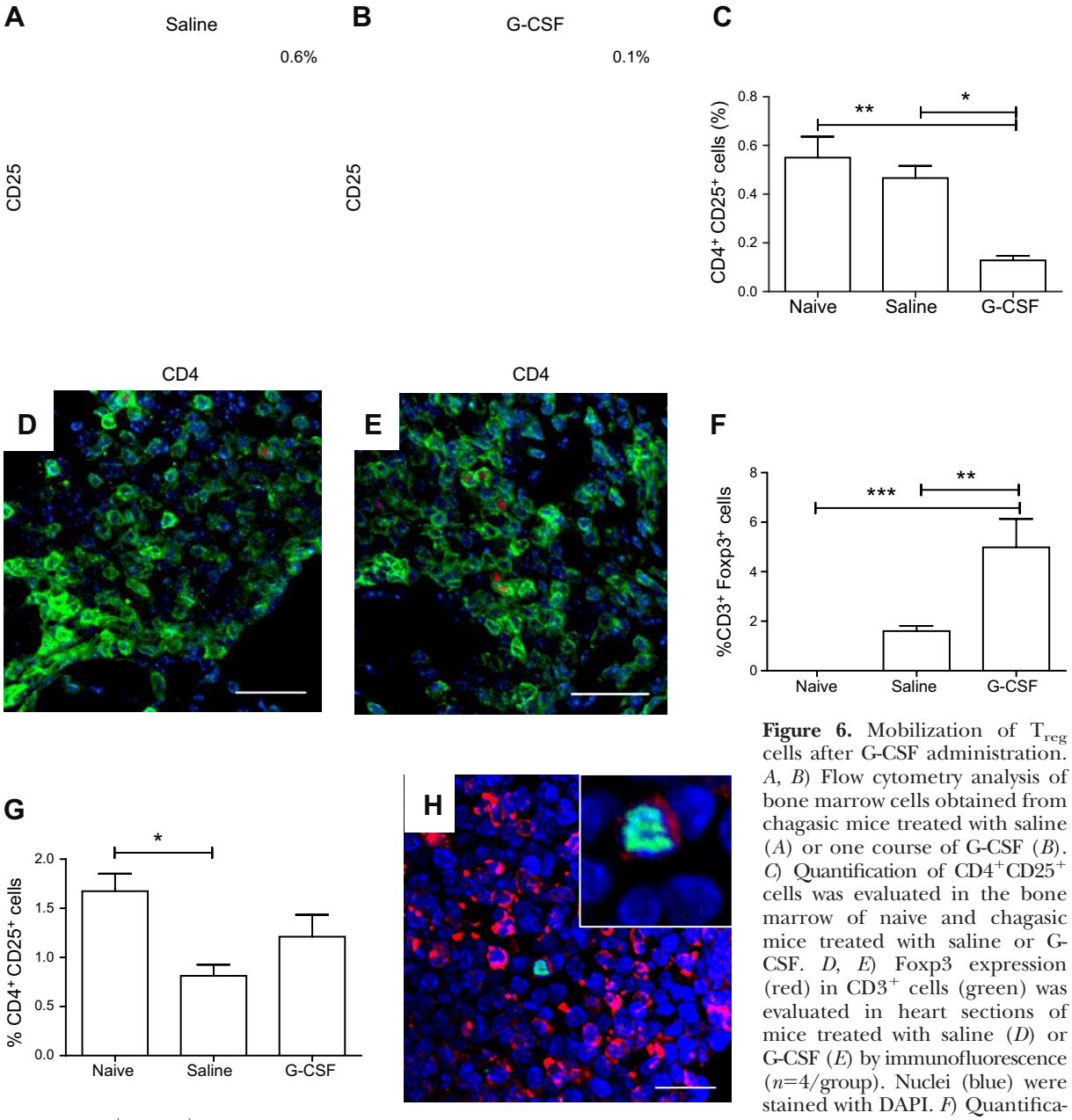

Figure 6. Mobilization of T_{reg} cells after G-CSF administration. *A*, *B*) Flow cytometry analysis of bone marrow cells obtained from chagasic mice treated with saline (*A*) or one course of G-CSF (*B*). *C*) Quantification of $CD4^+CD25^+$ cells was evaluated in the bone marrow of naive and chagasic mice treated with saline or G-CSF. *D*, *E*) Foxp3 expression (red) in $CD3^+$ cells (green) was evaluated in heart sections of mice treated with saline (*D*) or G-CSF (*E*) by immunofluorescence (n=4/group). Nuclei (blue) were stained with DAPI. *F*) Quantification of $CD3^+Foxp3^+$ cells in hearts of naive and chagasic mice treated with saline or G-CSF. *G*) Quantification of $CD4^+CD25^+$ cells was evaluated in the spleens of naive and chagasic mice treated with saline or G-CSF. Bars represent means ± SEM. *H*) Spleen section of a G-CSF-treated mouse, stained with anti-Foxp3 (green) and anti-IL-10 (red) antibodies. Nuclei (blue) were stained with DAPI. $*P < 0.05$; $**P < 0.01$; $***P < 0.001$.

crucial for limiting parasite replication (20, 27). On the other hand, an intense Th1 response will enhance heart inflammation (23), and elevated TNF-α may affect cardiomyocyte contraction (28). Exacerbated production of IFN-γ against *T. cruzi* antigens favors the development of a strong Th1 response in symptomatic cardiac patients, which leads to the progression of heart disease (20, 29). Despite the observed suppression of IFN-γ and TNF-α after G-CSF administration in chagasic mice, this therapy did not increase the parasite load, suggesting that the immune response against the parasite is still effective.

Previous reports have shown immune deviation induced after G-CSF treatment (30). In our model of Chagas disease, we did not observe an increase in IL-4, a marker of the Th2-type response. In addition, we found a significant decrease in *Tbet* mRNA, a transcriptional factor essential for Th1-polarized immune responses, but we did not observe a significant difference in gene expression levels for GATA3, essential for Th2 responses, in the hearts of G-CSF-treated mice. Therefore, our results do not indicate a shift toward a Th2 profile after G-CSF administration in chagasic mice, but rather a suppression of the Th1-type immune response found in chronic chagasic mice.

In addition to cytokines, the expression of adhesion molecules important to cell migration, such as syndecan-4 and ICAM-1, already shown to be elevated in the

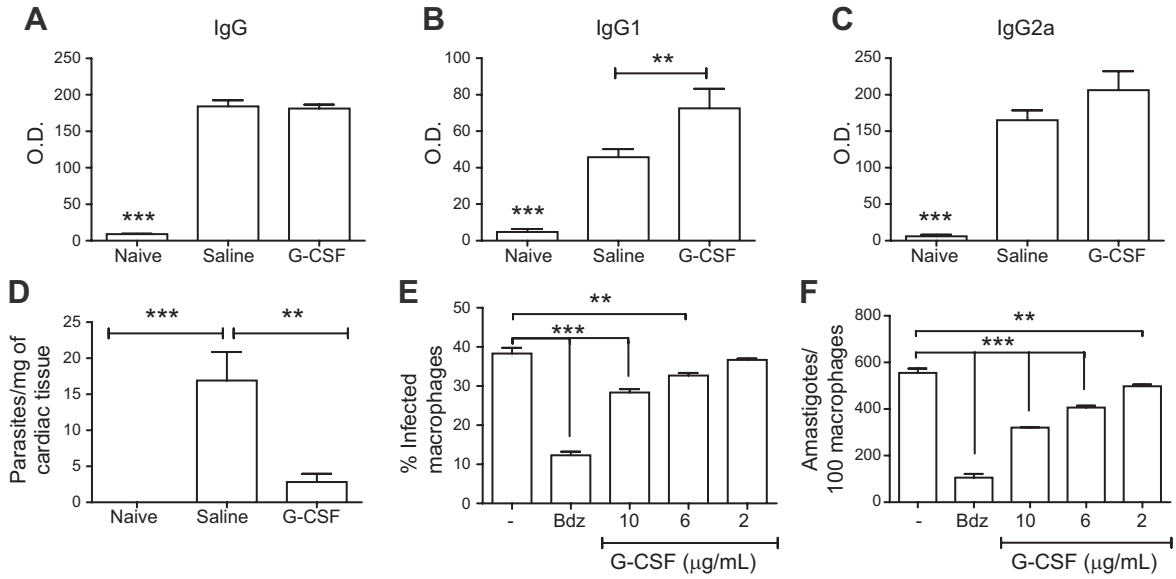

Figure 7. Effects of G-CSF on anti-*T. cruzi* antibody production and on the parasite. *A*–*C*) Serum samples from normal and *T. cruzi*-infected mice treated with saline or G-CSF (3 courses) were obtained 2 mo after treatment. Anti-*T. cruzi* levels of total IgG (*A*), IgG1 (*B*), and IgG2 (*C*) antibodies were determined by ELISA. Bars represent means ± SEM of 5–10 mice/group. *D*) Heart fragments obtained from normal and *T. cruzi*-infected mice treated with saline or G-CSF (3 courses) were used for DNA extraction and RT-qPCR analysis for quantification of parasite load. *E, F*) Mouse peritoneal macrophages were infected with *T. cruzi* and treated with G-CSF (3 and 10 μg/ml) or benznidazole (10 μg/ml), a standard drug. Numbers of infected cells (*E*) and amastigotes (*F*) were determined by counting hematoxylin and eosin-stained cultures. Values represent means ± SEM of triplicate determinations obtained in 1 of 2 experiments performed. $^{**}P < 0.01$; $^{***}P < 0.001$.

hearts of chronic chagasic mice (19, 29), was reduced after G-CSF therapy. TNF-α induces ICAM-1 expression, thus increasing endothelial adhesiveness for leukocytes (31). Syndecan-4 is a transmembrane heparan sulfate proteoglycan that acts cooperatively with integrins in generating signals necessary for the assembly of actin stress fibers and focal adhesions (32–34). Because TNF-α up-regulates syndecan-4 expression (35), the decreased expression in endothelial cells in the hearts of chagasic mice may be a consequence of the TNF-α down-regulation observed after G-CSF administration. Taken together, the decreases in syndecan-4 and ICAM-1 may contribute to a reduction in cell migration into the myocardium and, consequently, reduced inflammation.

Another important action of G-CSF in the Chagas disease model, as well as in other models of ischemic heart disease, is reduced fibrosis (17, 36). This may be due to the modulation in the heart of fibrogenic mediators, such as galectin-3, which have been shown to play important roles in fibrosis deposition and in heart failure (37). Galectin-3 expression was found in activated myocardial macrophages and is increased by IFN-γ (38, 39). In addition, the administration of recombinant galectin-3 in rats induced cardiac fibroblast proliferation, collagen production, and left ventricular dysfunction (38). Moreover, galectin-3 is known to play important roles in the regulation of inflammatory responses, including suppression of T-cell apoptosis (40). In fact, in our previous study, we observed an increase in apoptosis in the hearts of chagasic mice treated with G-CSF (16), correlating with the decrease of galectin-3 found herein.

TABLE 1. *Effects of G-CSF in axenic cultures of* T. cruzi *(Colombian strain)*

Drug	Conc. (μg/ml)	% Inhibition	
		Epimastigotes	Trypomastigotes
G-CSF	3	0.52 ± 0.52	1.90 ± 0.90
	10	2.58 ± 0.66	12.85 ± 1.43*
	30	9.60 ± 1.34**	24.28 ± 2.51***
Benznidazole	30	96.78 ± 0.06***	100***

Values are means ± SEM of 3 independent experiments. $^{*}P < 0.05$; $^{**}P < 0.01$; $^{***}P < 0.001$.

We observed suppression of inflammatory mediators after G-CSF administration, which was accompanied by an increase in IL-10 production in the hearts and spleens of chagasic mice. This is an important regulatory cytokine already shown to be associated with an improved outcome in chronic chagasic patients (20). Studies in noninfectious disease models have shown that G-CSF administration can induce both increases in IL-10 and TGF-β and mobilization of T_{reg} cells from the bone marrow (12, 41, 42). Evidence for the suppressive effects of G-CSF-mobilized T_{reg} cells are shown in a model of diabetes, in which isolated G-CSF-mobilized T_{reg} cells protected naive recipients against diabetogenic lymphocytes (42). Natural T_{reg} cells have emerged as potential immune tolerance mediators after immunotherapy in allergic diseases, comprising a population of circulating T cells that express the IL-$10^{+}CD4^{+}CD25^{+}$ phenotype involved in the ameliora-

tion of symptoms (43–45). The coexpression of IL-10 in T_{reg} cells, which demonstrated increased frequency after G-CSF treatment, suggests that these cells are a source of IL-10. In fact, the production of IL-10 has been described as one of the mechanisms by which T_{reg} cells exert their suppressive activity (46).

G-CSF administration had a systemic effect on the immune response, as shown by the reduction in- inflammatory mediators such as TNF-α and IFN-γ in the spleen and sera of chagasic mice. Although we did not observe significant alterations in IL-17 in the hearts of G-CSF-treated mice, G-CSF administration did affect splenetic IL-17 levels. In contrast to the work in naive mice performed by Hill *et al.* (47), we did not observe IL-17 induction after G-CSF administration in chronically infected mice. Concomitant with the reduction in inflammatory mediators, we observed increased production of IL-10 in the spleens of G-CSF-treated mice. $FoxP3^+$ cells also were costained for IL-10 in the spleens of chagasic mice treated with G-CSF, suggesting a role of this cell population in the modulatory action induced by G-CSF.

T_{reg} cells constitute an anti-inflammatory T-cell population associated with immune regulation, which may prevent tissue damage caused by parasite-triggered immune responses (48). T_{reg} cells expressing $CD4^+CD25^+$ cells have recently been associated with the expression of the regulatory lineage factor Foxp3 and are responsible for maintaining self-tolerance (49, 50). The increased percentage of T_{reg} cells in the spleens and lymph nodes of G-CSF-treated mice caused by mobilization of bone marrow-resident T_{reg} cells has been described previously (41). This mobilization of T_{reg} cells after G-CSF administration seems to be due to the reduced expression of SDF1, the CXCR4 ligand, in the bone marrow. Rutella *et al.* (51) reported that G-CSF induces an increase in T_{reg} cells in the peripheral blood of normal human recipients. Recent investigations evaluating the frequency of T_{reg} cells during early and late indeterminate forms of Chagas disease have shown a correlation between the severity of the CCC and a lower frequency or suppressive activity of $CD4^+CD25^+$ cells (52–54). Thus, our data corroborate these findings, because an inverse correlation between the percentage of T_{reg} cells, inflammatory cells, and cytokines in the heart of chagasic mice was found when G-CSF- and saline-treated mice were compared.

One important issue raised was whether the suppressive effects of G-CSF could interfere with the control of *T. cruzi* infection. The levels of anti-*T. cruzi* IgG antibodies in the sera of chagasic mice were not reduced after G-CSF treatment. More importantly, by using a very sensitive quantification method (18), we found a decrease in parasite load in the hearts of chronic chagasic mice treated with G-CSF compared with that in saline-treated mice, suggesting that this cytokine could have a direct effect on parasite elimination. To address this question, we evaluated the effects of G-CSF *in vitro*, in 3 parasitic forms. Although G-CSF had little effect on the viability of epimastigote form, it did significantly affect the forms found in the mammalian hosts (trypomastigotes and amastigotes) in a concentration-dependent manner. In fact, previous reports have shown that other cytokines, such as GM-CSF and TNF-α, can have direct effects on the parasite and interfere with *T. cruzi* infection (55). Taken together, our data indicate that parasitism reduction may be a positive effect of G-CSF therapy.

In conclusion, the present study reinforces our previous work, in which we demonstrated improvement in cardiopulmonary function after G-CSF administration, by revealing its potent anti-inflammatory properties in a model of parasite-driven heart disease. More importantly, we demonstrated the modulation of pathogenic immune responses without affecting the control of infection, a feature highly desired in the clinical setting. Finally, our results reinforce the possibility of clinical applications of G-CSF, a well-tolerated drug with few side effects, in the treatment of patients with CCC. FJ

The authors thank Kyan Allahdadi for careful review of the article. This work was supported by grants from the Brazilian Ministry of Sciences and Technology (MCT), Conselho Nacional de Pesquisas (CNPq), Financiadora de Estudos e Projetos (FINEP), Fundação Oswaldo Cruz (FIOCRUZ), and Fundação de Amparo as Pesquisas do Estado da Bahia (FAPESB). J.F.V. and A.C.D.A. were recipients of a Coordination for the Improvement of Higher Education Personnel (CAPES) doctoral scholarship from the Universidade Estadual de Feira de Santana/Programa de Pós-graduação em Biotecnologia (UEFS/PPgBIOTEC) and Rede Nordeste de Biotecnologia (RENORBIO) graduate programs, respectively. B.S.F.S. holds a CNPq doctoral scholarship, and C.S.M. holds a FAPESB master scholarship. M.B.P.S. and R.R.-D.-S. are recipients of CNPq senior fellowships.

REFERENCES

1. Franco-Paredes, C., Von, A., Hidron, A., Rodríguez-Morales, A. J., Tellez, I., Barragán, M., Jones, D., Náquira, C. G., and Mendez, J. (2007) Chagas disease: an impediment in achieving the millennium development goals in Latin America. *BMC Int. Health Hum. Rights* **7,** 1–6
2. Hotez, P. J., Bottazzi, M. E., Franco-Paredes, C., Ault, S. K., and Roses-Periago, M. (2008) The neglected tropical diseases of Latin America and the Caribbean: estimated disease burden and distribution and a roadmap for control and elimination. *PLoS Negl. Trop. Dis.* **2,** 1–11
3. Franco-Paredes, C., Bottazzi, M. E., and Hotez, P. J. (2009) The unfinished public health agenda of Chagas disease in the era of globalization. *PLoS Negl. Trop. Dis.* **3,** 1–4
4. World Health Organization. Chagas disease. Retrieved November 1, 2012, from http://www.who.int/mediacentre/factsheets/fs340/en/index.html
5. Bocchi, E. A., Bellotti, G., Mocelin, A., Uip, D., Bacal, F., Higuchi, M. L., Amato-Neto, V., Fiorelli, A., Stolf, N. A., Jatene, A. D., and Pileggi, F. (1996) Heart transplantation for chronic Chagas' heart disease. *Ann. Thorac. Surg.* **61,** 1727–1733
6. Von-Aulock, S., Boneberg, E. M., Diterich, I., and Hartung, T. (2004) Granulocyte colony-stimulating factor (filgrastim) treatment primes for increased ex vivo inducible prostanoid release. *J. Pharmacol. Exp. Ther.* **308,** 754–759
7. Hartung, T., Docke, W. D., Gantner, F., Krieger, G., Sauer, A., Stevens, P., Volk, H. D., and Wendel, A. (1995) Effect of granulocyte colony-stimulating factor treatment on ex vivo blood cytokine response in human volunteers. *Blood* **85,** 2482–2489

8. Boneberg E. M., and Hartung, T. (2002) Molecular aspects of anti-inflammatory action of G-CSF. *Inflamm. Res.* **51,** 119–128
9. Iwanaga, K., Takano, H., Ohtsuka, M., Hasegawa, H., Zou, Y., Qin, Y., Odaka, K., Hiroshima, K., Tadokoro, H., and Komuro, I. (2004) Effects of G-CSF on cardiac remodeling after acute myocardial infarction in swine. *Biochem. Biophys. Res. Commun.* **325,** 1353–1359
10. Harada, M., Qin, Y., Takano, H., Minamino, T., Zou, Y., Toko, H., Ohtsuka, M., Matsuura, K., Sano, M., Nishi, J., Iwanaga, K., Akazawa, H., Kunieda, T., Zhu, W., Hasegawa, H., Kunisada, K., Nagai, T., Nakaya, H., Yamauchi-Takihara, K., and Komuro, I. (2005) G-CSF prevents cardiac remodeling after myocardial infarction by activating the Jak-Stat pathway in cardiomyocytes. *Nat. Med.* **11,** 305–311
11. Higuchi, T., Yamauchi-Takihara, K., Matsumiya, G., Fukushima, N., Ichikawa, H., Kuratani, T., Maehata, Y., and Sawa, Y. (2008) Granulocyte colony-stimulating factor prevents reperfusion injury after heart preservation. *Ann. Thorac. Surg.* **85,** 1367–1373
12. Rutella, S., Zavala, F., Danese, S., Kared, H., and Leone, G. (2005) Granulocyte colony-stimulating factor: a novel mediator of T cell tolerance. *J. Immunol.* **175,** 7085–7091
13. Sakaguchi, S. (2005) Naturally arising Foxp3-expressing $CD25^{+}CD4^{+}$ regulatory T cells in immunological tolerance to self and non-self. *Nat. Immunol.* **6,** 345–352
14. Rutella, S., Pierelli, L., Bonanno, G., Sica, S., Ameglio, F., Capoluongo, E., Mariotti, A., Scambia, G., d'Onofrio, G., and Leone, G. (2002) Role for granulocyte colony-stimulating factor in the generation of human T regulatory type 1 cells. *Blood* **100,** 2562–2571
15. Rossetti, M., Gregori, S., and Roncarolo, M. G. (2010) Granulocyte-colony stimulating factor drives the in vitro differentiation of human dendritic cells that induce anergy in naive T cells. *Eur. J. Immunol.* **40,** 3097–3106
16. Macambira, S. G., Vasconcelos, J. F., Costa, C. R., Klein, W., Lima, R. S., Guimarães, P., Vidal, D. T., Mendez, L. C., Ribeiro-Dos-Santos, R., and Soares, M. B. (2009) Granulocyte colony-stimulating factor treatment in chronic Chagas disease: preservation and improvement of cardiac structure and function. *FASEB J.* **23,** 3843–3850
17. Federici, E. E., Abelmann, W. H., and Neva, F. A. (1964) Chronic and progressive myocarditis and myositis in C3H mice infected with *Trypanosoma cruzi*. *Am. J. Trop. Med. Hyg.* **13,** 272–280
18. Schijman, A. G., Bisio, M., Orellana, L., Sued, M., Duffy, T., Mejia Jaramillo, A. M., Cura, C., Auter, F., Veron, V., Qvarnstrom, Y., Deborggraeve, S., Hijar, G., Zulantay, I., Lucero, R. H., Velazquez, E., Tellez, T., Sanchez Leon, Z., Galvão, L., Nolder, D., Monje Rumi, M., Levi, J. E., Ramirez, J. D., Zorrilla, P., Flores, M., Jercic, M. I., Crisante, G., Añez, N., De Castro, A. M., Gonzalez, C. I., Acosta Viana, K., Yachelini, P., Torrico, F., Robello, C., Diosque, P., Triana Chavez, O., Aznar, C., Russomando, G., Büscher, P., Assal, A., Guhl, F., Sosa Estani, S., DaSilva, A., Britto, C., Luquetti, A., and Ladzins, J. (2011) International study to evaluate PCR methods for detection of *Trypanosoma cruzi* DNA in blood samples from Chagas disease patients. *PLoS Negl. Trop. Dis.* **5,** 1–13
19. Soares, M. B., de Lima, R. S., Rocha, L. L., Vasconcelos, J. F., Rogatto, S. R., dos Santos, R. R., Iacobas, S., Goldenberg, R. C., Iacobas, D. A., Tanowitz, H. B., de Carvalho, A. C., and Spray, D. C. (2010) Gene expression changes associated with myocarditis and fibrosis in hearts of mice with chronic chagasic cardiomyopathy. *J. Infect. Dis.* **202,** 416–426
20. Gomes, J. A., Bahia-Oliveira, L. M., Rocha, M. O., Martins-Filho, O. A., Gazzinelli, G., and Correa-Oliveira, R. (2003) Evidence that development of severe cardiomyopathy in human Chagas' disease is due to a Th1-specific immune response. *Infect. Immun.* **71,** 1185–1193
21. Köberle, F. (1968) Chagas' disease and Chagas' syndromes: the pathology of American trypanosomiasis. *Adv. Parasitol.* **6,** 63–116
22. Soares, M.B., Silva-Mota, K.N., Lima, R.S., Bellintani, M.C., Pontes-de-Carvalho, L., and Ribeiro-dos-Santos, R. (2001) Modulation of chagasic cardiomyopathy by IL-4: dissociation between inflammatory and tissue parasitism. *Am. J. Pathol.* **159,** 703–709
23. Soares, M. B. P., Pontes-de-Carvalho, L., and Ribeiro-dos-Santos, R. (2001) The pathogenesis of Chagas' disease: when autoimmune and parasite-specific immune responses meet. *An. Acad. Bras. Cienc.* **73,** 547–559
24. Bahia-Oliveira, L. M. G., Gomes, J. A. S., Rocha, M. O. S., Moreira, M. C., Lemos, E. M., Luz, Z. M., Pereira, M. E., Coffman, R. L., Dias, J. C., Cançado, J. R., Gazzinelli, G., and Corrêa-Oliveira, R. (1998) IFN-γ in human Chagas' disease: protection or pathology? *Braz. J. Med. Biol. Res.* **31,** 127–131
25. Galhardo, M. C. G., Martins, I. A., Hasslocher-Moreno, A., Xavier, S. S., Coelho, J. M., Junqueira, A. C., and dos Santos, R. R. (1999) Reactivation of *Trypanosoma cruzi* infection in a patient with acquired immunodeficiency syndrome. *Rev. Soc. Bras. Med. Trop.* **32,** 291–294
26. Campos, S. V., Strabelli, T. M., Amato Neto, V., Silva, C. P., Bacal, F., Bocchi, E. A., and Stolf, N. A. (2008) Risk factors for Chagas' disease reactivation after heart transplantation. *J. Heart Lung Transplant.* **27,** 597–602
27. Tadokoro, C. E., and Abrahamsohn, I. A. (2001) Bone marrow-derived macrophages grown in GM-CSF or M-CSF differ in their ability to produce IL-12 and to induce IFN-γ production after stimulation with *Trypanosoma cruzi* antigens. *Immunol. Lett.* **77,** 31–38
28. Ferrari, R. (1999) The role of TNF in cardiovascular disease. *Pharmacol. Res.* **40,** 97–105
29. Soares, M. B., Lima, R. S., Souza, B. S. F., Vasconcelos, J. F., Rocha, L. L., Dos Santos, R. R., Iacobas, S., Goldenberg, R. C., Lisanti, M. P., Iacobas, D. A., Tanowitz, H. B., Spray, D. C., and Campos de Carvalho, A. C. (2011) Reversion of gene expression alterations in hearts of mice with chronic chagasic cardiomyopathy after transplantation of bone marrow cells. *Cell Cycle* **10,** 1448–1455
30. Sloand, E., Kim, S., Maciejewski, J., Van Rhee, F., Chaudhuri, A., Barrett, J., and Young, N. S. (2000) Pharmacologic doses of granulocyte colony stimulating factor affect cytokine production by lymphocytes in vitro and in vivo. *Blood* **95,** 2269–2274
31. Ledebur, H. C., and Parks, T. P. (1995) Transcriptional regulation of the intercellular adhesion molecule-1 gene by inflammatory cytokines in human endothelial cells. Essential roles of a variant NF-κB site and p65 homodimers. *J. Biol. Chem.* **270,** 933–943
32. Horowitz, A., Tkachenko, E., and Simons, M. (2002) Fibroblast growth factor-specific modulation of cellular response by syndecan-4. *J. Cell Biol.* **157,** 715–725
33. Ishiguro, K., Kojima, T., and Muramatsu, T. (2003) Syndecan-4 as a molecule involved in defense mechanisms. *Glycoconj. J.* **19,** 315–318
34. Hamon, M., Mbemba, E., Charnaux, N., Slimani, H., Brule, S., Saffar, L., Vassy, R., Prost, C., Lievre, N., Starzec, A., and Gattegno, L. (2004) A syndecan-4/CXCR4 complex expressed on human primary lymphocytes and macrophages and HeLa cell line binds the CXC chemokine stromal cell-derived factor-1 (SDF-1). *Glycobiology* **14,** 311–313
35. Zhang, Y., Pasparakis, M., Kollias, G., and Simons, M. (1999) Myocyte-dependent regulation of endothelial cell syndecan-4 expression. Role of TNF-alpha. *J. Biol. Chem.* **274,** 14786–14790
36. Angeli, F. S., Amabile, N., Shapiro, M., Mirsky, R., Bartlett, L., Zhang, Y., Virmani, R., Chatterjee, K., Boyle, A., Grossman, W., and Yeghiazarians, Y. (2010) Cytokine combination therapy with erythropoietin and granulocyte colony stimulating factor in a porcine model of acute myocardial infarction. *Cardiovasc. Drugs Ther.* **24,** 409–420
37. Joo, H. G., Goedegebuure, P. S., Sadanaga, N., Nagoshi, M., and Von Bernstorff, W., and Eberlein, T. J. (2001) Expression and function of galectin-3, a β-galactoside-binding protein in activated T lymphocytes. *J. Leukoc. Biol.* **69,** 555–564
38. Sharma, U. C., Pokharel, S., Brakel, T. J. V., van Berlo, J. H., Cleutjens, J. P., Schroen, B., André, S., Crijns, H. J., Gabius, H. J., Maessen, J., and Pinto, Y. M. (2004) Galectin-3 marks activated macrophages in failure-prone hypertrophied hearts and contributes to cardiac dysfunction. *Circulation* **110,** 3121–3128
39. Reifenberg, K., Lehr, H. A., Torzewski, M., Steige, G., Wiese, E., Küpper, I., Becker, C., Ott, S., Nusser, P., Yamamura, K., Rechtsteiner, G., Warger, T., Pautz, A., Kleinert, H., Schmidt, A., Pieske, B., Wenzel, P., Münzel, T., and Löhler, J. (2007) Interferon-γ induces chronic active myocarditis and cardiomyopathy in transgenic mice. *Am. J. Pathol.* **171,** 463–472

40. Rabinovich, G. A., Ramhorst, R. E., Rubinstein, N., Corigliano, A., Daroqui, M. C., Kier-Joffé, E.B., and Fainboim, L. (2002) Induction of allogenic T-cell hyporesponsiveness by galectin-1-mediated apoptotic and non-apoptotic mechanisms. *Cell Death Differ.* **9,** 661–670
41. Zou, L., Barnett, B., Safah, H., Larussa, V. F., Evdemon-Hogan, M., Mottram, P., Wei, S., David, O., Curiel, T. J., and Zou, W. (2004) Bone marrow is a reservoir for $CD4^+CD25^+$ regulatory T cells that traffic through CXCL12/CXCR4 signals. *Cancer Res.* **64,** 8451–8455
42. Kared, H., Masson, A., Adle-Biassette, H., Bach, J. F., Chatenoud, L., and Zavala, F. (2005) Treatment with granulocyte colony-stimulating factor prevents diabetes in NOD mice by recruiting plasmacytoid dendritic cells and functional $CD4^+CD25^+$ regulatory T-cells. *Diabetes* **54,** 78–84
43. Francis, J. N., Till, S. J., and Durham, S. R. (2003) Induction of IL-$10^+CD4^+CD25^+$ T cells by grass pollen immunotherapy. *J. Allergy Clin. Immunol.* **111,** 1255–1261
44. Gardner, L. M., Thien, F. C., Douglass, J. A., Rolland, J. M., and O'Hehir, R. E. (2004) Induction of T 'regulatory' cells by standardized house dust mite immunotherapy: an increase in $CD4^+CD25^+$interleukin-10^+ T cells expressing peripheral tissue trafficking markers. *Clin. Exp. Allergy* **34,** 1209–1219
45. Urry, Z., Chambers, E. S., Xystrakis, E., Dimeloe, S., Richards, D. F., Gabryšová, L., Christensen, J., Gupta, A., Saglani, S., Bush, A., O'Garra, A., Brown, Z., and Hawrylowicz, C. M. (2012) The role of 1α,25-dihydroxyvitamin D_3 and cytokines in the promotion of distinct $Foxp3^+$ and IL-10^+ $CD4^+$ T cells. *Eur. J. Immunol.* **42,** 2697–2708
46. Morris, E. S., MacDonald, K. P., Rowe, V., Johnson, D. H., Banovic, T., Clouston, A. D., and Hill, G. R. (2004) Donor treatment with pegylated G-CSF augments the generation of IL-10-producing regulatory T cells and promotes transplantation tolerance. *Blood* **103,** 3573–3581
47. Hill, G. R., Olver, S. D., Kuns, R. D., Varelias, A., Raffelt, N. C., Don, A. L., Markey, K. A., Wilson, Y. A., Smyth, M. J., Iwakura, Y., Tocker, J., Clouston, A. D., and Macdonald, K. P. (2010) Stem cell mobilization with G-CSF induces type 17 differentiation and promotes scleroderma. *Blood* **116,** 819–828
48. Belkaid, Y., Blank, R. B., and Suffia, I. (2006) Natural regulatory T cells and parasites: a common quest for host homeostasis. *Immunol. Rev.* **212,** 287–300
49. Itoh, M., Takahashi, T., Sakaguchi, N., Kuniyasu, Y., Shimizu, J., Otsuka, F., and Sakaguchi, S. (1999) Thymus and autoimmunity: production of $CD25^+CD4^+$ naturally anergic and suppressive T cells as a key function of the thymus in maintaining immunologic self-tolerance. *J. Immunol.* **162,** 5317–5326
50. Shevach, E. M. (2009) Mechanisms of $foxp3^+$ T regulatory cell-mediated suppression. *Immunity* **30,** 636–645
51. Rutella, S., Bonanno, G., Pierelli, L., Mariotti, A., Capoluongo, E., Contemi, A. M., Ameglio, F., Curti, A., De Ritis, D. G., Voso, M. T., Perillo, A., Mancuso, S., Scambia, G., Lemoli, R. M., and Leone, G. (2004) Granulocyte colony-stimulating factor promotes the generation of regulatory DC through induction of IL-10 and IFN-α. *Eur. J. Immunol.* **34,** 1291–1302
52. Vitelli-Avelar, D. M., Sathler-Avelar, R., Dias, J. C. P., Pascoal, V. P., Teixeira-Carvalho, A., Lage, P. S., Elói-Santos, S. M., Corrêa-Oliveira, R., and Martins-Filho, O. A. (2005) Chagasic patients with indeterminate clinical form of the disease have high frequencies of circulating $CD3^+CD16^-CD56^+$ natural killer T cells and $CD4^+CD25^{High}$ regulatory T lymphocytes. *Scand. J. Immunol.* **62,** 297–308
53. De-Araújo, F. F., Vitelli-Avelar, D. M., Teixeira-Carvalho, A., Antas, P. R., Assis Silva Gomes, J., Sathler-Avelar, R., Otávio Costa Rocha, M., Elói-Santos, S. M., Pinho, R. T., Correa-Oliveira, R., and Martins-Filho, O. A. (2011) Regulatory T cells phenotype in different clinical forms of Chagas' disease. *PLoS Negl. Trop. Dis.* **5,** 1–8
54. Guedes, P. M., Gutierrez, F. R., Silva, G. K., Dellalibera-Joviliano, R., Rodrigues, G. J., Bendhack, L. M., Rassi, A.. Jr., Rassi, A., Schmidt, A., Maciel, B. C., Marin Neto, J. A., and Silva, J. S. (2012) Deficient regulatory T cell activity and low frequency of IL-17-producing T cells correlate with the extent of cardiomyopathy in human Chagas' disease. *PLoS Negl. Trop. Dis.* **6,** 1–11
55. Olivares-Fontt, E. O., de Baetselier, P., Heirman, C., Thielemans, K., Lucas, R., and Vray, B. (1998) Effects of granulocyte-macrophage colony-stimulating factor and tumor necrosis factor alpha on *Trypanosoma cruzi* trypomastigotes. *Infect. Immun.* **66,** 2722–2727

Received for publication February 20, 2013.
Accepted for publication August 5, 2013.

ANEXO IV

Assessment of Galectin-3 Polymorphism in Subjects with Chronic Chagas Disease

Gabriela da Silva Cruz[1], Ana Luiza Dias Angelo[1], Ticiana Ferreira Larocca[1,2,3], Carolina Thé Macedo[1,2,3], Márcia Noya- Rabelo[2], Luís Claudio Lemos Correia[2], Jorge Andion Torreão[2], Bruno Solano de Freitas Souza[1,3], Ricardo Ribeiro dos Santos[1,3], Milena Botelho Pereira Soares[1,3]

Centro de Biotecnologia e Terapia Celular – Hospital São Rafael[1]; Departamento de Cardiologia - Hospital São Rafael[2]; Centro de Pesquisas Gonçalo Moniz - FIOCRUZ[3], Salvador, BA - Brazil

Abstract

Background: Galectin-3, a β-galactoside binding lectin, has been described as a mediator of cardiac fibrosis in experimental studies and as a risk factor associated with cardiovascular events in subjects with heart failure. Previous studies have evaluated the genetic susceptibility to Chagas disease in humans, including the polymorphisms of cytokine genes, demonstrating correlations between the genetic polymorphism and cardiomyopathy development in the chronic phase. However, the relationship between the galectin-3 single nucleotide polymorphism (SNP) and phenotypic variations in Chagas disease has not been evaluated.

Objective: The present study aimed to determine whether genetic polymorphisms of galectin-3 may predispose to the development of cardiac forms of Chagas disease.

Methods: Fifty-five subjects with Chagas disease were enrolled in this observational study. Real-time polymerase chain reaction (PCR) was used for genotyping the variants rs4644 and rs4652 of the galectin-3 gene.

Results: For the SNP rs4644, the relative risk for the cardiac form was not associated with the genotypes AA (OR = 0.79, p = 0.759), AC (OR = 4.38, p = 0.058), or CC (OR = 0.39, p = 0.127). Similarly, for the SNP rs4652, no association was found between the genotypes AA (OR = 0.64, p = 0.571), AC (OR = 2.85, p = 0.105), or CC (OR = 0.49, p = 0.227) and the cardiac form of the disease.

Conclusion: Our results showed no association between the different genotypes for both SNPs of the galectin-3 gene and the cardiac form of Chagas disease. (Arq Bras Cardiol. 2015; [online].ahead print, PP.0-0)

Keywords: Chagas Disease; Galectin 3; Heart Failure; Polymorphism, Genetic; Chagas Cardiomyopathy

Introduction

Chagas disease (CD), caused by the intracellular parasite *Trypanosoma cruzi*, is a major public health problem in Latin America and affects millions of people worldwide[1]. About 30% of the patients develop chronic cardiomyopathy, which is the most severe form of CD and associated with worse prognosis in heart failure[2]. Since there is no effective treatment in this stage of the disease, it is crucial to identify biomarkers that might be used in the early detection of cardiac disease and prognostic stratification.

Previous studies have evaluated the genetic susceptibility to CD in humans. Polymorphisms of molecules involved in host damage, induced by the parasite, such as IL-4, IL-6, IL-10, IL-12, TNF-α, and IFN-γ have been determined in subjects with the disease, demonstrating the association between genetic polymorphism and the development of cardiomyopathy in the chronic phase of CD[3-8].

Recently, our group has demonstrated that the galectin-3 gene is overexpressed in the heart of animals chronically infected with *Trypanosoma cruzi*[9,10]. Galectin-3 is a member of the galectin family that binds β-galactosides and is produced by activated macrophages and fibroblasts[11]. It has been shown to be a mediator of cardiac fibrosis in experimental studies[11,12] and to be related to cardiovascular events and heart failure severity[13,14].

Previous studies have shown that genetic variants at two galectin-3 gene single nucleotide polymorphism (SNP) sites (rs4644 and rs4652, corresponding to *LGALS3* +191 A>C and *LGALS3* +292 A>C, respectively) are able to change the protein levels[15]. Galectin-3 plays an important role in inflammation and fibrosis process, and the relationship between the SNPs in the galectin-3 gene and the phenotypic variations in CD have not been evaluated. We hypothesized that galectin-3 SNPs can influence the development of cardiac forms of Chagas disease. Therefore, the present study aimed to evaluate the correlation of genetic polymorphisms of galectin-3 with severity of the cardiac form of Chagas disease.

Mailing Address: Ticiana Ferreira Larocca •
Av. São Rafael, 2152. Postal Code 41253-190. São Marcos, Salvador, BA - Brazil
Email: ticiana@cbtc-hsr.org
Manuscript received May 21, 2015; revised manuscript June 01, 2015; accepted June 23, 2015

DOI: 10.5935/abc.20150105

Methods

Study population

A retrospective observational study was performed between January 2011 and December 2013. A convenience sample of 55 subjects attending the CD outpatient clinic at Hospital São Rafael was studied.

Inclusion criteria were: CD diagnosis confirmed microbiologically by two serological tests (indirect hemagglutination and indirect immunofluorescence), and age from 18 to 70 years. Exclusion criteria were: previous myocardial infarction or history of coronary artery disease, primary valve disease, dialysis treatment for end-stage renal disease, active liver disease, hematologic, neoplastic or bone diseases, and contraindications to magnetic resonance imaging (MRI).

The study complied with the Declaration of Helsinki and was approved by the Ethics Committee. All subjects signed a written informed consent before their inclusion in the study. All subjects underwent a structured medical history and physical examination, blood analysis, 12-lead Electrocardiography (ECG), chest X-Ray, 24-h Holter monitoring, conventional Doppler echocardiogram, and cardiac magnetic resonance.

Genotyping of galectin-3 gene SNPs

Samples of genomic DNA were obtained from peripheral blood mononuclear cells. DNA extraction was performed using the commercial kit QIAamp DNA Blood Mini Kit (Qiagen GmbH, Hilden, Germany), according to the manufacturer's recommendations. The samples were stored in a freezer at -20°C. Genotyping of the SNPs rs4644 and rs4652 of the galectin-3 gene was performed by real-time polymerase chain reaction (PCR) using TaqMan® (Life Technologies, Carlsbad, USA), and the SNPs were amplified using the TaqMan® Universal PCR protocol (Life Technologies). Genotypes of each SNP were determined using the Sequence Detection System software version 1.3.1 (Life Technologies). The probes and primers for the selected SNPs were supplied by the same company.

Doppler echocardiogram

Standard transthoracic echocardiographic examination was performed using the Vivid 7 digital ultrasound system (GE Vingmed Ultrasound AS, Horten, Norway). Three cardiac cycles were stored in cineloop format for offline analysis. Left ventricle (LV) and left atrial dimensions were measured according to the American Society of Echocardiography's recommendations[16]. The LV ejection fraction (LVEF) was measured using the biplane Simpson's method.

Cardiac magnetic resonance imaging

Cardiac magnetic resonance imaging was performed using a Sigma HDx 1.5-T system (General Electric; Fairfield, CT, USA). For assessment of the LV function, electrocardiography-gated, breath-hold long-axis, short-axis, and four-chamber views were acquired in the same location in different sequences. Acquisition parameters used for the dynamic sequence included a repetition time (RT) of 3.5 ms, an echo time (ET) of 1.5 ms, flip angle of 60°, a receiver bandwidth of 125 kHz, a 35 x 35 cm field of view (FOV), a matrix of 256x148, a temporal resolution (TR) of 35 ms, and a slice thickness of 8.0 mm without gap. Delayed enhancement images were acquired every heartbeat, 10 to 20 min after the administration of a gadolinium-based contrast (0.1 mmol/kg) using RT of 7.1 ms, ET of 3.1 ms, flip angle of 20°, first cardiac phase, views per segment 16/32, matrix size of 256 x 192, slice thickness of 8.0 mm, gap between slices of 2 mm, field of view 32 to 38 cm, inversion time 150 to 300 ms, receiver bandwidth of 31.25 kHz, number of excitations of 2. The myocardial delayed enhancement (MDE) technique was used to investigate myocardial fibrosis, which was estimated by a quantitative visual method.

Statistical analysis

Categorical data were expressed as numbers (percentages, 95% confidence interval), and continuous data were expressed as mean ± SD or median (interquartile range). The genotype distribution of the SNPs rs4644 and rs4652 (AA, AC and CC) in subjects with indeterminate form of CD was compared with that in subjects with the cardiac form of CD using the Chi-square test or the Fisher's exact test. The percentage of myocardial fibrosis was compared between the groups with the 3 different genotypes Kruskal-Wallis test. Mann-Whitney test was used to assess differences in the median of myocardial fibrosis between subjects with and without the SNPs. The association between the cardiac form of CD and each of the genotypes (AA, AC and CC) was estimated by Odds Ratio (OR) and 95% confidence interval (CI). Cases with missing data were dropped from the analysis. Analyses were performed using SPSS version 20.0 (IBM), and $p < 0.05$ (two-tailed) was considered statistically significant.

Results

Clinical and imaging characteristics

The study comprised 55 subjects, 42% were men, with mean age of 58 ± 9 years. The prevalence of hypertension, diabetes, hypercholesterolemia and smoking were 71, 14, 42 and 27% respectively. Regarding the clinical forms, the subjects were distributed as follows: 16 (29%) with the indeterminate form (subjects with no evidence of cardiac involvement or heart failure), 16 (29%) with the cardiac form without ventricular dysfunction and 23 (42%) with the cardiac form with ventricular dysfunction. Seventeen subjects were in NYHA (New York Heart Association) functional class III-IV (31%). The mean LVEF, measured using the biplane Simpson's method, was 54 ± 15%, and the median percentage of myocardial fibrosis was 9.4% (2.2-17.3). Clinical and demographic characteristics of the subjects are described in Table 1.

Genotyping of LGALS3 SNPs

The SNPs genotype distribution is described in Table 2. There was no significant association between *LGALS3* genotypes (AA, AC, CC) of the SNPs rs4644 and rs4652 and the presence of the cardiac form of CD. For the SNP rs4644, the relative risk of the cardiac form was not associated with the genotype AA (OR = 0.79, 95%CI = 0.17 to 3.63, p = 0.759), AC (OR = 4.38, 95%CI = 0.87 to 22.02, p = 0.058), or CC

Table 1 - Subjects' clinical and demographic characteristics

	Subjects (n = 55)
Male gender	23 (41.8)
Age (years)	58 ± 9
Indeterminate form	16 (29)
Cardiac form without ventricular dysfunction	16 (29)
Cardiac form with ventricular dysfunction	23 (42)
NYHA III ou IV	17 (30.9)
Hypertension	39 (70.9)
Diabetes	8 (14.5)
Current smoking	15 (27.3)
Hypercholesterolemia	23 (41.8)
RBBB	27 (49.1)
Hemoglobin (g/dl)	14.0 ± 0.97
Creatinin (mg/dl)	0.87 ± 0.16
LVEF (%)	53.7 ± 15.4
LVESV (ml)	79.1 ± 65.4
LVEDV (ml)	177.3 ± 80.6
LVmass (g)	172.8 ± 57.3
Myocardial fibrosis (%)	9.4 (2.2-17.3)*

*Data are expressed as number (percentage) for categorical variables, and as mean ± SD or median (interquartile interval) for continuous variables; NYHA: New York Heart Association CMR: RBBB: Right bundle-branch block; LVEF: Left ventricular ejection fraction; LVESV: Left ventricular end-systolic volume; LVEDV: Left ventricular end-diastolic volume; LV: Left ventricular mass. *n = 40 (delayed enhancement cardiac magnetic resonance).*

Table 2 - Genotype and allele frequency of LGALS3 + 191 and LGALS3+292 in 16 subjects with the indeterminate form and 39 subjects with the cardiac form of Chagas disease

LGALS3 polymorphism	Indeterminate form (n=16)	Cardiac form (n = 39)	OR (95% CI)	p value
***LGALS3* +191**				
AA	3 (19, 7-43)	6 (15, 7-30)	0.79 (0.17-3.63)	0.759
AC	2 (12, 4-36)	15 (38, 25-54)	4.38 (0.87-22.02)	0.058
CC	11 (69, 44-86)	18 (46, 32-61)	0.39 (0.11-1.33)	0.127
***LGALS3* +292**				
AA	3 (19, 7-43)	5 (13, 6-27)	0.64 (0.13-3.06)	0.571
AC	4 (25, 10-50)	19 (49, 34-64)	2.85 (0.78-10.40)	0.105
CC	9 (56, 33-77)	15 (38, 25-54)	0.49 (0.15-1.58)	0.227

Data are expressed as number (percentage, 95% confidence interval).

(OR = 0.39, 95%CI = 0.11 to 1.33, p = 0.127). Similarly, for the SNP rs4652, the genotypes AA (OR = 0.64, 95%CI = 0.13 to 3.06, p = 0.571), AC (OR = 2.85, 95%CI = 0.78 to 10.40, p = 0.105), and CC (OR = 0.49, 95%CI = 0.15 to 1.58, p = 0.227) were not associated with the cardiac form of CD.

The SNP rs4644 genotype frequencies were not statistically different between the subjects with the indeterminate form and with the cardiac form of CD. (AA [19% *vs* 15%, p = 0.710], AC [12% *vs* 38%, p = 0.106] and CC [69% *vs* 46%, p = 0.149]) (Figure 1). In subjects with the indeterminate form, the most frequent genotype was the CC genotype, with a significantly higher prevalence than the genotypes AA and AC (p = 0.011 and p = 0.003, respectively). In subjects with the cardiac form, two genotypes were found to be more prevalent, AC and CC, as compared with the AA genotype (p = 0.04 and p = 0.006, respectively), with no difference between the prevalence of AC and CC (p = 0.647).

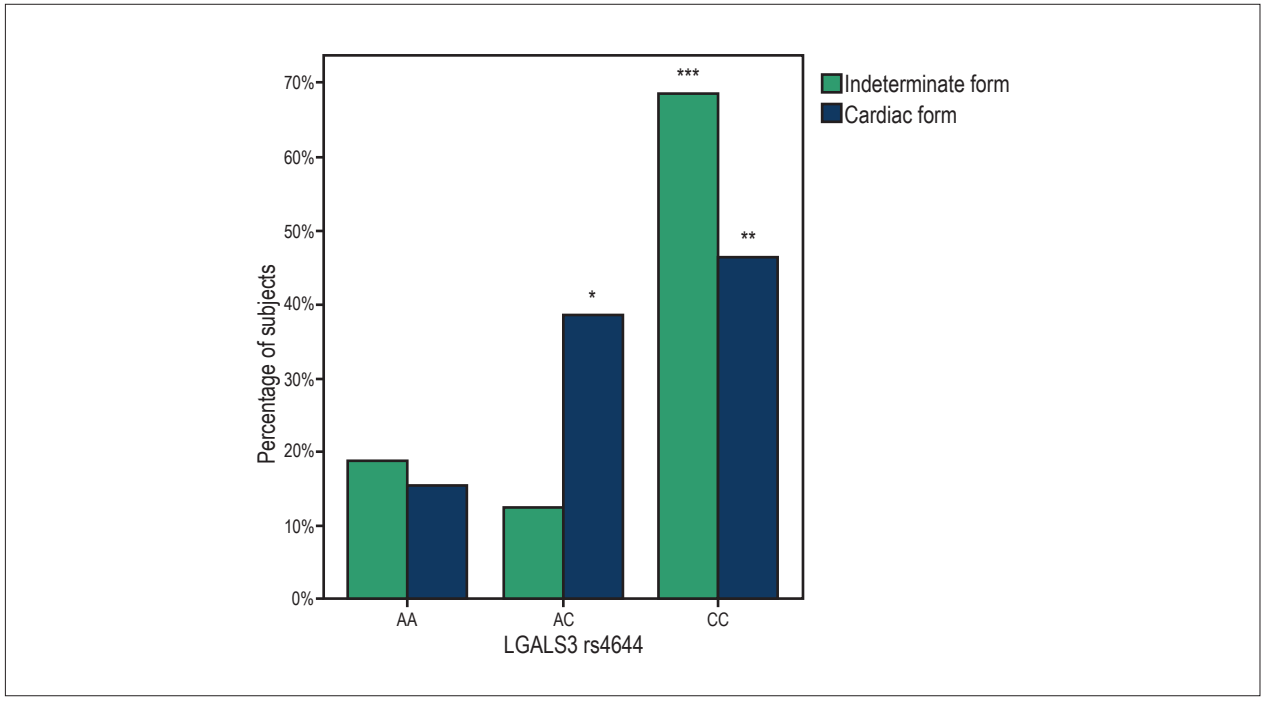

Figure 1 - *Prevalence of the genotypes AA, AC and CC of the LGALS3 rs4644 in the indeterminate form and cardiac form of Chagas disease. The p-values using two-sided Fisher's exact test were p = 0.710, p = 0.106 and p = 0.149, respectively. * p = 0.04, compared to AA genotype; ** p = 0.006, compared to AA genotype AA; *** p = 0.011, compared to AA genotype, and p = 0.003, compared to AC genotype*

Similar results were observed for the SNP rs4652 genotype distribution between the groups (Figure 2). In subjects with the indeterminate form and subjects with the cardiac form of CD, respectively, the prevalence of the AA genotype was 19% *vs* 13% (p = 0.678), the prevalence of AC was 25% *vs* 49% (p = 0.138), and the prevalence of CC was 56% *vs* 38% (p = 0.249). In subjects with the indeterminate form, there was no significant difference between the three genotypes (AA *vs* CC, p = 0.066; AA *vs* AC, p = 1.00; and AC *vs* AA, p = 0.149). Similarly to the SNP rs4644, in subjects with the cardiac form, genotypes AC and CC were more prevalent, as compared with genotype AA (p = 0.001 and p = 0.018, respectively), with no difference between the prevalence of AC and CC (p = 0.494).

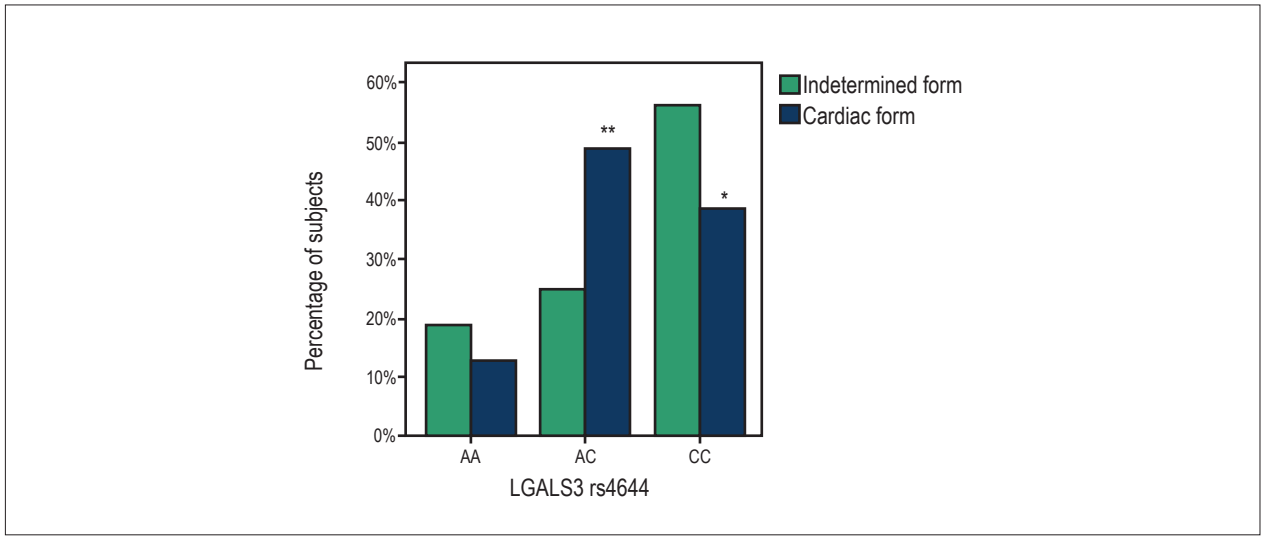

Figure 2 - *Prevalence of the genotypes AA, AC and CC of the LGALS3 rs4652 in the indeterminate form and cardiac form of Chagas disease. The p-values using two-sided Fisher's exact test were p = 0. 678, p = 0.138 and p = 0.249, respectively; * p = 0.018, compared to the AA genotype; ** p = 0.001, compared to the AA genotype*

Myocardial fibrosis

There was no statistically significant difference in the median percentage of myocardial fibrosis between subjects with and without the presence of any of the SNPs rs4644 and rs4652 genotypes (Table 3).

The median percentage of myocardial fibrosis was not statistically different between the AA, AC and CC genotypes (p = 0.508), or between SNP rs4644 and SNP rs4652 (p = 0.903 (Figure 3).

Discussion

This study evaluated the association between genetic variants of the *LGALS3* gene, encoding for galectin-3, and disease severity in subjects with CD. Since galectin-3 has been previously found to be highly correlated with fibrosis, we also evaluated the association of the three genotypes of the SNPs rs4644 and rs4652 with myocardial fibrosis. We found no significant difference in the prevalence of any of the genotypes between the subjects with the indeterminate form and the cardiac form of the disease. Also, there was no difference in the median of myocardial fibrosis between subjects with the AA, AC and CC genotypes of the SNPs in question.

The genetic predisposition to galectin-3 polymorphism has been previously associated with rheumatoid arthritis, another inflammatory disease. Hu et al[15] described an association between this rheumatic disease and the *LGALS3* +292C allele. Although we have shown that the *LGALS3* +191C and *LGALS3* + 292C allele carriage was relatively high in subjects with the cardiac form of CD, the CC genotype, at least for the SNP rs4644, was relatively more frequent among subjects with the indeterminate form. Thus, we could not confirm the possible role of the presence of CC genotype or AA genotype for both SNPs as a protective or a risk factor for developing the cardiac form of CD. Similarly, no relationship between the genetic polymorphisms in the gene encoding galectin-3 and the median of myocardial fibrosis was observed.

Conclusion

Studies at the levels of genes and proteins contribute to the understanding of the role of genetic variants in the etiology of diseases, as well as to elucidate their potential as

Table 3 – Median percentage of myocardial fibrosis in subjects with and without galectin-3 SNPs by genotype

	Without the SNP	With the SNP	p value
rs4644 AA	4.3 (0.0-14.4)	1.6 (0.0-4.7)	0.261
rs4644 AC	4.4 (0.0-9.8)	1.6 (0.0-19.2)	0.969
rs4644 CC	1.6 (0.0-15.0)	5.2 (0.2-18.5)	0.441
rs4652 AA	4.3 (0.0-14.0)	2.0 (0.3-10.6)	0.743
rs4652 AC	4.4 (0.0-10.0)	1.7 (0.0-15.1)	0.862
rs4652 CC	1.9 (0.0-14.1)	4.8 (0.0-10.0)	0.681

SNP: Single nucleotide polymorphism; Data are expressed as median (interquartile interval); p-values of Mann-Whitney U test.

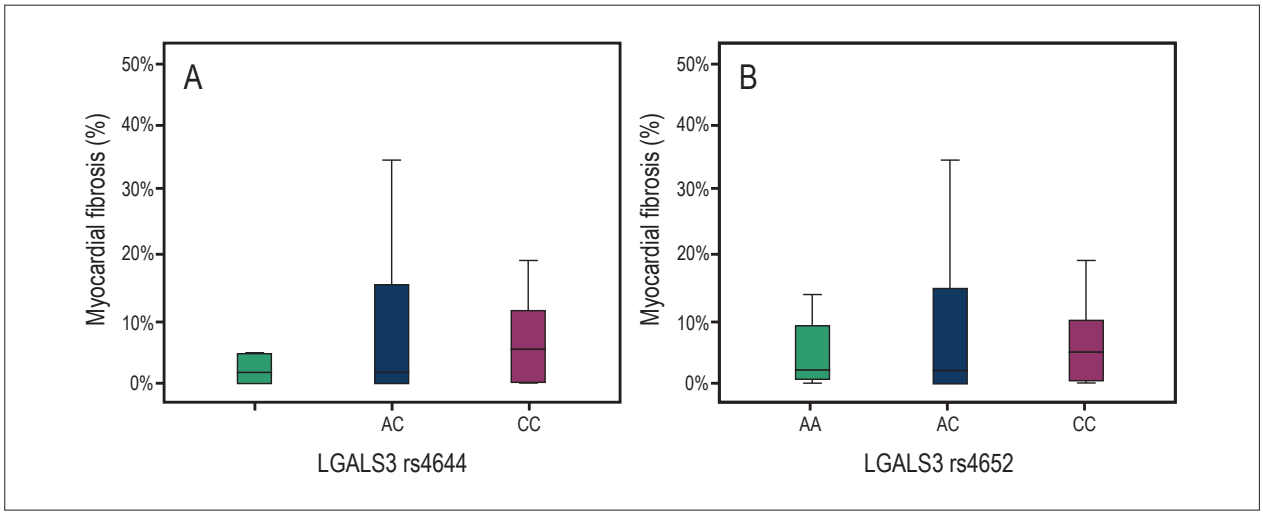

Figure 3 - *Percentage of myocardial fibrosis in subjects with the AA, AC and CC genotypes of the LGALS3 rs4644 (A) and rs4652 (B), p = 0.508 and p = 0.903, respectively.*

therapeutic targets, risk predictors and prognostic markers. Our findings did not lead to a significant conclusion on the role of galectin-3 polymorphism in the development of the cardiac form of CD. In addition, further studies with long-term follow up are necessary to evaluate whether other genetic variants play a role in inflammation and fibrosis in the indeterminate form of CD, to identify possible variants associated with disease progression in CD.

Acknowledgments

The authors thank Dr. Kyan James Allahdadi, PhD, for carefully reviewing the manuscript.

Author contributions

Conception and design of the research: Cruz GS, Angelo ALD, Souza BSF, Santos RR, Soares MBP; Acquisition of data: Cruz GS, Angelo ALD, Larocca TF, Macedo CT, Noya- Rabelo M, Torreão JÁ; Analysis and interpretation of the data: Cruz GS, Angelo ALD, Larocca TF, Macedo CT, Noya- Rabelo M, Correia LCL, Torreão JA, Souza BSF, Soares MBP; Statistical analysis: Cruz GS, Angelo ALD, Larocca TF, Noya- Rabelo M, Correia LCL; Obtaining financing: Santos RR, Soares MBP; Writing of the manuscript: Cruz GS, Larocca TF, Souza BSF; Critical revision of the manuscript for intellectual content: Cruz GS, Angelo ALD, Larocca TF, Macedo CT, Noya- Rabelo M, Correia LCL, Souza BSF, Santos RR, Soares MBP.

Potential Conflict of Interest

No potential conflict of interest relevant to this article was reported.

Sources of Funding

This study was funded by FAPESB.

Study Association

This study is not associated with any thesis or dissertation work.

References

1. World Health Organization. Chagas disease: control and elimination. Geneva; 2010.
2. Silva CP, Del Carlo CH, Oliveira Junior MT, Scipioni A, Strunz-Cassaro C, Ramirez JA, et al. Why do patients with chagasic cardiomyopathy have worse outcomes than those with non-chagasic cardiomyopathy? Arq Bras Cardiol. 2008;91(6):358-62.
3. Beraún Y, Nieto A, Collado MD, González A, Martín J. Polymorphisms at tumor necrosis factor (TNF) loci are not associated with Chagas' disease. Tissue Antigens. 1998;52(1):81-3.
4. Costa GC, da Costa Rocha MO, Moreira PR, Menezes CA, Silva MR, Gollob KJ, et al. Functional IL-10 gene polymorphism is associated with Chagas disease cardiomyopathy. J Infect Dis. 2009;199(3):451-4.
5. Drigo SA, Cunha-Neto E, Ianni B, Mady C, Faé KC, Buck P, et al. Lack of association of tumor necrosis factor-alpha polymorphisms with Chagas disease in Brazilian patients. Immunol Lett. 2007;108(1):109-11.
6. Flórez O, Martín J, González CI. Interleukin 4, interleukin 4 receptor-α and interleukin 10 gene polymorphisms in Chagas disease. Parasite Immunol. 2011;33(9):506-11.
7. Torres OA, Calzada JE, Beraún Y, Morillo CA, González A, González CI, et al. Lack of association between IL-6-174G/C gene polymorphism and Chagas disease. Tissue Antigens. 2010;76(2):131-4.
8. Zafra G, Morillo C, Martín J, González A, González CI. Polymorphism in the 3' UTR of the IL12B gene is associated with Chagas' disease cardiomyopathy. Microbes Infect. 2007;9(9):1049-52.
9. Soares MB, Lima RS, Souza BS, Vasconcelos JF, Rocha LL, Dos Santos RR, et al. Reversion of gene expression alterations in hearts of mice with chronic chagasic cardiomyopathy after transplantation of bone marrow cells. Cell Cycle. 2011;10(9):1448-55.
10. Vasconcelos JF, Souza BS, Lins TF, Garcia LM, Kaneto CM, Sampaio GP, et al. Administration of granulocyte colony-stimulating factor induces immunomodulation, recruitment of T regulatory cells, reduction of myocarditis and decrease of parasite load in a mouse model of chronic Chagas disease cardiomyopathy. FASEB J. 2013;27(12):4691-702.
11. Sharma UC, Pokharel S, van Brakel TJ, van Berlo JH, Cleutjens JP, Schroen B, et al. Galectin-3 marks activated macrophages in failure-prone hypertrophied hearts and contributes to cardiac dysfunction. Circulation. 2004;110(19):3121-8.
12. Liu YH, D'Ambrosio M, Liao TD, Peng H, Rhaleb NE, Sharma U, et al. N-acetyl-seryl-aspartyl-lysyl-proline prevents cardiac remodeling and dysfunction induced by galectin-3, a mammalian adhesion/growth-regulatory lectin. Am J Physiol Heart Circ Physiol. 2009;296(2):H404-12.
13. Felker GM, Fiuzat M, Shaw LK, Clare R, Whellan DJ, Bettari L, et al. Galectin-3 in ambulatory patients with heart failure: results from the HF-ACTION study. Circ Heart Fail. 2012;5(1):72-8.
14. Fermann GJ, Lindsell CJ, Storrow AB, Hart K, Sperling M, Roll S, et al. Galectin 3 complements BNP in risk stratification in acute heart failure. Biomarkers. 2012;17(8):706-13.
15. Hu CY, Chang SK, Wu CS, Tsai WI, Hsu PN. Galectin-3 gene (LGALS3) +292C allele is a genetic predisposition factor for rheumatoid arthritis in Taiwan. Clin Rheumatol. 2011;30(9):1227-33.
16. Lang RM, Bierig M, Devereux RB, Flachskampf FA, Foster E, Pellikka PA, et al; Chamber Quantification Writing Group; American Society of Echocardiography's Guidelines and Standards Committee; European Association of Echocardiography. Recommendations for chamber quantification: a report from the American Society of Echocardiography's Guidelines and Standards Committee and the Chamber Quantification Writing Group, developed in conjunction with the European Association of Echocardiography, a branch of the European Society of Cardiology. J Am Soc Echocardiogr. 2005;18(12):1440-63.

ANEXO V

INTERNATIONAL JOURNAL OF Experimental Pathology

Int. J. Exp. Path. (2014)

ORIGINAL ARTICLE

Bone marrow cells migrate to the heart and skeletal muscle and participate in tissue repair after *Trypanosoma cruzi* infection in mice

Bruno S. d. F. Souza*,†,[1], Carine M. Azevedo*,†,[1], Ricardo S. d. Lima*, Carla M. Kaneto†, Juliana F. Vasconcelos*,†, Elisalva T. Guimarães*, Ricardo R. dos Santos*,† and Milena B. P. Soares*,†

*Centro de Pesquisas Gonçalo Moniz, Fundação Oswaldo Cruz, Salvador, Brazil and †Centro de Biotecnologia e Terapia Celular, Hospital São Rafael, Salvador, Brazil

INTERNATIONAL JOURNAL OF EXPERIMENTAL PATHOLOGY

doi: 10.1111/iep.12089

Received for publication: 22 December 2013
Accepted for publication: 29 May 2014

Correspondence:
Milena B. P. Soares
Centro de Biotecnologia e Terapia Celular
Hospital São Rafael. Av. São Rafael 2152. São Marcos 41253-190
Salvador BA
Brazil
Tel.: 55 71 3281 6455
Fax: 55 71 3281 6489
E-mail: milena@bahia.fiocruz.br

[1]These authors have equally contributed to this work.

SUMMARY

Infection by *Trypanosoma cruzi*, the aetiological agent of Chagas disease, causes an intense inflammatory reaction in several tissues, including the myocardium. We have previously shown that transplantation of bone marrow cells (BMC) ameliorates the myocarditis in a mouse model of chronic Chagas disease. We investigated the participation of BMC in lesion repair in the heart and skeletal muscle, caused by *T. cruzi* infection in mice. Infection with a myotropic *T. cruzi* strain induced an increase in the percentage of stem cells and monocytes in the peripheral blood, as well as in gene expression of chemokines SDF-1, MCP1, 2, and 3 in the heart and skeletal muscle. To investigate the fate of BMC within the damaged tissue, chimeric mice were generated by syngeneic transplantation of green fluorescent protein (GFP^+) BMC into lethally irradiated mice and infected with *Trypanosoma cruzi*. Migration of GFP^+ BMC to the heart and skeletal muscle was observed during and after the acute phase of infection. GFP^+ cardiomyocytes and endothelial cells were present in heart sections of chimeric chagasic mice. GFP^+ myofibres were observed in the skeletal muscle of chimeric mice at different time points following infection. In conclusion, BMC migrate and contribute to the formation of new resident cells in the heart and skeletal muscle, which can be detected both during the acute and the chronic phase of infection. These findings reinforce the role of BMC in tissue regeneration.

Keywords
bone marrow cells, Chagas disease, chimeric mice, myocytes, tissue repair

Chagas disease is a zoonosis caused by the flagellate parasite *T. cruzi*. The disease is endemic in Latin American countries and continues to represent a major public health problem (Schofield *et al.* 2006). The prevalence of human *T. cruzi* infection is estimated at 15–16 million cases, with approximately 75–90 million people currently at risk of infection (Coura & Dias 2009).

The acute phase of the disease is transient and characterized by the presence of trypomastigote forms in the peripheral blood and amastigote proliferation within several host cell types (Koberle 1968). An intense inflammatory reaction is triggered by the presence of the parasite within tissues, resulting in a destruction of unparalleled proportions in the myocardium (Andrade 1983; Rassi *et al.* 2010), which, following the parasitaemia control, undergo a regenerative process. In humans, the acute phase regresses spontaneously after approximately 12 months (Andrade 1983; Rassi *et al.* 2010). About 30% of individuals infected by *T. cruzi* develop the symptomatic chronic cardiac form of the disease, for which there is no effective treatment (Andrade 1983). Thus, a more complete understanding of the cells and molecules that naturally participate in tissue repair in Chagas disease may open new avenues for the development of novel therapies.

Stem cell-based therapies represent a new frontier for the treatment of chronic degenerative diseases, including those affecting muscle and heart tissues. The bone marrow is an easily accessible source of stem cells, and its potential therapeutic applications have been intensely investigated. A number of studies have shown that bone marrow cells (BMC) migrate to injured organs, such as skeletal muscle and heart (Bianco *et al.* 2001; Goldenberg *et al.* 2008; Cao *et al.* 2009), leading to the formation of new specialized cells.

Specifically, we have observed that the transplantation of BMC obtained from both chagasic and naïve mice reduces the inflammatory infiltrates and fibrosis in the heart of chronically infected chagasic mice. Interestingly, BMC transplantation not only reduced inflammation and fibrosis, but also led to the formation of new cardiomyocytes (Soares *et al.* 2004, 2007). However, it is still not clear whether BMC are differentiating into GFP^+ cardiomyocytes during different stages of the cardiomyopathy development and how BMC are specifically attracted to the sites of damaged tissue. Here, the mobilization and recruitment of bone marrow cells were studied in mice infected with *T. cruzi*. Secondly, the migration and fate of BMC during the development of Chagas disease were studied in infected BMC chimeras. By performing these experiments, we present evidence regarding the contribution of bone marrow-derived cells, as well as the role of inflammatory mediators, in lesions affecting the heart and skeletal muscle.

Materials and methods

Animals

Six- to eight-week-old female C57BL/6 mice were used as recipients for the production of chimeric animals. Four-week-old male C57BL/6 mice, transgenic for enhanced green fluorescent protein (GFP), were used as bone marrow cells donors for reconstitution of irradiated mice. All mice were raised and maintained in the animal facilities at the Gonçalo Moniz Research Center, FIOCRUZ/BA, and provided with rodent food and water *ad libitum*.

Ethical approval

Animals were handled according to the NIH guidelines for animal experimentation. All procedures described had prior approval from the local animal ethics committee.

Generation of chimeric mice

C57BL/6 female mice were irradiated with 6 Gy for bone marrow cell depletion in a ^{137}Caesium source irradiator (CisBio International, Codolet, France). Bone marrow cells were obtained from femurs and tibiae from male GFP-transgenic mice and used to reconstitute irradiated mice. The mononuclear cells were purified by centrifugation in Ficoll gradient at 1000 ***g*** for 15 min (Histopaque 1119 and 1077, 1:1; Sigma-Aldrich, St. Louis, MO, USA). After two washings in DMEM medium (Sigma-Aldrich), the cells were filtered over nylon wool and resuspended in saline, and 200 µl was injected intravenously at 1×10^7 cells per mouse in all irradiated mice.

Parasites and infection

Trypomastigotes of the myotropic Colombian *T. cruzi* strain (Federici *et al.* 1964) were obtained from culture supernatants of infected LLC-MK2 cells. Infection of normal and chimeric mice was performed by intraperitoneal injection of 100 or 1000 *T. cruzi* trypomastigotes in saline respectively. Chimeric mice were infected 30 days after bone marrow transplantation. Parasitaemia of infected mice was evaluated at various time points following infection by counting the number of trypomastigotes in peripheral blood aliquots. Twenty-eight days after infection, chimeric animals were treated daily for 1 week with 40 mg/kg of benznidazole (Lafepe, Recife, Brazil) diluted in saline to control the parasitaemia.

Morphometric analysis

Groups of animals were euthanized 33, 66 and 192 days after infection, and different organs were removed and fixed in 10% buffered formalin. Tissue sections were analysed by light microscopy following paraffin embedding and then stained using a standard haematoxylin/eosin protocol. Inflammatory cells infiltrating heart and skeletal tissues were counted using a digital morphometric evaluation system. Images were digitalized using a colour digital video camera adapted to a microscope. The images were analysed using the Image Pro Plus Program (Media Cybernetics, San Diego, CA, USA), where inflammatory cells were counted and integrated with respect to area. Ten fields (100 μm^2) per section were counted in one section per heart.

Sample preparation and real-time RT-PCR

The RNA was harvested from hearts and skeletal muscle and isolated with TRIzol reagent (Invitrogen, Carlsbad, CA, USA) using concentration determined by photometric measurement. The RNA quality was analysed in 1.2% agarose gel. High-Capacity cDNA Reverse Transcription Kit (Applied Biosystems, Foster City, CA, USA) was used to synthesize cDNA from 2 µg of RNA following the manufacturer's recommendations. Real-time RT-PCR assays were performed to detect the expression levels of different genes, using commercial probes, as follows: *Sdf-1/CxCl12* (Mm 00443552_m1), *Ccl2/MCP-1* (Mm 00441242_m1), *Ccl8/MCP-2* (Mm 01297183_m1), *Ccl7/MCP-3* (Mm 00443113_m1), *IGF-1* (Mm00439561_m1) and *VEGF* (Mm00437304_m1). Amplification of qRT-PCR mixtures was performed with Universal Master Mix (Applied Biosystems) and the 7500 Real-Time PCR System (Applied Biosystems), under standard thermal cycling

conditions, comprised of 10 min polymerase activation at 95 °C, 40 cycles at 95 °C for 15 s and 60 °C for 60 s. Experiments with coefficients of variation >5% were excluded. A no-template control and no-reverse transcription control (No-RT) were also included. The results are presented as the fold increase of expression from the individual mRNAs, with the target internal control *GADPH*, using the cycle threshold method.

Immunofluorescence analysis

Ten-micrometre frozen sections or 5-μm paraffin-embedded sections of hearts, livers, spleen and skeletal muscle were obtained and used for detection of GFP^+ cells. The following primary antibodies were used: chicken anti-GFP (1:500; Aves Labs, Tigard, OR, USA), rabbit anti-myosin (1:200, Sigma-Aldrich), rabbit anti-von Willebrand Factor (1:50; Zymed Laboratories, San Francisco, CA, USA), mouse anti-PCNA (1:200; Dako Denmark A/S, Glostrup, Denmark) biotinylated with Dako Ark kit and mouse anti-Pax-7 (1:200; DSHB, Iowa city, IA, USA) stained using M.O.M. kit (Vector Labs, Burlingame, CA, USA). Secondary antibodies, anti-chicken Alexa Fluor 488 conjugated (1:200; Molecular Probes, Carlsbad, CA, USA) and anti-rabbit Alexa Fluor 568 conjugated (1:200; Molecular Probes), were used. For biotinylated antibodies stained sections, we used streptavidin Alexa Fluor 568 conjugated (1:200; Molecular Probes). Some heart sections were stained with phalloidin Alexa fluor 633 conjugated (1:100; Molecular Probes). Nuclei were counterstained with 4,6-diamidino-2-phenylindole (DAPI) (Vector Labs). Images were collected using the confocal microscope, FluoView 1000 (Olympus, Tokyo, Japan).

Flow cytometry analysis

Quantification of GFP^+ cells was performed in blood samples obtained from naïve, bone marrow chimeric mice (one month after reconstitution) and GFP-transgenic control mice. Quantitative analysis of Sca-1^+ and monocytes cells was performed in the blood of non-infected and acute chagasic mice, by flow cytometry. Cells were stained with labelled anti-mouse CD45 PE-Cy5.5, CD11b APC, CD34 PE, CD90 APC, SCA-1 FITC, F4/80 PerCP-Cy5 and Ly-6C/6G APC-Cy7 antibodies (BD Biosciences, San Diego, CA, USA) for 20 min, at room temperature. Red blood cells were lysed with lysis solution for 10 min at room temperature. Cells were washed twice with phosphate buffered saline (PBS), resuspended in 500 μl of PBS and then analysed using the cell analyser, LSRFortessa with FACSDiva software version 6.1.3 (BD Biosciences). To confirm the presence of GFP^+ cells in chimeric mice, blood samples from irradiated and reconstituted mice were evaluated after 30 days of transplantation. Blood samples obtained from wild-type and GFP-transgenic C57BL/6 mice were used as negative and positive controls respectively. Acquisition and analysis were performed using a FACScalibur cytometer with the CellQuest software (BD Biosciences). At least 10,000 events were collected.

Statistical analyses

Statistical comparisons between groups were performed by Student's *t*-test when comparing two groups and analysis of variance (ANOVA) followed by Tukey's test for multiple comparisons, using GraphPad Prism program (Software Inc., San Diego, CA, USA) version 5.0. Results were considered significant when $P < 0.05$.

Results

Infection with T. cruzi *increases percentage of circulating stem cells and monocytes as well as chemokines expression in the heart and skeletal muscle*

The mobilization of different cell subpopulations from the bone marrow was evaluated in the peripheral blood taken from C57BL/6 mice infected with Colombian *T. cruzi* strain. At the peak of infection (30 days after infection), a significant increase in the number of Sca-1^+ cells and monocytes was observed in infected mice, when compared to naïve controls (Table 1). The Sca-1^+ cells expressed either mesenchymal stem cell markers ($CD90^+$ $CD45^-$) or hematopoietic progenitor cell phenotype ($CD34^+$ $CD45^+$). Two monocyte subpopulations, expressing $LY6C^{hi}$ and $LY6C^{lo}$, were also observed (Table 1).

The expression of chemokines participating in the recruitment of macrophages and stem cells was investigated at the transcriptional level by qRT-PCR in the heart and skeletal muscle. Gene expression of SDF-1 (CXCL12) in the heart was found to be similar between naïve and *T. cruzi*-infected mice. In contrast, SDF-1 expression in skeletal muscles increased in *T. cruzi*-infected mice in comparison with naïve mice (Figure 1). The expression of MCP1, 2 and 3 genes was significantly increased in both heart and muscle tissues of infected mice when compared to naïve mice (Figure 1).

Table 1 Acute infection with *T. cruzi* induces the mobilization of Sca-1^+ and monocytes to the peripheral blood

Cell subpopulation	Uninfected	Infected	*P* value
MSC ($Sca1^+$ $CD90^+$ $CD45^-$)	0.23 ± 0.03	1.26 ± 0.18	<0.01
HSC ($Sca1^+$ $CD34^+$ $CD45^+$)	0.30 ± 0.06	1.71 ± 0.32	<0.05
MNC $F4/80^+$ $CD11b^-$ $LY6C^{lo}$	2.17 ± 0.20	42.70 ± 1.96	<0.0001
MNC $F4/80^+$ $CD11b^+$ $LY6C^{hi}$	10.90 ± 0.95	54.95 ± 1.93	<0.0001

Data represent the cell subpopulation% of naïve ($n = 3$) and infected ($n = 8$) mice and were expressed as means ± SEM. Statistical analysis was performed using Student's *t*-test. MSC, mesenchymal stem cells; HSC, hematopoietic stem cells; MNC, monocytes.

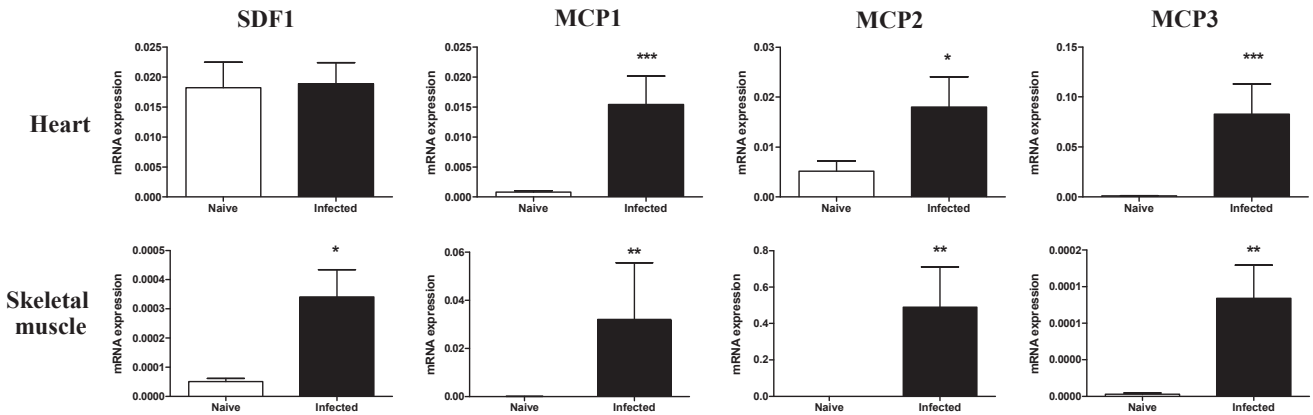

Figure 1 Gene expression of chemokines in the heart and skeletal muscle. Heart and skeletal muscle samples of uninfected or chagasic mice (33 days postinfection) were removed and analysed by qRT-PCR for the expression of SDF-1 and MCP 1, 2 and 3. Data represent the mean ± SEM of 5–8 mice per group. *$P < 0.05$; **$P < 0.01$; ***$P < 0.001$.

Presence of GFP⁺ cells in the heart and skeletal muscle of T. cruzi*-infected chimeric mice*

To investigate the fate of mobilized bone marrow cells following *T. cruzi* infection, we generated bone marrow chimeric mice by transplanting GFP⁺ bone marrow cells into lethally irradiated C57BL/6 recipients (Figure 2). Bone marrow reconstitution was confirmed by quantification of GFP⁺ cells by flow cytometry analysis (Figure 3 a–c). One month after reconstitution, chimeric mice were infected with 100 *T. cruzi* trypomastigotes and treated for 1 week with benznidazole, 28 days postinfection, to reduce mortality rate associated with the infection in chimeric mice. A decrease of parasitaemia levels in these animals was observed 30 days postinfection (Figure 3d). The numbers of inflammatory cells in the heart and skeletal muscle were quantified. As shown in Figure 3e, the number of inflammatory cells in the heart tissue was higher during the peak of parasitaemia (33 days after infection), decreasing after 192 days of infection. In contrast, the number of inflammatory cells remained elevated in skeletal muscle at all analysed time points (Figure 3f).

Each time point analysed revealed the presence of GFP⁺ cardiomyofibres. The GFP⁺ cardiomyocytes were positively stained with an anti-myosin antibody or phalloidin (Figure 4a–c) and were visualized as a group of adjacent cells or individual cells within the myocardium. In contrast, heart sections of uninfected chimeric mice had sparse or no GFP⁺ cells present (Figure 4d). The GFP⁺ cells found in the hearts of uninfected chimeric mice did not present characteristic cardiomyocyte morphology, as well as a lack myosin expression.

A significant number of GFP⁺ myofibres were found at all analysed time points (Figure 5a–c). The number of GFP⁺/myosin⁺ myofibres in skeletal muscle did not correlate with the severity of tissue inflammation. However, GFP⁺ myofibres were not observed in skeletal muscle sections obtained from uninfected chimeric mice, which included mice euthanized on day 192 (Figure 5d).

In addition to myofibres, GFP⁺ cells were found within endothelial cells of chagasic heart blood vessels (Figure 6a), but were not observed in uninfected chimeric mice (Figure 6b). A subpopulation of these GFP⁺ cells was positive for von Willebrand factor, an endothelial cell marker. However, GFP⁺ satellites cells were not found in skeletal muscle of chimeric mice at any of the time points analysed, as shown by Pax7 stain (Figure 6c and d). GFP⁺ cells were also observed in other organs of chimeric chagasic mice, such as liver and spleen (data not shown).

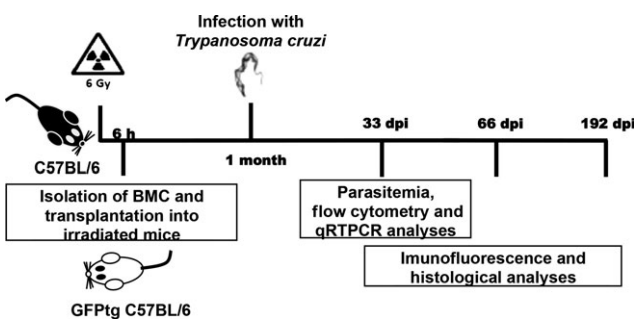

Figure 2 Generation of GFP⁺ bone marrow chimeric mice. Lethally irradiated wild-type C57BL/6 mice were transplanted with bone marrow obtained from C57BL/6 GFP transgenic mice.

Presence of proliferating GFP⁺ cells in inflammatory foci

Heart and skeletal muscle sections from chimeric mice euthanized at different time points following infection presented a massive influx of GFP⁺ inflammatory cells. Some GFP⁺ cells observed in inflammatory infiltrates of cardiac

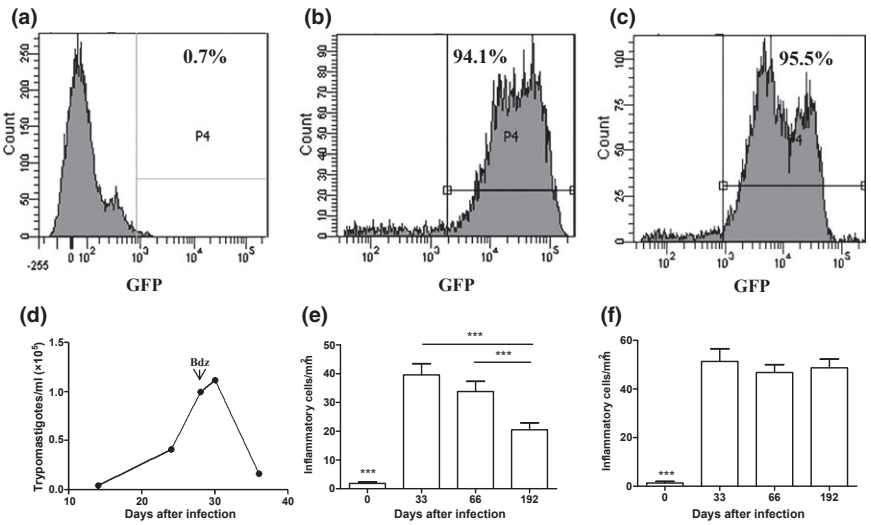

Figure 3 Infection of bone marrow chimeric mice with *T. cruzi*. Reconstitution of bone marrow chimeric mice was confirmed by flow cytometry analysis of GFP$^+$ cells in the blood. (a), naïve mouse. (b), GFP-transgenic mouse. (c), chimeric mouse (one month after transplantation). One month after transplantation, chimeric mice were infected with 100 Colombian strain *T. cruzi* and treated with benznidazole (bdz) 28 days later. (d) Blood parasitaemia of *T. cruzi*-infected chimeric mice. Quantification of inflammation in the heart (e) and skeletal muscle (f) at various times after infection of chimeric mice. Data represent the mean ± SEM of 3–5 mice per group. ***$P < 0.001$.

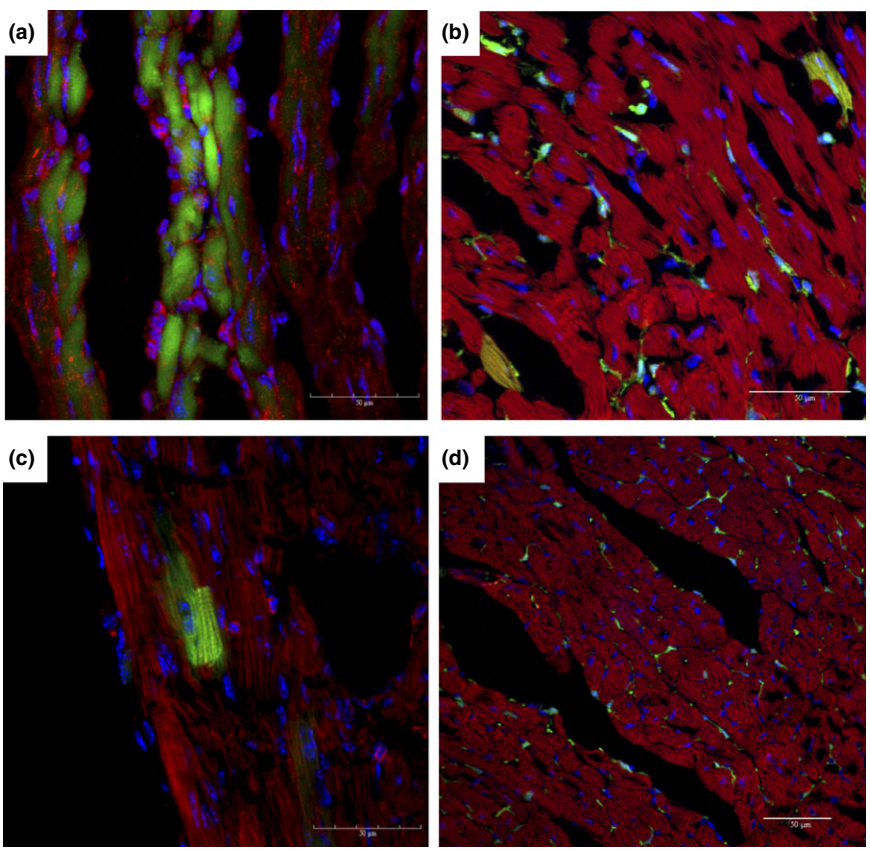

Figure 4 Presence of GFP$^+$ cells in the hearts of chagasic chimeric mice. Hearts of chimeric mice euthanized at different time points after infection with *T. cruzi* were analysed by confocal microscopy. GFP$^+$ (green) myosin$^+$ (a) or F actin$^+$ (b–d) (red) cardiomyocytes were found in heart sections of mice after 33 (a), 60 (b) and 192 (c) days of infection. (d) Heart section of an uninfected chimeric mouse. Nuclei were stained with DAPI (blue).

and skeletal muscle displayed positive nuclear staining for PCNA, a marker of cell proliferation (Figure 6e and f). Cardiomyocytes expressing PCNA were found in chimeric chagasic mice (Figure 6e'). However, myofibres expressing GFP and PCNA were not found in any heart or skeletal muscle sections analysed.

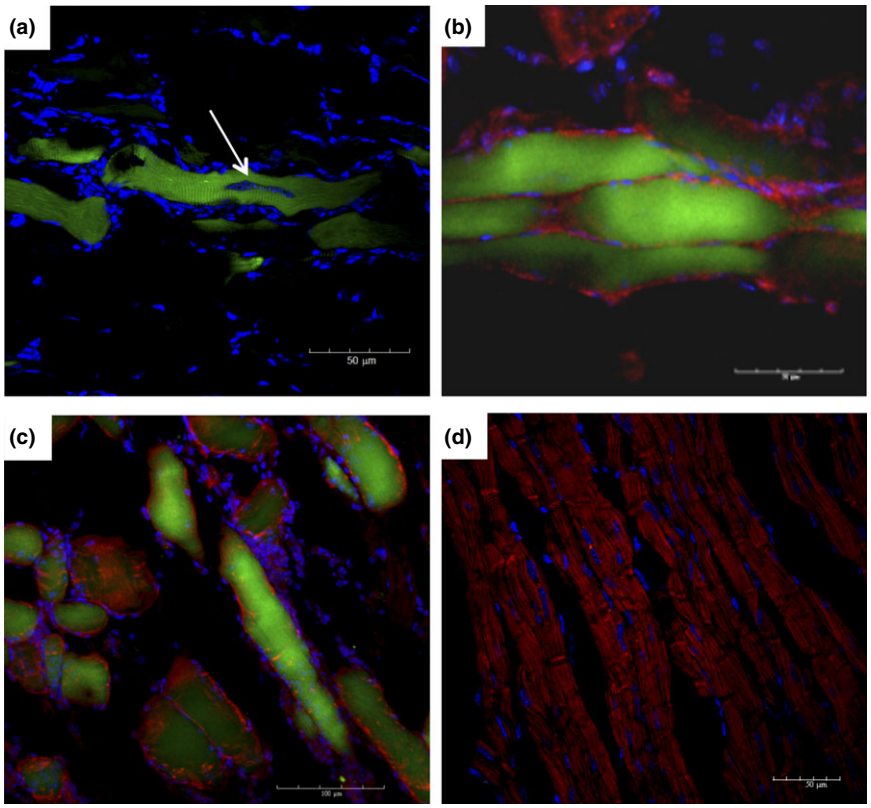

Figure 5 Presence of GFP$^+$ cells in skeletal muscle of chagasic chimeric mice. Skeletal muscle of chimeric mice euthanized at different time points after infection with *T. cruzi* was analysed by immunofluorescence microscopy. (a) Parasite nest within a GFP$^+$ myofibre (arrow) after 33 days of infection. (b and c) GFP$^+$ (green) myosin$^+$ (red) myofibres were found in skeletal muscle sections obtained from mice after 60 (B) and 192 (c) days of infection. (d) Skeletal muscle section obtained from an uninfected chimeric mouse. Sections were stained with anti-myosin antibody (red) and DAPI (blue).

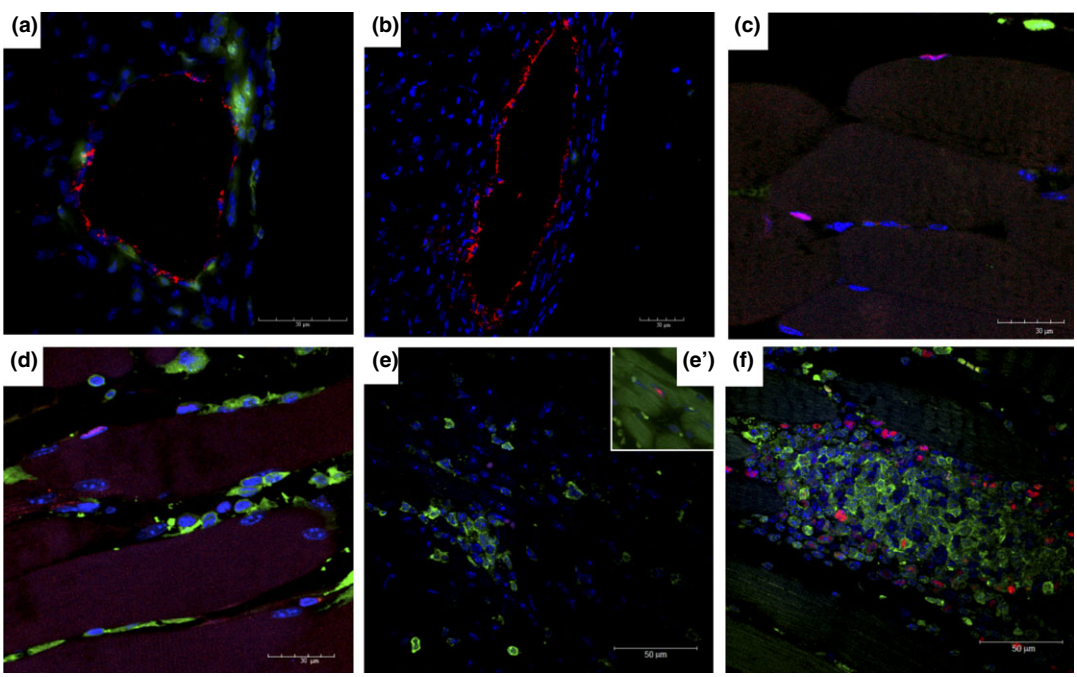

Figure 6 Characterization of GFP$^+$ cells in different organs of *T. cruzi*-infected chimeric mice. GFP$^+$ cells (green) were observed to be associated with blood vessels in the hearts of mice 33 days after infection (a), but not in uninfected chimeric mice (b). In red, staining for von Willebrand factor. Satellite cells Pax7$^+$ in skeletal muscle sections of naïve (c) and *T. cruzi*-infected mice (d) 33 days after infection. Presence of GFP$^+$ (green) proliferating PCNA$^+$ cells (red) in the inflammatory infiltrates of the heart (e) and PCNA$^+$GFP$^-$ cardiomyocytes stained with phalloidin (green; e') and skeletal muscle (f) tissue, 33 days postinfection. Nuclei were stained with DAPI (blue).

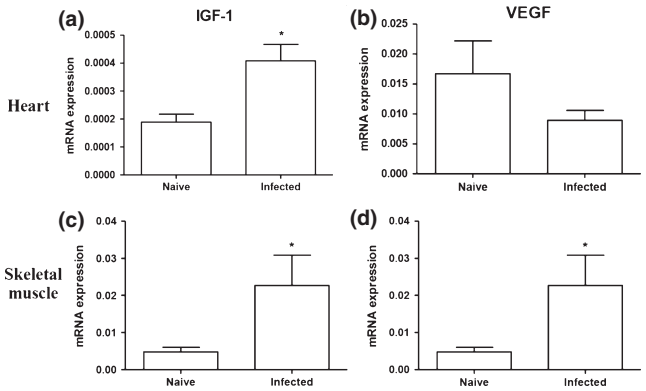

Figure 7 Expression of IGF-1 and VEGF in the heart and skeletal muscle. Naïve and *T. cruzi*-infected mice (33 days of infection) were euthanized to evaluate the gene expression of IGF-1 (a and c) and VEGF (b and d) by qRT-PCR. Data represent the mean ± SEM of 5–8 mice per group. $*P < 0.05$

Acute T. cruzi *infection upregulates the gene expression of IGF-1 and VEGF*

The mRNA expression of IGF-1 and VEGF was investigated in the skeletal muscle and hearts of *T. cruzi*-infected mice by qRT-PCR. A significant increase in IGF-1 mRNA levels was observed in both heart and skeletal muscle samples of infected mice, when compared to normal mice (Figure 7). In contrast, VEGF mRNA levels were significantly increased in the skeletal muscle, but not in the hearts of infected mice, when compared to normal mice (Figure 7).

Discussion

In the present study, we demonstrated that infection with *T. cruzi* can induce chemokine expression in inflamed tissues that continuously recruit bone marrow-derived cells to the peripheral blood and their contribution to the formation of resident cells in the heart and skeletal muscle tissues.

Chemokines MCP-1, -2, and -3 were also previously described to be highly expressed in the hearts of chagasic mice (Soares *et al.* 2010) and may induce the recruitment of monocytes and lymphocytes. It has been recently shown that some monocyte subpopulations can differentiate into specialized cell types, including endothelial cells and myocytes (Kodama *et al.* 2005; Kuwana *et al.* 2006), and may contribute to the GFP^+ myocytes and endothelial cells observed in our study.

While MCPs play a role in the recruitment of immune cells, it is well known that SDF-1/CXCR4 is a major axis of stem cell chemotaxis. A recent study utilizing an alternative mouse model of Chagas disease also failed to detect a raise in the expression of SDF-1 in the heart and showed that hematopoietic stem cells (i.e. $CD34^+$) were not recruited to the heart during infection (González *et al.* 2013). In our study, we observed an increased SDF-1 expression in the skeletal muscles and detected increased numbers of $CD34^+$ cells in the peripheral blood, suggesting that $CD34^+$ cells could be recruited to different inflamed tissues, as evidenced by the presence of GFP^+ resident cells in the tissues analysed.

Post-natal cardiomyogenesis has been reported to occur in mice and humans, at a low frequency (about 1% per year), a process that declines considerably with age (Garbern & Lee 2013). New cardiomyocytes can be generated from stem cells (Laflamme *et al.* 2002; Agbulut *et al.* 2003; Deb *et al.* 2003; Fogt *et al.* 2003; Thiele *et al.* 2004) or by dividing mature cardiomyocytes (Senyo *et al.* 2013). Here, we detected the presence of bone marrow-derived cardiomyocytes, as well as the proliferation of pre-existing cardiomyocytes (GFP^- $PCNA^+$). Similarly, Arnaiz *et al.* (2002) observed proliferating cardiomyocytes ($PCNA^+$) after different periods of infection by *T. cruzi* in rats (Arnaiz *et al.* 2002).

Previous studies have reported a low-frequency presence of bone marrow-derived skeletal myocytes following acute myotoxic injury (Corbel *et al.* 2003; Rudnick 2003). It has been suggested that these cells result from fusion between damaged myofibres and bone marrow-derived cells (Rudnick 2003). The frequency of bone marrow-derived myocytes was found to be higher in a Duchenne muscular dystrophy experimental model, which may result from a selective advantage (Dezawa *et al.* 2005). In the present study, we showed that persistent inflammation leads to an increased number of bone marrow-derived cells compared with those previously reported in acute injury experimental models.

Skeletal muscle regeneration is a dynamic process that occurs with the contribution of different stem cells sources, including skeletal muscle side population cells, bone marrow-derived cells, mesoangioblasts and pericytes (Otto *et al.* 2009). These cells can contribute to the satellite cell niche or to the generation of myofibres through other pathways (Xynos *et al.*, 2010).

The fusion process is a physiological mechanism by which myoblasts form multinucleated muscle fibres, becoming a syncytium. A previous study demonstrated that macrophages play an important role in muscle regeneration (Arnold *et al.* 2007) by producing growth factors for myogenic progenitors that can also undergo fusion with myofibres (Camargo *et al.* 2003). Thus, as there is a potent mobilization of two different monocyte populations ($Ly6C^{lo}$ e $Ly6C^{hi}$) and the presence of macrophages in the inflammatory foci, our data suggest that these cells are fusing with myocytes in our model of *T. cruzi* infection. Additionally, we found an increase in IGF-1 and VEGF gene expression upon *T. cruzi* infection. These factors have been implicated in the promotion of tissue repair by angiogenesis induction and promote muscle regeneration, two processes in which macrophages have been shown to play key roles (Lu *et al.* 2011; Santini & Rosenthal 2012).

Bone marrow-derived cells expressing satellite cell markers have been observed following bone marrow transplants in association with myofibres (Labarge & Blau 2002; Dreyfus *et al.* 2004). Camargo *et al.* (2003) also made this

observation, although at a low frequency, following hematopoietic stem cell transplantation in a cardiotoxin-induced injury model (Camargo *et al.* 2003). In our study, we did not observe any bone marrow-derived cells (GFP^+) expressing the satellite cell marker pax7, which seems to favour a fusion process rather than a transdifferentiation mechanism, in this model of *T. cruzi* infection.

In conclusion, we have demonstrated that bone marrow cells actively participate in the pathogenesis and regeneration process that occurs naturally in damaged skeletal muscles and hearts of an experimental model of Chagas disease. These observations support the potential benefits of bone marrow cell therapy during the chronic phase of Chagas disease, to increase a regeneration process that naturally occurs.

Acknowledgements

This work was supported by CNPq, FAPESB, FINEP and FIOCRUZ. The authors wish to thank Geraldo Pedral Sampaio for technical assistance in flow cytometry and Dr. Kyan James Allahdadi for careful revision of the manuscript.

References

Agbulut O., Menot M.L., Li Z. *et al.* (2003) Temporal patterns of bone marrow cell differentiation following transplantation in doxorubicin-induced cardiomyopathy. *Cardiovasc. Res.* **58**, 451–459.

Andrade Z.A. (1983) Mechanisms of myocardial damage in *Trypanosoma cruzi* infection. *Ciba Found. Symp.* **99**, 214–233.

Arnaiz M.R., Fichera L.E. & Postan M. (2002) Cardiac myocyte hypertrophy and proliferating cell nuclear antigen expression in Wistar rats infected with *Trypanosoma cruzi*. *J. Parasitol.* **88**, 919–925.

Arnold L., Henry A., Poron F. *et al.* (2007) Inflammatory monocytes recruited after skeletal muscle injury switch into antiinflammatory macrophages to support myogenesis. *J. Exp. Med.* **204**, 1057–1069.

Bianco P., Riminucci M., Gronthos S. & Robey P.G. (2001) Bone marrow stromal cells: nature, biology, and potential applications. *Stem Cells* **19**, 180–192.

Camargo F.D., Green R., Capetanaki Y., Jackson K.A. & Goodell M.A. (2003) Single hematopoietic stem cells generate skeletal muscle through myeloid intermediates. *Nat. Med.* **9**, 1520–1527.

Cao F., Sun D., Li C. *et al.* (2009) Long-term myocardial functional improvement after autologous bone marrow mononuclear cells transplantation in patients with ST-segment elevation myocardial infarction: 4 years follow-up. *Eur. Heart J.* **30**, 1986–1994.

Corbel S.Y., Lee A., Lin Y. *et al.* (2003) Contribution of hematopoietic stem cells to skeletal muscle. *Nat. Med.* **9**, 1528–1532.

Coura J.R., Dias J.P.C. (2009) Epidemiology, control and surveillance of Chagas disease 100 years after its discovery. *Mem. Inst. Oswaldo Cruz* **104**(Suppl 1), 31–40.

Deb A., Wang S., Skelding K.A., Miller D., Simper D. & Caplice N.M. (2003) Bone marrow-derived cardiomyocytes are present in adult human heart: a study of gender-mismatched bone marrow transplantation patients. *Circulation* **107**, 1247–1249.

Dezawa M., Ishikawa H., Itokazu Y. *et al.* (2005) Bone marrow stromal cells generate muscle cells and repair muscle degeneration. *Science* **309**, 314–317.

Dreyfus P.A., Chretien F., Chazaud B. *et al.* (2004) Adult bone marrow-derived stem cells in muscle connective tissue and satellite cell niches. *Am. J. Pathol.* **164**, 773–779.

Federici E.E., Abelmann W.H. & Neva F.A. (1964) Chronic and progressive myocarditis and myositis in C3H mice infected with *Trypanosoma cruzi*. *Am. J. Trop. Med. Hyg.* **13**, 272–280.

Fogt F., Beyser K.H., Poremba C., Zimmerman R.L. & Ruschoff J. (2003) Evaluation of host stem cell-derived cardiac myocytes in consecutive biopsies in long-term cardiac transplant patients. *J. Heart Lung Transplant.* **22**, 1314–1317.

Garbern J.C. & Lee R.T. (2013) Cardiac stem cell therapy and the promise of heart regeneration. *Cell Stem Cell* **12**, 689–698.

Goldenberg R.C., Jelicks L.A., Fortes F.S. *et al.* (2008) Bone marrow cell therapy ameliorates and reverses chagasic cardiomyopathy in a mouse model. *J. Infect. Dis.* **197**, 544–547.

González M.N., Dey N., Garg N.J. & Postan M. (2013) Granulocyte coloning-stimulating factor partially repairs the damage provoked by *Trypanosoma cruzi* in murine myocardium. *Int. J. Cardiol.* **168**, 2567–2574.

Koberle F. (1968) Chagas' disease and Chagas' syndromes: the pathology of American trypanosomiasis. *Adv. Parasitol.* **6**, 63–116.

Kodama H., Inoue T., Watanabe R. *et al.* (2005) Cardiomyogenic potential of mesenchymal progenitors derived from human circulating CD14+ monocytes. *Stem Cells Dev.* **14**, 676–686.

Kuwana M., Okazaki Y., Kodama H., Satoh T., Kawakami Y. & Ikeda Y. (2006) Endothelial differentiation potential of human monocyte-derived multipotential cells. *Stem Cells* **24**, 2733–2743.

Labarge M.A. & Blau H.M. (2002) Biological progression from adult bone marrow to mononucleate muscle stem cell to multinucleate muscle fiber in response to injury. *Cell* **111**, 589–601.

Laflamme M.A., Myerson D., Saffitz J.E. & Murry C.E. (2002) Evidence for Cardiomyocyte Repopulation by Extracardiac Progenitors in Transplanted Human Hearts. *Circ. Res.* **90**, 634–640.

Lu H., Huang D., Ransohoff R.M. & Zhou L. (2011) Acute skeletal muscle injury: CCL2 expression by both monocytes and injured muscle is required for repair. *FASEB J.* **25**, 3344–3355.

Otto A., Collins-Hooper H. & Patel K. (2009) The origin, molecular regulation and therapeutic potential of myogenic stem cell populations. *J. Anat.* **215**, 477–497.

Rassi A. Jr, Rassi A. & Marin-Neto J.A. (2010) Chagas disease. *Lancet* **375**, 1388–1402.

Rudnick M.A. (2003) Marrow to muscle, fusion versus fusion. *Nat. Med.* **9**, 1461–1462.

Santini M.P. & Rosenthal N. (2012) Myocardial regenerative properties of macrophage populations and stem cells. *J. Cardiovasc. Transl. Res.* **5**, 700–712.

Schofield C.J., Jannin J. & Salvatella R. (2006) The future of Chagas disease control. *Trends Parasitol.* **22**, 583–588.

Senyo S.E., Steinhauser M.L., Pizzimenti C.L. *et al.* (2013) Mammalian heart renewal by pre-existing cardiomyocytes. *Nature* **493**, 433–436.

Soares M.B., Lima R.S., Rocha L.L. *et al.* (2004) Transplanted bone marrow cells repair heart tissue and reduce myocarditis in chronic chagasic mice. *Am. J. Pathol.* **164**, 441–447.

Soares M.B., Garcia S., Campos de Carvalho A.C. & Ribeiro dos Santos R. (2007) Cellular therapy in Chagas' disease: potential

applications in patients with chronic cardiomyopathy. *Regen. Med.* **2**, 257–264.

Soares M.B., de Lima R.S., Rocha L.L. *et al.* (2010) Gene expression changes associated with myocarditis and fibrosis in hearts of mice with chronic chagasic cardiomyopathy. *J. Infect. Dis.* **202**, 416–426.

Thiele J., Varus E., Wickenhauser C., Kvasnicka H.M., Metz K.A. & Beelen D.W. (2004) Regeneration of heart muscle tissue: quantification of chimeric cardiomyocytes and endothelial cells following transplantation. *Histol. Histopathol.* **19**, 201–209.

Xynos A., Corbella P., Belmonte N., Zini R., Manfredini R. & Ferrari G. (2010) Bone marrow-derived hematopoietic cells undergo myogenic differentiation following a Pax-7 independent pathway. *Stem Cells.* **28**, 965–973.